Physiological and Functional Characterisation of RafS, a Ribosome Associated Factor of Mycobacteria

Nandita Keshavan

Imperial College London Doctoral Thesis
Department of Life Sciences
(PhD. Molecular Microbiology)
2014

Declaration of Originality

I declare that I have performed all of the work and analysed all of the data in this thesis, with the exception of the translation assays which were conducted by Dr. Rashid Akbergenov and also four growth curve assays (Figures 3.4 and 3.5) that were carried out by Josephine Choo.

Copyright Declaration

Abstract

Tuberculosis (TB) is a leading cause of death from a single infectious agent and infects one third of the world's population in a latent form. Latent TB is characterised by presence of TB antigens but a lack of symptoms of TB. Latent TB is associated with the persistent form of *Mycobacterium tuberculosis,* and is a reservoir from which symptomatic infection arises. Non-replicating persistence (NRP) is postulated to be a reversible state characterised by lack of replication, decreased metabolic activity and increased antimicrobial resistance.

To achieve viable persistence, NRP cells have been postulated to require stabilisation of cellular structures needed for stress tolerance and for the transition from NRP to active replication. This study investigates the hypothesis that ribosome stabilisation assists in mycobacterial stress tolerance and persistence. RafS is a novel mycobacterial ribosome associated factor and putative ribosome stabilisation factor. The physiological roles and functional characteristics of RafS are investigated in this study.

The role of RafS in *M. smegmatis* (Msm) and *M. tuberculosis* (Mtb) physiology were investigated. Competitive survival assays between wild type and $\Delta rafS_{Mtb}$ illustrated that $RafS_{Mtb}$ confers a competitive advantage during survival under nutrient limitation. $RafS_{Msm}$ and $RafH_{Mtb}$ were found to significantly inhibit *in vitro* translation. Furthermore, $RafS_{Msm}$ and $RafH_{Mtb}$ inhibited *in vitro* translation of mRNA with and without Shine Dalgarno sequences. It was determined that $RafS_{Msm}$ is dispensable for growth and survival in several conditions and also for mature biofilm and pellicle formation. Also, $RafS_{Msm}$ is dispensable for tolerance of heat, acid and antibiotic stress. Ribosomal profiling indicated no significant effect of $rafS_{Msm}$ deletion on ribosomal subunit association in log phase and stationary phase rich media cultures. These findings are discussed in the context of mycobacterial growth, survival, stress tolerance and persistence mechanisms.

Acknowledgements

Firstly, I must thank my supervisor Dr. Huw Williams for his regular guidance and feedback on written and presented material throughout the PhD. He made several suggestions for experiments which were essential to this project. He also facilitated collaborations and gave constructive feedback during the writing of this thesis. I am also grateful for having had the opportunity to attend an international TB conference in Whistler.

Secondly, my sincere thanks goes to the post-doctoral researcher Dr. Kathryn Lougheed for teaching me several methods in the initials stages, for her feedback in meetings and for teaching and supervising my containment level 3 (CL3) work during this project. She was also very helpful in ordering materials for the project and in $RafH_{Mtb}$ protein purification.

My sincere thanks goes to Dr. Rashid Akbergernov and Prof. Erik Bottger (University of Zurich) for their assistance with the translation assays. I thank Rashid who carried out the translation assays and provided me with raw data and methods. I am greatly indebted to Dr. Brian Robertson who gave of his time and supervised my CL3 work and who also participated in discussion regarding the *M. tuberculosis* data.

Thanks also goes to Prof. Steven Curry and post doctoral researcher Dr. Eoin Leen (Imperial College) for their advice regarding bioinformatic programs. I specially thank Dr. Eoin Leen who helped me at short notice by rendering predicted protein structures in PyMol. I also thank Dr. Brian Robertson and Dr. John Rossiter who were members of my progress review panel for their constructive feedback. I thank Dr. Kerstin Williams and Heather Coombe who maintained the CL3 suite.

I thank the undergraduates Josephine Choo and John Fielden for their work during the PhD. I thank Dr. Mike Brownleader (Generon) for his suggestion regarding centrisart protein concentration. I thank Andrej Trauner for his input regarding ribosomal profiling. Also, valuable were the input of the members of the Williams lab Chandrika Nair, Rebecca Price and Katie Farrant. I am also grateful to Dr. Christoph Engl and Dr. Parul Mehta from the Martin Buck lab for their general advice. Thanks is also due to Dr. Peter Lund from the University of Birmingham for his discussions regarding biofilm assays.

I am very grateful for the assistance of Mr. Ian Morris and Ms. Fiona May in several material, equipment or admin-related matters and also washing and delivery services in our building. Thanks also goes to Timber Tech's, Dr. Bob Coutts's, Dr. Pietro Spanu's, Dr. John Rossiter's and Prof. Martin Buck's and other labs from whom I borrowed equipment or materials when needed. I would also like to thank the Constant systems team for mediating servicing of the cell disruptor. I also thank the thesis examiners Prof. Paul Langford and Prof. Graham Stewart who provided important feedback on the thesis.

I am grateful to the government of Trinidad and Tobago for providing me with a scholarship which financed the tuition fees during this project and other research funding bodies that have contributed to this project. I also thank Imperial College for the graduate school courses that I took during the PhD. I must also thank my family, in particular my parent, siblings and friends for their support throughout the project.

Contents

List of Figures

List of Tables and Abbreviations

Abbreviation	Expansion
AES	Allelic exchange substrate
ATP	Adenosine triphosphate
CFU	Colony forming units
DR	Downstream homology region
EHR	Enduring Hypoxic Response
FPLC	Fast Protein Liquid Chromatography
GTP	Guanosine triphosphate
HdB	Hartmann de Bont
HPF	Hibernation Promoting Factor
iTRAQ	Isobaric tags for relative and absolute quantitation

IFN	Interferon
IPTG	Isopropyl-β-D-thio-galactoside
LB	Luria Broth
MABA	Microplate Alamar Blue Assay
MIC	Minimum inhibitory concentration
Msm	*Mycobacterium smegmatis*
Mtb	*Mycobacterium tuberculosis*
NRP	Non-Replicating Persistence
OADC	Oleic acid albumin dextrose catalase supplement
PPD	Purified Protein Derivative
PCR	Polymerase Chain Reaction
PY	Protein Y
Raf	Ribosome Associated Factor
RMF	Ribosome Modulation Factor
SDS PAGE	Sodium Dodecyl Sulfate Polyacrylamide Gel Electrophoresis
TB	Tuberculosis
TNF	Tumour Necrosis Factor
UR	Upstream homology region

1. Introduction

1.1 Scope of the Introduction

The introduction aims to provide an overview of *Mycobacterium tuberculosis*, aspects of tuberculosis (TB) pathology, latent TB and *in vitro* stress models. Subsequently, bacterial translation, *Escherichia coli* ribosome stabilisation and putative mycobacterial ribosome stabilisation factors (Raf proteins) are described. Finally, the main research objectives of the project are outlined.

1.2 *Mycobacterium tuberculosis* and tuberculosis (TB)

1.2.1 *Mycobacterium tuberculosis*, TB and latent TB

Mycobacteria belong to the phylum Actinobacteria, which is known for its high morphological diversity (Servin *et al.,* 2008). Actinobacteria are found in aquatic and terrestrial habitats worldwide and produce a variety of extracellular enzymes and secondary metabolites (Falkinham *et al.,* 2009, Ventura *et al.,* 2007). The genus *Mycobacterium* includes the pathogens, *Mycobacterium tuberculosis* and *Mycobacterium leprae* which are causative agents of TB and leprosy, respectively (Henriques *et al.,* 2000).

During the industrial revolution, TB was responsible for 1 in 4 deaths (Donoghue, 2009). In 2010, an estimated 1.3 million people died from TB and an estimated 8.6 million new TB cases arose (WHO Report 2013). Biological and socioeconomic factors contribute to the spread of TB, such as HIV-related immunodeficiency, prevalence of drug-resistant TB, poor sanitation and overcrowding (Rustad *et al.,* 2009). Furthermore, the current Bacillus Calmette-

Guerin (BCG) vaccine primarily protects young children and leprosy patients from TB, but provides variable protection (0 – 80%) against infectious pulmonary TB in adults (Singh *et al*., 2014).

Latent TB is defined by the absence of clinical TB symptoms along with a positive reaction to the purified protein derivative (PPD) skin test (Barry *et al.,* 2009). Globally, an estimated 1.8 billion people are PPD+. The actual value may be lower than estimated due to false positive results if an immune response to PPD is elicited by antigens from other mycobacteria, such as *Mycobacterium bovis* in the BCG vaccine. A more specific latent TB diagnostic test which detects interferon-γ (IFN-γ) produced *in vitro* in response to *M. tuberculosis* antigens has been developed (Barry *et al.,* 2009).

Current antibiotics target actively replicating bacteria and are not effective against latent stage TB. The current first-line regimen for treating active TB consists of isoniazid, a rifamycin, pyrazinamide and ethambutol and the length of treatment (6 months) reflects the difficulty of eradicating *M. tuberculosis*. Factors such as reduced patient compliance or antibiotic inefficacy contribute to the formation of genetic antibiotic resistance. Koul *et al.* highlighted that a drug regime of reduced duration and lower dosing frequency is needed (Koul *et al.,* 2011).

Latent TB and TB reactivation are major public health concerns and new antimicrobial strategies are needed to target latent TB bacilli, whose antibiotic-tolerance is phenotypic in nature and distinct from genetic antibiotic resistance. Latent bacilli act as a reservoir from which actively replicating transmissible bacilli can arise and the emergence of bacilli from latency to active TB is known as reactivation. TB reactivation occurs mostly in highly oxygenated regions, while

latency is associated with reduced oxygen. Immunodeficiency and diabetes are risk factors which increase the chances of reactivation (Barry *et al.,* 2009).

1.2.2 *M. tuberculosis* lung pathogenesis and granuloma formation

M. tuberculosis is well-adapted for lung pathogenesis and a single bacterium is sufficient to cause infection (Russell *et al*., 2007). *M. tuberculosis* is a facultative intracellular parasite of macrophages and bacilli undergo an elaborate struggle with the immune system in order to gain a stronghold in infected lungs. *M. tuberculosis* exploits immune-mediated damage to spread within infected lungs, which show a gradation of stages in which calcified tuberculous lesions with few viable bacteria become caseous lesions which themselves become sources of actively replicating bacteria (Barry *et al*., 2009).

When aerosols carrying TB bacilli are inhaled into the lungs, the bacilli undergo internalisation by macrophages. Here, *M. tuberculosis* undergoes rapid replication, arrests phagosome maturation and prevents phagosome acidification and accumulation of hydrolytic enzymes (Rengarajan *et al.,* 2005). In quiescent macrophages, *M. tuberculosis* bacilli are retained in the recycling endosomal pathway, a state protected from lytic enzymes of the lysosome, where iron is accessible for incorporation into several enzymes and proteins. In the presence of activating cytokines, macrophages can deliver the bacilli to acidic lysosome-like vacuoles.

Activated macrophages exhibit low oxygen levels and produce nitric oxide and related radicals, conditions that are unfavourable for *M. tuberculosis* active

replication and metabolism. However, latent TB bacilli are postulated to result from *M. tuberculosis* entering a non-replicating persistent state for survival in the stressful environment of granulomas. Granulomas are avascular lesions that suppress bacterial growth due to oxygen and nutrient deprivation, acidic pH and nitric oxide production. Several types of granulomas have been identified which suggests that a spectrum of pathology is characteristic of pulmonary TB infections (Table 1.1) (Russell *et al.,* 2007).

Table 1.1. Types and features of TB granulomas suggest that a spectrum of pathology is characteristic of pulmonary TB infections (Barry *et al*., 2009).

Type of granuloma	Features		
	Most prevalent in active and/or latent TB	Composition	*M. tuberculosis* bacilli primary location
Non-necrotising granuloma	Active TB	mostly macrophages with some lymphocytes	macrophages
Caseous granuloma	Active and latent TB	epithelial macrophages, neutrophils, lymphocytes, sometimes surrounded by peripheral fibrosis; centre is caseous and hypoxic and contains dead host cells	macrophages, in the centre and possibly in the fibrotic rim
Fibrotic granuloma	Latent TB	mostly fibroblasts, with minimal macrophages	Unknown

Granulomas aid in limiting the spread of *M. tuberculosis*, and yet also harbour latent bacilli for decades. Several immune factors contribute to granuloma formation, such as activating cytokine TNFα (tumour necrosis factor alpha) which mediates phagocyte migration and aggregation to form granulomas. Mycobacteria themselves produce a potent initiator of granuloma formation, cord factor, suggesting that they are well adapted to and may even benefit from survival within granulomas.

Zebrafish embryos are employed for investigating *Mycobacterium marinum* infections due to their transparency during the first 3 weeks of development which allows real-time monitoring of host-pathogen interactions and fluorescent transgenic immune cells within the host. Studies of *M. marinum* infections have revealed mechanisms of bacterial spread within granulomas, such as uninfected macrophage attraction to infected macrophage aggregates and inter-macrophage bacterial transfer (Pozos *et al*., 2004). During reactivation, granulomas caseate and cavitate, releasing viable bacilli into the lung. Reactivated bacilli can induce a productive cough that facilitates dissemination to new hosts (Höner zu Bentrup *et al.,* 2001).

1.3 *M. tuberculosis* stress adaptations

1.3.1 *M. tuberculosis* non-replicating persister (NRP) cells tolerate unfavourable conditions

Non-replicating persister cells (NRP cells) are postulated to be responsible for the latent asymptomatic phase in TB-infected individuals. NRP is postulated to be a reversible state characterised by (i) lack of replication (ii) decreased metabolic activity and (iii) increased antimicrobial resistance. It has been suggested that the use of the term 'dormancy' to refer to the NRP state is inappropriate because bacterial mRNA transcripts are found in lung tissue in the latent stage of disease, indicating that latent bacilli retain some metabolic activity. Unfavourable conditions in granulomas are postulated to encourage the development of stress-resistant NRP cells. (Höner zu Bentrup *et al.,* 2001).

The Cornell mouse model is an example of an animal model that was designed to isolate *M. tuberculosis* persister cells. In this model, after infecting mice with *M. tuberculosis*, chemotherapy was administered and the infection was thus reduced to a point at which no bacterial colonies were isolated when tissue homogenates were plated on nutrient agar. From these samples, persistent bacteria were retrieved by spontaneous reactivation of the infection or by immuno-suppressive corticosteroid therapy (Guirado *et al*., 2013).

Persistence mechanisms are widely investigated using *in vitro* models due to cost effectiveness, rapidity and reproducibility of preliminary results. *M. bovis* (BCG), *M. smegmatis* and *M. marinum* predominate in the literature as models for studying *M. tuberculosis*. The use of *M. tuberculosis* in growth-based experiments is limited

by its slow growth and it being a biosafety level 3 human pathogen (Shiloh *et al.,* 2010).

The mechanisms by which actively growing mycobacteria undergo a shift to become NRP cells and maintain viability remain to be understood. Several processes have been identified that are essential for NRP bacteria viability, including NAD^+ and ATP synthesis and maintenance of the proton motive force. While protein synthesis is greatly reduced, expression of genes encoding several alternative sigma factors is greatly enhanced, suggesting that these genes may be involved in mediating adaptations to persistence (Rustad *et al.,* 2009).

The majority of sporulation genes are not required for mycobacterial virulence in macrophages and to date, sporulation has not yet been conclusively demonstrated in *M. tuberculosis* (Russell *et al*., 2007). However, spore-like forms were reported by Ghosh *et al*. (Kirsebom lab), who suggested that sporulation occurs at a low rate in *M. marinum* and *M. bovis* BCG (Ghosh *et al.,* 2009). Traag *et al.* conducted similar experiments but did not detect spores in *M. marinum* cultures (Traag *et al.,* 2010). Singh *et al* (Kirsebom lab), suggested that since the signal that triggers sporulation is not yet known, the existence of spore-like forms is not easily reproduced (Singh *et al.,* 2010).

Ovoid forms were also suggested to be an NRP cell morphology. Anuchin *et al.* observed non-plateable ovoid forms in *M. smegmatis* cultured under nitrogen-limitation. Ovoid forms showed increased antimicrobial and heat resistance, diminished metabolic activity and diminished colony forming unit (CFU) viability. Ovoid forms could be stored for up to 5 months and recovered to become rod-

shaped cells (Anuchin *et al*., 2009). To date, these NRP cell morphologies have not been conclusively accepted.

1.3.2 *In vitro* mycobacterial stress mechanisms

1.3.2.1 Coping with reduced oxygen: *M. tuberculosis* hypoxic stress tolerance and the DosR regulon

Bacterial cells employ respiratory reactions to oxidise metabolites for generating energy. Oxygen is important for the functioning of the electron transport chain, where the energy generated from the transfer of electrons across a series of cytochromes is coupled to ATP synthesis and oxygen is the terminal electron acceptor for this process (Cecchini *et al.,* 2003). As described in section 2.2, hypoxia is an important stress condition which *M. tuberculosis* faces in the environment of the granuloma. This leads to the question as to how does *M. tuberculosis* survive hypoxia?

Several models have been developed for investigating mycobacterial stress mechanisms. According to the Wayne hypoxia model, NRP cells can be obtained by culturing *M. tuberculosis* in a sealed vessel with a defined culture-to-headspace ratio with gentle mixing. This model is convenient for investigating genes involved in stress adaptation, due to gradual oxygen depletion and nutrient starvation during extended stationary phase (Wayne *et al.,*1996).

Regarding the metabolic pathways used to generate energy in hypoxic *M. tuberculosis*, many genes predicted to be involved in *M. tuberculosis* anaerobic respiration are surprisingly repressed or not induced, suggesting that much remains to be understood as to how *M. tuberculosis* remains viable during persistence (Rustad *et al.,* 2009). Key regulons involved in hypoxic adaptation are the DosR (dormancy survival) and EHR (enduring hypoxic response) regulons (Leistikow *et al*., 2010, Rustad *et al*., 2008). Blocking expression of the DosR regulon had little effect

on subsequent expression of the EHR. The EHR regulon contains 230 genes and is important for the long-term maintenance of the hypoxic response (Rustad *et al*., 2008).

The DosR regulon is a set of 48 coregulated genes which is induced by three factors which inhibit aerobic respiration: hypoxia, NO, and CO. Control and induction of the DosR regulon is mediated by a three-component regulatory system composed of DosS and DosT, two sensor histidine kinases that bind NO and CO, and a response regulator, DosR (Honaker *et al.* 2009, Leistikow *et al*,. 2010). The genes of the DosR regulon contain a consensus sequence to which DosR binds, known as the DosR binding motif (Gautam *et al*., 2011). DosR genes upregulated during *M. tuberculosis* persistence include universal stress proteins, nitroreductases, diacylglycerol acyl transferases, heat shock proteins, and ferredoxins.

The DosR regulon is primarily involved in the *M. tuberculosis* initial hypoxic response where it is responsible for (i) mediating a shift away from oxygen consumption which is necessary for optimal transition of *M. tuberculosis* to aerobic growth from an anaerobic or an NO-induced NRP state and (ii) maintenance of ATP levels and balancing of the redox state (NAD/NADH ratio) under hypoxic conditions (Gerasimova *et al.,* 2011). It has also been suggested that the DosR regulon plays an important role in reducing growth prior to transitioning to the NRP form (Hett *et al.,* 2008). Deletion of DosR was associated with a reduction in the abundance of 70S associated ribosomes in hypoxic *M. smegmatis* cultures (Trauner *et al.,* 2012). This is described further in section 1.3.6.

1.3.2.2 *M. tuberculosis* nutrient starvation stress tolerance: investigating energy-limitation responses

Given that *M. tuberculosis* undergoes nutrient starvation in granulomas and that metabolites are important for generating energy in bacteria, mechanisms of nutrient starvation stress tolerance are of significant interest in the study of mycobacteria. The Loebel model investigated survival of NRP bacilli in general nutrient starvation in oxygen-rich conditions (in phosphate-buffered saline, where nutrients were absent).

Loebel *et al.* found that nutrient-starved *M. tuberculosis* bacilli survive for long periods of time *in vitro* and undergo a drastic reduction in respiration over the first 96 hours of starvation (*Loebel et al.*, 1933). Betts *et al.* adapted the Loebel model to investigate changes in *M. tuberculosis* gene expression under general nutrient starvation using microarray analysis and found that 279 genes were upregulated and 323 genes were downregulated after 96 hours of culture (Betts *et al*., 2002).

This study provided evidence for the slowdown of the transcription apparatus, energy metabolism, lipid biosynthesis and cell division in addition to induction of the stringent response and other genes that may play a role in maintaining long-term survival (Betts *et al*., 2002). It also leads to further questions as to the effectors of slowdown of these essential cellular processes.

Smeulders *et al.* showed that *M. smegmatis* remained viable over 650 days after a reduction in viability under carbon, nitrogen and phosphorous starvation (Smeulders *et al*., 1999). A study investigating *M. smegmatis* survival under nutrient starvation in a chemostat model found three mechanisms that the bacteria employed (i) alteration of metabolism to minimise waste (ii) production of new compounds to

scavenge resources and (iii) utilisation of alternative energy sources (Berney *et al*. 2010).

1.3.2.3 The stringent response is a bacterial amino acid starvation response that is induced in nutrient-starved *M. tuberculosis*

The stringent response is an amino acid starvation response that has been studied extensively in *E. coli* and other gram negative bacteria. As mentioned in section 1.3.2.2, induction of the stringent response was observed in a study of the differential expression of *M. tuberculosis* genes in general nutrient starvation (Betts *et al*., 2002)

The stringent response is regulated by the alarmone guanosine tetraphosphate (ppGpp), a small molecule regulator of transcription of genes regulating growth and survival. ppGpp is produced from pppGpp, which itself is produced from ATP and GTP by the enzymes RelA and SpoT of the RelA/SpoT (RSH) family. RelA is bound to a subset of ribosomes and is activated in response to uncharged tRNA in the ribosomal A-site during amino acid starvation. SpoT is activated by a range of other starvation stresses.

ppGpp binds near the active site of RNA polymerase (RNAP) and plays a role in repressing rRNA synthesis and ribosome production. Genes negatively regulated by ppGpp include genes involved in DNA replication, ribosome assembly, translation, fatty acid production and cell wall synthesis. Genes positively regulated by ppGpp include genes involved in amino acid biosynthesis and proteolysis and

stress tolerance genes, such as osmotic and oxidative stress genes and genes encoding universal stress proteins (Magnusson *et al.,* 2005).

In *M. tuberculosis*, RelA and SpoT have a single homologue, RelMtb, which catalyzes (p)ppGpp synthesis and hydrolysis (Avarbock *et al.* 2005). Loss of RelMtb was associated with impaired survival under nutrient starvation and under extended anaerobic incubation. Also, the stringent response is essential for *M. tuberculosis* long term survival in a TB mouse model (Primm *et al.,* 2000) (Dahl *et al.,* 2003).

1.4 Bacterial ribosome structure and translation

1.4.1 Bacterial ribosome structure

Protein synthesis, also known as translation, is the process by which the message encoded by mRNA is translated into specific amino acids that comprise proteins. Given the vast changes in transcription observed in nutrient-starved *M. tuberculosis* described in section 1.3.2.2 and the hypoxic and stringent stress responses described in sections 1.3.2.1 and 1.3.2.3 respectively, it is apt to investigate whether further regulation occurs at the translation level in *M. tuberculosis* as a result of energy limitation stresses.

Ribosomes are structures that mediate translation and comprise ribosomal RNA (rRNA) and proteins (r proteins). The majority of ribosomal proteins are less than 20 kDa in molecular weight. Ribosomal subunits contain rRNA molecules that form a scaffold upon which r proteins bind (Broderson *et al*. 2005). The subsequent information presented in section 1.4 is based on a text by Anders Liljas unless otherwise indicated (Liljas, 2004).

Ribosomes are RNA-protein structures that mediate translation or protein synthesis. Bacterial ribosome subunits are named according to their sedimentation coefficients; the large subunit is termed the 50S subunit and the small subunit is termed the 30S subunit. The two subunits when bound together form the 70S ribosomal subunit. These sizes are shared by chloroplast, archaea and plant mitochondrial ribosomes, whereas eukaryote ribosomes are composed of the 60S large subunit and the 40S small subunit, which together form the 80S ribosome.

The 50S ribosomal subunit contains 23S and 5S rRNA whereas the 30S subunit contains 16S rRNA. The rRNA molecules provide bindings sites to r proteins, which in turn stabilise the rRNA structure. Ribosome crystal structures indicate extensive rRNA interactions with r proteins. rRNA molecules form double-stranded helices, which themselves form secondary structures comprising kinks and turns stabilised by hydrogen bonds. Kink-turn structures have been associated with binding to r proteins. Notably, the region of the small subunit that interfaces the large subunit is distinctly protein-poor.

The r proteins are primarily globular and exhibit acidic surface and internal basic regions that neutralize the negative charge of rRNA. A repeatedly occurring motif, the RNA recognition motif (RRM) is composed of alternating β strands and α helices in a pattern known as “split β-α-β”. Also common are OB-fold (oligonucleotide binding) domains which contain β sheets. Some proteins also bind zinc, magnesium and monovalent ions.

Arrangement of rRNA helices in the small (30S) subunit allows flexibility which is important for its functionality. The large subunit mediates peptidyl transfer in the peptidyl transfer centre. Large subunit 23S rRNA contains 6 interwoven domains that form a stable core. Interactions between rRNA and r proteins in the large subunit are more extensive than those of the small subunit. Two flexible side protuberances, L1 and the L12 stalk, are functionally important. The entry site of the incoming amino acid is known as the A site and the site of polypeptide chain formation is known as the P site. The polypeptide exit tunnel allows passage of the nascent polypeptide chain to the exterior and its external side is protein-rich.

In the 70S ribosome, translational activities mainly occur at the subunit interface and ribosome dynamic properties depend on inter-subunit bridges that hold ribosomal subunits together. 12 intersubunit bridges have been mapped to specific proteins and helices in the 30S and 50S subunits. The bridges are dynamic and change or break in response to the changes that occur at the subunit interface.

1.4.2 Bacterial translation

During translation, ribosomes select amino acids in the order needed to form the primary structure of polypeptides which form proteins. Ribosome association refers to the joining of 50S and 30S subunits to form 70S ribosomes. Ribosome dissociation refers to the separation of 70S ribosomes into 50S and 30S subunits. Ribosome association and dissociation are key processes in the ribosome cycle. Translation takes place in three main stages;

1. Initiation, the process of mRNA recognition and mRNA positioning.
2. Elongation, the process of polypeptide chain building based on codon-anticodon recognition.
3. Termination, the conclusion of polypeptide building and ribosome recycling. During initiation, messenger RNA (mRNA) is threaded through two tunnels, which are responsible for:

(i) binding mRNA

(ii) decoding the mRNA message.

1.4.2.1 Translation initiation

Initiation begins with the 30S subunit recognising the mRNA molecule; the Shine-Dalgarno (A- and G- rich) sequence of the mRNA 5' end is recognized by the anti-Shine-Dalgarno sequence of the 30S subunit's 16S rRNA 3' end. Recognition between these sequences anchors the mRNA to the 30S subunit. In a process known as mRNA adaptation, the initiator codon, an RNA triplet found in mRNA, positioned in the P-site is recognized by the initiator tRNA anticodon.

Subsequent codons are recognized by complementary anticodon RNA triplets in tRNA carrying specific amino acids. tRNAs bound to rRNA at the A and P sites base pair to mRNA for mRNA decoding. Codon-anticodon recognition produces small subunit anti-codon stem loop conformation changes, which mediates a movement known as "closure". Initiation factors IF1, IF2 and IF3 mediate fMet-tRNA positioning in the P site and IF2 catalyses subunit association. Functions of initiation factors are shown in Table 1.2.

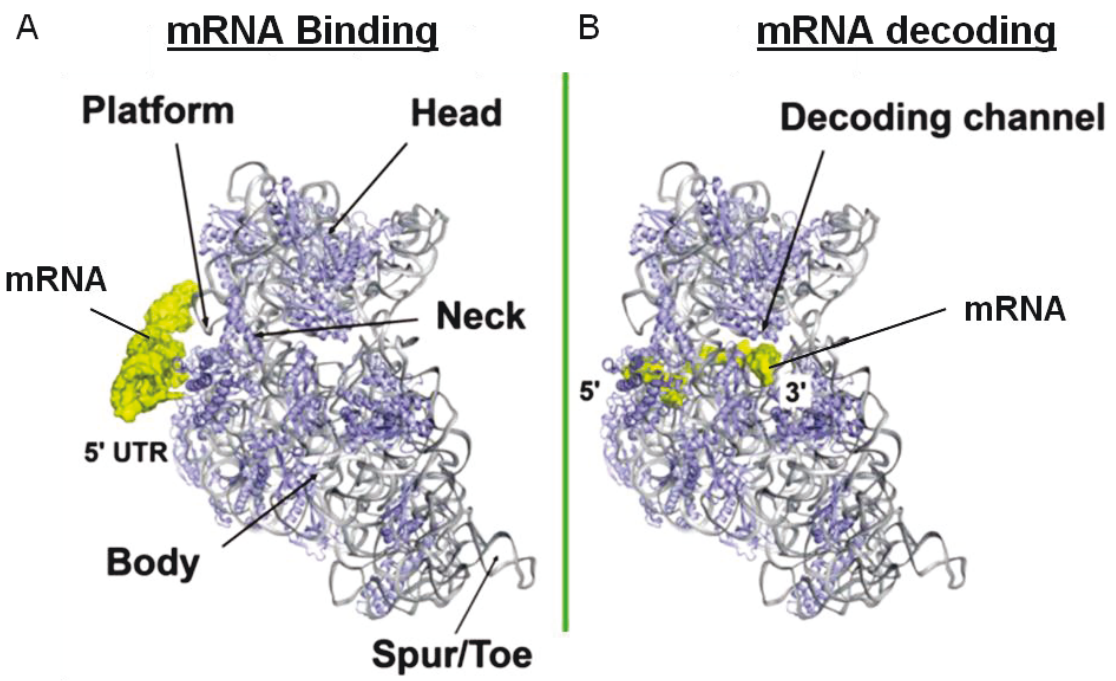

Figure 1.1. Models for mRNA binding and decoding at the 30S ribosomal subunit during bacterial translation initiation. An mRNA molecule is shown in yellow and the 30S ribosomal subunit is shown in lilac. (A) mRNA binding: An mRNA molecule is recruited on the 30S subunit platform. mRNA 5' Shine-Dalgarno (A- and G- rich) sequence recognition by the anti-Shine-Dalgarno sequence of the 30S subunit 16S rRNA 3' end anchors the mRNA to the 30S subunit. (B) mRNA decoding: During a process known as mRNA adaptation, the mRNA moves into the mRNA decoding channel, a groove located at the neck of the 30S subunit. During this process, the mRNA unfolds and codons are exposed for recognition by tRNA anti-codons and the mRNA and adjustment of the mRNA in the decoding centre is mediated by initiation factors and fMet-tRNA^{fMet}. mRNA adaptation leads to recruitment of the 50S ribosomal subunit and formation of an active 70S initiation complex. Initiation factors assist in ensuring fidelity of mRNA binding and in maintaining the rate of initiation complex formation. Image adapted from Simonetti *et al*., 2009.

Table 1.2. Functions of translation initiation factors. (Liljas, 2004).

Initiation factor	Function
IF1	• stimulates ribosome subunit dissociation • stimulates IF2 binding • assists in directing the initiator tRNA to the P site
IF2	• associates the pre-initiation complex (mRNA+30S subunit+ IFs) to the large subunit
IF3	• prevents association between the two ribosomal subunits before initiation is complete (interaction site with intersubunit bridge has been confirmed) • promotes 70S ribosome dissociation and maintains a pool of free 30S ribosomal subunits • directs initiator tRNA to the P-site • influences kinetics and fidelity of codon-anticodon recognition

1.4.2.2 Elongation

Subsequently, the large ribosomal subunit binds and elongation begins. The sites at which tRNA interact with the large subunit are present in a tunnel at the subunit interface known as the peptidyl transferase centre. These sites, in order of tRNA migration during translation are as follows;

1. T-site: entry site where tRNA bound with elongation factor EF-Tu is located
2. A-site: site for aminoacyl tRNA complexes
3. P-site: site for peptidyl tRNA complexes

4. E-site: exit site where deacetylated tRNA is located before exiting the ribosome.

The A, P and E sites are the tRNA binding sites of the ribosome. Of these, the A and P sites play a significant role in elongation and reactions in these sites are catalysed by the rRNA component of the ribosome (Broderson *et al*., 2005). During elongation, each amino acid is added to the growing polypeptide chain after codon-anti-codon interaction, in a process known as decoding.

The aa-tRNA amino acid end contacts the 50S subunit peptidyl transferase centre. The aa-tRNA anticodon end contacts the mRNA decoding site of the 30S subunit, where it is bound to its corresponding mRNA codon in the A site (Fig. 1.2). A peptide bond then forms between the amino acid of the tRNA in the A site and the amino acid of the charged tRNA in the P site. The growing polypeptide chain is transferred to the tRNA in the A site. This tRNA is then known as the peptidyl tRNA. Elongation factors EFTu and EFG assist in this process and their main features are included in Table 1.3.

The peptidyl-tRNA in the A site carrying the nascent polypeptide chain is to be shifted to the P site so that another aatRNA can bind at the A-site, in a process known as translocation. To achieve this, the ribosome undergoes a “ratchet-like” movement, an approximately 10^{o} anticlockwise rotation of the 30S subunit relative to the large subunit induced by EF-G:GTP. This mediates (i) tRNA shifting from the A- and P- sites to the P- and E-sites respectively and (ii) movement of mRNA to expose the next codon in the A-site (Fig. 1.2), allowing entry of the next aa-tRNA and mRNA codon. Upon dissociation of EF-GDP, the ribosome returns to its original subunit orientation.

Table 1.3. Features of key translation elongation factors. (Liljas, 2004).

Elongation factor	Features
EF-Tu	• binds aminoacyl tRNAs to the A site and protects aminoacyl tRNAs from hydrolysis • GTP hydrolysis induces a conformational change to activate EF-Tu. EF-Tu mediates removal of GDP from the ribosome
EF-G	• translocase; mediates translocation of peptidyl tRNA and mRNA after peptidyl transfer ("ratchet-like" movement) • GTP hydrolysis induces a conformational change to activate EF-G

1.4.2.3 Termination

Translation is terminated when a stop codon is encountered. The stop codon is recognized by class 1 termination factors which hydrolyse the polypeptide from the tRNA. Ribosome recycling allows binding of new mRNA to the ribosome, since the previous mRNA and deacetylated tRNAs exit the ribosome and the ribosomal subunits are dissociated from each other. This process is mediated by ribosome recycling factor, RRF, which binds across the A and E sites. Ribosomes interact with membrane proteins via the 50S subunit which contains a polypeptide exit tunnel, a non-polar tunnel in which the nascent polypeptide chain travels out of the ribosome, and is protected from digestion by proteolytic enzymes. Protein folding occurs when polypeptide chain emerges from the ribosome (Broderson *et al*., 2005).

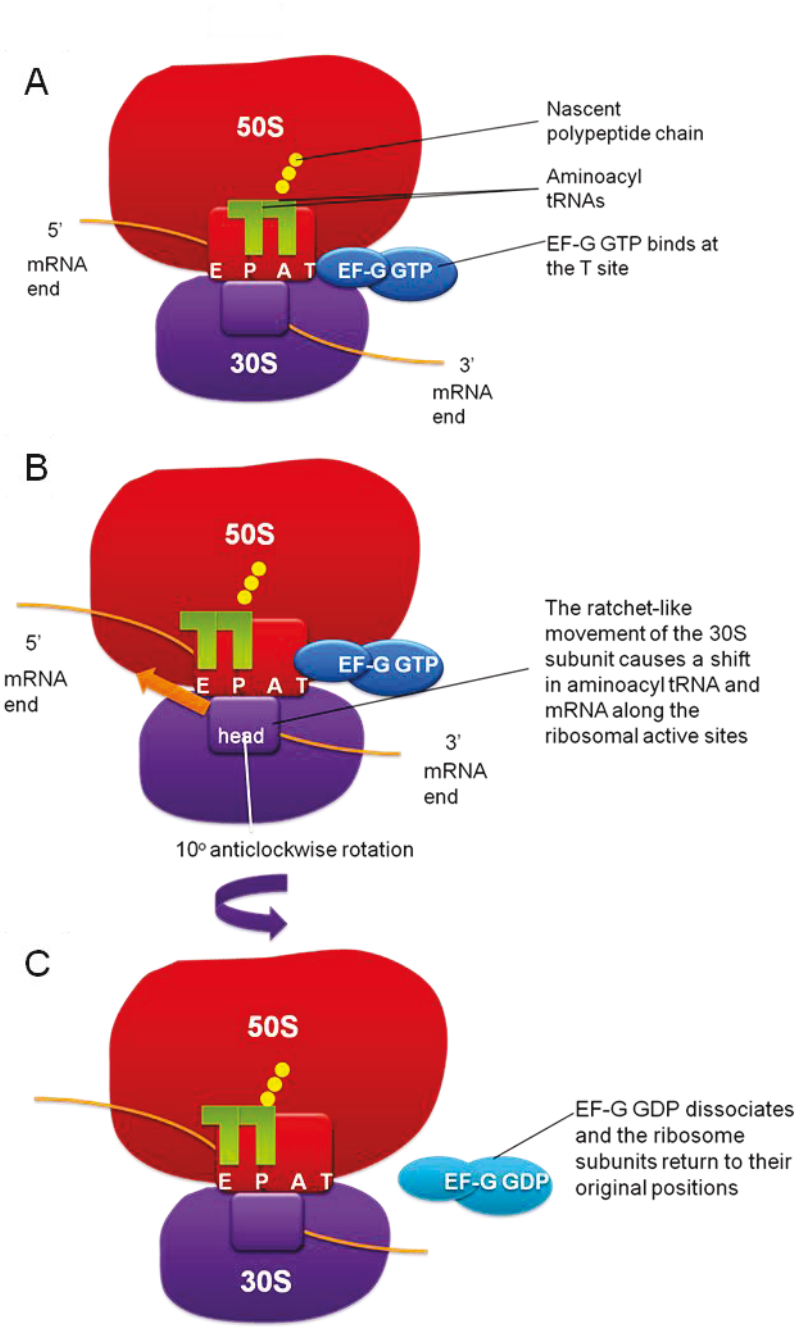

Figure 1.2. Translocation: the post-peptide bond formation “ratchet-like” movement of the 30S ribosomal subunit during elongation. (A) Pre-translocation conformation of ribosome subunits (B) “Ratchet-like” movement: anticlockwise rotation of the 30S subunit head relative to the 50S subunit which induces movements of the aatRNA and mRNA along the ribosomal active sites. (C) Ribosome subunits return to their original conformation. Aminoacyl tRNAs (green), mRNA (orange), 30S (purple) and 50S (red) subunits and EF-G GTP (dark blue) and EF-G GDP (pale blue) are shown.

1.5 Bacterial ribosome stabilisation

1.5.1 Ribosome stabilisation is a form of bacterial translational regulation associated with nutrient starvation

Studies of ribosomal heterogeneity and specialisation in bacteria and eukaryotes refuted the view that ribosomes and translation are unchanging entities (Gilbert *et al.,* 2010). An example of a specialised ribosome is the stabilised ribosome. Ribosome stabilisation is defined as the association of ribosomal subunits or ribosomes which renders them translationally inactive. Ribosome stabilisation is a means of exit from the ribosome cycle and is a form of translational regulation found in several bacterial and eukaryotic species (Ortiz *et al.,* 2010, Krokowski *et al.,* 2011).

E. coli stationary phase ribosomes were found to have lower affinity for ribosome initiation and dissociation factors compared to log phase ribosomes, suggesting that ribosome stabilisation and translation inhibition may be important adaptations during stationary phase (Yoshida *et al.,* 2009). Evidence describing ribosome stabilisation in *E. coli* is described in sections 1.5.2 and 1.5.3.

1.5.2 *Escherichia coli* stabilised ribosomes exist as both 70S monomers and 100S dimers

In *Escherichia coli* (*E. coli*), ribosome stabilisation results in the formation of both 70S ribosome monomers and 100S ribosome dimers. The 70S monomer is formed by the association of the 50S and 30S ribosomal subunits. The 100S dimer is a higher order ribosomal structure that is formed when two 70S ribosomes are joined together via their 30S subunits. It has been shown to be translationally inactive (Wada *et al.,* 1995). The 30S subunits contact each other in two regions (Fig. 1.3) (Ortiz *et al.,* 2010).

Ortiz *et al.* investigated 100S dimer formation and distribution in different growth phases. Cryoelectron tomography indicated that an estimated 10% to 20% of stabilised ribosomes formed 100S dimers in minimal media stationary phase. The cellular distribution of the 100S dimers indicated that in this condition, they cluster together. The proportion of 100S dimers was lower in exponential phase and clustering of 100S dimers was not observed. Furthermore, addition of amino acids resulted in reduction of 100S dimers in stationary phase cells (Ortiz *et al.,* 2010). Taken together, these data suggested a role for 100S dimer formation in tolerance of stationary phase nutrient starvation in *E. coli*.

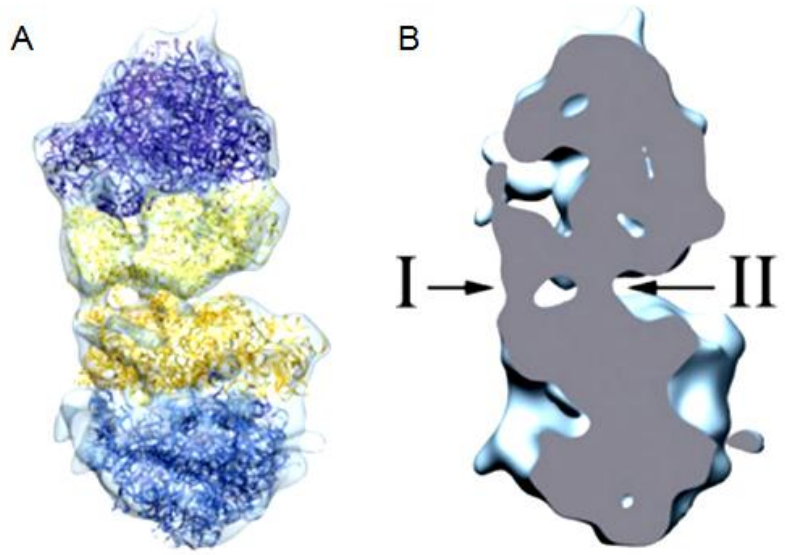

Figure 1.3. Cryo-electron tomography-derived structure of the *E. coli* 100S dimer, a stabilised ribosomal form of *E. coli* found most abundantly in minimal media stationary phase cultures. (A) Averaged 100S ribosome density map based on cryo-electron tomograms of *E. coli* grown to stationary phase in minimal media with 70S ribosome crystal structure docked into the density map. 50S ribosome subunits are shown in blue and 30S subunits are shown in yellow. (B) Cross-section of the 100S ribosome density map from (A). Two major contact regions between the 70S ribosome particles (I and II) were identified. Ribosomal proteins S9, S10, and the 16S rRNA helix 39 were located near region 1 and protein S2 was located near region 2. Imaged adapted from Ortiz *et al*., 2010.

1.5.3. *E. coli* ribosome stabilisation factors

1.5.3.1 *E. coli* ribosome stabilisation factors affect ribosomal subunit association

Since 100S dimers are translationally inactive ribosomal forms, 100S dimerisation is an example of ribosome stabilisation (see section 1.5.2). Given that 100S dimers and 70S monomers potentially play a role in nutrient starvation tolerance, their discovery led to further questions regarding the factors responsible for ribosome stabilisation. Three ribosome stabilisation factors (RSFs) are responsible for *E. coli* ribosome stabilisation; protein Y (also known as YfiA) (PY), ribosome modulation factor (RMF) and hibernation promoting factor (HPF).

The effect of RSFs on ribosome subunit association suggested a role for these proteins in ribosome stabilisation. Ribosome profiling indicated that RMF and HPF are involved in the sequential conversion of 70S monomers to 100S dimers as follows:

1. RMF causes dimerisation of 70S ribosome monomers to form 90S dimers. (Wada *et al.,* 1995).
2. HPF, also known as Yhbh, binds to 90S dimers and converts them to 100S dimers. (Ueta *et al*., 2008).

Polikanov *et al.* determined high resolution crystal structures of RMF, HPF and YfiA in complex with the *Thermus thermophilus* ribosome. The structures indicated the binding sites of these proteins and mechanisms by which they inhibit translation. The findings regarding RMF, HPF and PY are described sections 1.5.3.2, 1.5.3.3 and 1.5.3.4, respectively (Polikanov *et al.,* 2012).

Compared to ribosome stabilisation in *E. coli*, in *Lactococcus lactis,* YfiA is necessary and sufficient for 100S ribosome dimerisation. Furthermore, *yfiA* deletion diminished survival in energy starving conditions (Puri *et al.,* 2014). This indicates that in some organisms, ribosome stabilisation can be mediated by a single factor. Since the docking sites of *E. coli* ribosome stabilisation factors have been characterised and this gives insight into their mechanism, the remainder of this section describes the ribosome stabilisation factors of *E. coli*.

1.5.3.2 *E. coli* RMF (Ribosome Modulation Factor) prevents mRNA binding to the ribosome, inhibits translation and promotes 90S ribosome dimer formation

RMF was found to bind to stationary phase ribosomes in *E. coli* and was associated with ribosome dimer formation. RMF is synthesised prior to stationary phase and also in a slowly growing nutrient-starved state. Deletion of *rmf* was associated with decreased survival of *E. coli* in 5 hours of acid stress culture at pH3 (El-Sharoud *et al*., 2007). Also, deletion of *rmf* was associated with decreased survival of *E. coli* in 100 minutes of heat stress at 50^{o}C.

This viability defect in heat stress was more pronounced for *E. coli* stationary phase cells lacking *rmf*, whose ribosomes also showed a defect in thermal stability as shown by differential scanning calorimetry. Deletion of *rmf* was also associated with a decrease in the abundance of 100S ribosome dimers under heat stress in stationary phase. Taken together, the data indicated a significant role for *rmf* in tolerance of acid and heat stress during stationary phase (Niven *et al.,* 2004).

Furthermore, RMF is a significant inhibitor of *in vitro* translation; RMF inhibited both phage MS2 and polyU mRNA *in vitro* translation (Wada *et al*., 1995 and Yoshida *et al*., 2009). The gene encoding RMF is widely present in gammaproteobacteria, but is not present in any other bacteria (Ueta *et al*., 2013). Polikanov *et al.* later showed that RMF binds to 3 nucleotides of 3' end 16S rRNA at the anti-Shine-Dalgarno region (Fig. 1.4).

By occupying this position, RMF blocks access of the mRNA Shine-Dalgarno (SD) sequence to the 30S ribosomal subunit, thus preventing translation initiation. Furthermore, RMF involvement in the dimerisation of 30S subunits is supported by the observation that 30S subunits dimerise *in vitro* upon the addition of RMF (Polikanov *et al.,* 2012).

Polikanov *et al* identified the two points of contact between the 30S subunits that had been described previously by Ortiz *et al*. (Polikanov *et al.,* 2012, Ortiz *et al*., 2010). RMF-induced 30S subunit dimerisation was not a result of RMF proteins contacting each other, suggesting that 30S subunits directly contact each other during dimerisation. Polikanov *et al*. hypothesised that the binding of RMF to two 30S subunits induces a conformational change which allows the 30S subunits to contact each other and that binding of HPF further stabilises 100S dimer formation (Polikanov *et al.,* 2012).

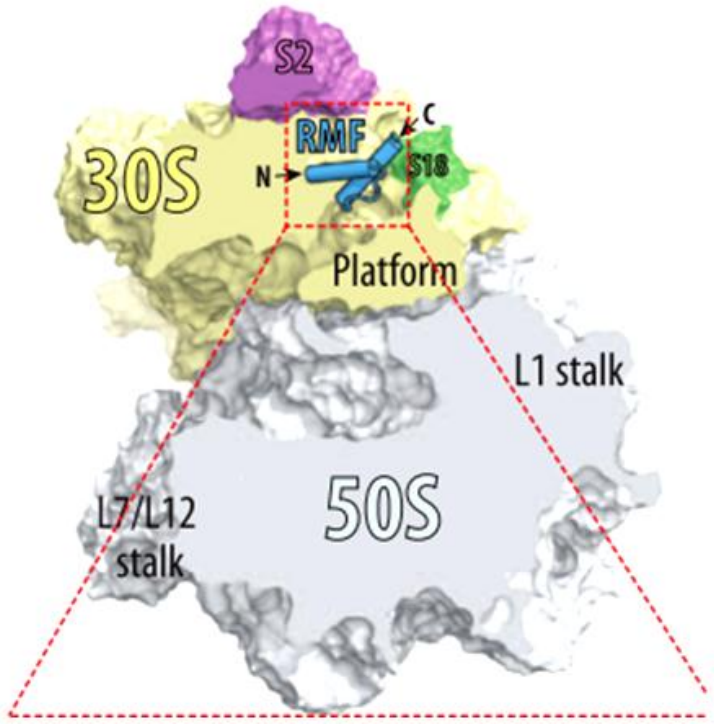

Figure 1.4. *E. coli* RMF blocks access of mRNA to the 30S ribosomal subunit, preventing translation initiation. RMF mediates dimerisation of 70S ribosomes to form 90S stabilised ribosome dimers, a process which is mediated by joining of 30S subunits. RMF (blue) binds to 3 nucleotides of 3' end 16S rRNA at the anti-Shine-Dalgarno region and prevents recognition of the Shine-Dalgarno sequence of mRNA by the ribosome. The image shown is based on a high resolution crystal structure of RMF in complex with the *Thermus thermophilus* ribosome. Figure adapted from Polikanov *et al.* 2012.

1.5.3.3 *E. coli* HPF (Hibernation Promoting Factor) promotes 100S ribosome dimer formation whereas PY inhibits 100S ribosome dimer formation

According to Polikanov's HPF-ribosome and PY-ribosome crystal structures (described in section 1.5.3.1), HPF and PY both bind at the channel of the 30S subunit that lies between the head and body, where tRNAs and mRNA bind during protein synthesis. Although their binding sites overlap, they have opposing roles; HPF promotes 100S dimer formation whereas PY inhibits its formation.

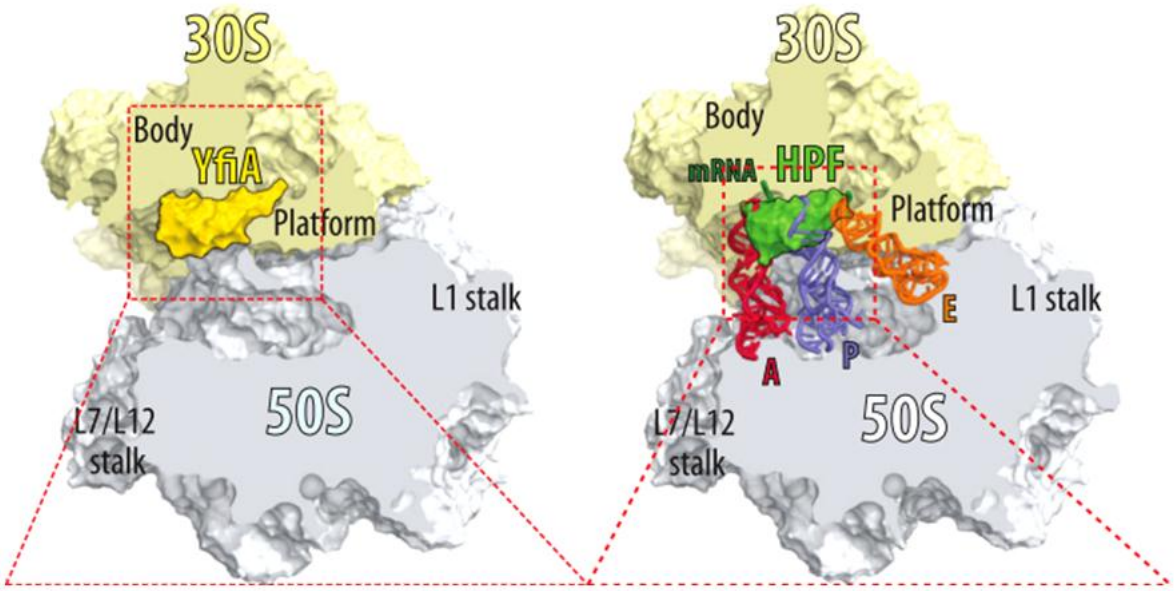

Figure 1.5. PY (YfiA) (yellow) and HPF (green) bind at the channel between the head and body of the 30S subunit, where tRNAs and mRNA bind during protein synthesis. HPF promotes 100S dimer formation whereas PY inhibits 100S dimer formation. The image shown is based on high resolution crystal structures of PY and HPF in complex with the *Thermus thermophilus* ribosome. Figure adapted from Polikanov *et al.* 2012.

In *E. coli,* HPF is a significant inhibitor of phage MS2 mRNA translation (SD present) but is not a significant inhibitor of polyU mRNA translation (Ueta *et al.,* 2008). On the other hand, PY inhibits translation of both GFP (SD present) and polyU mRNA (Agafonov *et al.,* 2001). In *E. coli*, RMF and HPF together are responsible for mediating ribosome dimerisation.

IF3 is an initiation factor that dissociates 70S ribosomes into individual subunits. Although IF3 is capable of removing HPF from the ribosome, 100S dimers stabilised by both RMF and HPF were found to be unaffected by incubating with IF3 (Yoshida *et al.*, 2009). However, 100S ribosome dimerisation is rapidly reversed by adding nutrients. Upon transferring *E. coli* cells from nutrient starvation to fresh medium, RMF and HPF exit 100S dimers within 1 minute of transfer and cells start to proliferate within 6 minutes (Aiso *et al*., 2005).

E. coli HPF is known as a "short HPF" since it lacks a long C-terminal extension. Short HPFs are predominantly present amongst gammaproteobacteria (e.g. *E. coli, Salmonella* Typhimurium*, Yersinia pestis, Klebsiella pneumonia, Pseudomonas fluorescens and Vibrio cholerae).* "Long HPFs" had longer C-terminal extensions and did not require RMF for 100S ribosome formation.

"Long HPFs" were characteristic of non-gammaproteobacteria (e.g. *Bacillus subtilis, Staphylococcus aureus*, *Streptococcus pyogenes, M. tuberculosis and Borrelia burgdorferi*) (Ueta *et al.,* 2008, Ueta *et al.,* 2013). In *Staphylococcus aureus,* SaHPF is a homologue of HPF but no RMF homolog exists. Unlike in *E. coli* where 100S dimers are found exclusively in stationary phase, 100S dimers exist in all growth phases of *S. aureus* and the highest levels of 100S dimers are found at the transition from exponential phase to stationary phase.

Given that 100S ribosome dimer formation is not a feature of mycobacterial ribosome stabilisation (Trauner, 2010), the promotion of 70S ribosome monomer formation is a putative ribosome stabilisation mechanism in mycobacteria. Since PY promotes 70S ribosome monomer formation, the findings regarding PY are addressed in the subsequent section (1.5.3.4).

1.5.3.4 PY (*E. coli*) promotes 70S ribosomal monomer formation and inhibits 100S ribosome dimer formation.

PY, also known as YfiA, is an RSF and S30AE protein of 70S *E. coli* ribosomes. S30AE proteins are prevalent amongst several bacterial and cyanobacterial species (see section 4.1). Agafonov *et al.* carried out studies regarding PY's effect on *in vitro* translation and determined that PY inhibited GFP mRNA translation and polyU mRNA translation (Ribosome: PY 1:1 and 1:4 respectively) (Agafonov *et al.,* 2001). Deletion of *yfia* did not affect growth and viability in 8 days of culture (Ueta *et al*., 2005).

PY is bound to ribosomes during stationary phase at 37°C (Maki *et al.* 2000; Agafonov *et al*. 2001). When initially discovered, PY was shown to increase the proportion of 70S monomers (Agafonov *et al.,* 1999). Deletion of *yfiA* was associated with an increase in 100S dimer formation; *ΔyfiA* (RMF and HPF present) showed a higher proportion of 100S dimers than wild type, whereas 100S dimers were not isolated from *Δhpf* (RMF and YfiA present) (Ueta *et al*., 2008). These findings suggested that PY activity is anti-ribosome dimerisation.

Supporting this anti-dimerisation role, PY was suggested to block the binding of RMF and HPF to the ribosome. The long C-terminal extension of PY has been

shown to overlap with the binding site of RMF (Figure 1.6). Thus, prevention of RMF binding is a suggested mechanism that explains the anti-dimerisation effect of PY (Polikanov *et al.,* 2012). Furthermore, PY also occupies the same binding site as HPF and stabilises the 30S subunit in its apo-conformation i.e. the 30S subunit conformation without RMF bound.

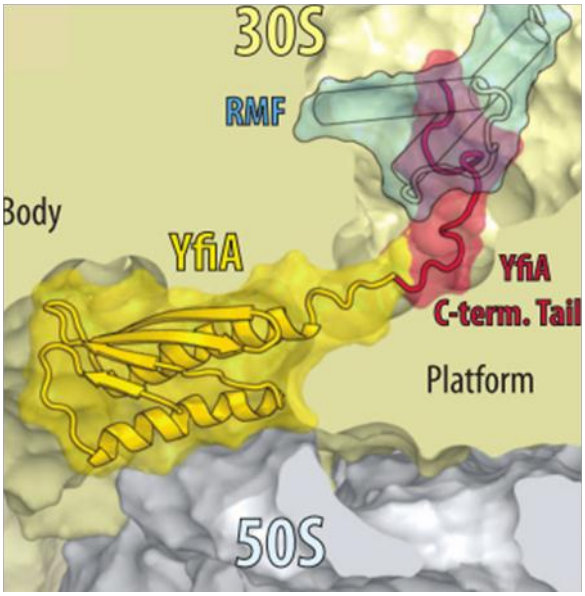

Figure 1.6. The binding site of PY which overlaps with that of RMF supports its anti-ribosome dimerisation role in *E. coli*. The long C-terminal extension (red) of PY (yellow) is shown to overlap with the binding site of RMF (blue). Prevention of RMF binding to the 30S ribosome is suggested to explain the anti-dimerisation effect of PY. The image shown is based on high resolution crystal structures of PY and RMF in complex with the *Thermus thermophilus* ribosome. Figure adapted from Polikanov *et al.* 2012.

1.5.3.5 PY (*E. coli*) is an auxiliary factor in cold acclimation

The binding of PY at the 30S ribosomal subunit mRNA channel and PY's inhibition of GFP and polyU mRNA translation were established (sections 1.5.3.3 and 1.5.3.4. Here, I review the findings of Di Pietro *et al.* which challenge the previous hypothesis that PY is a central regulator during cold shock tolerance (Wilson *et al.* 2004).

During cold shock at 15^{o}C*, E. coli* cells are known to undergo transient growth arrest and an acclimation phase characterised by bulk protein synthesis repression and expression of cold shock genes. Cold shock mRNA regulatory elements render cold shock mRNAs suitable for translation in cold conditions (Di Pietro *et al.* 2013). Although it had been suggested that PY may play a central role in repressing bulk protein synthesis during cold shock– in particular repression of non-cold shock protein synthesis (Wilson *et al,* 2004),

Di Pietro's findings indicated that in cold acclimation, PY does not play a central regulatory role in growth, in maintaining viability or in repressing bulk protein synthesis. The following findings regarding PY illustrate its non-central role during cold shock:

1. PY was dispensable for growth at 37^{o}C and at 10^{o}C.
2. PY was dispensable for viability in cold shock after growth at 37^{o}C.
3. At 15^{o}C, translation assays indicated partial inhibition of translation achieved at the highest amounts of PY added (80 pmol) and that inhibition varied depending on the mRNA employed.
4. Translation of several cold shock mRNA was strongly inhibited. With *cspA* cold shock (cs) mRNA, strong inhibition of translation (80%) was seen when

PY was pre-incubated with 50S and 30S subunits, prior to the addition of initiation factors. At 15^{o}C, inhibition of translation of *cspA* mRNA (cs) was 55%. At 37^{o}C, inhibition of translation of *cspG* mRNA (cs) was 45% (Di Pietro *et al.* 2013).

PY acts as an auxiliary factor in cold acclimation:

1. PY played a partial role in reducing bulk protein synthesis, as was determined by investigating the effect of *yfiA* deletion on cell lysate protein content in cells undergoing cold shock; For *in vitro* translation at 15^{o}C versus at 37^{o}C, translation inhibition was higher at 40 – 50% versus at 20 – 30%, respectively.
2. PY appeared to increase translation resumption efficiency upon exiting the cold acclimation phase (Di Pietro *et al.* 2013).

Taken together, Di Pietro's findings suggest a non-central role for PY in protein synthesis regulation during cold acclimation and that PY-mediated inhibition of translation is mRNA-specific and temperature-specific.

1.5.3.6 PY stabilisation of 70S ribosome monomers is most effective when ribosomes are dissociated and when initiation factors are absent

Further to Polikanov's findings regarding PY's docking site at the 30S ribosomal subunit and Agafonov's findings regarding PY-mediated *in vitro* inhibition of translation, Di Pietro's findings indicated that (i) the translation inhibition mechanism of PY involves PY binding 30S ribosomal subunits to prevent initiation

complex formation and that (ii) PY binding to the ribosome is most effective when ribosomes are dissociated and when initiation factors are absent (Polikanov *et al.,* 2012, Agafonov *et al.,* 2001).

The findings of Di Pietro *et al.* indicated that:

1. PY bound rapidly and tightly to 30S subunits and slowly and weakly to 50S subunits as shown by fluorophore tagging and binding affinity studies of PY-ribosome interaction. This agrees with PY's known binding site as determined by Polikanov (Polikanov *et al.,* 2012).
2. PY accelerated the kinetics of idle 70S ribosome formation by approximately two-fold. This agrees with PY's known activity in promoting 70S ribosome monomer formation (Ueta *et al.* 2005).
3. PY did not destabilise fMet-tRNA once it was correctly positioned on the ribosome, suggesting that PY does not compete effectively with initiation factors for binding to the 30S subunit.
4. When pre-incubated with 30S subunits without initiation factors, PY was associated with a two-fold reduction in fMet-tRNA and initiation factor binding to the 30S subunit (Di Pietro *et al*. 2013).

Without pre-incubating PY with dissociated ribosomes in the absence of initiation factors, PY-mediated inhibition of initiation complex formation is scarce. This suggests that it is worthwhile to investigate PY's inhibitory activity in conditions where initiation factors are less abundant, such as in energy-limiting conditions when the nutrient supply is low. This may lead towards a better understanding of the conditions contributing to ribosome stabilisation and how PY is regulated accordingly.

Furthermore, studies that investigate the ribosome stabilisation activity of PY in conditions of nutrient starvation are lacking, and based on the mechanistic model presented, further investigations of the role of PY in translation inhibition during starvation stress tolerance is warranted.

1.6 Investigating mycobacterial ribosome stabilisation

1.6.1 The mycobacterial ribosome stabilisation hypothesis

The mycobacterial ribosome stabilisation hypothesis states that in mycobacteria, the association of 50S and 30S ribosomal subunits results in the formation of inactive 70S stabilised ribosomes (Trauner *et al*., 2010). 70S stabilised ribosomes were postulated to be the sole stabilised form of ribosomes since higher order ribosomal structures such as 100S dimers were found to be absent in *M. smegmatis* and *M. bovis*.

The mycobacterial ribosome stabilisation hypothesis stated above is a general hypothesis that is not limited to a specific condition. A more specific hypothesis was postulated to address mycobacterial ribosome stabilisation in NRP cells (see section 1.6.2). *M. smegmatis* ribosome subunit composition was investigated in hypoxic stasis by investigating changes in RNA biosynthesis levels, rRNA stability and ribosomal sucrose gradient profiling. The 70S ribosome was shown to be the predominant form in normoxic, hypoxic and carbon starved *M. smegmatis* stasis (Trauner, 2010). Also, the DosR regulon was shown to play a role in ribosome subunit association in hypoxic stasis. These findings are described in section 1.6.2.

1.6.2 The mycobacterial ribosome stabilisation NRP hypothesis

M. tuberculosis NRP cells are in a state of non-replicating persistence as described in section 1.3.1 and the mechanisms that allow NRP persistence and survival despite unfavourable conditions in granulomas are being investigated. The general hypothesis of macromolecular stability in NRP cells is that the stabilisation of essential cellular structures is needed for the transition from NRP to active replication (Leistikow *et al*., 2010).

More specifically, the mycobacterial ribosome stabilisation hypothesis states that ribosomes must be stabilised in NRP cells in order to be available during active replication, when conditions are favourable for return to active growth. In addition to the ribosome stabilisation hypothesis, it has been postulated that the ability to sense and respond to environmental stimuli is needed so that entry into and exit from the NRP state is regulated according to conditions present (Dworkin *et al*., 2010). Thus, putative ribosome stabilisation factors are postulated to mediate ribosome stabilisation and assist in regulating mycobacterial stress tolerance and persistence.

1.6.3 DosR is necessary and sufficient for *M. smegmatis* ribosome subunit association in hypoxic stasis

The DosR regulon plays a role in the initial hypoxic response in *M. tuberculosis* and is described in section 1.3.2.1. Trauner determined that the DosR regulon plays a role in promoting 70S ribosome monomer formation in *M. smegmatis* hypoxic stasis cultures. Although *dosR* deletion did not appear to affect the level of 70S ribosomes in normoxic stasis, 50S ribosomes were the predominant form isolated from Δ*dosR* mutant hypoxic stasis cultures (Trauner *et al*., 2010, Trauner *et al*., 2012). This suggested that DosR is necessary and sufficient for *M. smegmatis* ribosome subunit association in hypoxic stasis.

In *M. smegmatis*, the transition from active growth to hypoxic stasis is characterised by a decrease in rRNA biosynthesis levels, suggesting that ribosome assembly is reduced in stationary phase. In Δ*dosR* mutants, the decrease in rRNA levels during prolonged hypoxia was more rapid, suggesting that DosR plays a role in maintaining rRNA levels in hypoxic stasis (Trauner *et al*., 2010). The role of DosR in 70S ribosomal subunit association supported the mycobacterial ribosome stabilisation NRP hypothesis (see section 1.6.2).

During hypoxic stasis in *M. smegmatis*, a marked decrease in the proportion of 30S subunits compared to 50S subunits was observed. In Δ*dosR* mutants, this effect was more pronounced, suggesting that DosR plays a role in maintaining 30S subunit levels in hypoxic stasis. Given that *E. coli* RSFs bind at the 30S subunit (see section 1.5.3), the role of DosR is maintaining 30S subunit levels led to the question as to whether a putative RSF in *M. smegmatis* was regulated by DosR (see section 1.6.4).

1.6.4 RafS and RafH are putative mycobacterial ribosome stabilisation factors

Given that DosR was found to play a role in mycobacterial ribosome subunit association in hypoxic stasis (section 1.6.3) and ribosome 100S dimerisation in *E. coli* occurs in minimal media (section 1.5.2), proteomic analysis was conducted on ribosomes obtained from hypoxic and carbon-starved stasis *M. smegmatis* cultures to investigate whether putative ribosome stabilisation factors were bound to the ribosomes.

Two hypothetical proteins were found to bind to *M. smegmatis* ribosomes under hypoxic and carbon-starved stasis. MSMEG_3935 and MSMEG_1878, were bound to ribosomes in hypoxic stasis. MSMEG_1878 was also bound to ribosomes in carbon-starved stasis. In active normoxic growth, these proteins were not bound to ribosomes in significant amounts (Trauner, 2010).

MSMEG_3935 and MSMEG_1878 were found to be S30AE proteins containing the S30AE domain, a ribosome-binding domain, and are homologous to *M. tuberculosis* S30AE proteins Rv3241c and Rv0079, respectively (95% and 80% protein sequence identity with their respective *M. tuberculosis* homologues, NCBI blastp). The S30AE domain contains two alpha helices and a four-stranded beta sheet (Zhukov *et al.,* 2007). This domain is also present in PY (section 1.5.3). Further details of the bioinformatic characteristics of these proteins are described in section 4.1.

The mycobacterial S30AE proteins were named ribosome associated factors (Raf proteins). MSMEG_1878 and Rv3241c were named $RafS_{Msm}$ and $RafS_{Mtb}$ and MSMEG_3935 and Rv0079 were named $RafH_{Msm}$ and $RafH_{Mtb}$, respectively. The

role of $RafS_{Msm}$ and $RafS_{Mtb}$ in ribosome stabilisation was the main hypothesis investigated in this project and research aims are outlined in section 1.8.

1.6.5 *M. smegmatis* $RafH_{Msm}$ is a putative ribosome stabilisation factor that plays a role in maintaining rRNA stability and viability in hypoxic stasis and in maintaining viability in heat stress

$RafH_{Msm}$ was found to be a member of the DosR regulon, since its upstream region contained an element that is regulated by DosR. Furthermore, $RafH_{Msm}$ was absent from Δ*dosR* mutant ribosomes (Trauner, 2010). Phenotypic and complementation analysis of Δ$rafH_{Msm}$ and Δ*dosR* mutants indicated that $rafH_{Msm}$ contributes to Δ*dosR* mutant phenotypes (Trauner, 2010, Trauner *et al*., 2012).

1. Δ$rafH_{Msm}$ rRNA stability is compromised during prolonged hypoxic stasis, suggesting that $RafH_{Msm}$ plays a role in maintaining rRNA stability in hypoxic stasis.
2. Δ$rafH_{Msm}$ viability is impaired during prolonged hypoxic stasis, but to a lesser extent than for Δ*dosR*, suggesting that $RafH_{Msm}$ plays a role in maintaining viability in hypoxic stasis.
3. Δ$rafH_{Msm}$ viability is impaired in heat stress at 55^{o}C to a similar extent as for Δ*dosR*. Provision of $rafH_{Msm}$ in *trans* fully restored the Δ*dosR* phenotype

1.7 Investigating RafS, a putative ribosomal stabilisation factor in mycobacteria

1.7.1 Gene environment of RafS

Notably, the genome of *M. leprae* was found to contain *rafS,* but not *rafH,* suggesting that investigation of a role of RafS in non-tuberculous mycobacteria is also warranted. Miotto *et al* identified the presence of a small RNA at the negative strand of the 5' untranslated region ≤ 80 bp upstream of the Rv3241c gene by global RNA-seq analysis of exponentially growing cultures of *M. tuberculosis* H37Rv. The presence of a -10 consensus sigma factor a promoter sequence was also found to be associated with this sRNA.

Also, the sRNA was visualised by northern blot analysis of exponential and stationary phase cultures. Sig a is a primary sigma factor associated with regulation of gene expression during the exponential growth phase. Regulatory RNA species function via a range of mechanisms and the function of the sRNA upstream of Rv3241c is yet unknown (Miotto *et al*., 2012).

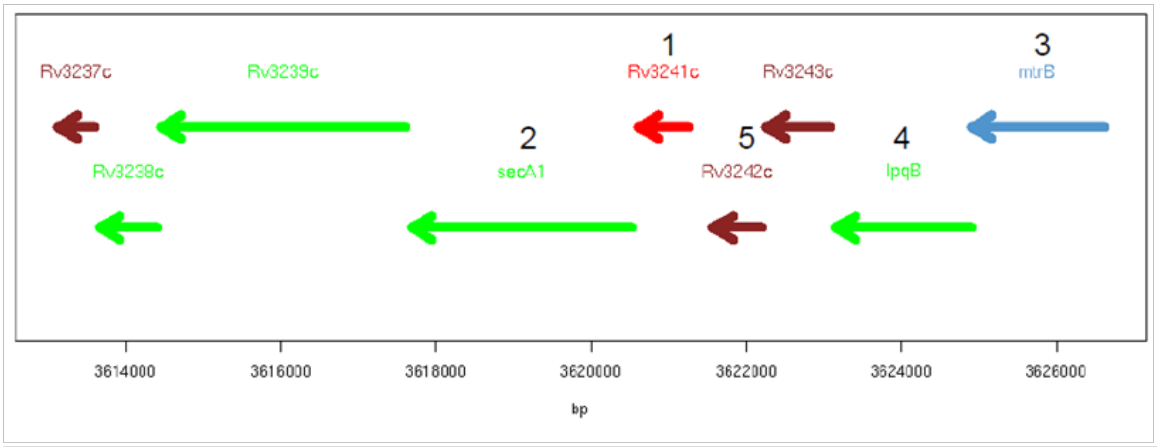

Number	Annotation
1	Rv3241c, S30AE protein
2	secA1, Probable preprotein translocase SecA1 1 subunit. SecA1 is involved in protein export. Interacts with the SECY/SECE subunits. SECA has a central role in coupling the hydrolysis of ATP to the transfer of PRE-secretory periplasmic and outer membrane proteins across the membrane.
3	Mtrb, Two component sensory transduction histidine kinase MtrB|
4	lpqB, probable conserved lipoprotein B, unknown function
5	Rv3242c, contains purine/pyrimidine phosphoribosyl transferases signature

Figure 1.7. Gene environment of *rafS*$_{Mtb}$ (Rv3241c) in the *M. tuberculosis* genome (Tuberculist). Available gene annotations are indicated. SecA is involved in protein export across the cytoplasmic membrane (Hou *et al.,* 2008).

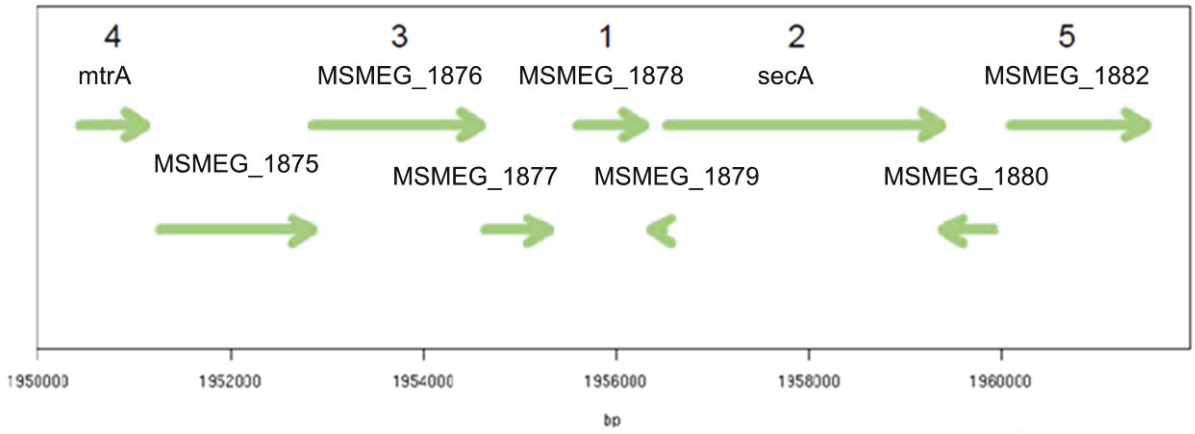

Number	Annotation
1	MSMEG_1878, S30AE protein
2	secA, subunit of pre-protein translocase secA, unknown function
3	MSEMG_1876, LpqB protein, unknown function
4	mtrA, DNA-binding response regulator MtrA
5	Acyltransferase

Figure 1.8. Gene environment of *rafS*$_{Msm}$ (MSMEG_1878) in the *M. smegmatis* genome (Smegmalist). Available gene annotations are indicated.

1.7.2 RafS$_{Mtb}$ expression is upregulated in nutrient-starved *M. tuberculosis* and in early lung infection of an *M. tuberculosis* –infected guinea pig model

RafS$_{Msm}$ was found to bind ribosomes in *M. smegmatis* hypoxic and carbon-starved stasis (see section 1.6.3). As previously mentioned in section 1.3.2.2, Betts *et al*. identified several *M. tuberculosis* H37Rv genes that were upregulated in nutrient-starved stasis. Of these genes, it was determined that *rafS*$_{Mtb}$ (Rv3214c) was significantly upregulated after 4 hours of stationary phase general nutrient starvation (PBS) ($p = 2 \times 10^{-6}$), and *rafS*$_{Mtb}$ expression was 3.18 fold higher than in active growth in rich media.

In the same model, *rafS*$_{Mtb}$ was also significantly upregulated after 24 hours of stationary phase general nutrient starvation (PBS) ($p = 3.3 \times 10^{-4}$) and *rafS*$_{Mtb}$ expression was 2.07 fold higher than in active growth in rich media. At 96 hours, no significant difference in *rafS*$_{Mtb}$ gene expression was observed. The data suggested the role of $RafS_{Mtb}$ in tolerance of early nutrient starvation in 2 to 24 hour standing cultures is worth further investigation.

In comparison, expression of *rafH*$_{Mtb}$ was significantly down-regulated (10.2 fold) in general nutrient starvation (Figure 1.8). Also down-regulated at 96 hours were several genes involved in energy metabolism, lipid biosynthesis, polyketide and non-ribosomal peptide synthesis and genes encoding ribosomal proteins. Among the characterised genes that were upregulated at 96 hours were transcriptional regulators of the GntR, ArsR, Lrp/AsnC families (Betts *et al*., 2002).

However, Beste *et al.* detected that transposon mutant *ΔrafH*$_{Mbo}$ was one of 29 mutants with reduced fitness in fast growth (doubling time = 23 days) in a carbon-limited chemostat (probability of false prediction <0.1), suggesting a role for *rafH*$_{Mtb}$ in carbon starvation in a continuous culture fast growth *M. bovis* BCG chemostat model (Beste *et al*. 2009).

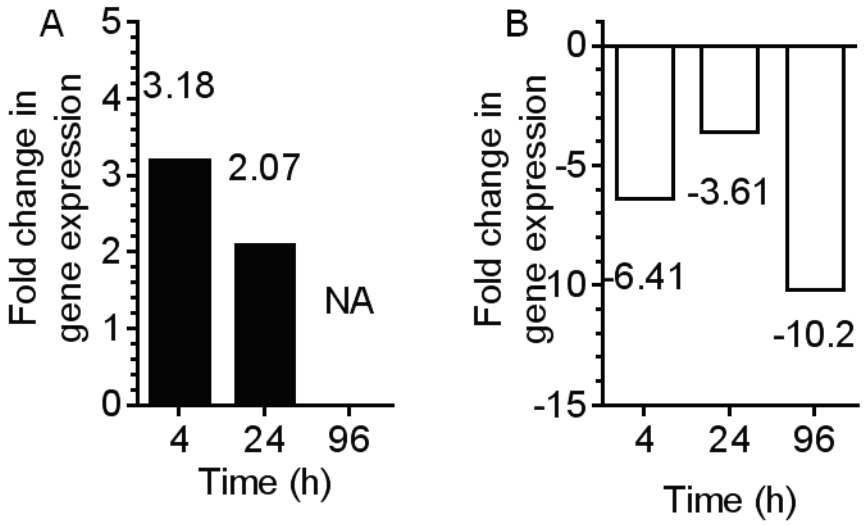

Figure 1.9 *M. tuberculosis* Raf protein expression is altered during general nutrient starvation in standing cultures. (A) $RafS_{Mtb}$ expression is significantly upregulated in early nutrient starvation (PBS). (B) $RafH_{Mtb}$ expression is significantly downregulated in 4 to 96 hour nutrient starvation (PBS). Image generated based on data from Betts *et al*., 2002. Fold change in gene expression was compared in *M. tuberculosis* stationary phase general nutrient starvation versus active growth in rich media (Betts *et al*., 2002).

Kruh *et al.* employed mass spectrometry to investigate the expressed proteome in early and chronic stages of *M. tuberculosis* disease in a guinea pig model. $RafS_{Mtb}$ was one of the 310 proteins detected in 30-day infected lungs and was absent from those identified from 90-day infected lungs and those identified in uninfected lungs (Kruh *et al*., 2010). This finding suggested that the activity of $RafS_{Mtb}$ is likely to be most relevant to early (30 day) *M. tuberculosis* infection. The findings presented in this section supported our investigation of Raf proteins, which is discussed in the next section.

1.8 Investigating RafS-mediated ribosomal stabilisation in mycobacteria: project rationale and aims

The role of RafS has not been investigated prior to the start of this project. This project investigates the role of putative RSFs, $RafS_{Msm}$ and $RafS_{Mtb}$ using physiological and biochemical approaches. Further details of the discovery of the Raf proteins and the findings regarding $RafH_{Msm}$ are described in section 1.6.3. The mycobacterial ribosome stabilisation hypothesis states that in mycobacteria, the association of 50S and 30S ribosomal subunits results in the formation of inactive 70S stabilised ribosomes. We investigated the hypothesis that RafS is an RSF which plays a role in stress tolerance in *M. smegmatis* and in *M. tuberculosis*.

Given the association of $RafS_{Mtb}$ expression with nutrient limitation and guinea pig lung infection described in section 1.7.2, physiological studies were employed to investigate the role of $RafS_{Msm}$ in growth and stasis during nutrient abundance and limitation. The role of $RafS_{Msm}$ in mature biofilm and pellicle formation, in competitive survival and in resuscitation from prolonged stasis were also investigated. Regarding biochemical investigations, I employed ribosomal profiling to investigate whether $RafS_{Msm}$ plays a role in stabilisation of a subset of ribosomes during active growth and early stationary phase. Also, the effect of purified $RafS_{Msm}$ and $RafH_{Mtb}$ on *in vitro* translation was investigated. The role of $RafS_{Mtb}$ in growth and competitive survival was investigated.

In summary, the project's aims were to investigate:

1. the effect of *rafS*$_{Msm}$ deletion on active growth, survival, resuscitation and competitive fitness in nutrient abundance and starvation,
2. the effect of *rafS*$_{Mtb}$ deletion on active growth and competitive fitness in prolonged stationary phase,
3. the effect of *rafS*$_{Msm}$ deletion on pH, heat and antibiotic stress tolerance,
4. the effect of *rafS*$_{Msm}$ deletion on mature biofilm and pellicle formation,
5. bioinformatic features of Raf proteins,
6. the effect of RafS and RafH on *in vitro* translation,
7. the effect of *rafS*$_{Msm}$ deletion on ribosome subunit association in active growth and stationary phase.

2. Materials and Methods

2.1 Media and Chemicals

M. smegmatis and *E. coli* strains were routinely cultured at 37°C in LB Tween 80 and LB media, respectively. Media was prepared and sterilised by autoclaving at 121^{o}C for 15 mins. 7H9 (BD) medium was used for culturing *M. tuberculosis* and for carrying out the MABA assay. 7H11 agar (BD or Sigma) was used for culturing *M. tuberculosis*. Antibiotics (Sigma) were prepared by dissolving in distilled water and filter-sterilising using a 0.2 µm pore syringe filter (Nalgene).

2.1.1 Media formulations

Luria Broth (LB)

Components per L:

5 g Yeast extract (Fisher Sci.), 5 g NaCl (Sigma), 10 g Tryptone (Fisher Sci.), 15g Agar (Sigma) (for LB agar only).

Trace compounds: 0.01 g EDTA, 0.1 g $MgCl_2 \cdot 6H_2O$, 1 mg $CaCl_2 \cdot 2H_2O$, 0.2 mg $NaMoO4 \cdot 2H_2O$, 0.4 mg $CoCl_2 \cdot 6H_2O$, 1 mg $MnCl_2 \cdot 2H_2O$, 2 mg $ZnSO_4 \cdot 7H_2O$, 5 mg $FeSO_4 \cdot 7H_2O$, 0.2 mg $CuSO_4 \cdot 5H_2O$

LB Kan 40	40 µg/ml kanamycin (Sigma)
LB Hyg 50	50 µg/ml hygromycin (Sigma)
LB Hyg 100	100 µg/ml hygromycin (Sigma)
LB Amp 100	100 µg/ml ampicillin (Sigma)
LB Chlor 20	20 µg/ml chloramphenicol (Sigma)
LB C 20, A 100	20 µg/ml chloramphenicol (Sigma) 100 µg/ml ampicillin (Sigma)

7H9 medium

4.7 g Middlebrook 7H9 broth powder (BD), 2 ml glycerol (Sigma), 0.05 % (v/v) Tween 80 (Sigma), make to 900 ml with dH_2O. 100 ml of sterile Middlebrook OADC supplement (BD) added after autoclaving and stored at 4 ^oC.

Components per L:

Ammonium sulphate 0.5 g, L-Glutamic Acid 0.5 g, sodium citrate 0.1 g, pyridoxine 1.0 mg, biotin 0.5 mg, disodium phosphate 2.5 g, monopotassium phosphate 1.0 g, ferric ammonium citrate 0.04 g, magnesium sulphate 0.05 g, Calcium Chloride 0.5 mg, zinc sulphate 1.0 mg, copper sulphate 1.0 mg

Middlebrook OADC enrichment approximate formula per liter sodium chloride 8.5 g, bovine albumin (Fraction V) 50.0 g dextrose 20.0 g, catalase 0.03 g

7H11 agar

21 g Middlebrook 7H11 broth powder (BD), 5 ml glycerol (Sigma), is made to 900 ml with dH_2O. 100 ml of sterile Middlebrook OADC supplement (BD) is added after autoclaving along with hygromycin antibiotic where needed (50 ug/ml)

Components per L:

Enzymatic Digest of Casein 1g, Disodium Phosphate 1.5 g,

Monopotassium Phosphate 1.5 g, Ammonium Sulfate 0.5 g,

Monosodium Glutamate 0.5 g, Sodium Citrate 0.4 g,

Ferric Ammonium Citrate 0.04 g, Magnesium Sulfate 0.05 g, Copper Sulfate 0.001 g, Pyridoxine 0.001 g ,Zinc Sulfate 0.001 g Biotin 0.0005 g, Malachite Green 0.00025 g, Agar 13.5 g, Middlebrook OADC Enrichment Approximate Formula Per Liter Sodium Chloride 8.5 g, Bovine Albumin (Fraction V) 50.0 g

Dextrose 20.0 g, Catalase 0.03 g

Hartmans-de Bont (HdB) minimal medium

Components per L
3.88 g K_2HPO_4, 2.13 g NaH_2PO_4. $2H_20$, 2.0 g $(NH_4)_2S0_4$,
8 ml 10 % glycerol (Sigma), 0.05 % (v/v) Tween 80 (Sigma), trace compounds (as below).
Trace compounds: 0.1 g $MgCl_2$. $6H_20$, 10 mg EDTA, 2 mg $ZnSO_4$. $7H_20$, 1 mg $CaCl_2$ $2H_20$, 5 mg $FeSO_4.7H_20$, 0.2 mg Na_2MoO_4. $2H_20$, 0.2 mg of $CuSO_4.5H_20$, 0.4 mg of $CoCl_2$. $6H_20$, 1 mg $MnCl_2.2H_20$.

M63 minimal medium

10X M63 salt solution was made with 2 g $(NH4)_2$ SO_4, 13.6 g KH_2PO_4 and 0.5 mg $FeS0_4.7H_20$ per L and autoclaved. A 20% glucose solution was made by dissolving 200 g glucose per L and autoclaving. 1 L M63 media was made by mixing 100 ml 10X M63 Salt solution and 100 ml 20% glucose to achieve a final percentage of 2%. Freshly made filter-sterilised casamino acids (BD) were added to achieve a final percentage of 0.5% (made from acid hydrolyzed casein with low sodium chloride and iron concentrations). Sterile supplements were added to achieve final concentrations of 1 mM $MgS0_4.7H_20$ and 0.7 mM $CaCl_2$.

2.1.2 Chemical Formulations

Chemical formulations are listed below unless stated elsewhere.

PBS: Phosphobuffer saline (Components per L)	8 g NaCl (Sigma), 0.2 g KCl (Sigma), 1.44g Na2HPO4 (Sigma) and 0.24 g KH2PO4 (Sigma), adjusted to pH 7.4 with conc. HCl and autoclaved. For PBS-20% glycerol, glycerol 200 ml glycerol were added
CTAB: cetyl trimethyl ammonium bromide (Components per L)	100 ml 1 M Tris HCl pH 8.0, 280 ml 5 M NaCl, 40 ml of 0.5 M EDTA, 20 g of CTAB (cetyltrimethyl ammonium bromide)

2.2 Bacterial strains, plasmids and primers

Bacterial strains, plasmids and primers are shown in Tables 2.1, 2.2 and 2.3, respectively. Plasmid constructs are shown in Table 2.4. Overnight cultures were grown by inoculating bacteria from an agar plate to 5 ml of LB supplemented with appropriate antibiotics in a 50 ml plastic centrifuge tube (BD) and then incubating overnight at 37^{o}C shaking at 200 rpm (*E. coli*) or 150 rpm (*M. smegmatis*). Strains were stored in 50% glycerol stocks at -80^{o}C.

Table 2.1: Bacterial strains employed in this study.

Strain	Description/ relevant genotype	Source
M. smegmatis mc^2155	Wild type *Mycobacterium smegmatis*	Laboratory strain
M. tuberculosis H37Rv	Wild type virulent *Mycobacterium tuberculosis* strain	Laboratory strain
E. coli HB101 Competent Cells	*F–, thi-1, hsdS20 (rB–, mB–), supE44, recA13, ara-14, leuB6, proA2, lacY1, galK2, rpsL20 (strr), xyl-5, mtl-1.* High Transformation efficiency 10^8cfu/µg; employed as an intermediate cloning strain	Pr*Omega*
E. coli GM2163 cells	*F– dam-13::Tn9 (Camr) dcm-6 hsdR2 (rk –mk+) leuB6 hisG4 thi-1 araC14 lacY1 galK2 galT22 xylA5 mtl-1 rpsL136 (Strr) fhuA31 tsx-78 glnV44 mcrA mcrB1* Dam and Dcm methylase deficient and deficient for plasmid recombination; employed as an intermediate cloning strain due to lack of methylation of CCWGG restriction sites	Laboratory Strain
E. coli Rosetta™	*F– ompT hsdSB(rB– mB–) gal dcm pRARE2 (CamR)* pRARE2 supplies tRNAs for the codons AUA, AGG, AGA, CUA, CCC, and GGA BL21 DE3 derivative increases codon usage of *E. coli;* employed as a recombinant protein expression strain	Novagen

Table 2.2. Plasmids employed in this study for mutant cloning.

Plasmid	Selection in media	Strains	Usage
PCR®-Blunt 4-TOPO® (Invitrogen)	LB Kan 40	*E. coli* HB101	Amplification of cloning inserts
pYUB854 (Kessel et al., 2008)	LB Hyg 100 (*E. coli*) LB Hyg 50 (Msm) 7H9 Hyg 50 (Mtb)	*E. coli* HB101, *M. smegmatis* mc^2155, *M. tuberculosis* H37Rv	Mycobacterial- *E. coli* shuttle plasmid used in the preparation of the linear allelic substrate
pJV53 (Kessel et al., 2008)	LB Kan 40 LBT Kan 40	Electrocompetent *M. smegmatis* mc^2155 and *M. tuberculosis* H37Rv	Acetamide-induced expression of Che9c gp60 and gp61 enzymes which enhance homologous recombination of dsDNA in mycobacteria
pET15b (Novagen)	LB Amp 100	Rosetta™ *E. coli* (Novagen)	Expression of His-tagged proteins for protein purification
pMV361	LB Kan 40 LBT Kan 40	*E. coli* HB101, *M. smegmatis* mc^2155	Mycobacterial- *E. coli* shuttle plasmid, Integrating vector for overexpression and mutant complementation in *M. smegmatis* mc^2155

Table 2.3 Primers used for PCR amplification and screening (obtained from Sigma and stored at -20^{o}C)

Number	Primer Name	5' to 3' Sequence
1	1878_UR_F	ggtacctcgctcttggccgctacgccg
2	1878_UR_R	tctagaatggcttgacatacttggcaactcgtttc
3	1878_ DR_F	gctagcctggcctgaccggccgac
4	1878_ DR_Rnew	actagtggggtcatgccggagaggatg
5	3241dnF	tctagaatccgtctggcgtgatcggcg
6	3241dnR	ggtaccgtagtccttgtcgcggctgaacag
7	3241upF	actagtgaccgcgacacttggtgtgtgcttg
8	3241upR	aagcttacctgaatccacggctagccttgacatacg
9	D1878_Screen_F	gcgtggcgtgaagcaactttcgg
10	D1878_Screen_R	acgatccgcgcgaactcctggt
11	D3241c_Screen_F	gaaagcgtgattacccaattgag
12	D3241c_Screen_R	cgtagagccggaagtagttc
13	Msm_1878_F_ NF	caattgtaatgtcaagccattcgatggattcaagc
14	Msm_1878_R_CR	aagctttcaggccaggcggatcag
15	Msm_1878_NR	aagcttttagtcgttgtagcgcgcctc
16	Msm_1878_CF	caattgtaatgggcgtcgccgagcac
17	NewMtb_3241c _F_NF	caattgtaatgtcaaggctagccgtg
18	NewMtb_3241c _R_CR	aagcttttatctggtgttgaagccgt
19	Mtb_3241c _NR	aagcttttatctggtgttgaagccgttctc
20	Mtb_3241c _CF	caattgtaatgccagccgaggcacac
21	Corrected3241c_forpET15b_F	catatgatgtcaaggctagccgtggatt
22	3241c_forpET15bR	ggatcctcacgccagacggatcaacc
23	Corrected 1878_forpET15b_F	catatgatgtcaagccattcgatggattcaa
24	1878_forpET15b_R	ggatcctcaggccaggcggatcagc
25	Rv0079_forpET15b_F	catatggtggaaccgaaacgcagtcg
26	Rv0079_forpET15b_R	ggatcctcatgccagaccgtcggcaa
27	3935_forpET15b_F	catatgatggacgtcgatgtgtcgacc
28	3935_forpET15b_R	ggatccctagccgtccgcaggggt
29	3241c_forpET15b_F	catatgtagtggattcaggtcaggttctg
30	3241c_forpET15bR	ggatcctcacgccagacggatcaacc

Table 2.4. List of plasmids constructed in this study

	Plasmid Name	Insert length (bp)
1	pYUB854:*rafS*$_{Msm}$ AES	3431
2	pYUB854: *rafS*$_{Mtb}$ AES	3890
3	pET15b: *rafH*$_{Mtb}$	822
4	pET15b: *rafH*$_{Msm}$	777
5	pET15b: *rafS*$_{Mtb}$	660
6	pET15b: *rafS*$_{Msm}$	693
7	pMV361: *rafS*$_{Msm}$	693
8	pMV361: *rafS*$_{Msm}$ N	498
9	pMV361: *rafS*$_{Msm}$ C	201
10	pMV361: *rafS*$_{Mtb}$	660
11	pMV361: *rafS*$_{Mtb}$ N	438
12	pMV361: *rafS*$_{Mtb}$ C	228

2.3 Molecular biology techniques

2.3.1 Preparation of pellets for mycobacterial colony PCR or gDNA extraction

In a class III laboratory, single *M. tuberculosis* colonies were isolated on 7H11 agar. 10 ml 7H9 stationary phase cultures (37^{o}C, 125 rpm) were harvested (10 mins, 2000 g) and boiled for 10 mins to heat kill. All manipulations were then carried out in the Class II laboratory. Single *M. smegmatis* colonies were isolated on LB agar. 50 ml LBT stationary phase cultures (37^{o}C, 150 rpm) were harvested by centrifugation (15 mins, 4000 rpm).

2.3.2 Extraction of genomic DNA from mycobacteria: CTAB method

Mycobacterial cell pellets prepared as described (section 2.3.1) and were resuspended in 5 ml distilled water and 500 µl lysozyme (10 mg/ml) and vortexed and incubated at 37 ^{o}C for 1 hour. 60 µl proteinase K (10 mg/ml) and 700 µl 10% SDS were added and the mixture was vortexed and incubated at 65^{o}C for 10 mins. 7 ml chloroform/iso-amylalcohol mix (24:1) were added and the mixture vortexed and centrifuged for 5 mins at 18 000 g. 5.5 ml of the top phase was recovered and an equal volume of isopropanol was added and incubated at -20 ^{o}C for 30 mins. The DNA was pelleted by centrifugation at 13 000 rpm for 20 mins and the pellet washed with 70% ethanol, air dried and resuspended in 500 µl distilled water.

2.3.3 Polymerase Chain Reaction (PCR) and agarose gel electrophoresis

PCR was performed using DNA Engine DYAD (MJ Research) with *Pfu* DNA polymerase (Pr*Omega*) or *Taq* DNA polymerase (Fermentas) with associated buffers and a 2mM dNTP mix from Fermentas. Primers used are shown in Table 2.3. The PCR program was carried out as shown (Table 2.5). To improve annealing, 2.5 µl DMSO were added per 25 µl reaction. Each 25 µl reaction also contained 5 µl diluted primers and 0.5 µl template DNA. Gradient PCR was carried out to determine the optimal annealing temperature where required.

Analysis of PCR products was carried out using gel electrophoresis. Agarose gels used were composed of 1% (w/v) agarose and SYBR® Safe DNA gel stain (Invitrogen) in a 1:10 000 dilution. Gel images were obtained using the Gel Doc feature of the Quantity One program (Bio-Rad). The 1 kb Fermentas bench top ladder was used routinely.

Table 2.5 PCR thermal cycling conditions used during gene cloning.

PCR Step	Temperature (^{o}C)	Duration	Number of cycles
1. Initial Incubation	95	2 mins	1
2. Denaturation	95	30 s	
3. Annealing	varies	30 s	30
4. Elongation	72	varies	
5. Final Extension	72	10 mins	1
6. Soak	4	Indefinite	1

2.3.4 Restriction enzyme digestion, ligation and transformation

Fast digest® restriction enzymes and associated green buffers (Fermentas) were used according to the manufacturer's instructions. Digested fragments were purified from agarose gels using the QIAGEN® Gel extraction kit according to the manufacturer's instructions. Ligations were carried out using the Fermentas DNA Ligation Kit according to the manufacturer's recommendations, using a 3:1 molar ratio of insert to vector.

1 µg of plasmid DNA, prepared using the Mini Prep kit (QIAGEN®), or ligation product was added to 100 µl of chemically competent cells and the mixture was incubated on ice for 20 min. The cells were heat shocked at 42˚C for 45 sec, returned to ice for a further 2 min and then allowed to recover in 1 ml LB at 37˚C, 150 rpm, for 1 hour. This suspension was pelleted and resuspended in 100 µl media and spread onto LB plates with an appropriate selection marker and incubated at 37˚C overnight.

2.3.5 Preparation and transformation of electrocompetent *M. smegmatis* cells

The method used for electroporation was based on that of Bibb *et al.* (Bibb et al., 2002). Electrocompetent cells were prepared by growing an Msm culture to mid-log phase (OD_{600} 0.5–0.7), harvesting and washing them three times in cold 50 ml 10% glycerol and resuspending them in the same buffer. The cells were stored in 400 µl aliquots at -80^{o}C. For transforming these cells by electroporation, 400 µl of electrocompetent Msm cells were mixed with 100 ng of DNA and transferred to a

chilled 0.2 cm electrocuvette (BioRad). The cells were electroporated using Gene Pulser (BioRad) set to 2.5 kV and 25 µF and the pulse controller set to 1000 Ω.

The cells were allowed to recover in 2 ml of LB medium for 6 hours and then pelleted and resuspended in 100 µl of LB which was plated onto LB antibiotic plates. Plates were incubated at 37˚C for 2 to 3 days. Individual colonies were streaked onto fresh antibiotic containing plates. For preparing recombineering electrocompetent cells, the above method was used to insert pJV53 into Msm. Msm:pJV53 was grown to mid-log phase with 0.2% acetamide and electrocompetent cells were prepared again as described. These cells were electroporated with the linear allelic exchange substrate (AES).

2.3.6 Preparation and transformation of electrocompetent *M. tuberculosis* cells

M. tuberculosis H37Rv:pJV53 was grown on 7H11 OADC agar, at 37 ^{o}C, and subcultured in 7H9, with 0.05% Tween 80, 20 µg/ml kanamycin and 0.2% succinate, to mid log phase (7 to 10 days at 37 ^{o}C, 125 rpm). 10 ml cultures were incubated in 125 ml flasks. The cultures were induced with 0.2% acetamide and incubated for 24 h at 37 ^{o}C. Electrocompetent cells were prepared by harvesting and washing thrice in 25 ml 10% glycerol and resuspending in the same buffer.

For transforming these cells by electroporation, 200 µl of electrocompetent *M. tuberculosis* cells were mixed with 100 ng of linear AES and transferred to a 0.2 cm electrocuvette (BioRad). The cells were electroporated at 2.5 kV, 25 µF and 1000 Ω. The cells were allowed to recover in 2 ml of 7H9 medium for 24 hours and then pelleted and resuspended in 100 µl of 7H9 which was plated onto LB kanamycin

plates. Plates were incubated at 37˚C for 21 days. Individual colonies were sub-cultured onto 7H11 OADC hygromycin 50 µg/ml agar (Bibb *et al.*, 2002).

2.3.7 Mycobacterial recombineering and complementation

Mycobacterial recombineering was carried out using the method of Kessel *et al.* (Kessel *et al.,* 2007). Upstream and downstream regions flanking the gene to be deleted were amplified by PCR with appropriate restriction sites. Gel electrophoresis was used to confirm successful PCR amplification of the UR and DR regions and products were cloned into PCR®-4Blunt-TOPO (Invitrogen) and amplified in dam/dcm methylase deficient *E. coli* or HB101 *E. coli*. Sequencing (Beckman Coulter genomics) was done to confirm that the inserts were of the correct sequence. UR and DR inserts were digested from PCR®-4Blunt-TOPO and obtained using gel electrophoresis.

Plasmid pYUB854 was digested with appropriate restriction enzymes and incubated with 1 µl thermosensitive alkaline phosphatase (TSAP) (Thermosci) to prevent religation. The DR insert was ligated to linear pYUB854 with T4 DNA ligase (Thermosci) and the resulting plasmids were isolated and digested with appropriate restriction enzymes. After confirming that the DR insert was present, the UR insert was then ligated to linear $rafS_{Msm}$. The resulting plasmids were digested to confirm that both UR and DR inserts were present. The pYUB854/rafS UR/DR plasmid was digested with appropriate restriction enzymes to obtain the linear AES.

The pJV53 plasmid encoding recombineering mycobacteriophage Che9c enzymes gp60 (exonuclease) and gp61 (recombinase) to enhance recombination of

a double stranded linear AES was inserted by electroporation into electrocompetent wild type *M. smegmatis* and gp60 and gp61 expression was induced with 0.2% acetamide, after which competent cells were prepared. The linear AES was electroporated into these cells and colonies were obtained from hygromycin (50 µg/ml) selective plates. A pure mutant colony was identified from electroporation plates and screened using colony PCR.

For complementation of *ΔrafS* mutants by insertion of pMV361/*rafS* (Kan^R), $\Delta rafS_{Msm}1$:pJV53 was subcultured four times on plain LB agar to allow cells that have lost pJV53 to predominate due to the selective advantage of not needing to produce proteins involved in kanamycin resistance. Similarly, *Δ*$rafS_{Mtb}2$:pJV53 and *Δ*$rafS_{Mtb}3$:pJV53 strains were subcultured seven times on plain 7H9 agar.

Single colonies were streaked onto agar both with and without kanamycin (40 µg/ml). Colonies absent from the Kan+ plate but present on the Kan- plate were considered to lack pJV53. Subsequently, electrocompetent cells were prepared and pMV361/*rafS* was electroporated into these cells. Colony PCR was used to confirm that endogenous *rafS* gene was absent from the complemented mutant.

2.4 Physiological assays

2.4.1 Preparation of *M. smegmatis* stationary phase starter cultures

M. smegmatis was streaked onto plain LB agar and incubated for 2 days at 37^{o}C. After ensuring there were no contaminants visible, a streak of cells was inoculated to a falcon tube with 5 ml media or 50 ml media in a 250 ml conical flask incubated at 37^{o}C at 150 rpm for 20 hours. Cultures were verified to be in stationary phase by measuring optical density at 600nm.

2.4.2 Optical density measurement

For bacterial cultures, OD_{600nm} was measured in a spectrophotometer (WPA) using the appropriate media as a blank. 1 ml samples were read in 1.5 ml plastic cuvettes (BRAND). The sample was diluted with the appropriate media if the reading measured greater than 1. Similarly, other measurements were taken for other samples at the optical density indicated.

2.4.3 *M. smegmatis* normoxic growth curve assays

Stationary phase starter cultures were prepared as described and inoculated into 50 ml media in 250 ml glass conical flasks with sponge bungs (standard normoxia with culture: air ratio of 1:5). These were incubated at 37^{o}C at 150 rpm on an orbital shaker. Samples were taken at intervals indicated and OD_{600nm} was measured as described.

2.4.4 *M. smegmatis* Colony Forming Unit (CFU) assays

M. smegmatis CFU assays were carried out by adding 10 µl per culture to 90 µl of LBT media in a sterile 96 well plate (BD falcon). In subsequent wells containing 90 µl of LBT media, 10 µl per well was transferred to the next column of wells with a multichannel pipette (Eppendorf) and mixed. In this manner, 7 serial dilutions were carried out. 10 µl of each dilution was spotted onto a petri dish with approximately 50 to 60 ml LB agar. The plates were incubated for 3 to 4 days at 37^{o}C and colonies were counted and recorded with the appropriate dilution factor. CFU cell count estimates (CFU/ml) were calculated using the equation below:

$$CFU\ estimate\ = Colony\ count \times 100\ \times 10^{dilution\ factor}$$

2.4.5 *M. smegmatis* survival and resuscitation assays

Stationary phase LBT starter cultures were prepared as described. For survival assays in normoxia, per strain, 0.1 ml of each stationary phase culture were inoculated into 5 ml sterile media in 50 ml falcon tubes (BD) capped with sterile sponge bungs and incubated at 37^{o}C at 150 rpm. Sterile water was added uniformly at intervals to account for loss of water due to evaporation. For survival assays in hypoxic stasis, intact plastic 125 ml conical flasks (Corning) were autoclaved with 100 ml media with orange caps.

These caps were then replaced with sterile rubber suba-seal bungs after adding 1 ml stationary phase culture inocula. CFU assays were carried out at the intervals specified. For survival assays in 0% glycerol HdB and PBS, 100 ml per

stationary phase culture were pelleted and resuspended in 100 ml of sterile distilled water and by centrifugation at 2000 g to remove nutrients.

The pellets were then resuspended in plastic 125 ml conical flasks (Corning) and sealed as described above. For CFU sampling, each seal was wiped with 70% ethanol and CFU assay samples were obtained by extraction with BD Microlance 3 25G x 5/8" 0.5 mm x 16 mm needles with 2 ml syringes (BD). For resuscitation assays, 1 ml of each culture were added to 50 ml LBT in glass conical flasks with sponge bungs and OD_{600nm} was monitored at intervals indicated. Growth curve sampling was carried out described as for the normoxic growth curve assays. After plotting CFU/ml (vertical axis) versus time (d) (horizontal axis), significance testing was carried out (section 2.6).

2.4.6 *M. smegmatis* and *M. tuberculosis* survival competition assay

Independent wild type and *ΔrafS* stationary phase starter cultures were set up as described. A 3 ml mixed inoculum was made by adjusting individual strain levels as calculated based on the final target of OD_{600nm} 0.5 per strain using the following equation and adding an appropriate volume of sterile distilled water to make up the final 3 ml volume:

$$Volume\ of\ culture\ required\ for\ inoculation\ = \frac{0.5}{Optical\ density\ of\ stationary\ phase\ culture} \times 3$$

200 µl of mixed inoculum were added per 5 ml media in 50 ml Falcon tubes (BD). CFU sampling was carried out after vortexing tubes at intervals indicated and *ΔrafS*$_{Msm}$ and mixed colony counts were recorded and CFUs calculated. Percentage

abundance of the *ΔrafS* mutant was calculated using the following equation and assay replicates with *ΔrafS* starting percentage abundance greater than or equal to 50% were carried forward for further CFU sampling:

$$\Delta rafS \text{ percentage abundance} = \frac{\Delta rafS \text{ colony count}}{\text{Total colony count}} \times 100$$

2.4.7 *M. smegmatis* Microtitre plate alamar blue assay (MABA) for investigation of chemical stress susceptibility assay

Minimum inhibitory concentrations (MICs) were determined for wild type *M. smegmatis* using the MABA assay (Collins *et al*., 1997, Lougheed *et al.,* 2011). Stationary phase LBT starter cultures were prepared as described. 100 µl per *M. smegmatis* stationary phase LBT starter culture were inoculated to 50 ml LBT and incubated (37 ^{o}C, 150 rpm) up to mid-log phase (OD_{600nm} approximately 0.5).

Cells were harvested and washed thrice with sterile PBS and then resuspended in sterile PBS + 20 % glycerol and stored in 100 µl aliquots in sterile 1 ml Eppendorf tubes at -80 ^{o}C. 100 µl of cells were plated on plain LB to and incubated (37 ^{o}C) to check for growth of contaminants. Chemicals (Sigma) were dissolved according to the manufacturer's recommendations, filter sterilised (0.2 µm pore size) and stored at -20 ^{o}C. Stock concentrations were determined based on published MIC data.

Outer perimeter wells of clear 96 well plates (BD Falcon) were filled with 200 µl sterile distilled water to protect experimental wells from dehydration. 180 µl media were added to the first column and 90 µl sterile media were added to the remaining

columns. 1 µl 200X chemical stock solution was added to the first column. Two-fold serial dilutions were performed by transferring 90 µl across the columns of the microplate with a multichannel pipette for each chemical in triplicate and using new sterile tips for each transfer. The 10th column contained media only and cell only controls in triplicate. Frozen cells were thawed and diluted (10 µl in 10 ml 7H9) and then 10 µl of this cell suspension were added to each well excluding media only wells. Plates were incubated at 37 ^{o}C for 66 hours.

20 µl alamar blue (Pr*Omega*) were added to each well and the plates were incubated for a further 6 hours, giving a total of 72 hours, after which MICs were visually determined. Wells with blue fluid were taken to contain cells which were not viable. Wells with pink fluid were taken to contain cells which were viable. Wells which contained purple fluid were also considered to contain viable cells (although less than in pink wells).

The lowest chemical concentration which inhibited viability (giving a blue colour) was taken to be the MIC. Fold differences in mean MICs were calculated as shown (equation 1). 95% confidence intervals were calculated using Microsoft Excel. Fold differences less than or equal to 2 fold were considered to be insignificant (van de Kasteele *et al.*, 2012). A decreased MIC indicates greater antibiotic susceptibility.

Equation 1: $Fold\ difference\ in\ MIC = \frac{\text{Mean MIC of wild type}}{\text{Mean MIC of } \Delta\text{rafSMsm}}$

2.4.8 *M. smegmatis* mature biofilm formation assay

Stationary phase LBT starter cultures were prepared as described. 1 ml M63 media were added per well of a 24 well non-tissue culture treated plate (BD). Stationary phase cultures were centrifuged for 2 mins at 5 g to remove clumps and

10 µl of each culture supernatant were inoculated per well. The plates were incubated in normoxia for 4 days at 30^0C or 5 days at 28.5^0C. Biofilm formation at the interface of the solid surface and liquid medium was checked (biofilm formation in a ring shape on walls of the well). Culture was removed from wells by briskly shaking to remove. Plates were submerged in a tray of water and then vigorously shaken to remove liquid over a waste tray.

1 ml 0.5% crystal violet (SIGMA) were added per well and stained for 10 min and then removed. The plate was washed twice in a fresh distilled water tray, shaking out as much liquid as possible after each wash and vigorously tapped onto paper towels to remove excess liquid. The plates were allowed to dry in a fume cabinet for 20 mins and 1 ml 95% ethanol were added per and incubated covered for 1 hour. 1 ml of the suspension was transferred to cuvettes and optical density ($OD_{570\ nm}$) was measured.

2.4.9 *M. smegmatis* pellicle assay

Pellicle assays were adapted based on a method by B. Khoo (American Society for Microbiology Microbe online library; http://www.microbelibrary.org/; web page is no longer available). Stationary phase LBT starter cultures were prepared as described. 5 ml 7H9 OADC without Tween were aseptically added to sterile glass test tubes with steel caps. Stationary phase cultures were centrifuged for 2 mins at 200 rpm to remove clumps and 10 µl of each culture supernatant were inoculated per tube and incubated at 37^oC for 48 hours. Photographs of the pellicle formed at the air-liquid interface were obtained.

2.4.10 *M. smegmatis* acid pH stress assay

Sterile LBT media at pH 3, 5 and 7 were prepared. Actual pHs were measured with a pH meter and recorded. 2 ml of each medium were added to a sterile 24 well plate (BD). Stationary phase LBT starter cultures were prepared as described. 18 ml of each stationary phase culture was centrifuged at 2 000 g and each pellet was resuspended in 90 µl media. 10 µl of the suspension were added to each well and mixed. The plates were incubated at 37^{o}C and CFU assays were carried out at 0, 3 and 6 hours. Significance testing was carried out (section 2.6).

2.4.11 *M. smegmatis* heat stress survival assay

Stationary phase LBT starter cultures were prepared as described and transferred to an incubator at 55^{o}C at 150 rpm, ensuring even distance from the fan. CFU assays were carried out at intervals indicated. Significance testing was carried out (section 2.6).

2.4.12 Preparation of *M. tuberculosis* stationary phase starter cultures

M. tuberculosis was streaked onto plain 7H11 agar with a 10 µl sterile plastic loop and incubated for 7 days at 37^{o}C. After ensuring there were no contaminants visible, a streak of cells was inoculated to a new plastic 125 ml conical flask with plastic caps (Corning) with 50 ml 7H9 media and incubated at 37^{o}C at 125 rpm for 10 days. Cultures were verified to be in stationary phase by measuring optical density at 600nm.

2.4.13 *M. tuberculosis* growth curve assay

M. tuberculosis stationary phase starter cultures were prepared as described. 1 ml per starter culture was subcultured into 50 ml of 7H9 media in new sterile 125 ml plastic conical flasks (Corning) and incubated at 37^{o}C at 125 rpm. OD_{600nm} measurement in a spectrophotometer was carried out at intervals indicated.

2.4.14 *M. tuberculosis* CFU assays

CFU assays were carried out by sampling 10 µl of culture and adding to 90 µl of 7H9 media in a 96 well plate. In subsequent wells containing 90 µl of media, 10 µl of each sample were transferred with a multichannel pipette to the next column of wells and mixed. In this manner, 7 serial dilutions were carried out. 10 µl of each dilution was spotted onto a petri dish with approximately 50 to 60 ml 7H11 agar. The plates were sealed with parafilm and incubated for 14 days at 37^{o}C and then colonies were counted and recorded with the corresponding dilution factor. CFU estimates (CFU/ml) were calculated using the equation below:

$$CFU\ estimate\ = Colony\ count \times 100\ \times 10^{dilution\ factor}$$

2.5 Biochemical methods

2.5.1 Recombinant protein induction and analysis

Strains were grown on LB AC plates overnight and used to inoculate 50 ml starter cultures, and grown at 150 rpm at 37^{o}C. Per strain, 1 ml overnight culture was used to inoculate 50 ml LB AC media and strains were grown until OD_{600nm} 0.5 to 0.8 at 150 rpm at 37^{o}C. The cultures were kept at 4^{o}C for 30 mins and then were adjusted to the final concentration of IPTG needed. The cultures were allowed to grow for another 3 h (or other time indicated) at 150 rpm at 37^{o}C and 1 ml culture was pelleted at 18 000 g and stored at -20^{o}C.

For recombinant protein expression analysis of small pellets, each pellet was resuspended in 1x primary amine free Bugbuster (Novagen) with 200 µl benzonase (Novagen) and 0.833 µl 1X rLysozyme (Merck). The mixture was incubated at room temperature for 20 mins, shaking at 20 rpm and then pelleted at 18 000 g for 20 mins at 4^{o}C. The supernatant (soluble fraction) was transferred to a fresh tube and insoluble fraction was labeled and both stored at -20^{o}C.

To confirm protein expression, insoluble pellets were resuspended in 50 µl distilled water. 10 µl Laemmli buffer loading dye (SIGMA) were added per 10 µl soluble and insoluble fractions, and incubated at 95^{o}C for 10 minutes to allow protein denaturation. SDS-PAGE gels were prepared and run as described in the next section with 4 µl of each insoluble fraction and 16 µl of each soluble fraction loaded per well.

2.5.2 SDS-PAGE

The composition of protein gels is given in Table 2.6. Protein samples were thawed at room temperature and insoluble fractions were resuspended in 50 µl deionised water. 10 µl of each sample was mixed with 10 µl 2X Laemmli buffer (Sigma) by vortexing and heated at 98^{o}C for 10 mins on the heat block. Samples were cooled and loaded to protein gels. 4 µl of each insoluble sample and 20 µl of each soluble fraction were loaded.

The ladder used was EZ RUN Rec Protein Ladder (10 to 200 kDa) (Fischer Scientific) or PageRuler Plus prestained protein ladder (10 to 250 kDa) (Thermosci). The gel was run at 135 V for 45 minutes and staining was carried out with Imperial™ Protein stain (Thermo Scientific) as recommended. Staining and destaining were carried out for 1 hour each at 20 rpm or destaining was carried out overnight.

Table 2.6. Composition of protein gels for SDS-PAGE. TEMED indicates Tetramethylethylenediamine. Acrylamide and APS were obtained from SIGMA.

12% Separating Gel Reagents	Amount per gel	4.5% Stacking Gel Reagents	Amount per gel
40% acrylamide	2.4 ml	40% acrylamide	0.3 ml
GLB (Gel Lower Buffer)	2 ml	GUB (Gel Upper Buffer)	0.66 ml
dH20	3.6 ml	Distilled H_20	1.68 ml
TEMED	8 µl	TEMED	10 µl
APS 10%	40 µl	APS 10%	20 µl
Final Volume	8 ml	Final Volume	2.64 ml

Gel Lower Buffer components per 500 ml
90.85g Tris, 20ml 10% SDS, adjusted to pH 8.8 with 10ml conc HCL

Gel Upper Buffer components per 500 ml
30.3g Tris, 20ml 10% SDS, adjusted to pH to 6.8 with approx. 20ml conc HCL

2.5.3 Scaled up recombinant protein induction and lysis for FPLC

Overnight cultures were set up in 250 ml glass flasks and in 50 ml LB AC and incubated as described in section 2.5.1. 25 ml of each starter culture was inoculated to 1 L LB AC and incubated as before, carrying out IPTG induction as required. The cultures were pelleted (8000 g, 10 mins, JA26 XP centrifuge (Beckman), JA14 rotor). Pellets were resuspended in 10 ml binding FPLC buffer B and sonicated for 2x 10 mins (40% power, 2 sec pulse) with a 5 minute interval between. Fractions were separated (16000 g, 45 min, 4°C, Avanti J 26 XP, J25.5 rotor). The supernatant was

transferred to a fresh tube and 40 µl elution buffer were added per ml sample and filtered with a 0.2 µM pore syringe filter (PALL).

2.5.4 FPLC protein purification

FPLC buffers were prepared using the His buffer kit (GE) as per the manufacturer's instructions. Binding buffer (A) (20 mM imidazole, 20 mM sodium phosphate, 500 mM NaCl, pH 7.4) and elution buffer (B) (500 mM imidazole, 20 mM sodium phosphate, 500 mM NaCl, pH 7.4) were prepared in deionised water and filtered using a vacuum pump and Millipore filter papers. With the AKTA-FPLC system (GE), a pump wash was carried out with buffers A and B for 5 mins.

A 1 ml His-trap column (GE) was attached to the platform, and buffer A was allowed through (5 mins, flow rate 0.5 or 1ml/min; maximum pressure alarm 0.6 MPa). The superloop sample end (GE) was manually washed with 5 ml buffer A and filled with filtered (PALL 0.2 µM pore syringe filter) protein sample, which was then injected to the column. The column was washed with buffer A until UV level dropped to 0 and then with a buffer A/B mix as required. Fractions were collected (serpentine, 12 mm tubes, 1 ml) and analysed by SDS-PAGE. Pure protein fractions were pooled and stored at 4^{o}C and concentrated the following day or immediately using Amicon (Millipore) or centrisart concentrators (Sartorius) as per the manufacturer's instructions with appropriate buffers (Tables 2.7, 2.8).

Table 2.7: Glycerol storage buffer compositions for Raf protein storage. Final concentrations of items are indicated.

Buffer component	$RafS_{Msm}$ storage buffer	$RafH_{Mtb}$ storage buffer
Tris-HCl	10 mM	20 mM
NaCl	50 mM	200 mM
Glycerol	10%	10%
DTT	-	2 mM
Final pH	7.4	8

Table 2.8: TAKM7 buffer compositions for Raf protein storage for translation assays. Final concentrations of items are indicated.

Buffer component	$RafS_{Msm}$ TAKM7 buffer	$RafH_{Mtb}$ TAKM7 buffer
Tris-HCl pH 7.6	20 mM	20 mM
NH_4Cl	70 mM	70 mM
Glycerol	10%	10%
KCl	30 mM	30 mM
$MgCl_2$	7 mM	7 mM
Final pH	7.4	8

2.5.5 Ribosomal Profiling

Buffers compositions are; ribosomal buffer (10 mM Tris-HCl (pH 7.4), 70 mM KCl, 1 or 10 mM $MgCl_2$), 15% sucrose (15% sucrose w/v, 50 mM Tris-HCl [pH 7.4], 25 mM KCl, 10 mM $MgCl_2$), 40% sucrose (40% sucrose w/v, 50 mM Tris-HCl [pH 7.4], 25 mM KCl, 10 mM $MgCl_2$), sucrose cushion (1.1 M sucrose w/v, 50 mM Tris-HCl [pH 7.4], 25 mM KCl, 10 mM $MgCl_2$). Buffers containing sucrose were autoclaved and pipetted aseptically.

Cultures were grown in LBT media in 2 L flasks at 37^{o}C at 150 rpm. For mid log profiling, stationary phase cultures were inoculated to 1L media and grown to an OD_{600nm} of 0.5 to 0.8. 2 L of culture were pelleted per strain. For stationary phase profiling, stationary phase cultures were inoculated to 2 x 400 ml media and a total of 800 ml culture was pelleted per strain (10 min per 250 ml culture, JA14 rotor, Avanti J-26XP centrifuge, 8000 g) and frozen at -20˚C.

The previous method (Trauner *et al.*, 2010) was modified to incorporate new equipment and improve accuracy of profiles. 13.2 ml thinwall polyallomer Beckman centrifuge tubes (Ref no. 331372) were used for centrifugation. For preparing sucrose gradients, a horizontal line was drawn 1.5 cm from the base of each gradient to indicate the end of fractionation. 5.5 ml sterile 40% sucrose were added to the tubes, covered and placed vertically in a -80^{o}C freezer. When frozen, 5.5 ml sterile 15% sucrose were added and the tubes were returned to the freezer. When needed, the frozen sucrose layers were thawed and equilibrated overnight at 4^{o}C on a flat surface.

For cell lysis, the French press was replaced with a cell disruptor. Cell pellets were thawed and resuspended in 10 ml ribosomal buffer and a manual cell homogeniser was used to disrupt clumps. Cell suspensions were lysed with a cell disruptor (30 kpsi twice per sample, 4^{o}C, Constant Systems). 50 ml distilled water and 50 ml ribosomal buffer were added to the cell disruptor prior to lysis. Between different strains, the cell disruptor was cleaned by adding 50 ml distilled water, 50 ml 70% ethanol, 50 ml distilled water and 50 ml ribosomal buffer in this order. At the end of lysis, 50 ml distilled water, 50 ml 70% ethanol and 50 ml distilled water were added for cleaning.

Cell lysates were centrifuged (Optima L100 XP, Sw41Ti rotor, 30,000 g, 30 min, 4°C) using ribosomal buffer for balancing. Clarified cell extracts were loaded onto 4 ml sucrose cushions and centrifuged (Optima L100 XP, Sw41Ti rotor, 31,000 g, 2 hours 30 min, 4°C) for ribosome pelleting. The supernatant was removed by decanting. The top half of the tube was removed with a pair of scissors to facilitate resuspension of the pellet. The ribosomal pellet was resuspended in cold 200 µl ribosomal buffer and incubated on ice for 20 mins before storing in eppendorf tubes at -80^{o}C.

Thawed ribosome pellets were loaded onto gradients, ensuring that the final levels were even, and centrifuged (Optima XP L100, 5 h, 35,000 rpm, 4 °C,SW 41-Ti rotor). 200 µl from the gradient meniscus was pipetted into the final well to obtain the reading for the last fraction. A 40 × 1.1 mm needle (BD) was used to pierce the tube base and fractions were collected in a 96-well plate (approximately 3 drops per well) upto the line drawn. 2 µl per fraction was read on the NanoDrop machine (Thermosci, nucleic acids module, absorbance wavelength 254 nm, 40% sucrose as blank).

Normalised fraction ratios were calculated per fraction number as shown (Equation 1A and 1B) (the last fraction was attributed fraction ratio 1 and the penultimate fraction was attributed fraction ratio 0.8). Normalised absorbance ratios were calculated per fraction as shown (Equation 2) (attributing the highest absorbance value as absorbance ratio 1). Ribosomal profiles were plotted with fraction ratio on the horizontal axis and absorbance ratio (254 nm) on the vertical axis. Ribosomal sub-species appear as a series of three peaks corresponding to the 70S, 50S and 30S species.

Equation 1A: $Fraction\ Ratio\ Divisor = \frac{Penultimate\ Fraction\ number}{0.8}$

Equation 1B: $Fraction\ ratio = \frac{Fraction\ number}{Fraction\ Ratio\ Divisor}$

Equation 2: $Absorbance\ ratio = \frac{Absorbance}{Highest\ absorbance\ value}$

2.5.6 Preparation of *M. smegmatis* S100 extract and ribosomes for translation assays

Buffers were prepared according to the following compositions: Homogenisation buffer (HB): pH 7.6, stored at 4°C 50 mM Tris, 100 mM NH_4Cl, 7 mM $MgCl_2$, 0.5 mM EDTA, 0.001%Tween 20, 5 mM β-Mercaptoethanol (added on the day of experiment). Sucrose cushion (SC): pH 7.6, stored at 4°C, 50 mM Tris, 350 mM NH_4Cl, 7 mM $MgCl_2$, 0.5 mM EDTA, 1.1 M sucrose, 0.001% 10% Tween 20, 3 mM β-Mercaptoethanol (added on the day of experiment).

Bacterial pellets were resuspended in 1.5 ml HB per gram wet pellet and vortexed. Pellets were lysed twice in a French press at 1020 psi using a 35 ml French Pressure Cell. 2 µl/g wet cell pellet RQ DNase was added after the first passage. The lysates were pooled after the second passage and stirred using a magnetic stirrer (max. 240 rpm). 1.5 g cold alumina per gram wet cell pellet were added to the lysate and stirred for 30 min.

The suspension was transferred to a Sorvall GSA tube (SLA1500, 250 ml) and spun at 3600 rpm (2000g) for 10 min to pellet the alumina. The speed was increased to 8000 rpm (10000g) and spun for 30 more min to pellet cell debris. The supernatant was filtered through an autoclaved tea filter and transferred into Sorvall SS34 tubes and spun at 16000 rpm (30000g) for 30 min. The supernatant (S30 extract) was transferred into a 200 ml measuring cylinder on ice avoiding the pellet and white layer at the surface.

13 ml of S30 extract was layered slowly onto Beckman Ti 50.2 tubes with 9 ml sucrose cushion and spun at 33000 rpm (~100000g) for 16 hrs overnight. This resulted in the S100 extract (supernatant) and ribosomal pellet. Three quarter of S100 extract (supernatant) was transferred into a measuring cylinder, also taking the upper yellow part of the sucrose cushion. S100 was dialysed with dialysis tubing (MWCO 6000-8000) in TAKM7 buffer.

S100 extract was added to 20 ml Vivaspin™ concentrators (MWCO 6000-8000) equilibrated with TAKM7 and spun at 4600 g in a Heraeus centrifuge at 4°C (ca. 3300 rpm). The flow through was discarded regularly (after 30 min) and filled up with S100. S100 was concentrated to approx. 16 ml and 0.125 ml glycerol were added per ml S100 and mix gently with a pipette. Supernatant was transferred to a fresh tube and 500 µl aliquots were pipetted and frozen in liquid nitrogen and store at -80°C.

The remaining supernatant covering the ribosome pellet was discarded and the tubes were inverted. The ribosome pellet was washed twice with TAKM7, and pellets resuspended in approx. 2 ml TAKM7. 50 µl aliquots of the ribosome solution were frozen with liquid nitrogen and stored at -80 °C and these were known as non-dissociated ribosomes. Dissociated ribosomes were prepared by resuspending in 50mM Tris (pH7.6), 500 mM KCl, 0.05 mM $MgCl_2$ and 5 mM β-mercaptoethanol. Ribosome concentrations were determined by absorption measurements on the basis of 23 pmol ribosomes per A_{260} unit (Akbergenov *et al.*, 2011).

2.5.7 Preparation of mRNA for translation assays

Plasmids pZ296 (pT7-hRluc) and pZ547(pT7-*Omega* hFluc) were employed to prepare R-luc and *Omega* F-luc mRNA, respectively. Plasmid DNA was prepared by Midiprep (Qiagen) according to the manufacturer's instructions. The plasmid was resuspended in 450 µl water. 450 µl of plasmid was mixed with 45 µl NaAc [3M] and 1350 µl 100% ethanol, vortexed and then stored at -80 °C for > 40 mins. The mixture was centrifuged at, 4 °C, 18 000 rpm for 15 min and the supernatant was discarded. The pellet was washed with 500 µl 80% ethanol (pre-cooled to -20°C) and centrifuged for 10 mins, 4 °C, 18 000 g and the supernatant was discarded. The pellet was dried in a speed vacuum device for 10 minutes without heating, dissolved in 100 µl dH_20 and the DNA concentration was measured.

The plasmid was linearized with HindIII (digested overnight in HindIII 10X buffer) and plasmid linearisation was confirmed by agarose gel electrophoresis. 400 µl of Phenol: Chloroform: Isoamylalcohol mixture [25:24:1] was added to the restriction digest to purify the DNA. The mixture was vortexed 3 x 20 sec until the organic and inorganic phases homogenised. The mixture was centrifuged at 4 °C, 18 000 rpm for 15 min and the supernatant was transferred to a new tube. 400 µl chloroform were added and the mixture was vortexed 3 x 20 sec. The mixture was centrifuged at, 4 °C, 18 000 g for 15 min and the supernatant was transferred to a new tube.

DNA was precipitated by adding 40 µl sodium acetate [3M] (24.6 g in 100mL H_2O; adjusted to pH 5.2 with acetic acid) and 1200 µl 100% ethanol to the DNA and mixed by vortexing and then stored at -80 °C for 40 mins. The mixture was centrifuged at 4 °C, 18 000 g for 15 min and the supernatant was discarded. The

pellet was washed with 500 µl 80% ethanol (pre-cooled to -20 °C). The mixture was centrifuged at 4 °C, 18 000 g for 15 min and the supernatant was discarded. The pellet was dried in a speed vacuum device for 5 minutes without heating and dissolved in 200 µl distilled H_20.

For *in vitro* transcription, the reaction mixture was prepared as shown in table 2.9 in 1 x 2 ml tubes and incubated for 4 hours in a thermomixer (500 rpm). The reaction should appear turbid and it is then frozen overnight at -20^oC.

Table 2.9 *In vitro* transcription reaction mixture for mRNA preparation for translation assays

Component	Volume [µl]
Hepes [1M, pH 7.5]	160
$MgCl_2$ [1M]	50
DTT [1M] in dH_20	80
ATP [100mM]	80
CTP [100mM]	80
GTP [100mM]	80
UTP [100mM]	80
RNase Inhibitor	20
DNA	200
Spermidine [1M] in dH_20	4
dH_2O	1126
T7 RNA Polymerase	40 (+40 after 2 hours)
Total	2000

For RNA precipitation, the transcription reaction was thawed and centrifuged for 5 mins at 4 °C, 18 000 g. The supernatant was aspirated (approximately 2000 µl) into two 2 mL tubes and mixed in new tube with 450 µl LiCl [10M] per 1000 µl reaction. The pellet was resuspended in 1 ml dH_2O and mixed with a thermomixer, for 4 mins at 40 °C at 106 g. This mixture was centrifuged for 5 mins at 4 °C, at 18 000 g. 1 ml of supernatant was aspirated, mixed in a new tube with 450 µl LiCl [10M] and stored on ice. The steps in the last three sentences were repeated 5 to 7 times.

The RNA precipitation reaction was incubated on ice for at least 30 min. The mixture was centrifuged for 5 mins at 4 °C, at 18 000 g and the supernatant was discarded. Pellets were washed with ice-cold ethanol [80%]. The mixture was centrifuged for 5 mins at 4 °C, at 13000 rpm and the ethanol supernatant was discarded. Pellets were dried in a speed vacuum device for 1-2 min at 30°C. Pellets were pooled in a total of 400 µl dH_2O and stored at 4°C overnight to allow pellets to dissolve.

To each 400 µl RNA solution, 40 µl NaAc [3M] and 1200 µl 100% EtOH were added, shaken and stored at -80 °C for > 40 mins. The mixture was centrifuged for 5 mins at 4 °C, at 18 000 g and the supernatant was discarded. The pellet was washed with 500 µl 80% ethanol (pre-cooled to -20 °C). The mixture was centrifuged for 5 mins at 4 °C, at 18 000 g and the supernatant was discarded. The pellet was dried in a speed vacuum device without heat, dissolved in 150 µl dH_2O and the RNA concentration was measured. mRNA was adjusted to a final concentration of 2 µg/µl.; an aliquot of mRNA was diluted by mixing 1.5 µl mRNA with 148.5 µl 10 mM Tris HCl, pH 8.0 and measuring A_{260} and then diluting with water.

2.5.8 Preparation of translation pre-mix

The pre-mix used in translation assays was prepared with the components shown in Table 2.10.

Table 2.10 Components of the translation assay pre-mix (30 µl).

Component	Volume [µl]	Stock	Final Concentration
S30 Premix (Pr*Omega*)	12	NA	40% (vol/vol)
M. smegmatis S100 extract	6	NA	20%(vol/vol)
tRNAs (Sigma)	1.2	10 µg/µl	0.4 µg/µl
Amino acids (Sigma)	1.2	5 mM	200 µM
RNasin (Thermoscientific)	0.6	40 U/µl	0.8 U/µl
Protease Inhibitor (Roche)	0.6	50x	1x
mRNA	2	2 µg/µl	13.3 ng/µl
dH_2O	2.4	NA	NA
Total Premix Volume	26	NA	NA

2.5.9 Luciferase mRNA translation assay

M. smegmatis ribosomes and *M. smegmatis* S100 extract were prepared as described in section 2.5.6. *Omega* F-luc mRNA or *Renilla* R-luc mRNA was prepared as described in section 2.5.7. 7.5 pmol *M. smegmatis* ribosomes were incubated with 30 µl of a translation mixture pre-mix (Table 2.10, section 2.5.8) and Raf proteins stored in TAKM7 buffer (section 2.5.4) at 37^{o}C for the time indicated and stopped on ice. Pr*Omega* reagents were obtained from the Dual Luciferase Assay Kit (Pr*Omega*).

Where pre-incubation of Raf proteins without mRNA is indicated, mRNA was added after incubating ribosomes with all other components as specified. Paromomycine, served as a positive control in the concentrations indicated and Raf proteins were omitted in these controls. Non-dissociated or dissociated wild type ribosomes were used as specified. The dual luciferase assay was performed as specified by the manufacturer (Pr*Omega*). Bioluminescence was measured in a luminometer (FLx800; Bio-Tek Instruments).

2.5.10 PolyU mRNA translation assay

M. smegmatis ribosomes and S100 extract were prepared as described in section 2.5.6 and polyU mRNA was obtained from Sigma. 7 Non-dissociated or dissociated wild type ribosomes were employed as specified. 5 pmol *M. smegmatis* ribosomes were incubated with Raf proteins and 30 µl of a translation mixture pre-mix (composition indicated in Table 2.10, section 2.5.8) in TAKM7 buffer (section 2.5.4). ^{14C}Phe amino acids were the only amino acids supplied.

Where pre-incubation of Raf proteins without mRNA is indicated, mRNA was added after incubating the ribosomes with all other components as specified. The mixture was incubated at 37^{o}C for the time indicated and the reaction was then stopped on ice. For detection of ^{14C}Phe, RNA was hydrolysed with 5 ml of 5M KOH and protein was precipitated with 5% TCA. Each reaction mixture was filtered through a 0.45 mm nitrocellulose membrane and exposed to a phosphoimager screen for detection of ^{14C}Phe incorporation.

2.6 Statistical testing

Significance testing was carried out between data groups with one-way ANOVA with Holm-Šídák multiple comparison test and p-values were obtained using GraphPad Prism 6 software (GraphPad Prism version 6.00 for Windows, GraphPad Software, San Diego California USA, www.graphpad.com). P-value significance was described as listed by GraphPad Prism 6 with p-values greater than or equal to 0.05 being not significant, p-values between 0.01 and 0.05 being significant, p-values between 0.001 and 0.01 being very significant and p-values between 0.0001 and 0.001 being extremely significant.

3. Role of RafS in mycobacterial physiology

3.1 Role of RafS in mycobacterial physiology: aims

We investigated the hypothesis that the putative ribosome stabilisation factor RafS, plays a role in mycobacterial physiology in growth, survival and stress tolerance phenotypes. We aimed to construct and complement deletion mutants *ΔrafS*$_{Msm}$ and *ΔrafS*$_{Mtb}$ and investigate their physiological characteristics. *M. smegmatis* mutants expressing full length and truncated RafS genes were also constructed and investigated. Several assays were carried out in the model organism, *M. smegmatis* and key assays were carried out in *M. tuberculosis.*

3.2 Construction of *M. smegmatis* mutants

3.2.1 Construction of Δ*rafS*$_{Msm}$ and Δ*rafS*$_{Msm}$c *M. smegmatis* mutants.

I aimed to construct Δ*rafS*$_{Msm}$ and Δ*rafS*$_{Msm}$c mutants. I employed mycobacterial recombineering for Δ*rafS*$_{Msm}$ construction (Kessel *et al*., 2007). This involves cross over between a double stranded linear AES and the *M. smegmatis* wild type genome, resulting in the replacement of the endogenous *rafS*$_{Msm}$ gene from the wild type genome with a hygromycin resistance gene casette present within the AES. *ΔrafS*$_{Msm}$*c* refers to *ΔrafS*$_{Msm}$ complemented with a copy of *rafS*$_{\text{Msm}}$ whose expression is controlled by an *hsp60* promoter mediating constitutive expression included on an integrating plasmid (Materials and Methods section 2.3.7). Bacterial strain, plasmid and primer details are given in Materials and Methods tables 2.1., 2.2 and 2.3, respectively.

For construction of the linear AES, Upstream (UR) and downstream (DR) regions (821 bp and 721 bp, respectively) flanking the *rafS*$_{Msm}$ (MSMEG_1878) gene

were amplified by PCR of wild type *M. smegmatis* genomic DNA (Fig. 3.1A) (Table 2.3). The PCR products were cloned into PCR®-4Blunt-TOPO (Invitrogen) and amplified in *E. coli* GM2163 cells. The DR was inserted between NheI and SpeI restriction sites and the UR between KpnI and XbaI restriction sites of PCR®-4Blunt-TOPO. The UR and DR inserts were digested from TOPO/rafS$_{Msm}$UR and TOPO/rafS$_{Msm}$DR and sizes were confirmed by gel electrophoresis (Fig. 3.1B).

The pYUB854 plasmid containing the hygromycin resistance casette (Appendix Figure 1) was digested with NheI and SpeI and the DR insert was ligated to linear pYUB854 digested with NheI and SpeI. The pYUB854/rafS$_{Msm}$DR plasmids were isolated and digested with KpnI and XbaI so that the UR could be inserted. The UR was ligated to linear pYUB854/rafS$_{Msm}$DR. The resulting pYUB854/rafS$_{Msm}$UR/DR plasmid was digested with KpnI and SpeI to obtain the rafS$_{Msm}$ linear AES (3936 bp) and presence of UR and DR inserts was confirmed by restriction digest of the AES with KpnI and XbaI (UR) NheI and SpeI (DR) (Fig. 3.1 C). A summary of the mycobacterial recombineering strategy for construction of Δ*rafS$_{Msm}$* is shown in Figure 3.1D.

The recombineering helper plasmid pJV53 was electroporated into wild type *M. smegmatis*. 0.2% w/v acetamide was used to induce expression of gp60 and gp61, which assist in the recombination of the AES with the bacterial genome. The linear AES was electroporated into these cells and Hyg^R colonies were obtained on hygromycin selective plates. Colony PCR was used to screen electroporation colonies by amplifying a region surrounding the *rafS$_{Msm}$* upstream and downstream sequences in order to confirm successful insertion of the hygromycin resistance casette between *rafS$_{Msm}$* flanking regions (Fig. 3.2 A). Three *ΔrafS$_{Msm}$* mutants were obtained from three separate electroporations of the linear AES to recombineering

cells prepared from three separate *M. smegmatis* colonies and were named *ΔrafS$_{Msm}$1, ΔrafS$_{Msm}$2 and ΔrafS$_{Msm}$3.* These were called independent *ΔrafS$_{Msm}$* mutants. (Fig. 3.2 B).

The *ΔrafS$_{Msm}$1* strain was complemented with the plasmid pMV361/*rafS$_{Msm}$* (Kan^R) (Materials and Methods section 2.3.6). For this purpose, serial subculturing of *ΔrafS$_{Msm}$1:* pJV53 on plain LB agar was carried out to select for the loss of pJV53. Then, *ΔrafS$_{Msm}$1* colonies were streaked onto LB agar with and without kanamycin. Kan^S *ΔrafS$_{Msm}$1* colonies were isolated and electroporated with pMV361/*rafS$_{Msm}$* and Kan^R colonies were selected. The resulting *ΔrafS$_{Msm}$1*: pMV361/*rafS$_{Msm}$* strain was named *ΔrafS$_{Msm}$c*. *ΔrafS$_{Msm}$c* was confirmed to be hygromycin and kanamycin resistant and colony PCR was used to confirm that the endemic *rafS$_{Msm}$* gene was absent (Fig. 3.2 C).

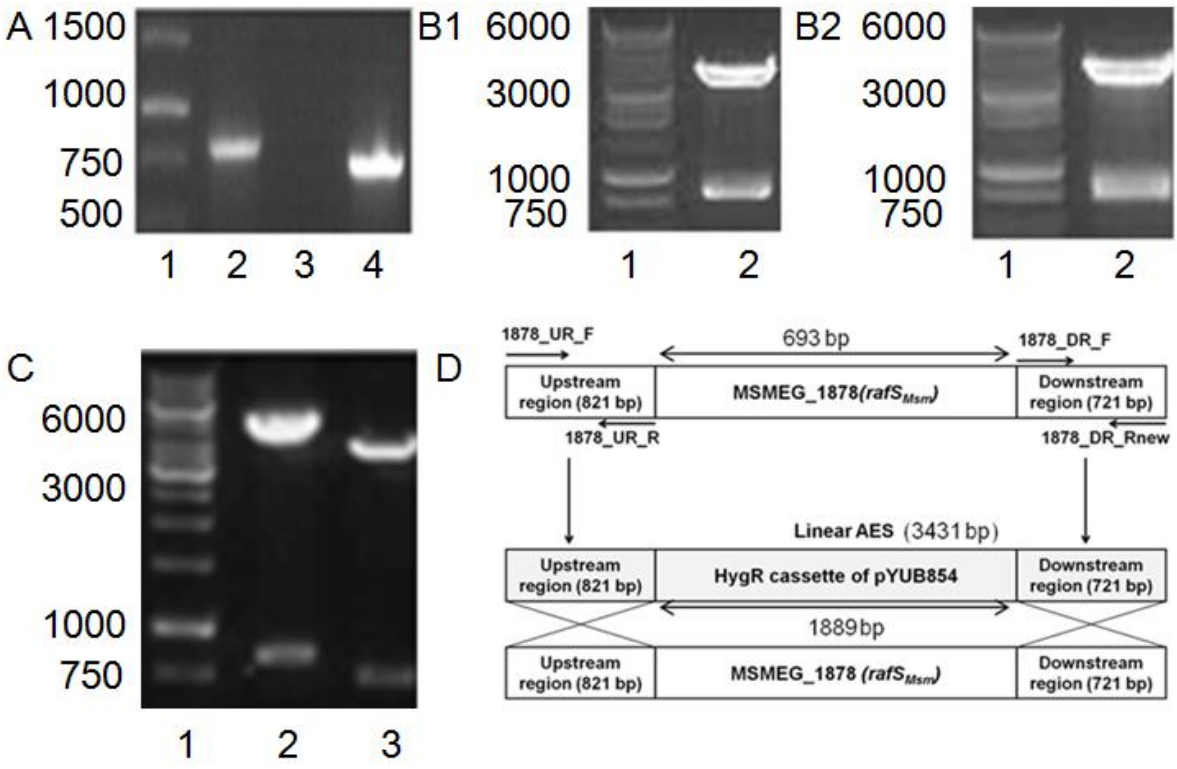

Figure 3.1 Construction of the *ΔrafS*$_{Msm}$ mutant by mycobacterial recombineering. Upstream (821 bp) and downstream (721 bp) regions flanking the *rafS*$_{Msm}$ gene were amplified from *M. smegmatis* wild type genomic DNA and a double stranded linear allelic exchange substrate (AES) carrying a hygromycin resistance cassette was constructed and exchanged with the endemic *rafS*$_{Msm}$ gene. (A) PCR amplification of *rafS*$_{Msm}$ upstream (lane 2) and *rafS*$_{Msm}$ downstream (lane 4) flanking sequences. (B) Restriction digest of upstream (B1 lane 2) and downstream (B2 lane 2) flanking sequences from TOPO/rafS$_{Msm}$UR and TOPO/rafS$_{Msm}$DR plasmids, respectively. (C) Restriction digest confirmation of presence of upstream (lane 2) and downstream (lane 3) sequences in the *rafS*$_{Msm}$ linear allelic exchange substrate. The pYUB854/rafS$_{Msm}$UR/DR plasmid was digested with KpnI and SpeI to obtain the rafS$_{Msm}$ linear AES (3936 bp) and presence of UR and DR inserts confirmed by restriction digest of the AES with KpnI and XbaI (UR) NheI and SpeI (DR). (D) Mycobacterial recombineering strategy for constructing ΔrafS$_{Msm.}$ AES indicates allelic exchange substrate. Primers for amplification of upstream and downstream regions are indicated adjacent to arrows. DNA ladder and band sizes in bp are indicated in lane 1 of each panel.

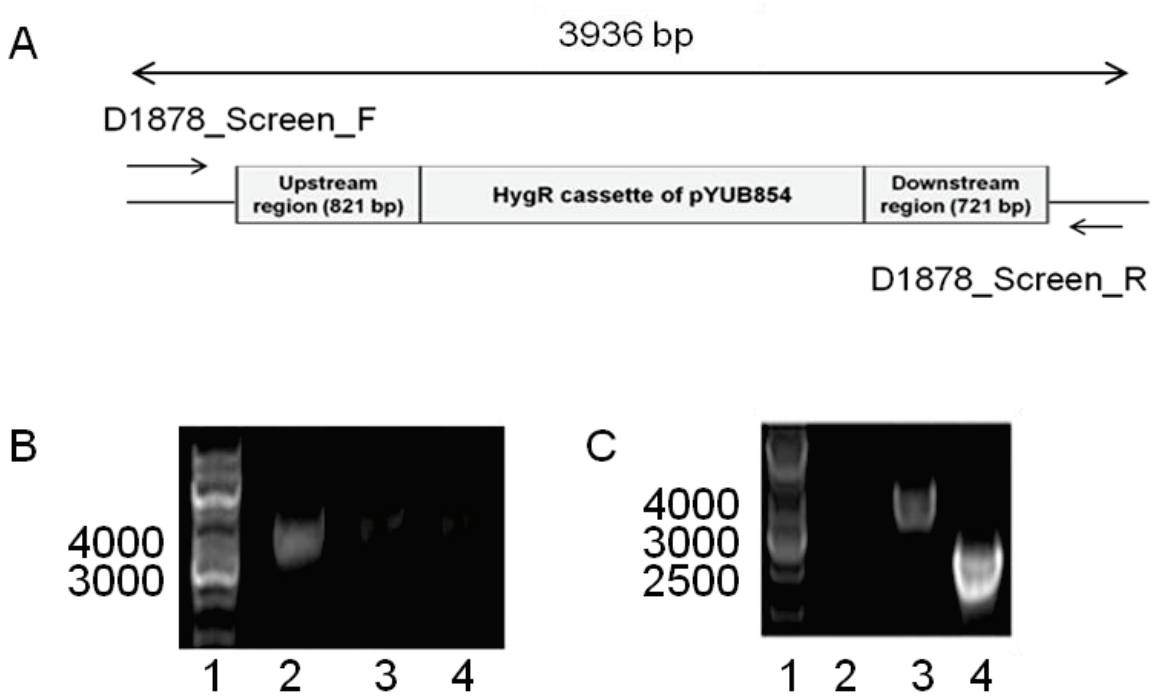

Figure 3.2 PCR confirmation of construction of 3 independent *ΔrafS*$_{Msm}$ mutants. After electroporation of the *rafS*$_{Msm}$ linear allelic exchange substrate (AES) into wild type *M. smegmatis* cells, colonies were screened for AES insertion by PCR amplification of the region surrounding the allelic exchange substrate. (A) Colony PCR strategy for amplifying the 3936 bp region surrounding the integrated AES after mycobacterial recombineering. Primers for PCR amplification are indicated adjacent to arrows. (B) Colony PCR confirmation of construction of *ΔrafS*$_{Msm}$*1* (lane 2), *ΔrafS*$_{Msm}$*2* (lane 3) and *ΔrafS*$_{Msm}$*3* (lane 4) independent mutants. The 3936 bp amplicon is shown in all lanes. (C) After complementation of the *ΔrafS*$_{Msm}$1 mutant, the PCR shown in (A) was used to confirm insertion of the AES in the *ΔrafS*$_{Msm}$c strain by amplification of the 3936 bp region (lane 3). The screening PCR shown in A was carried out on wild type *M. smegmatis* genomic DNA for comparison and lane 4 indicates an amplicon of 2740 bp which covers the region surrounding the endemic rafS$_{Msm}$ gene. DNA ladder and band sizes in bp are indicated in lane 1 in each panel.

3.2.2 Construction of *M. smegmatis* strains expressing RafS full length and truncated proteins

M. smegmatis strains expressing RafS full length and truncated proteins were constructed in order to investigate whether constitutive expression of Raf proteins affects physiological characteristics of *M. smegmatis*. We intended to investigate these strains under conditions for which *ΔrafS*$_{Msm}$ showed a significantly different phenotype to wild type *M. smegmatis*. Truncated RafS proteins were expressed to investigate the roles of individual domains.

Details of Raf protein structures based on bioinformatic predictions are given in section 4.2. Integrating vectors were constructed for constitutive expression of full length and truncated RafS proteins (in *M. smegmatis*) via the *hsp60* promoter of plasmid pMV361. Bacterial strain, plasmid and primer details are given in Materials and Methods tables 2.1., 2.2 and 2.3, respectively.

Candidate truncation regions were selected based on alignment with the short HPF protein PY which also contains an N terminal S30AE domain (See Figure 4.3 for predicted secondary structures of Raf proteins). For each protein, within the region after the S30AE domain, a specific truncation residue was chosen such that the residue has low helix, strand and buried index propensities based on Jpred secondary structure predictions (Cole *et al.,* 2008). The chosen truncation residues were 166 for RafS$_{Msm}$ and 141 for RafS$_{Mtb}$.

Full length *rafS*$_{Msm}$ and *rafS*$_{Mtb}$ and sequences of N and C terminal domains were amplified from *M. smegmatis* genomic DNA using primers 13 to 20 (Table 2.3). The 6 PCR products indicated (Fig. 3.3 A) were cloned into PCR®-4Blunt-TOPO

(Invitrogen) between MfeI and HindIII restriction sites and transformed into HB101 *E. coli*. Inserts were digested from 'TOPO/*rafS* expression sequence' plasmids with MfeI and HindIII and ligated to the linear pMV361 vector digested with MfeI and HindIII. The 'pMV361/rafS expression sequence' vectors were electroporated into wild type *M. smegmatis*. The electroporation colonies were screened by colony PCR to identify colonies with *rafS* expression sequences using primers 13 to 20 (Table 2.3). (Fig. 3.3 B, C).

A study containing evidence for changes in the annotation of the *M. tuberculosis* H37Rv genome suggested that $rafS_{Mtb}$ (Rv3241c) should be re-annotated such that its original length of 645 bp increases to 660 bp (Kelkar *et al.,* 2011). The Rv3241c gene would start at a site 15 bp upstream of the previously annotated site, causing substitution of the first methionine amino acid with the sequence "MSRLAV". Prior to knowing about the reannotation, I had completed construction of the vectors described. Subsequently, I re-constructed the pMV361/$rafS_{Mtb}$ and pMV361/$rafS_{Mtb}$N vectors with the new gene lengths as described.

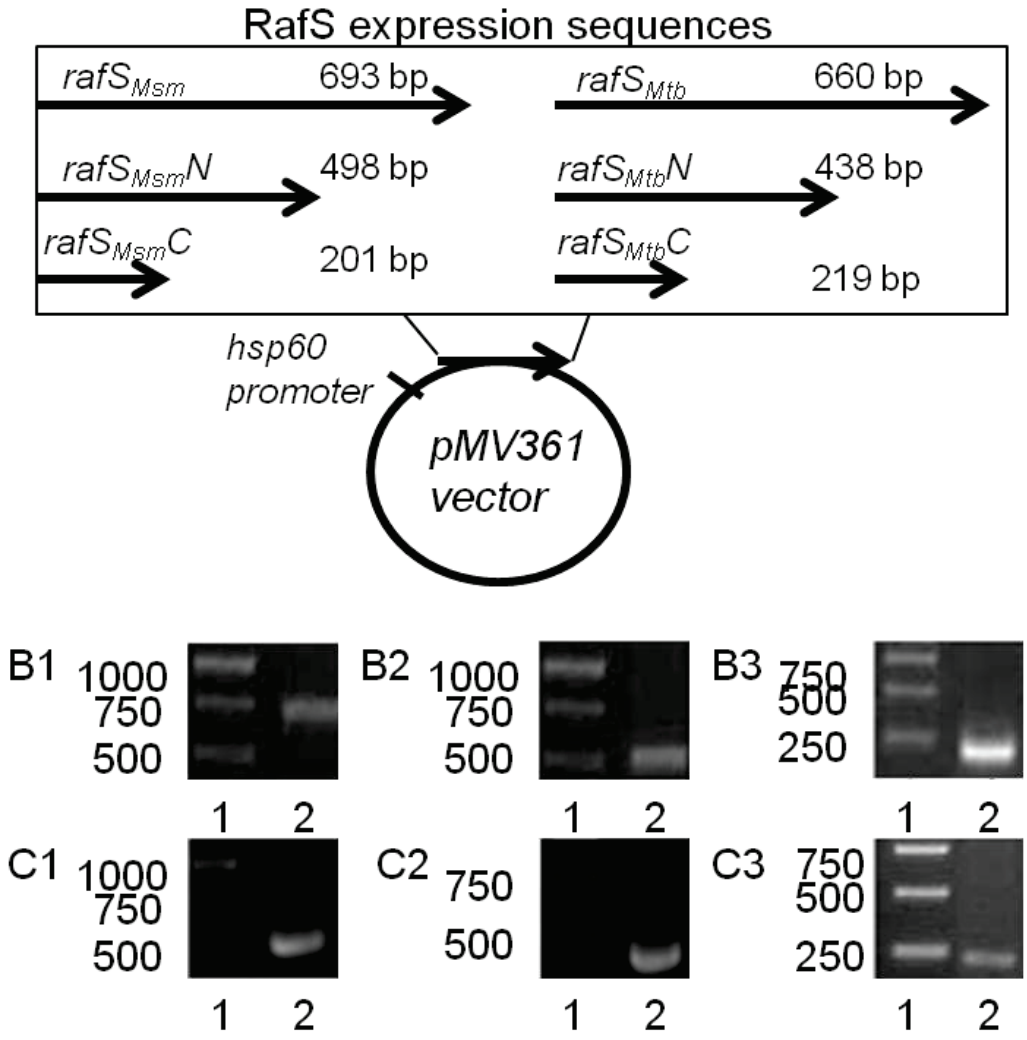

Figure 3.3 Construction of *M. smegmatis* plasmids expressing RafS full length and truncated proteins (A) Cloning strategy for construction of *M. smegmatis* strains expressing RafS full length and truncated proteins. Integrating pMV361 vectors were constructed for full length and truncated RafS protein constitutive expression in wild type *M. smegmatis* under the control of an *hsp60* promoter. Expression sequences are shown in black outlined boxes. (B, C) PCR confirmation of the presence of constitutive RafS expression sequences in *M. smegmatis*:pMV361/*rafS* expression sequence strains; (B) Expression sequences shown in lane 2 of each panel are $rafS_{Msm}$ (B1, 693 bp), $rafS_{Msm}$N (B2, 498 bp), $rafS_{Msm}$C (B3, 201 bp), $rafS_{Mtb}$ (C1, 660

bp) and *rafS*$_{Mtb}$N (C2, 438 bp) and *rafS*$_{Mtb}$C (C3, 219 bp). DNA ladder and band sizes in bp are indicated in lane 1 of each panel.

3.3 Role of RafS$_{Msm}$ in normoxic growth

3.3.1 Role of RafS$_{Msm}$ in normoxic growth in liquid media

The normoxic growth characteristics of wild type *M. smegmatis*, Δ*rafS*$_{Msm}$, and Δ*rafS*$_{Msm}$c strains in LBT and minimal HdB media were investigated. The Luria Bertani or LBT rich medium contained the complex carbon sources yeast extract and tryptone (peptides formed by casein digestion by trypsin). Hartman's de Bont minimal medium contained 0.04% glycerol as the sole carbon source (Materials and Methods sections 2.4.3, Appendix Table 1). No significant differences in strain growth characteristics in LBT or Hdb were observed (Fig. 3.4).

We next investigated the role of RafS$_{Msm}$ in growth during the transition from LBT stasis to active growth in HdB and also from HdB stasis to active growth in LBT. Transition from LBT to HdB (nutrient downshift) involves adjustment to utilisation of glycerol, the sole and limited carbon source. Transition from HdB to LBT (nutrient upshift) involves adjustment to utilisation of complex carbon sources present in tryptone and yeast extract. LBT stationary phase cultures subcultured to HdB showed no apparent differences in growth characteristics (Fig. 3.5 A). HdB stationary phase cultures subcultured to LBT media also showed no apparent differences in growth characteristics (Fig. 3.5 B) Taken together, the results indicated that RafS$_{Msm}$ is dispensable for normoxic growth in LBT and HdB media and for growth during nutrient downshift and upshift.

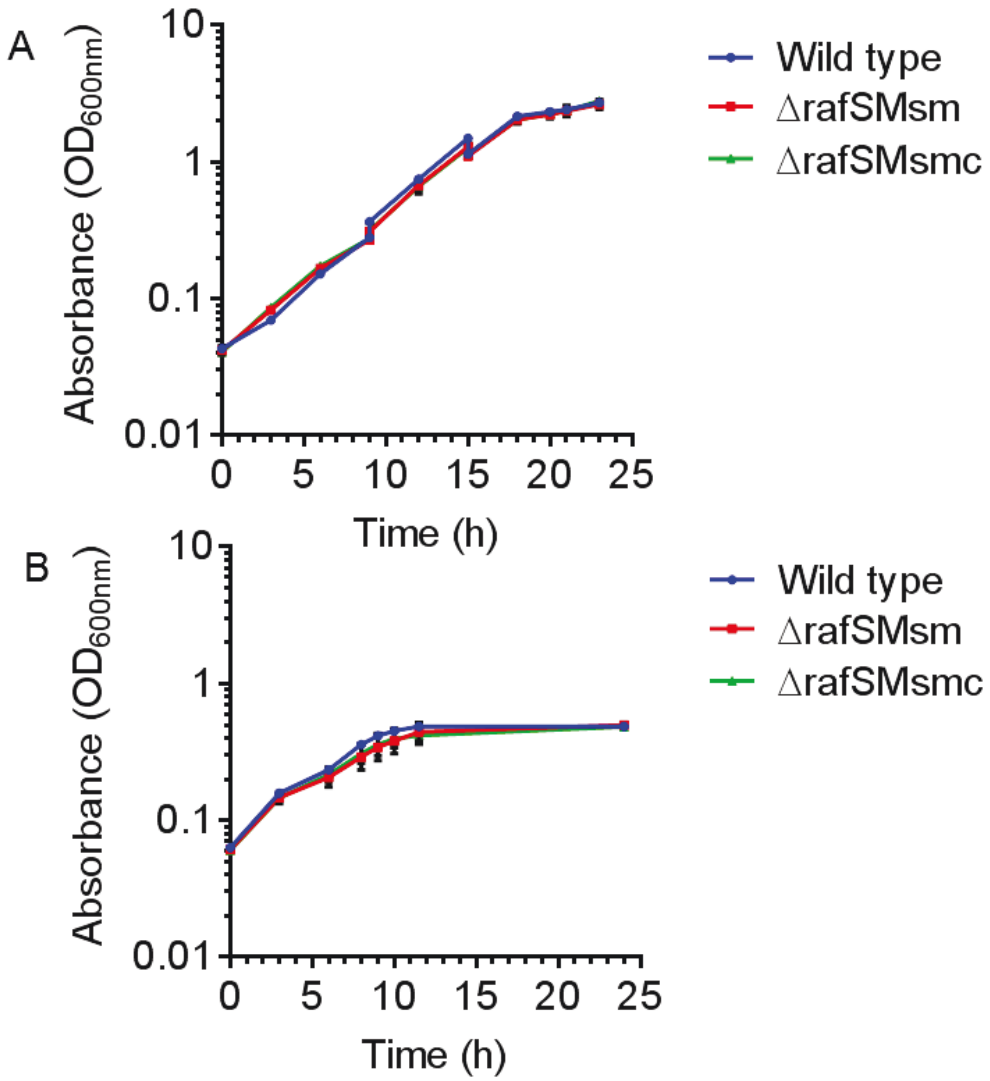

Figure 3.4. $RafS_{Msm}$ is dispensable for growth in LBT and HdB minimal media (normoxia). Growth of 3 wild type *M. smegmatis* replicates, 3 independent Δ*rafS*$_{Msm}$ mutant replicates and 3 Δ*rafS*$_{Msm}$*c* replicates was investigated. Average optical density (600nm) is plotted. Error bars indicate standard deviation. (A) Strains were cultured in LBT to stationary phase (3h duration) and subcultured to LBT to monitor early growth (0 to 9 h), active growth (9 to 15 h) and the transition to stationary phase (15 to 24 h). Growth curves were included in a single plot. (B) Strains were cultured in LBT to stationary phase (3h duration) and subcultured to HdB to monitor growth till stationary phase.

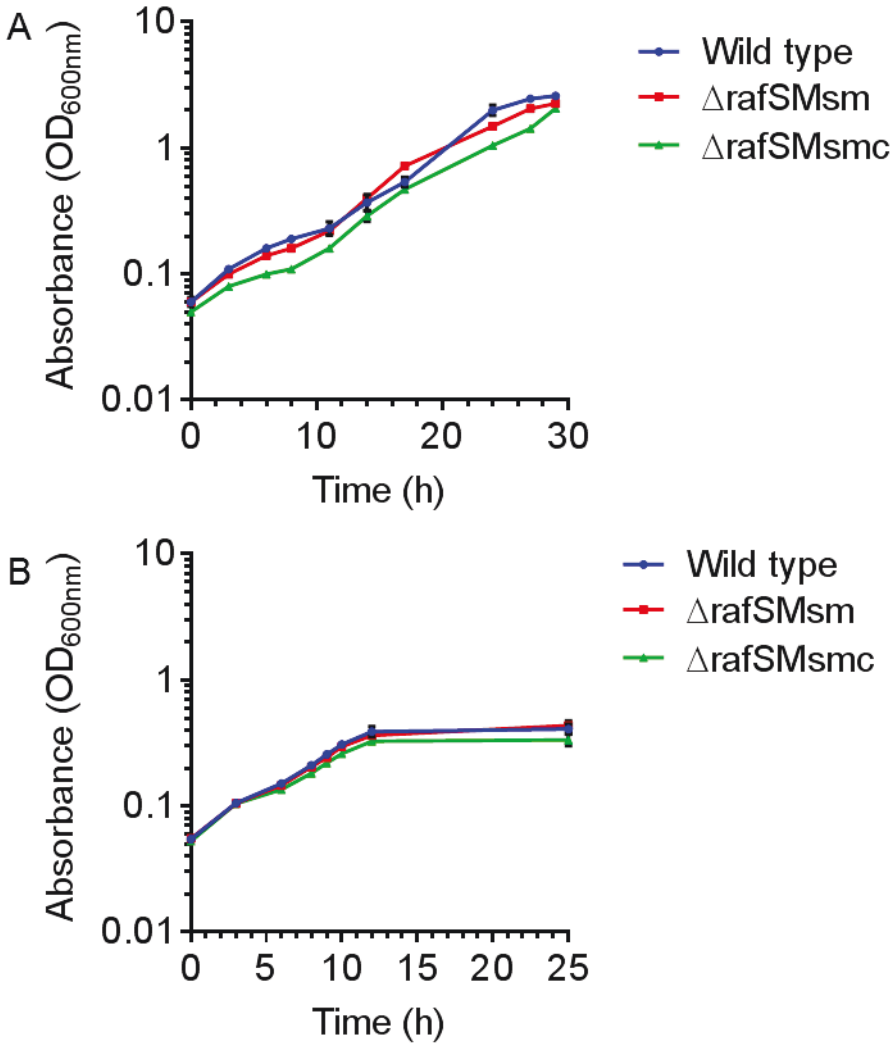

Figure 3.5. $RafS_{Msm}$ is dispensable for growth during nutrient downshift and upshift (normoxia). Growth of wild type *M. smegmatis,* Δ*rafS*$_{Msm}$ 2 and Δ*rafS*$_{Msm}$*c* (3 biological replicates each) was investigated. Average optical density (600nm) is plotted. Error bars indicate standard deviation. (A) $RafS_{Msm}$ is dispensable for growth during nutrient downshift. Strains were cultured in LBT to stationary phase (3h duration) and subcultured to HdB. (B) $RafS_{Msm}$ is dispensable for growth during nutrient upshift. Strains were cultured in HdB to stationary phase (9h duration) and subcultured to LBT in two independent LBT batches to monitor early growth (0 to 17 h) and entry into stationary phase from a low OD (24 to 29 h). Growth curves were included in a single plot.

We next investigated the growth characteristics of strains constitutively expressing full length and truncated rafS proteins via an *hsp60* promoter of the pMV361 integrating plasmid. Wild type *M. smegmatis*/pMV361, *M. smegmatis*/pMV361: *rafS*$_{Msm}$, *M. smegmatis*/pMV361: *rafS*$_{Msm}$*N* and *M. smegmatis*/pMV361: *rafS*$_{Msm}$*C* strains were cultured to late log phase in LBT media and no apparent differences in growth characteristics were observed (Fig. 3.6 A).

Growth characteristics of *M. smegmatis*/pMV361, *M. smegmatis*/pMV361: *rafS*$_{Mtb}$, *M. smegmatis*/pMV361: *rafS*$_{Mtb}$*N* strains in LBT media did not appear to be different (Fig. 3.6 B). Given the lack of difference in strain growth, I did not pursue characterisation of *M. smegmatis*/pMV361: *rafS*$_{Mtb}$*C.* The data indicated that constitutive expression of RafS$_{Msm}$ and RafS$_{Mtb}$ and truncated constructs in wild type *M. smegmatis* does not affect growth in LBT media.

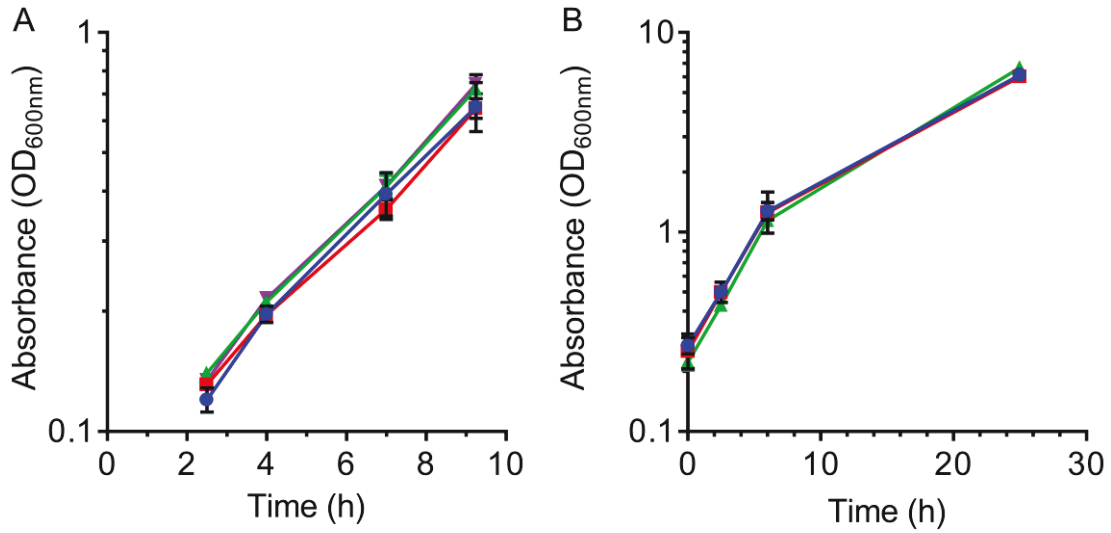

Figure 3.6. RafS protein constitutive expression does not affect growth of *M. smegmatis* in LBT (normoxia). Average optical density at 600nm is plotted. Error bars indicate standard deviation. (A) *M. smegmatis*/pMV361 (blue), *M. smegmatis*/pMV361: $rafS_{Msm}$ (red), *M. smegmatis*/pMV361: $rafS_{Msm}N$ (green) and *M. smegmatis*/pMV361: $rafS_{Msm}C$ (violet) strains (3 replicates each) were cultured to stationary phase (3h duration) and subcultured to LBT to monitor growth until late log phase. (B) *M. smegmatis*/pMV361 (blue), *M. smegmatis*/pMV361: $rafS_{Mtb}$ (red), *M. smegmatis*/pMV361: $rafS_{Mtb}N$ strains (green) (3 replicates each) were cultured to stationary phase in LBT (3h duration) and subcultured to LBT to monitor growth until stationary phase.

3.3.2 Role of $RafS_{Msm}$ in mature biofilm and pellicle formation

I next investigated whether $RafS_{Msm}$ plays a role in normoxic mature biofilm and pellicle formation (Materials and Methods sections 2.4.8, 2.4.9). Mature biofilms cultured in M63 minimal media for 4 days at 30^{o}C indicated no significant difference in biofilm formation (Fig 3.7 A). Mature biofilms cultured in M63 minimal media for 5 days at 28.5^{o}C also indicated no significant difference in biofilm formation (Fig 3.7 B). Pellicles cultured in 7H9 media in triplicate for 2 days at 37^{o}C indicated no apparent difference in pellicle formation in all strains investigated (Fig 3.7 C). Taken together, the data indicated that $RafS_{Msm}$ is dispensable for biofilm and pellicle formation.

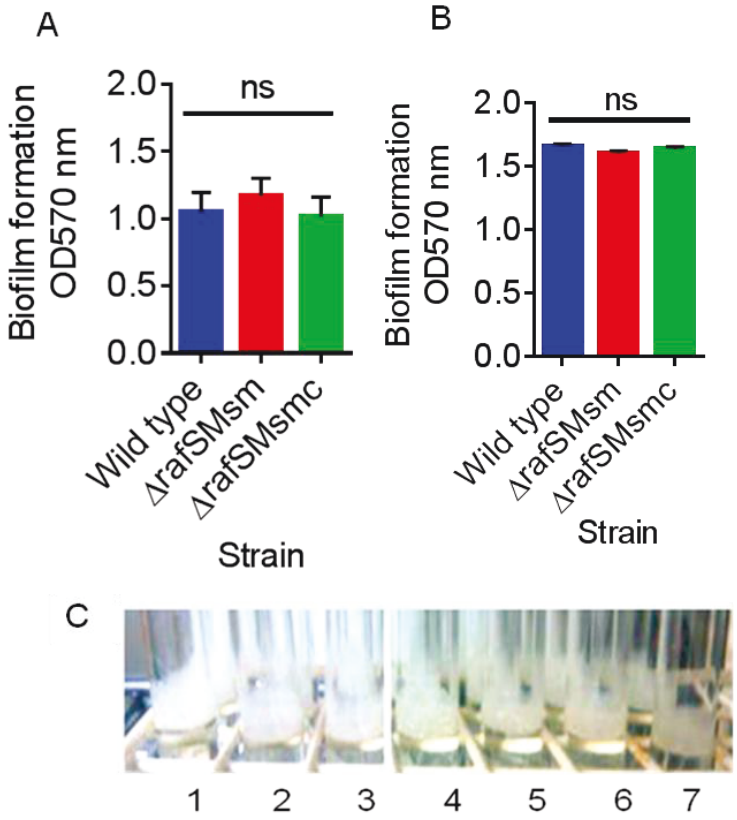

Figure 3.7. $RafS_{Msm}$ is dispensable for biofilm and pellicle formation. Mature biofilms were cultured in M63 minimal media for 4 days at 30°C (6 replicates per strain) (A), or at 5 days at 28.5°C (5 replicates per strain) (B) and stained with 0.5% crystal violet, solubilised with 95% ethanol and optical density at 570 nm was measured. Average optical density is plotted and strain names are indicated on the horizontal axis. Error bars indicate standard deviations. (C) $RafS_{Msm}$ is dispensable for pellicle formation *in vitro*. Pellicles were cultured in 7H9 media in triplicate for 2 days at 37°C (3 replicates per strain) and a representative photograph was taken of one representative replicate per strain. Wild type *M. smegmatis* (1), *Δ$rafS_{Msm}$* (2), *Δ$rafS_{Msm}$C* (3), *M. smegmatis:pMV361* (4), *M. smegmatis:pMV361/ $rafS_{Msm}$* (5), *M. smegmatis:pMV361/ $rafS_{Msm}$N* (6) and *M. smegmatis:pMV361/ $rafS_{Msm}$C* (7) pellicles are shown. Means were compared using a one-way ANOVA with Holm-Šídák multiple comparison test; ** indicates a very significant p-value between 0.001 and 0.01; ns indicates a non-significant p-value > 0.05.

3.4 Role of $RafS_{Msm}$ in tolerance of acid, heat and antibiotic stress

We investigated the role of $RafS_{Msm}$ in tolerance of acid stress, a condition present in granulomas and thus known to be physiologically relevant to *M. tuberculosis* pathology (Shleeva *et al.,* 2011). Short term survival assays were employed to investigate survival of stationary phase cells in LBT media at pH 2.73, 4.7 and 6.74 (normoxia) in a 24-well format (Materials and Methods section 2.4.10). The results indicated no significant differences between wild type and Δ*rafS$_{Msm}$1* viabilities (Fig. 3.8).

Since Δ*rafH$_{Msm}$* viability is impaired in heat stress at 55^{o}C (Trauner *et al*., 2010), we investigated the role of $RafS_{Msm}$ in tolerance of heat stress 55^{o}C. Differences in survival of wild type and *ΔrafS$_{Msm}$*1 stationary phase cells at 55^{o}C were investigated during a period of 6.5 h (Materials and Methods section 2.4.11). The data indicated no significant difference between wild type and *ΔrafS$_{Msm}$*1 viabilities (Fig. 3.9).

We also investigated the role of $RafS_{Msm}$ in antibiotic stress tolerance. Due to $RafS_{Msm}$ being a ribosome-binding protein (Trauner, 2010), we investigated antibiotic susceptibility to ribosome-targetting antibiotics. Antibiotics with non-ribosomal targets were also included for comparison. The microplate alamar blue assay (MABA) was employed for MIC determination in 7H9 (Fig. 3.10 A) and HdB media (Fig. 3.10 B) (Collins *et al.,* 1997) (Materials and Methods section 2.4.7).

Growth of wild type and *ΔrafS$_{Msm}$*1 strains was investigated in antibiotics at a 10-fold serial dilution concentration series starting from 200X reported MIC values over a period of 48 hours. Mean fold differences in between wild type and *ΔrafS$_{Msm}$*

MICs were less than 4-fold indicating no significant differences (van de Kassteele *et al.,* 2012). Taken together, the data indicated that $RafS_{Msm}$ was dispensable for short term viability in acid pH and heat stress and also for antibiotic tolerance in LBT and HdB minimal media in normoxia.

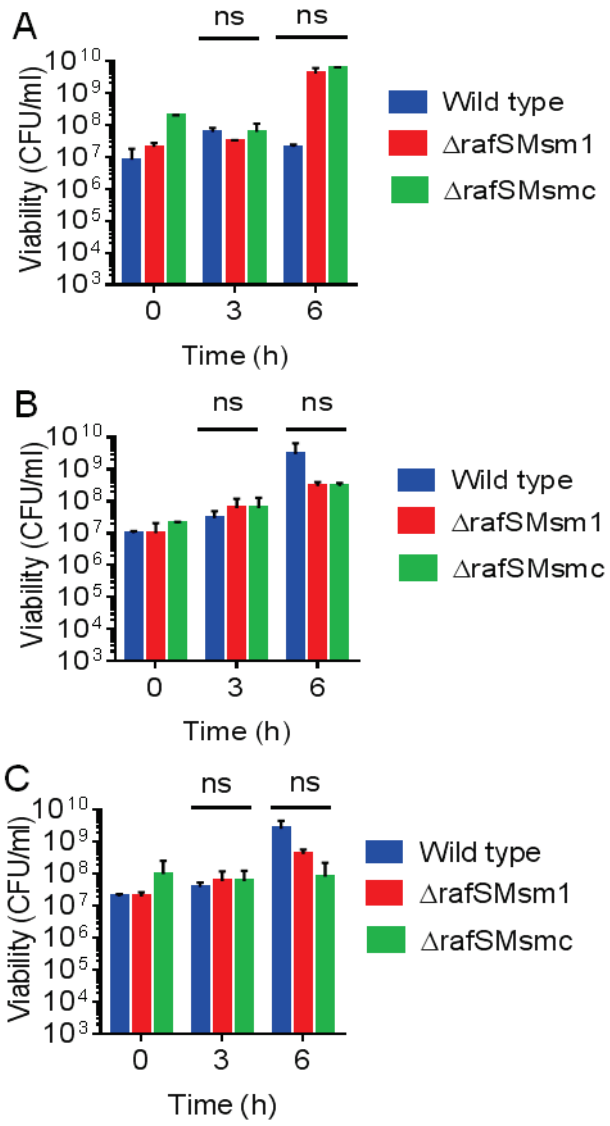

Figure 3.8. $RafS_{Msm}$ in dispensable for short term survival in acidic medium (normoxia). Wild type *M. smegmatis*, Δ*rafS*$_{Msm}$1 and Δ*rafS*$_{Msm}$C strains (3 biological replicates each) were cultured to stationary phase in LBT media (3h duration) and resuspended in 2 ml LBT media at pH 2.73 (A), pH4.7 (B) and pH 6.74 (C) in a 24 well plate to monitor viability over a 6 h period. 6 h means were compared using a one-way ANOVA with Holm-Šídák multiple comparison test; ns indicates a non-significant p-value > 0.05.

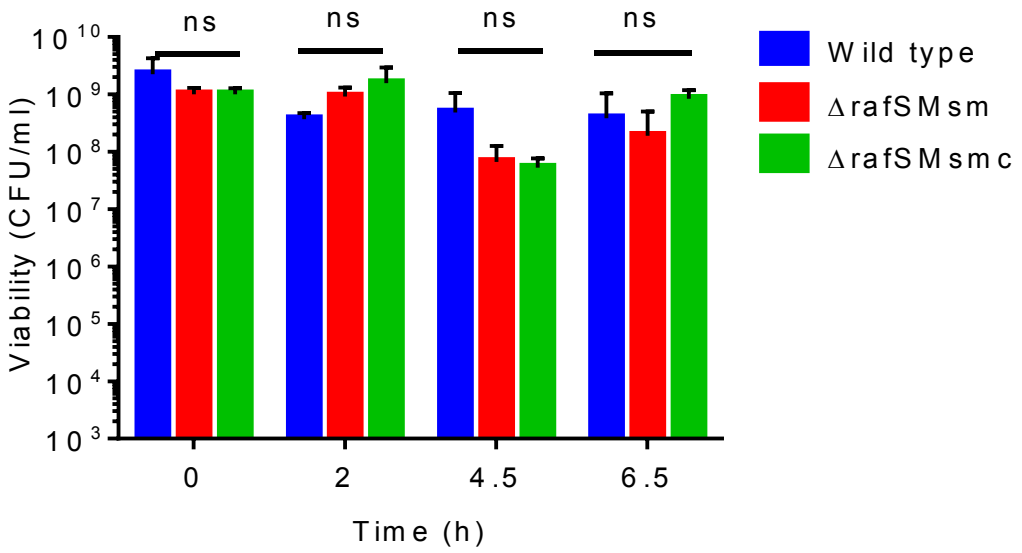

Figure 3.9. $RafS_{Msm}$ is dispensable for short term survival in heat stress (55^{o}C , normoxia). Wild type *M. smegmatis*, *Δ$rafS_{Msm}$*1, *Δ$rafS_{Msm}$*C strains (3 biological replicates each) were cultured to stationary phase in LBT media (3h duration) and transferred to an incubator at 55^{o}C, 150 rpm to monitor viability over a 6.5 h period. 6.5 h means were compared using a one-way ANOVA with Holm-Šídák multiple comparison test; ns indicates a non-significant p-value > 0.05.

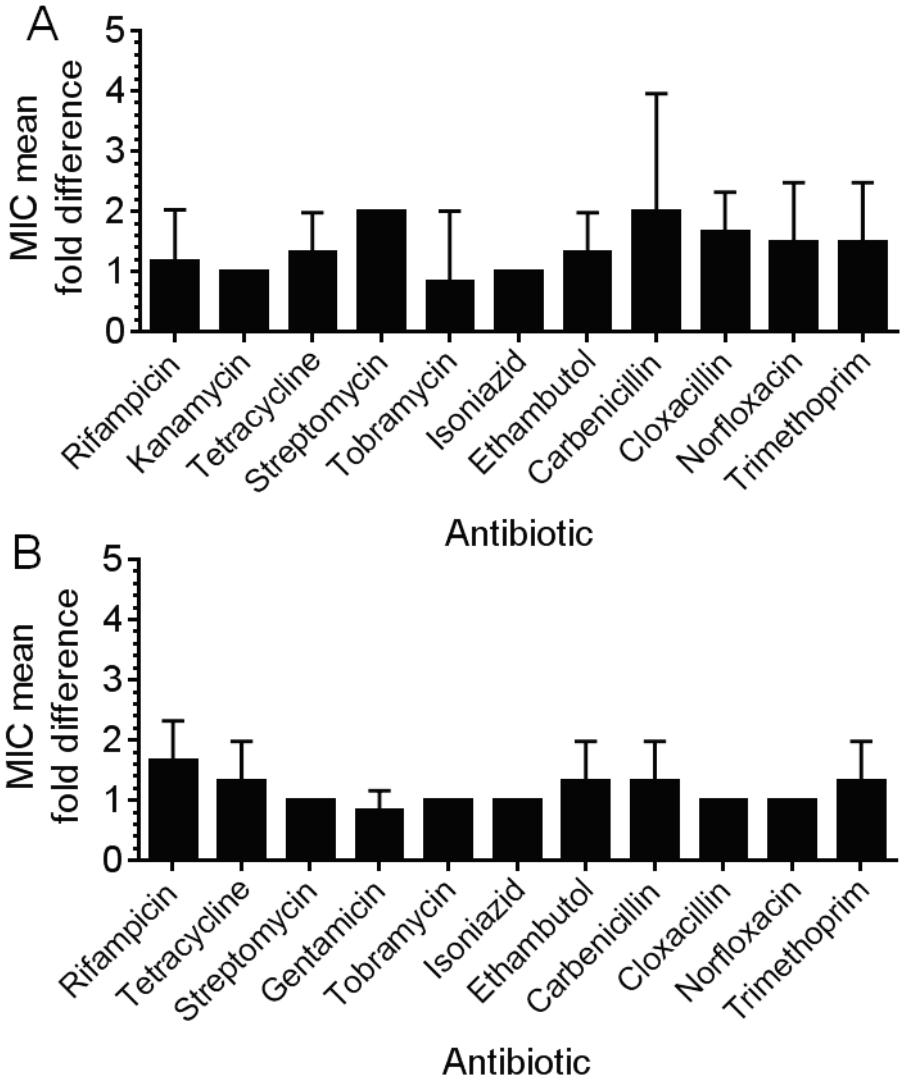

Figure 3.10. $RafS_{Msm}$ is dispensable for antibiotic tolerance in *M. smegmatis*. Wild type and *Δraf*S_{Msm}1 (3 biological replicates per strain) were cultured in media containing antibiotics at a 10 fold serial dilution concentration series starting from 200X reported MICs in 96 well plates in 7H9 rich medium (A) and in HdB minimal medium (0.04 % glycerol) (B) for 48 hours (normoxia), after which MICs (minimum inhibitory concentrations) were determined using alamar blue. Mean fold differences between wild type and *Δraf*S_{Msm} MICs are plotted and error bars indicate 95% confidence intervals.

3.5 Role of $RafS_{Msm}$ in stasis survival and resuscitation

As shown previously, *ΔrafH*$_{Msm}$ viability was compromised in 41 day hypoxic stasis (Trauner *et al*., 2012). Thus, survival assays were carried out in order to investigate whether *rafS*$_{Msm}$ plays a role in maintaining viability during normoxic and hypoxic stasis in rich and carbon-limited media. These assays were intended to investigate long term trends indicating differences in strain survival.

Normoxic survival assays were carried out in LBT and HdB (0.04% and 0% glycerol) stasis (Materials and Methods section 2.4.5). (See Appendix Table 2 for a summary of conditions investigated). The survival assay in normoxic LBT stasis indicated significantly lower *ΔrafS*$_{Msm}$ survival on the 44th day of LBT stasis (p= 0.0377). Also, this defect appeared to be complemented by the *ΔrafS*$_{Msm}$*c* mutant (Fig 3.10). This assay was not continued further due to the formation of large clumps in cultures of all strains that could not be disrupted by vortexing.

The survival assay in HdB (0.04% glycerol) also indicated no significant differences in strain survival in 72 days stasis (Fig 3.12 A). When a carbon source was not provided in the 0% glycerol HdB assay, 0.02% tyloxapol was employed as dispersal agent that is non-hydrolysable by mycobacteria and does not act as a carbon source in order to achieve stringent carbon starvation. No significant differences in strain survival were observed in 73 days HdB (0% glycerol) stasis (Fig 3.12 B).

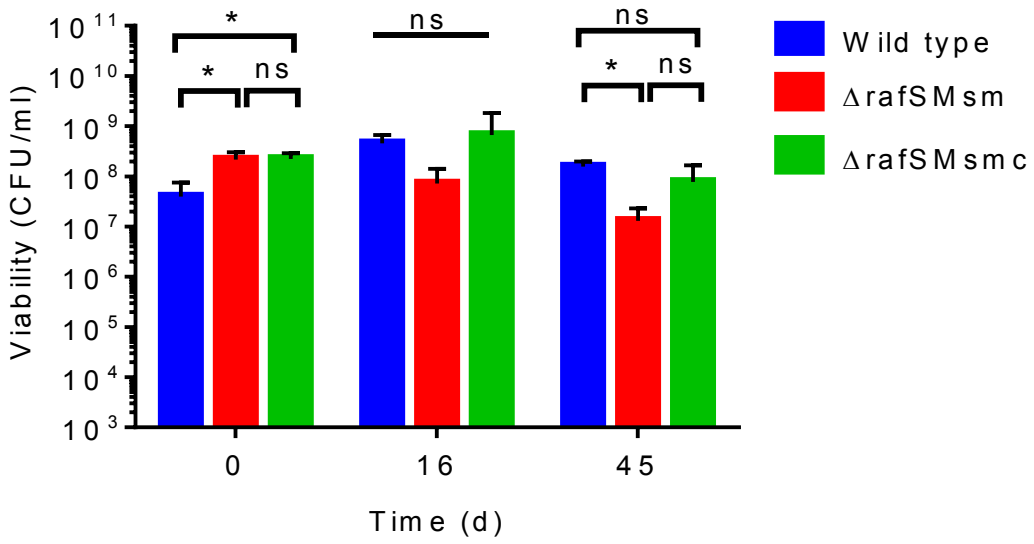

Figure 3.11. Role of $RafS_{Msm}$ in survival in normoxic LBT stasis. Wild type *M. smegmatis*, *Δ$rafS_{Msm}$1* and *Δ$rafS_{Msm}$C* strains (three biological replicates per strain) were cultured to normoxic stasis in LBT media (3h duration) and subcultured to LBT. Strains were allowed to grow to stationary phase at 150 rpm, 37^{o}C (1 day duration of growth to stasis) and CFU cell counts were obtained at days indicated. Day 0 indicates the CFU reading taken after subculturing strains from LBT stasis to LBT prior to long-term incubation. n = 3 except for day 45 *Δ$rafS_{Msm}$1* and *Δ$rafS_{Msm}$c* time points, where n = 2. Average CFU/ml were plotted. Error bars indicate standard deviation. Means were compared using a one-way ANOVA with Holm-Šídák multiple comparison test; ns indicates a non-significant p-value > 0.05; * : significant p = 0.01 to 0.05.

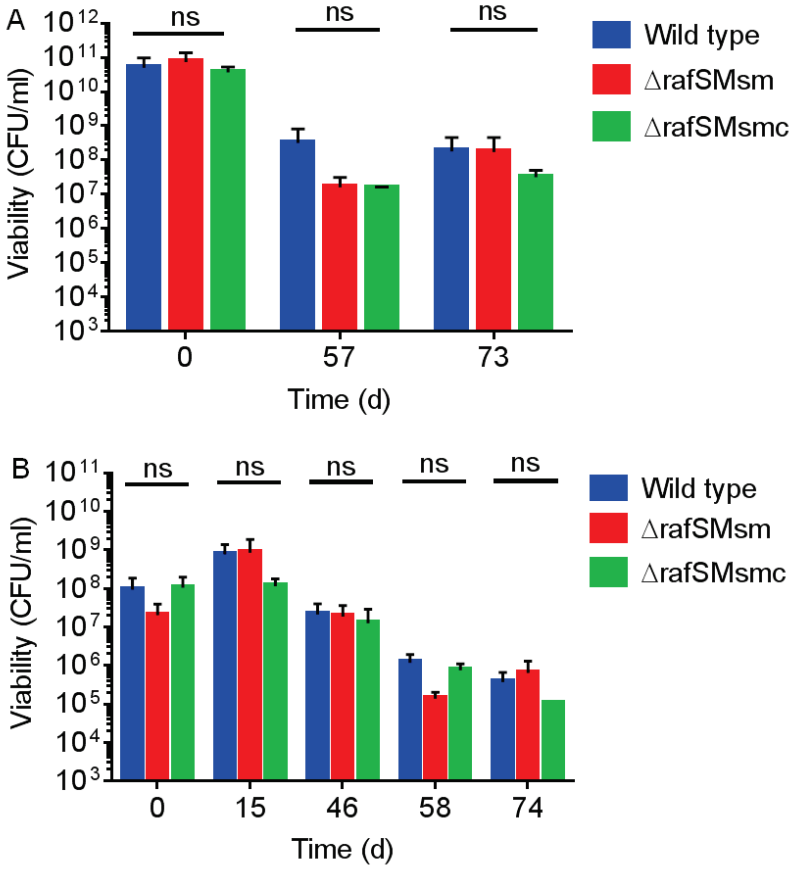

Figure 3.12. $RafS_{Msm}$ is dispensable for survival in normoxic HdB (0.04% (A) and 0% (B) glycerol stasis. (A) Wild type *M. smegmatis*, *Δ$rafS_{Msm}$1* and *Δ$rafS_{Msm}$C* strains (3 biological replicates per strain) were cultured to normoxic stasis in LBT (3h duration) and subcultured to the HdB (0.04% glycerol). Strains were allowed to grow in HdB to stationary phase at 150 rpm, 37°C (14 h duration of growth to stasis) and CFU cell counts were obtained at days indicated. Day 0 indicates the CFU reading taken after subculturing strains from LBT stasis to HdB, prior to long-term incubation. (B) Wild type *M. smegmatis*, *Δ$rafS_{Msm}$*1 and *Δ$rafS_{Msm}$C* strains (3 biological replicates per strain) were cultured to normoxic stasis in LBT (3h duration), pelleted and resuspended in HdB without glycerol (0.02% Tyloxapol). Cultures were incubated at 150 rpm, 37°C and CFU cell counts were obtained at days indicated. Day 0 indicates the CFU reading taken after resuspending strains from LBT stasis to HdB, prior to long-term incubation. Average CFU/ml were plotted. Error bars indicate standard deviation. Means were compared using a one-way ANOVA with Holm-Šídák multiple comparison test; ns: non-significant p-value > 0.05.

Hypoxic survival assays were carried out in LBT and HdB (0.04% glycerol) stasis (Materials and Methods section 2.4.5). The hypoxic stasis survival assay (255 days) in LBT indicated no significant differences in strain survival (Fig. 3.13 A). The hypoxic stasis survival assay in HdB (0.04% glycerol) (364 days) indicated an overall trend of no significant difference in strain viability between wild type and Δ*rafS*$_{Msm}$,

However, a significantly lower Δ*rafS*$_{Msm}$ viability than wild type (p= 0.0019) was observed at day 55, and this defect was not recovered in the complemented strain which also showed a viability defect at day 55 (wild type versus Δ*rafS*$_{Msm}$*c* p= 0.0019). Also, another significant Δ*rafS*$_{Msm}$*c* viability defect was observed at day 364 (wild type versus Δ*rafS*$_{Msm}$*c* p= 0.0116) (Fig. 3.13 B). It would be worthwhile to further investigate Δ*rafS*$_{Msm}$ viability defects around day 55 (HdB 0.04% glycerol, hypoxia) with more frequent viability testing before and after day 55. Also, employing an alternative complementation strain, such as one where *rafS*$_{Msm}$ is expressed under the control of its native promoter would be useful as a control.

We next investigated the role of RafS$_{Msm}$ in survival in oxygen-limited general nutrient starvation PBS stasis. The results indicated no significant differences in viabilities between strains in 345 days of stasis (Fig 3.14). Taken together, the data indicated that RafS$_{Msm}$ is dispensable for prolonged survival in normoxic LBT and HdB stasis and in hypoxic LBT and HdB stasis.

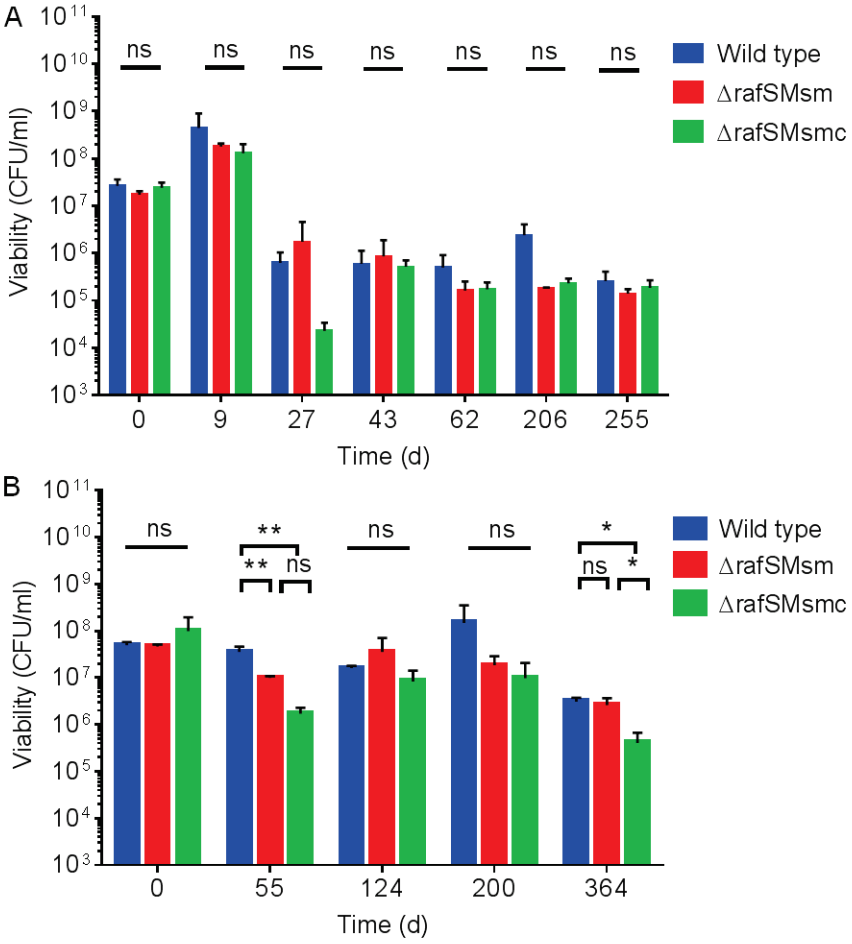

Figure 3.13. $RafS_{Msm}$ is dispensable for survival in hypoxic LBT and HdB (0.04% glycerol) stasis. Wild type *M. smegmatis*, *Δ$rafS_{Msm}$1* and *Δ$rafS_{Msm}$c* strains (3 biological replicates each) were cultured to normoxic stasis in LBT (3h duration) and then subcultured to LBT (A) or HdB (0.04% glycerol) (B) and grown to stationary phase in suba-sealed flasks. Cultures were incubated at 150 rpm, 37^{o}C and CFU cell counts were obtained at days indicated. Day 0 indicates the CFU reading taken after subculturing strains from LBT stasis to LBT or HdB, prior to long-term incubation. (A) A composite graph was obtained from two separate culture sets where the first set was sampled from days 0 to 43 and the second set which was set up at a later date from days 62 to 255. Average CFU/ml are plotted. Error bars indicate standard deviation. Means were compared using one-way ANOVA with Holm-Šídák multiple comparison test; ** : very significant p = 0.001 to 0.01; ns: non-significant p-value > 0.05.

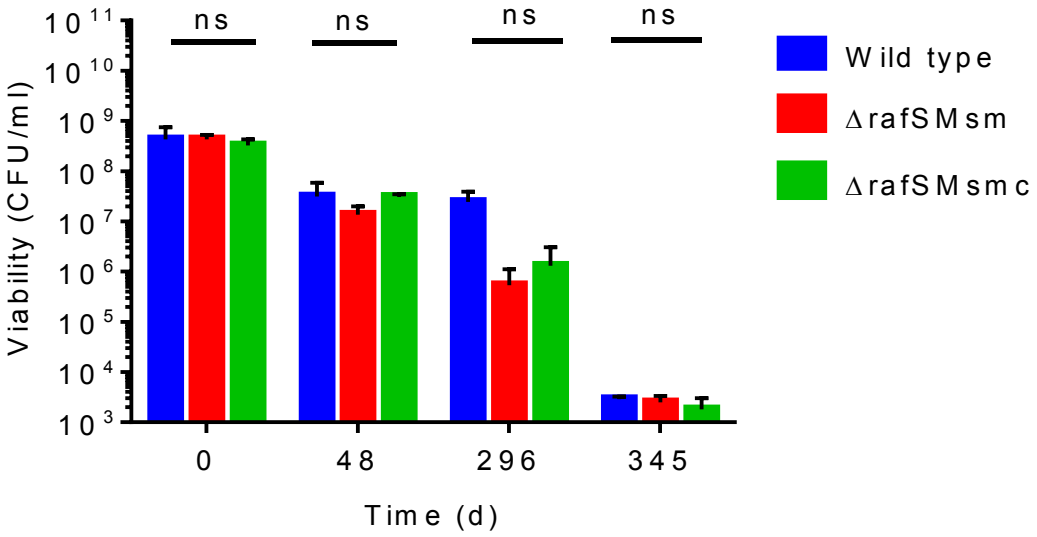

Figure 3.14. Role of $RafS_{Msm}$ in survival in PBS stasis (general nutrient starvation). Wild type *M. smegmatis*, *Δ$rafS_{Msm}$1* and *Δ$rafS_{Msm}$c* strains were cultured to normoxic stasis in LBT (3h duration) and cultures were pelleted. The pellets were resuspended in modified PBS and transferred to suba-sealed flasks (cultures not exposed to air). CFU cell counts were obtained at days indicated. Day 0 indicates the CFU reading taken after resuspending strains from LBT stasis to modified PBS, prior to long-term incubation. 3 biological replicates per strain are included except for *Δ$rafS_{Msm}$c* where 2 replicates are included. Average CFU/ml are plotted. n = 3 for all points except wild type day 48 where n=2. Error bars indicate standard deviation. Means were compared using one-way ANOVA with Holm-Šídák multiple comparison test; ns: non-significant p-value > 0.05.

Resuscitation of aged stasis cultures was carried out to investigate whether *$rafS_{Msm}$* deletion affects resuscitation of aged cultures in fresh LBT media (Materials and Methods section 2.4.5) (Fig. 3.15). An assumption was made that the viabilities of the inoculum cultures were not significantly different. This assumption was based on the lack of significant differences observed between strain viabilities in adjacent time points of the survival assays from which the inocula were derived.

Resuscitation of normoxic HdB (0.04% glycerol) stasis cultures indicated no significant differences in strain resuscitation characteristics, indicating dispensability of $RafS_{Msm}$ (Fig 3.14). Resuscitation of normoxic HdB (0 % glycerol), hypoxic LBT and hypoxic HdB (0.04% glycerol) stasis cultures also showed no apparent differences in resuscitation of all strains (Appendix Fig. 2). In the latter three experiments, two replicates per strain were obtained and further investigation of these conditions was not pursued since the data indicated that resuscitation was successful for all strains.

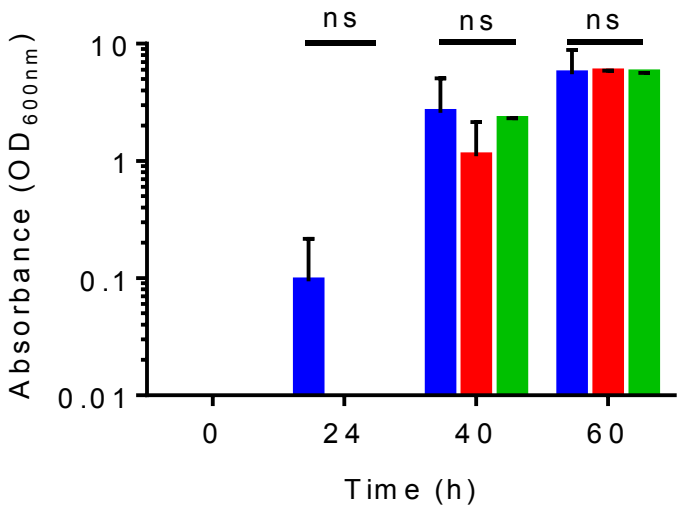

Figure 3.15. $RafS_{Msm}$ is dispensable during resuscitation of aged normoxic HdB stasis cultures in rich media (normoxia). Wild type *M. smegmatis* (blue), *Δ$rafS_{Msm}$1*(red) and *Δ$rafS_{Msm}$c* (green) day 65 0% glycerol, 0.02% Tyloxapol HdB normoxic aged cultures (3 biological replicates per strain) were resuscitated by sub-culturing 1 ml of each culture to fresh LBT medium and monitoring growth in normoxic conditions. Means were compared using one-way ANOVA with Holm-Šídák multiple comparison test; ns: non-significant p-value > 0.05.

3.6 Investigating the role of $RafS_{Msm}$ in competitive survival

We next investigated whether *rafS*$_{Msm}$ deletion affects strain fitness and survival when *ΔrafS*$_{Msm}$ is cultured in competition with wild type *M. smegmatis* (Materials and Methods section 2.4.6). The *ΔrafS*$_{Msm}$ strain (Hyg^R) was distinguished from the wild type in a mixed population by CFU enumeration using selective agar containing hygromycin. The LBT competition assay indicated no significant differences in strain survival (Fig. 3.16).

The HdB assay also indicated a trend of no significant difference in strain survival, other than at day 6 when *ΔrafS*$_{Msm}$ mutant survival was significantly lower than wild type (assay with two independent *ΔrafS*$_{Msm}$ mutants $p = 0.002$) (Fig. 3.17 A). Furthermore, I confirmed that this trend was similar upto 33 days with independent *ΔrafS*$_{Msm}$ mutant 3 (plotted separately, but derived from same experiment as Fig 3.18 A; day 6 $p = 0.0065$)) (Fig. 3.17 B). Taken together, the data from the LBT and HdB competition assays indicated that $RafS_{Msm}$ is dispensable for competitive survival in 27 days of rich stasis and in 32 days of carbon-limited normoxic stasis.

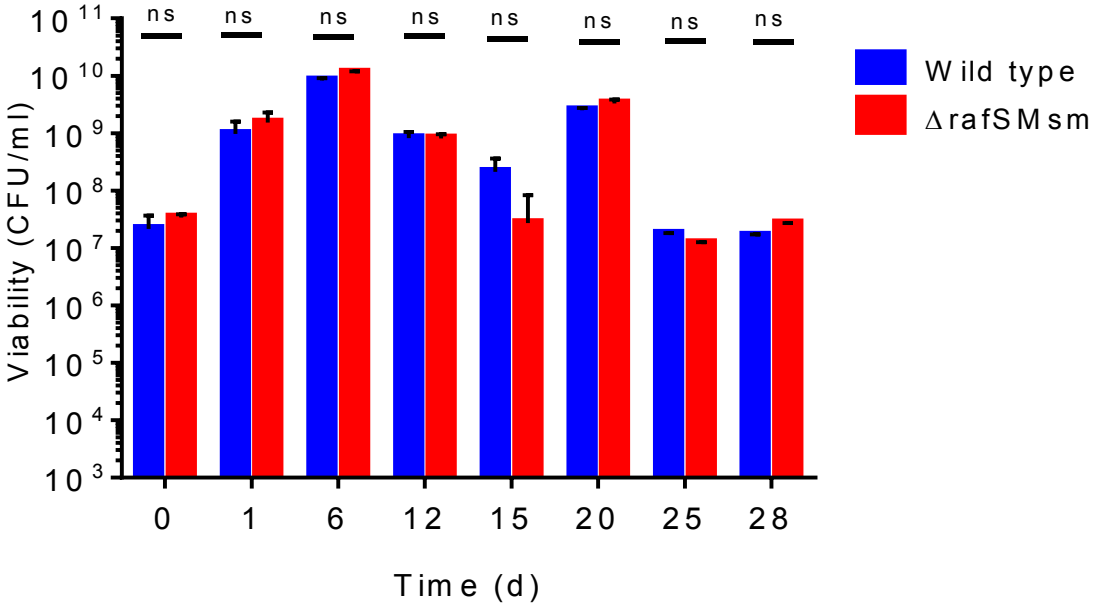

Figure 3.16. $RafS_{Msm}$ is dispensable during 28 day competitive LBT growth and stasis (normoxia). *M. smegmatis* wild type (3 biological replicates) and two independently constructed *Δ$rafS_{Msm}$* mutants (3 biological replicates each of *Δ$rafS_{Msm}$* mutants 2 and 3) were cultured to stasis in LBT media (3h duration), mixed in equal amounts and the mixture was subcultured to LBT media and incubated at 37°C. CFU readings were obtained on LB agar (total count) or LB agar with 50 µg/ml hygromycin (*Δ$rafS_{Msm}$* count). Day 0 indicates the CFU reading taken after subculturing strains from LBT stasis to LBT media, prior to long-term incubation. Average CFU values are indicated. Error bars indicate standard deviation. Means were compared using one-way ANOVA with Holm-Šídák multiple comparison test; ns: non-significant p-value > 0.05.

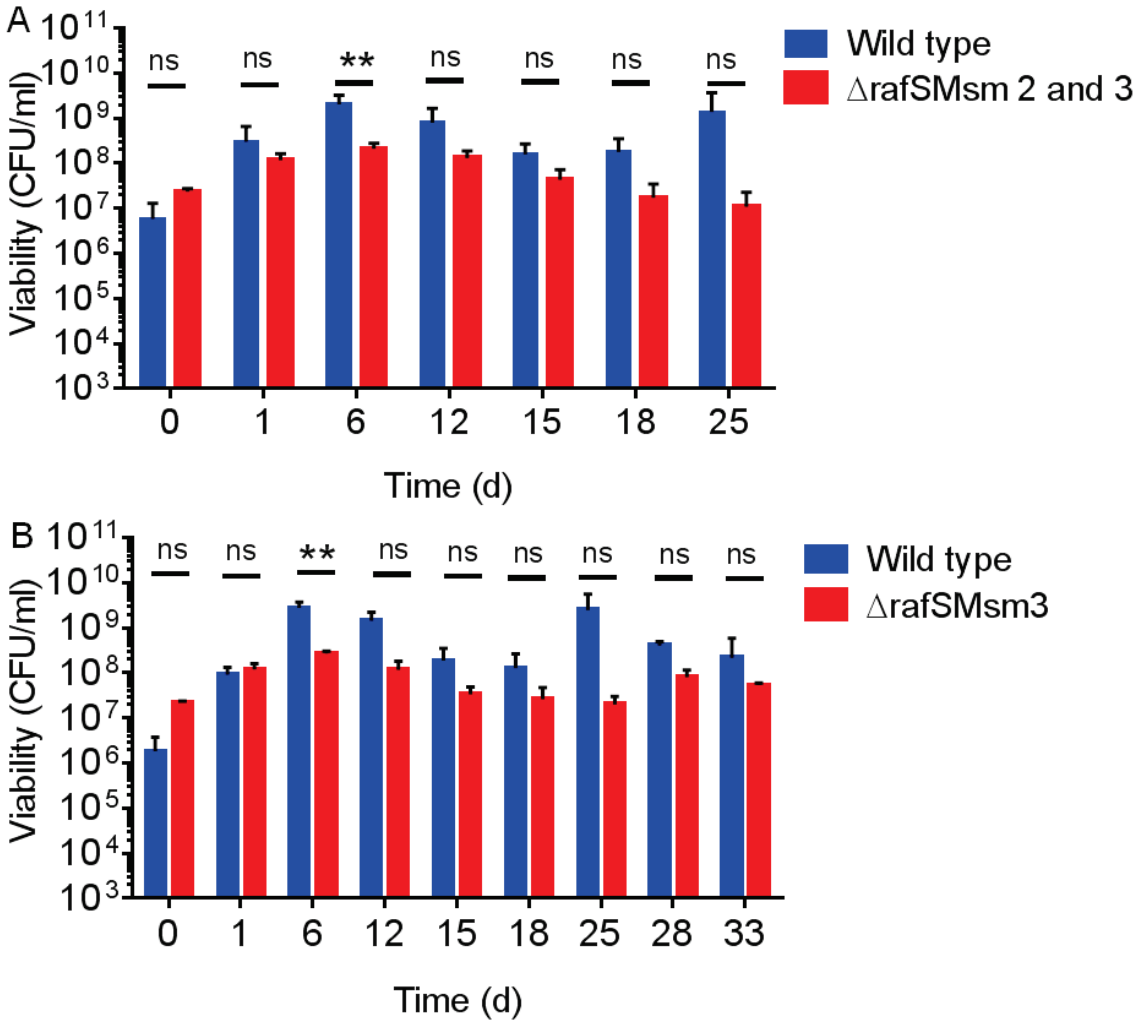

Figure 3.17. $RafS_{Msm}$ is dispensable for survival during 25 - 33 day competitive HdB growth and stasis (normoxia). (A) 25 day competition assay with *Δ$rafS_{Msm}$* mutants 2 and 3 (3 biological replicates each). *M. smegmatis* wild type (3 biological replicates) and two independently constructed *Δ$rafS_{Msm}$* mutants (3 biological replicates each of *Δ$rafS_{Msm}$* mutants 2 and 3) were cultured to stasis in LBT media (3 h duration), mixed in equal amounts and the mixture was subcultured to LBT media and incubated at 37^{o}C, 150 rpm. CFU readings were obtained on LB agar (total count) or LB agar with 50 µg/ml hygromycin (Δ*$rafS_{Msm}$* count). (B) 33 day competition assay with *Δ$rafS_{Msm}$* mutant 3 (3 biological replicates) derived from experiment described in (A). Average CFU values are indicated. Error bars indicate standard deviation. Means were compared using one-way ANOVA with Holm-Šídák multiple comparison test; ns: non-significant p-value > 0.05 ; ** : very significant p = 0.001 to 0.01.

3.7 Role of $RafS_{Mtb}$ in *M. tuberculosis* physiology

3.7.1 Construction of *Δ$rafS_{Mtb}$* mutants

Δ$rafS_{Mtb}$ deletion mutants were constructed in order to investigate key conditions informed by *M. smegmatis* investigations. The mycobacterial recombineering strategy for construction of *Δ$rafS_{Mtb}$* is summarised in Fig 3.18 G. Upstream and downstream regions (1014 bp *$rafS_{Mtb}$* UR and 987 bp *$rafS_{Mtb}$* DR, respectively) flanking the *Δ$rafS_{Mtb}$* (Rv3241c) gene were amplified by PCR of wild type *M. tuberculosis* genomic DNA using primers 3241upF, 3241upR, 3241dnF, 3241dnR (Table 2.3), (Fig. 3.18 A, B). Bacterial strain, plasmid and primer details are given in Materials and Methods tables 2.1., 2.2 and 2.3, respectively.

The PCR products were cloned into PCR®-4Blunt-TOPO (Invitrogen) and amplified in *E. coli* GM2163 cells. The *$rafS_{Mtb}$* DR was cloned between XbaI and KpnI restriction sites and the *$rafS_{Mtb}$* UR between SpeI and HindIII restriction sites (Materials and Methods sections 2.3.3, 2.3.4). For construction of the linear AES, the UR and DR inserts were digested from TOPO/ *$rafS_{Mtb}$* UR and TOPO/ *$rafS_{Mtb}$* DR, respectively (Materials and Methods section 2.3.7) (Fig 3.18 C, D).

The *$rafS_{Mtb}$* UR was ligated to linear pYUB854 digested with SpeI and HindIII. The resulting pYUB854/ *$rafS_{Mtb}$* UR plasmids were isolated and digested with SpeI and HindIII to confirm the presence of the UR (Fig 3.18 E). The DR insert was ligated to linear pYUB854/*$rafS_{Mtb}$* UR. pYUB854/*$rafS_{Mtb}$* UR/DR plasmids were digested to confirm UR and DR presence (Fig. 3.18 F). The pYUB854/*$rafS_{Mtb}$* UR/DR plasmid was digested with KpnI and SpeI to obtain the *$rafS_{Mtb}$* linear AES (4135 bp).

The recombineering helper plasmid pJV53 was electroporated into wild type *M. tuberculosis*. 0.2% w/v acetamide was used to induce expression of gp60 and gp61, which assist in recombination of the AES with the bacterial genome. The *rafS*$_{Mtb}$ AES was electroporated into acetamide-induced electrocompetent H37Rv:pJV53 cells. Hyg^R colonies were obtained on hygromycin plates (Materials and Methods section 2.3.6).

Several attempts were made to screen electroporation colonies with a single PCR covering the entire Hyg^R cassette, *rafS*$_{Mtb}$ upstream and downstream regions and peripheral regions to show successful replacement of the *rafS*$_{Mtb}$ gene with the Hyg^R cassette. Since these attempts were unsuccessful, I employed two colony PCRs which amplified the region surrounding the *rafS*$_{Mtb}$ DR region (Fig 3.18 A2, B3). Genomic DNA from 8 Hyg^R colonies from the electroporation plates was extracted as described (Materials and Methods section 2.3.1, 2.3.2). Regions surrounding the *rafS*$_{Mtb}$ downstream region (4135 bp; *ΔrafS*$_{Mtb}$ and 2888 bp; wild type) were amplified by PCR with the primers indicated (Fig 3.19).

PCR products from 5 colonies indicated *rafS*$_{Mtb}$ AES insertion (Fig. 3.19 A1). In these colonies, the wild type *rafS*$_{Mtb}$ gene was absent (Fig. 3.19 B1), whereas the positive control with wild type genomic DNA confirmed that the latter PCR was successful (Fig. 3.19 B2). Taken together, the analyses confirmed construction of 5 independent *ΔrafS*$_{Mtb}$ mutants, which were named *ΔrafS*$_{Mtb}$ 2, 3, 4, 5 and 6. I attempted to complement *ΔrafS*$_{Mtb}$ mutants 2 and 3 by inserting plasmid pMV361/ *ΔrafS*$_{Mtb}$, but was unable to unmark the *ΔrafS*$_{Mtb}$ mutants for this purpose, since the recombineering helper plasmid, pJV53 (Kan^R) was not lost despite 7 passages on plain 7H11 agar without kanamycin.

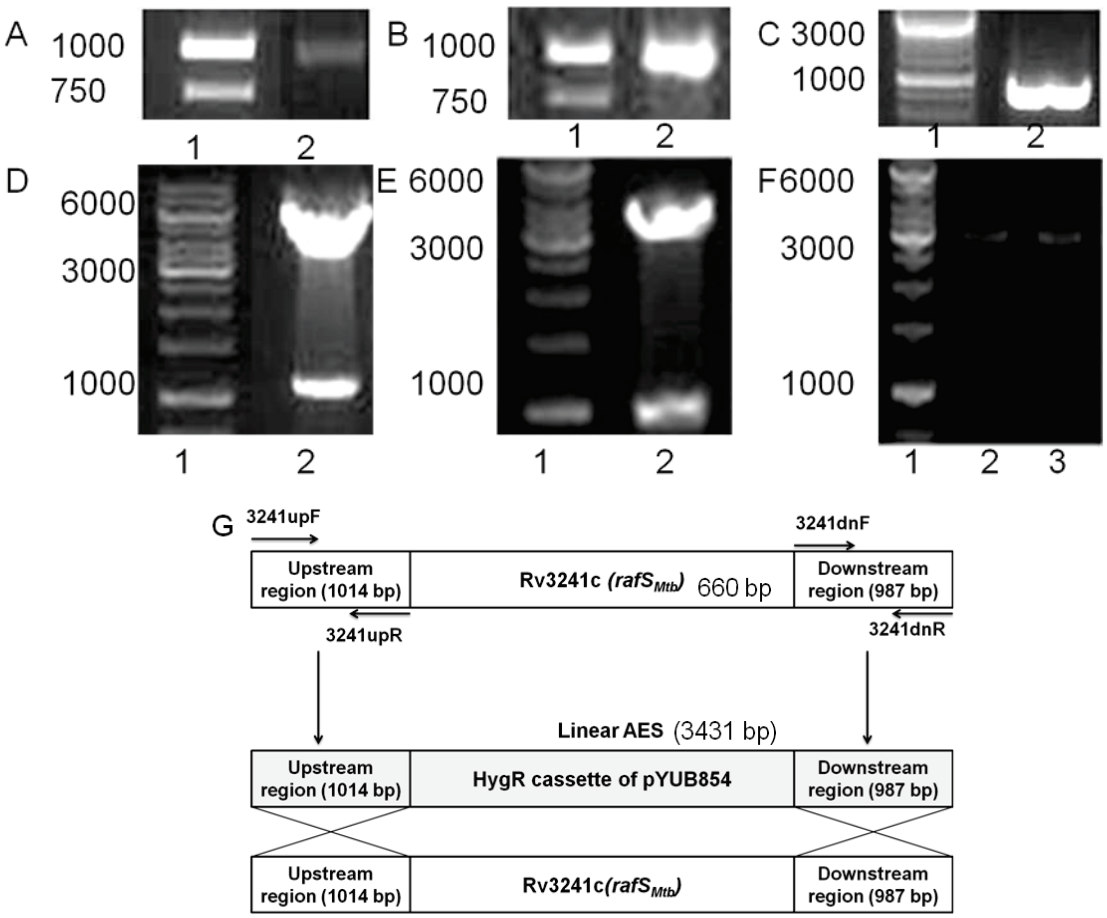

Figure 3.18. Gel electrophoresis analyses during construction of *ΔrafS*$_{Mtb}$ by mycobacterial recombineering. (A, B) PCR amplification of *rafS*$_{Mtb}$ upstream (UR) (A lane 2) and *rafS*$_{Mtb}$ downstream (DR) (B lane 2) regions. (C, D) Digest confirmation of *rafS*$_{Mtb}$ UR (C lane 2) and PCR confirmation of DR (D lane 2) inserts in TOPO vectors. (E) Digest confirmation of presence of UR insert in pYUB854/ rafS$_{Mtb}$ UR prior to DR insertion (lane 2). (F) Digest confirmation of *rafS*$_{Mtb}$ UR (lane 2) and DR (lane 3) in the linear allelic exchange substrate. DNA ladder and band sizes in bp are indicated in lane 1 of each panel. DR digestions were carried out with XbaI and KpnI UR digestions with SpeI and HindIII (G) Mycobacterial recombineering strategy for constructing *ΔrafS*$_{Mtb.}$ Upstream and downstream regions flanking Rv3241c (*rafS*$_{Mtb}$) were amplified and a double stranded linear allelic exchange substrate (AES) (gray) carrying a hygromycin resistance cassette was constructed and exchanged with endogenous Rv3241c. Primer names are indicated adjacent to arrows.

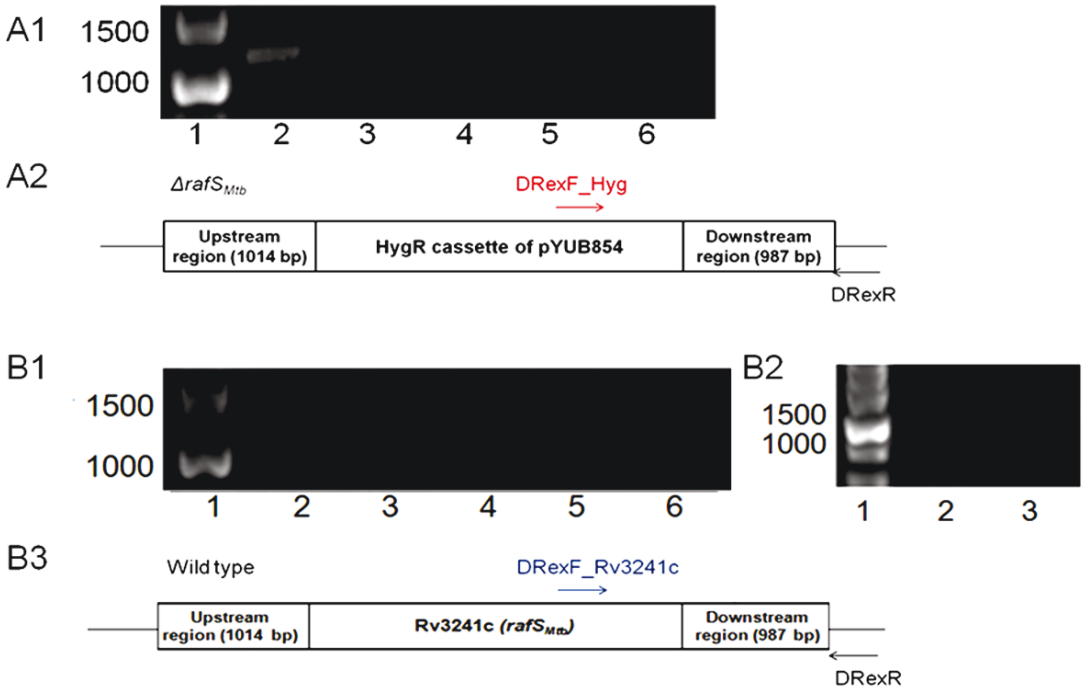

Figure 3.19. PCR confirmation of *rafS*$_{Mtb}$ deletion in *ΔrafS*$_{Mtb}$ 2, 3, 4, 5 and 6. The *rafS*$_{Mtb}$ AES (allelic exchange substrate) was electroporated into acetamide-induced electrocompetent *M. tuberculosis* H37Rv:pJV53 cells and genomic DNA was extracted from eight resulting Hyg^{R} colonies (colonies 2 to 6 are indicated in lanes to 2 to 6 of panels A1 and B1). Colony PCRs were employed to amplified the region surrounding the *rafS*$_{Mtb}$ DR region as shown in A2 and B3. (A1) Confirmation of *rafS*$_{Mtb}$ AES insertion (1168 bp PCR products) (lane 2). (B1) Confirmation of absence of the *rafS*$_{Mtb}$ gene (1201 bp PCR products absent) (lane 2). (B2) Confirmation of presence of *rafS*$_{Mtb}$ in a positive control PCR of *M. tuberculosis* H37Rv wild type genomic DNA (1201 bp PCR product present in B2 lane 2 and absent in no template negative control in lane 3). DNA ladder and band sizes in bp are indicated in lane 1 of each panel.

3.7.2 Role of $RafS_{Mtb}$ in active growth and in competitive survival

M. tuberculosis is known for its slow growth. In optimal laboratory growth conditions, a doubling time of 16 hours can be achieved, whereas in the human host, growth rates are dependent on the site and stage of infection. Active replication is characteristic of the acute phase of infection which precedes the persistent state. (Beste *et al*., 2009). I investigated the role of $RafS_{Mtb}$ in active growth of *M. tuberculosis* in 7H9 rich media (normoxia) (Materials and Methods section 2.4.13).

The 7H9 media contained glycerol, glutamic acid, oleic acid, bovine serum albumin and glucose which are potential carbon sources. It also contains the co-factor biotic and sodium citrate which facilitates citrate-mediated iron transport. The data indicated an overall trend of no apparent differences in strain growth characteristics other than between days 1 and 3 when a higher growth rate was observed for the wild type compared to $\Delta rafS_{Mtb}$ mutant (Fig. 3.20).

Since this trend did not continue, we concluded that there was no significant growth defect of the $\Delta rafS_{Mtb}$ mutants. It was observed that gas bubbles were exclusively present in all $\Delta rafS_{Mtb}$ mutant cultures and absent from the wild type cultures, indicating that the effect $rafS_{Mtb}$ deletion on $\Delta rafS_{Mtb}$ mutant metabolism warrants further investigation.

We next investigated the effect of $rafS_{Mtb}$ deletion on competitive survival in 7H9 rich normoxic stasis (Materials and Methods sections. 2.4.6, 2.4.14) (Fig 3.21). Given that the strains did not grow sufficiently in HdB media, we limited the investigation to 7H9 rich media. There were several difficulties in obtaining CFU data and this was due to agar dehydration during incubation which affected cell growth.

Towards the end of the assay, this problem was resolved by using thicker agar plates. Complete time points obtained were plotted and the experiment was discontinued beyond the time frame indicated due time limitations.

For the final time points obtained, we observed significantly higher wild type viabilities compared to *ΔrafS*$_{Mtb}$ (Assay 1, day 164 p = 0.0025, Assay 2 day 238 p = 0.0003) (Fig 3.21 A and B). The data thus far indicated that RafS$_{Mtb}$ is dispensable for normoxic active growth and plays a role in survival in 228 day normoxic competitive stasis in *M. tuberculosis* in rich medium. Further time points are needed to characterise the *ΔrafS*$_{Mtb}$ competitive survival defect.

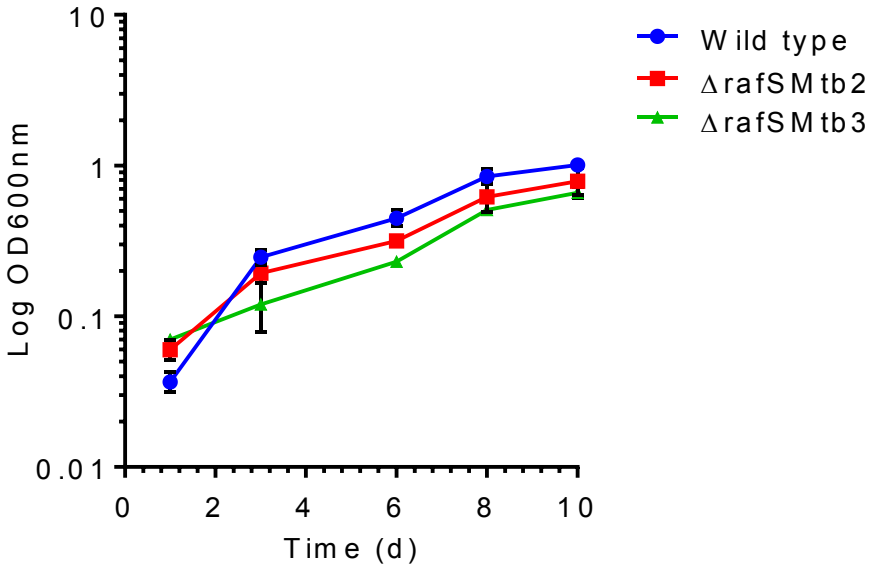

Figure 3.20. $RafS_{Mtb}$ is dispensable for growth of *M. tuberculosis* in rich 7H9 medium (normoxia). *M. tuberculosis* wild type H37Rv and two independently constructed *Δ$rafS_{Mtb}$* mutants were cultured in 7H9 medium at 37^{o}C, 125 rpm for 10 days. The strains were subcultured to 7H9 medium and growth of wild type H37Rv (3 biological replicates) and two independently constructed *Δ$rafS_{Mtb}$* mutants (3 biological replicates each of *Δ$rafS_{Mtb}$* mutants 2 and 3) and incubated at 37^{o}C, 125 rpm for 10 days. Growth was monitored at intervals indicated. Average optical density (OD600nm) is plotted. Error bars indicate standard deviation.

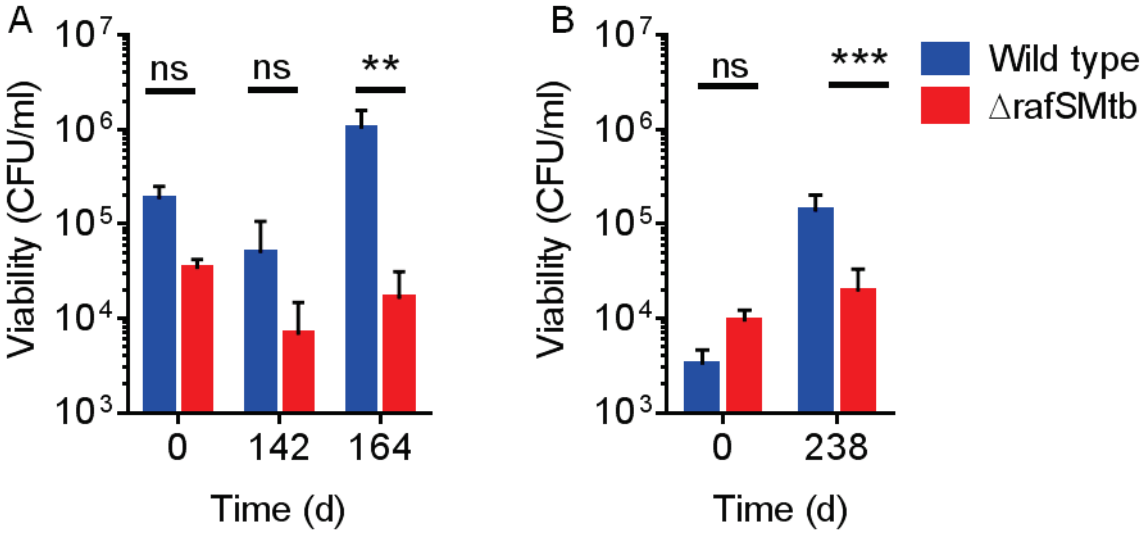

Figure 3.21. $RafS_{Mtb}$ plays a role in maintaining viability during competitive survival in normoxic 7H9 rich stasis (*M. tuberculosis* wild type versus *Δ$rafS_{Mtb}$* survival competition. *M. tuberculosis* H37Rv wild type (3 biological replicates) and two independently constructed *Δ$rafS_{Mtb}$* mutants (3 biological replicates each of *Δ$rafS_{Mtb}$* mutants 2 and 3) were cultured to stasis in 7H9 media (10 day duration), mixed in equal amounts and the mixture was subcultured to 7H9 media and incubated at 37°C. CFU readings were obtained on 7H11 agar (total count) or 7H11 agar with 50 µg/ml hygromycin (*Δ$rafS_{Mtb}$* count). (A) and (B) indicate independent experiments. Average CFU values are indicated. Error bars indicate standard deviation. Means were compared using one-way ANOVA with Holm-Šídák multiple comparison test; ns: non-significant p-value > 0.05; ** very significant p = 0.001 to 0.01; *** : extremely significant p = 0.0001 to 0.001).

3.8 RafS physiological findings: discussion

The findings presented thus far indicate that $RafS_{Msm}$ is dispensable in several conditions, including active normoxic growth, survival in normoxic and hypoxic stationary phase and stress tolerance. It would be useful to investigate $RafS_{Msm}$ expression levels and *Δ$rafS_{Msm}$* phenotypes in other nutrient starvation conditions, such as nitrogen and phosphate starvation which may then be used to inform further *Δ$rafS_{Mtb}$* characterization. Also, construction and characterization of a *Δ$rafS_{Msm}$ Δ$rafH_{Msm}$* mutant (double knockout) would be useful for investigating whether the deletion of both Raf proteins affects growth, survival and stress tolerance phenotypes.

$RafS_{Mtb}$ was found to play a role in long term survival in competitive normoxic stasis. Regarding the latter finding, a more detailed study is required to investigate the *Δ$rafS_{Mtb}$* competitive survival defect, particularly beyond day 142. Furthermore, these findings suggest that carrying out longer term competition assays may be worthwhile for $RafS_{Msm}$ characterization. For both genes, proteomic data will be useful to determine under which conditions Raf proteins are expressed.

Also, it remains to be investigated as to whether $RafS_{Mtb}$ plays a role in metabolism during active growth, given that bubbles were observed in *Δ$rafS_{Mtb}$* rich medium cultures. Further investigations will be needed to determine whether $RafS_{Msm}$ and $RafS_{Mtb}$ have different roles in *M. smegmatis* and *M. tuberculosis* respectively or whether some phenotypes overlap and are common to both genes. The findings in this chapter are discussed further in Chapter 5.

Chapter 4: RafS protein characteristics and effects on ribosome translation and subunit association

4.1 RafS protein characteristics and effects on ribosome translation and subunit association: aims

$RafS_{Msm}$ and $RafH_{Msm}$ had been found to bind *M. smegmatis* ribosomes during stasis (Trauner, 2010). Also, given the presence of the S30AE ribosome-binding domain in Raf proteins and the function of PY (an S30AE protein and RSF in *E. coli*), we aimed to investigate the hypothesis that RafS is a ribosome stabilisation factor in mycobacteria. For this purpose, the following were carried out:

1. Analysis of $RafS_{Msm}$ and $RafS_{Mtb}$ protein bioinformatic features and comparison to those of $RafH_{Msm}$ and $RafH_{Mtb}$.
2. Expression and purification of Raf proteins for biochemical assays.
3. Investigation of the effect of $RafS_{Msm}$ and $RafH_{Mtb}$ proteins on *in vitro* translation of *M. smegmatis* ribosomes.
4. Investigation of the role of $RafS_{Msm}$ in *M. smegmatis* ribosome subunit association.

4.2 Bioinformatic analysis of RafS proteins

4.2.1 Bioinformatic analysis of RafS proteins: aims

The following bioinformatic features of $RafS_{Msm}$ and $RafS_{Mtb}$ proteins were investigated:

1. taxonomical prevalence of $RafS_{Mtb}$-related proteins
2. conserved domain identification of RafS proteins
3. protein sequence alignment comparison of RafS and RafH proteins
4. predicted protein structures : structural comparison of RafS, RafH and *E. coli* PY and/or HPF
5. disordered and protein-binding regions of RafS proteins
6. putative N and C terminal domain regions and inter-domain linker regions of RafS proteins

4.2.2 RafS protein taxonomical coverage, conserved domain identification and sequence alignment analyses

Raf proteins are classified as “long HPFs” (hibernation promoting factors) due to their long C terminal extensions which differs from “short HPFs”, such as PY of *E. coli,* which contain shorter C terminal extensions (Trauner, 2010). The predicted molecular weights of $RafS_{Msm}$ and $RafS_{Mtb}$ proteins are 26.40 kDa and 24.53 kDa, respectively (ProtParam, Expasy). Further characteristics of Raf proteins, such as predicted stability and theoretical isoelectric point are listed in Appendix Table 3. We investigated the bioinformatic features of $RafS_{Msm}$ and $RafS_{Mtb}$ proteins including taxonomical coverage**,** conserved domain identification and sequence alignment.

Analysis of taxonomical coverage of RafS-related proteins was carried out based on the protein sequence of $RafS_{Mtb}$ (Rv3241c). This indicated predominant prevalence of RafS-related proteins in bacterial genera. There were 3792 RafS-related proteins in bacteria, 73 in cyanobacteria and 48 in eukaryotes (TB database) (Fig. 4.1 A). Phylogenetic analysis of Raf proteins indicated close phylogenetic similarity of $RafS_{Mtb}$ and the RafS homologue of *M. bovis,* which is an uncharacterized protein to date (MUSCLE-EBI) (Fig. 4.1 B). Notably, a RafS homologue is present in *M. leprae*, a mycobacterial species known for its conservative genome, whereas RafH is absent in *M. leprae*.

For $RafS_{Msm}$ and $RafS_{Mtb}$, conserved domains were found within both N terminal regions of $RafS_{Msm}$ (residues 30 to 145) and $RafS_{Mtb}$ (residues 15 to 110). The RafS conserved domains were the RaiA (ribosome associated inhibitor A) domain, yfiA (ribosome subunit interface protein), ribosome associated protein Y (Psrp-1) and the S30AE ribosome binding domain/sigma 54 modulation protein

(DELTA-BLAST) (Figure 4.2 A, B). Psrp-1 is a protein of unknown function found in the cyanobacterium Synechococcus PCC 7002 that is encoded by a light-repressed transcript whose expression was suppressed in the presence of light (Tan *et al*., 1994). NCBI DELTA-BLAST also indicated that 22 putative 30S ribosome subunit-binding sites were present within the putative S30AE domains of each RafS protein.

RafS and RafH protein sequence alignment (4 in total) indicated 69% protein sequence similarity between RafS and RafH proteins (EBI Clustal *Omega* alignment, percentage similarity obtained from T-Coffee 11) (Fig. 4.3 A). RafH protein sequences showed longer C-terminal extensions than RafS proteins. $RafS_{Msm}$ and $RafS_{Mtb}$ protein sequence alignment indicated 98% protein sequence similarity (EBI Clustal *Omega* alignment, percentage similarity obtained from T-coffee 11) (Fig. 4.3 B). Two regions of protein sequence dissimilarity between the RafS protein sequences were observed (Regions 1 and 2, Fig. 4.3 B). It remains to be understood as to whether these regions play a role in determining functional differences between $RafS_{Msm}$ and $RafS_{Mtb}$ proteins.

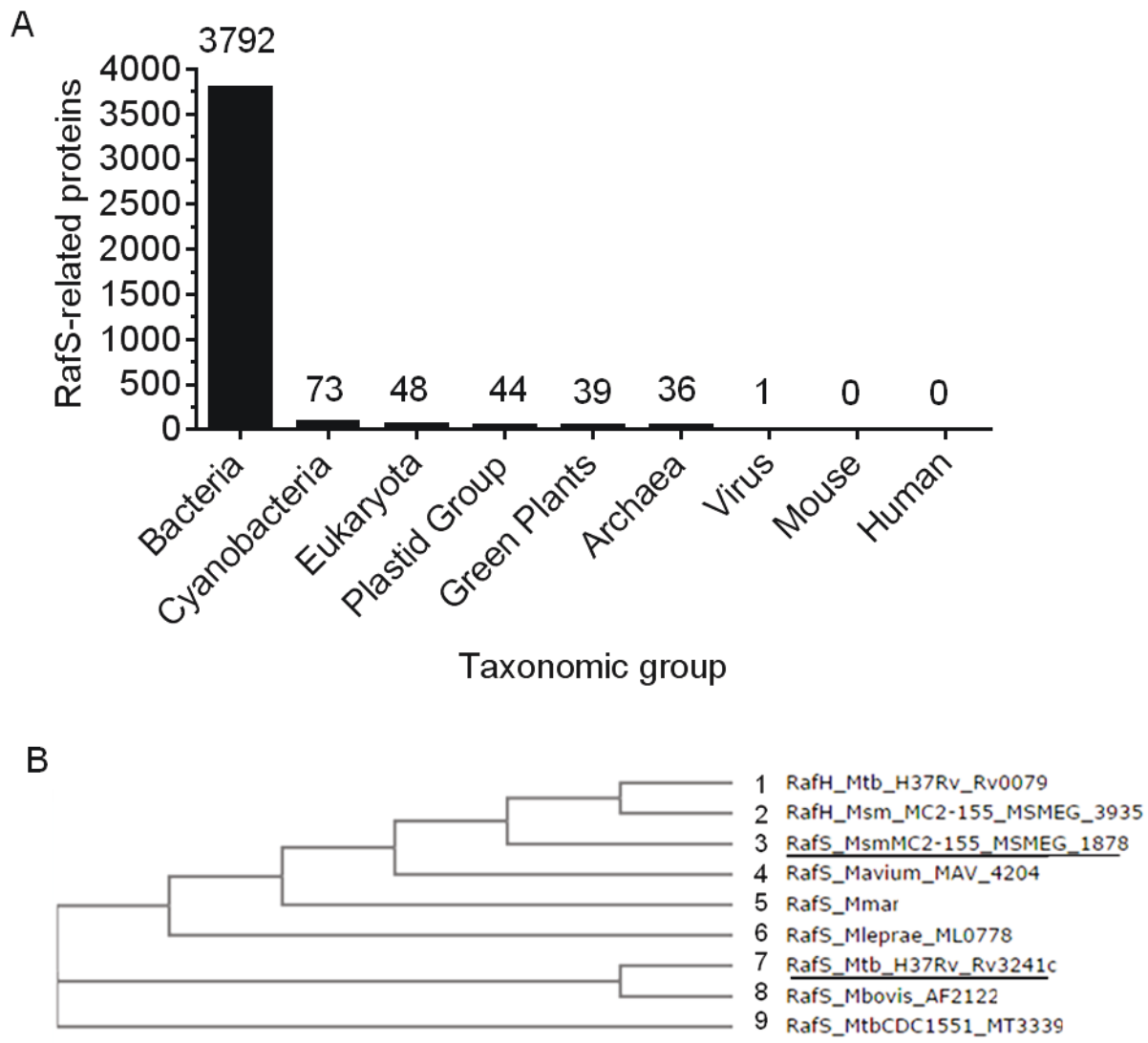

Figure 4.1. Taxonomic prevalence and phylogenetic similarity of RafS-related proteins (A) Taxonomic prevalence of RafS-related proteins based on protein sequence of Rv3241c ($RafS_{Mtb}$) (TB database). (B) Phylogenetic analysis of RafS-related proteins based on multiple sequence alignment (MUSCLE – EBI). RafS proteins investigated in this study are underlined. RafH-related proteins indicated are from the following species/strains; *M. tuberculosis* H37Rv (1), *M. smegmatis* MC2-155 (2). RafS-related proteins indicated are from the following species/strains; *M. smegmatis* MC2-155 (3), *M. avium*. (4), *M. marinum* (5), *M. leprae* (6), *M. tuberculosis* H37Rv (7), *M. bovis* (8) and *M. tuberculosis* CDC1551 (9).

Figure 4.2. Conserved domain analysis of $RafS_{Msm}$ (A) and $RafS_{Mtb}$ (B) protein sequences (NCBI DELTA-BLAST). Amino acid residue numbers are indicated. Brown triangles indicate 30S ribosome-binding sites. Conserved domains are indicated as follows; RaiA (ribosome associated inhibitor A) domain (❶), *yfiA* (ribosome subunit interface protein) (❷), Ribosome associated protein Y (Psrp-1) (❸) and the S30AE ribosome binding domain/sigma 54 modulation protein (❹). Conserved domains indicated were found in the regions of residues 30 - 145 for $RafS_{Msm}$ and 15 - 110 for $RafS_{Mtb}$.

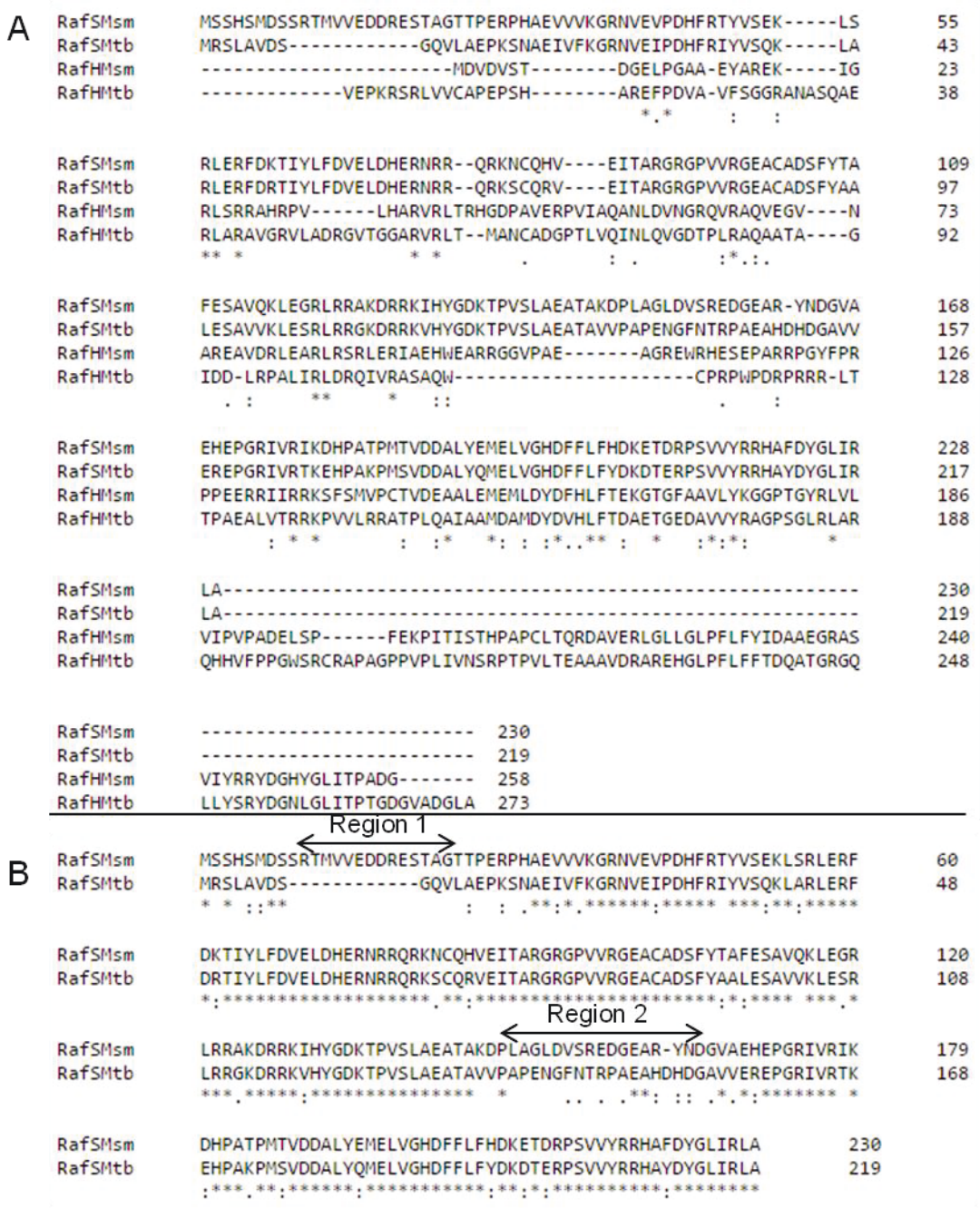

Figure 4.3. RafS and RafH multiple protein sequence alignment (EBI Clustal *Omega* 1.2.1). (A) Alignment of RafS and RafH protein sequences (69% sequence similarity). Sequences of $RafS_{Msm}$, $RafS_{Mtb}$, $RafH_{Msm}$ and $RafH_{Mtb}$ are indicated. (B) $RafS_{Msm}$ and $RafS_{Mtb}$ protein sequence alignment (98% sequence similarity) indicating 2 regions of sequence dissimilarity (Regions 1 and 2). Asterisks (*) indicate identical residues. Asterisks (*) indicate identical residues. Colons (:) indicate conservative substitutions and periods (.) indicate semi-conservative substitutions. Percentage sequence similarity was obtained from T-coffee 11 (EBI).

4.2.3 RafS and RafH: features of predicted protein structures

We investigated RafS and RafH predicted protein structures and compared them to that of PY (*E. coli*). Secondary structure-coloured, N to C terminus progression-coloured and confidence-coloured protein predicted structures of Raf proteins are shown in Figure 4.4. Raf protein predicted structures consisted of N terminal globular domains that adopt a βαββββα topology. For each RafS protein, this domain was found in the region previously defined as the S30AE conserved domain ($RafS_{Msm}$ 30 - 145 and $RafS_{Mtb}$ 15 - 110 of Figure 4.2) (Fig. 4.4 A).

Raf protein N-terminal domains are putative ribosome-binding domains that were predicted with high confidence and appeared structurally similar to that of PY (*E. coli* short HPF homologue) (Fig. 4.4 C). N-terminal Phyre2 and PSPIRED predicted secondary structures for $RafS_{Msm}$ and $RafS_{Mtb}$ agreed with each other (Buchan *et al*., 2013) (Appendix Figures 3 and 4). Raf protein C-terminal domains were predominantly predicted with lower confidence, indicating that similar structures are lacking among existing protein structures. The structural characteristics and roles of the C-terminal domains are yet unknown. A linker joining the N and C terminal domains is apparent in all Raf protein structures (Fig. 4.4 B).

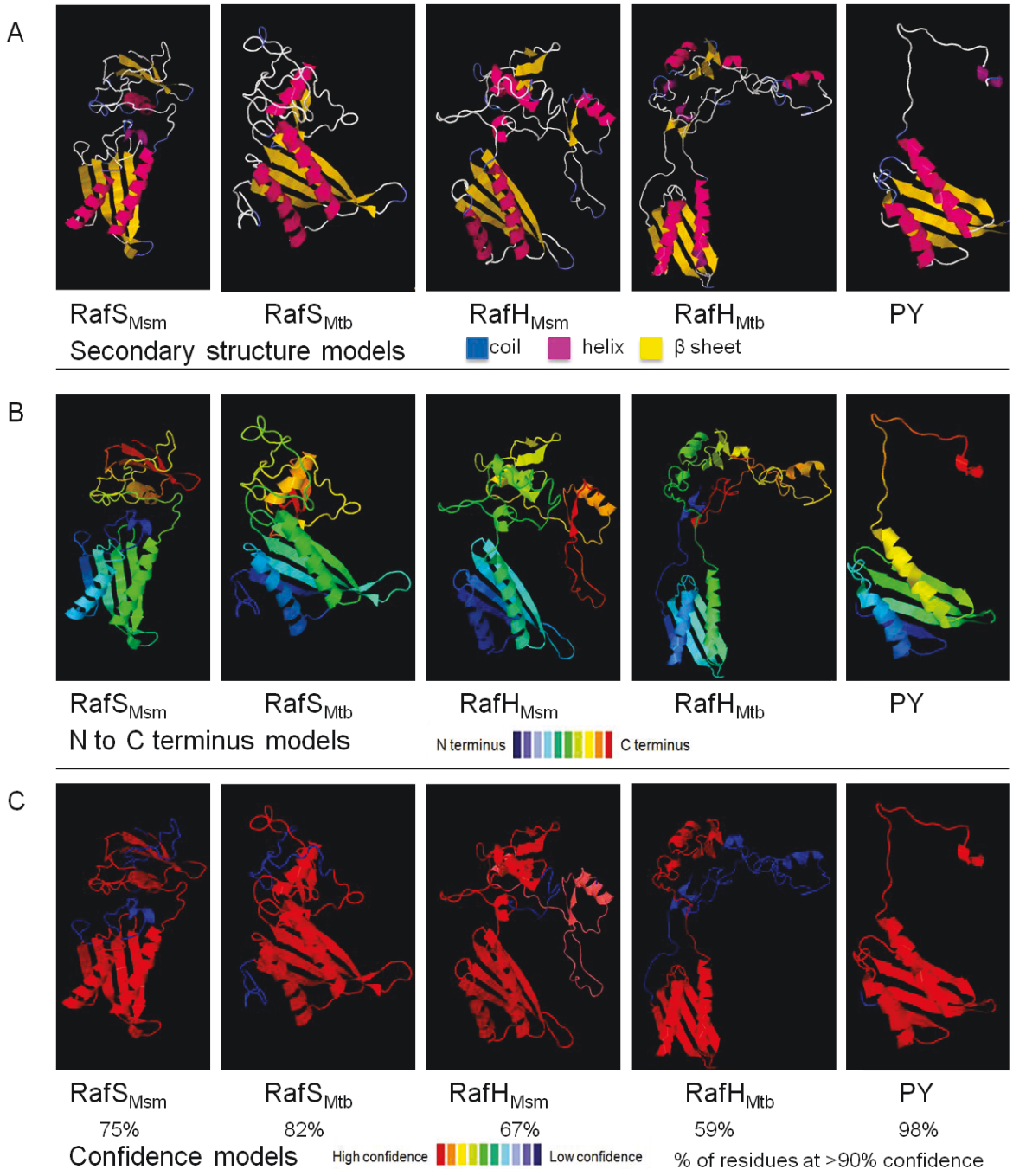

Figure 4.4. Predicted protein structures based on homology modeling of *M. smegmatis and M. tuberculosis* Raf proteins and of PY, an S30AE homologue in *E. coli* (Phyre2, Kelley *et al*., 2009). Models include (A) secondary structure-coloured (B) N to C terminus progression-coloured and (C) confidence-coloured protein structure predictions. Percentage of residues predicted with greater than 90% confidence is indicated. Protein sequences were obtained from Smegmalist, Tuberculist and NCBI online databases.

4.2.4 $RafS_{Msm}$ and $RafS_{Mtb}$: features of predicted protein structures

An overlay of $RafS_{Msm}$ and $RafS_{Mtb}$ predicted protein structures indicated apparent similarity of the N-terminal domain region, which agreed with the similarity observed based on individual structures displayed in Fig 4.4 (Fig. 4.5 A). Also, an overlay of $RafS_{Msm}$ and $RafS_{Mtb}$ predicted protein structures with those of $RafH_{Msm}$, HPF and PY (the latter two are *E. coli* homologues) indicated that these structures were predominantly similar at the N-terminal domain region (Fig. 4.5 B).

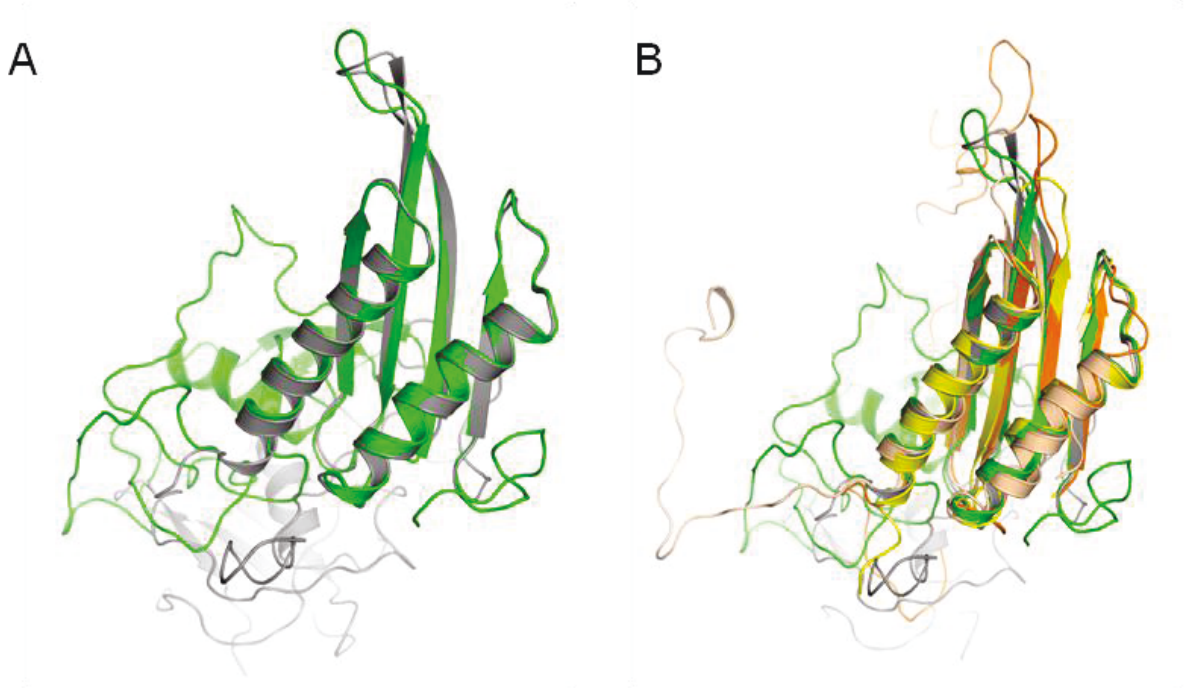

Figure 4.5. Structural overlays of $RafS_{Msm}$ and $RafS_{Mtb}$ predicted protein structures. Predicted protein structures obtained with Phyre2 (Kelley *et al*., 2009) were overlayed with PyMol (The PyMol Molecular Graphics System, Version 1.7.2, Schrodinger, LLC). Images were rendered with depth cuing (fading of posterior structure) for 3D effect. (A) Overlay of $RafS_{Msm}$ (gray) and $RafS_{Mtb}$ (green) predicted protein structures. (B) Overlay of $RafS_{Msm}$ (gray), $RafS_{Mtb}$ (green), $RafH_{Msm}$ (orange), HPF (yellow) and PY (wheat) predicted protein structures.

$RafS_{Msm}$ and $RafS_{Mtb}$ predicted protein structures were further investigated in order to identify putative domain boundaries and disordered and protein binding regions (Fig. 4.5 A). For both RafS proteins, protein-binding disordered regions were predicted at the N terminal starting sequence as follows; $RafS_{Msm}$ 0 – 25 (N1) and $RafS_{Mtb}$ 0 – 10 (N2) (Confidence score > 0.5) (Buchan *et al.*, 2013).

Also, disordered regions were predicted which overlap with predicted inter-domain boundary regions as follows; $RafS_{Msm}$ residues 125 – 175 (L1) and $RafS_{Mtb}$ residues 110 – 150 (L2) predicted disordered regions overlap with $RafS_{Msm}$ residues 125 – 150 (I1) and $RafS_{Mtb}$ residues 105 – 135 (I1) predicted domain boundary regions (Fig. 4.5 A, B). For both RafS proteins, 'N' regions overlapped with 'Region 1' of low protein sequence similarity. Also, predicted disordered and inter-domain boundary regions 'L' and 'I' overlapped with second region of low protein sequence similarity, 'Region 2', (refer to Fig. 4.2B for RafS protein sequence alignment).

Putative inter-domain linker regions identified by alignment termini profiling (region 'I' determined in Fig 4.6 B) were used to identify putative domains of RafS predicted protein structures. Based on this prediction, RafS protein domains were annotated as shown in Fig. 4.7. Binding of $RafS_{Msm}$ and $RafH_{Msm}$ to 30S subunits of stationary phase ribosomes has previously been shown by mass spectroscopy (Trauner, 2010). However, the binding site(s) of Raf proteins on the ribosome and location of Raf protein domains during docking to the ribosome is yet unknown.

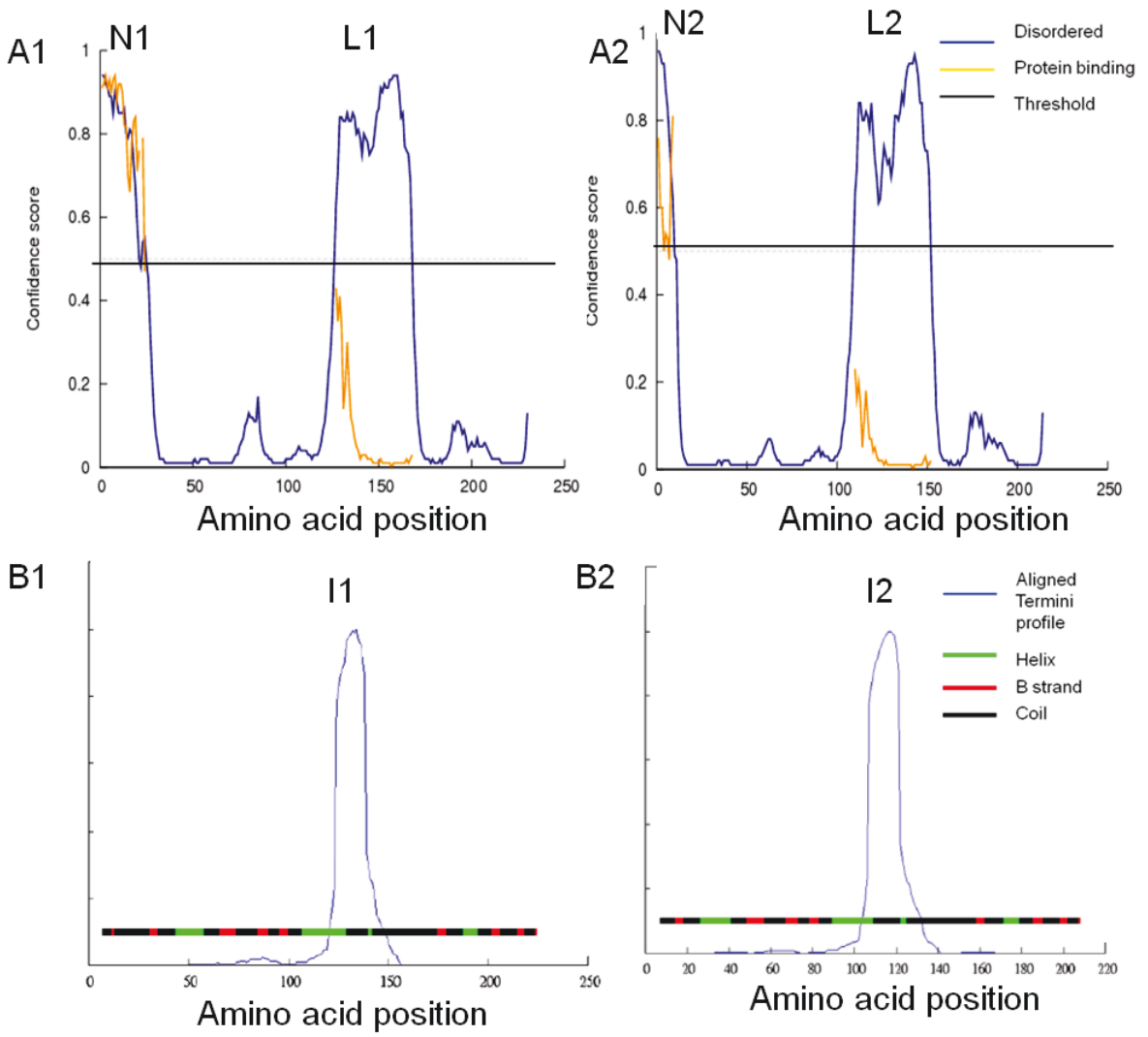

Figure 4.6. Prediction of RafS disordered, protein binding and domain boundary regions (PSPIRED server, Buchan *et al*., 2013). (A) $RafS_{Msm}$ (A1) and $RafS_{Mtb}$ (A2) predicted disordered and protein binding regions. Confidence score is shown on the vertical axis. A confidence score of greater than 0.5 (threshold indicated) is considered to be significant. Predicted protein binding disordered regions are indicated between residues 0 – 25 for $RafS_{Msm}$ (N1) and residues 0 – 10 for $RafS_{Mtb}$ (N2). Predicted disordered regions are indicated between residues 125 – 175 for $RafS_{Msm}$ (L1) and residues 110 – 150 for $RafS_{Mtb}$ (L2). (B) $RafS_{Msm}$ (B1) and $RafS_{Mtb}$ (B2) aligned termini profiles indicating the density of end points of PSI-BLAST alignments and putative domain boundaries. Predicted secondary structure is also indicated. Predicted inter-domain boundary regions are indicated between residues 125 – 150 for $RafS_{Msm}$ (I1) and residues 105– 135 for $RafS_{Mtb}$ (I2).

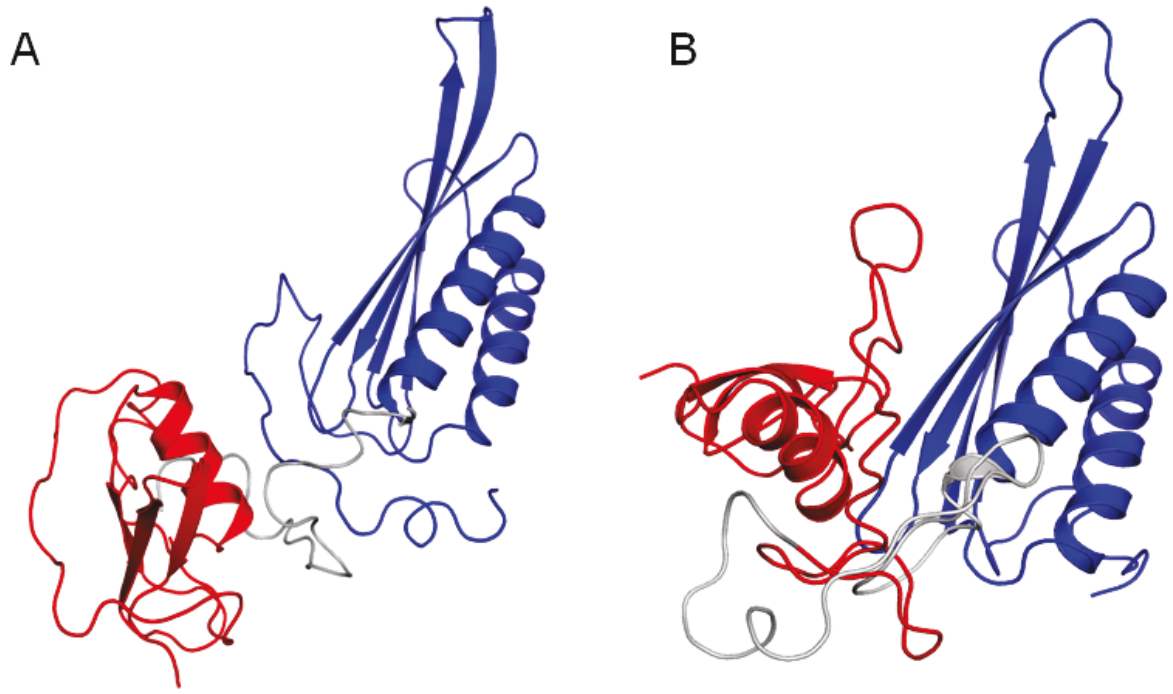

Figure 4.7. RafS protein structures indicating putative domains. Putative linker regions ($RafS_{Msm}$ 125 – 150 and $RafS_{Mtb}$ 105 – 135, shown in gray) were identified using PSPIRED alignment termini profiling (Buchan *et al.*, 2013). Predicted protein structures obtained with Phyre2 (Kelley *et al.*, 2009) were coloured according to domain with PyMol (The PyMol Molecular Graphics System, Version 1.7.2, Schrodinger, LLC). (A) $RafS_{Msm}$ predicted protein structure coloured by putative domain; putative N terminal putative ribosome-binding domain (blue), putative inter-domain linker (gray) and C terminal putative domain (red). (B) $RafS_{Mtb}$ predicted protein structure coloured by putative domain; putative N terminal putative ribosome-binding domain (blue), putative inter-domain linker (gray) and C terminal putative domain (red).

4.2.5 Bioinformatic analysis of RafS proteins: summary

In summary, bioinformatic predictions suggest that $RafS_{Msm}$ and $RafS_{Mtb}$ each contain:

1. a putative ribosome-binding N terminal globular domain of βαββββα topology, identified as the S30AE domain by conserved domain analysis and homologous to the N-terminal domains of $RafH_{Msm,}$ $RafH_{Mtb}$ and PY.
2. a putative N-terminal protein-binding disordered region (corresponding $RafS_{Msm}$ and $RafS_{Mtb}$ sequences differ).
3. a putative disordered inter-domain linker region (corresponding $RafS_{Msm}$ and $RafS_{Mtb}$ sequences differ).
4. a putative C-terminal domain of unknown function.

4.3 Raf protein expression and purification

4.3.1 Raf protein expression and purification: aims and mutant construction

We aimed to purify recombinant His-tagged RafS and RafH proteins for investigating biochemical characteristics of Raf proteins. To achieve this, the initial objective was to construct *E. coli* strains expressing N-terminal His-tagged Raf proteins (with 6 histidine residues), determine optimal conditions for soluble protein expression and carry out protein purification by immobilized metal (Ni^{2+}) ion affinity chromatography (IMAC) to obtain soluble Raf proteins.

The pET15b vector was chosen for induction of Raf protein expression with IPTG and N terminal 6-His tagging of expressed Raf proteins. Also, *E. coli Rosetta™:*pRARE cells (Novagen) were employed as expression strains for the recombinant Raf proteins. The pRARE plasmid carried by the expression strain supplies tRNAs for the codons AUA, AGG, AGA, CUA, CCC and GGA, providing for "universal" translation, to avoid limiting translation codon usage to those supplied by *E. coli.* Bacterial strain, plasmid and primer details are given in Materials and Methods tables 2.1., 2.2 and 2.3, respectively.

Full length gene sequences of Rv0079 ($RafH_{Mtb}$), MSMEG_3935 ($RafH_{Msm}$), Rv3241c ($RafS_{Mtb}$) and MSMEG_1878 ($RafS_{Msm}$) were amplified by PCR from genomic DNA using primers 21 to 30 (Table 2.3). PCR products were sub-cloned into PCR®-4Blunt-TOPO in *E. coli* HB101, between NdeI and BamHI restriction sites. Inserts were confirmed to be of correct size and sequence by colony PCR and sequencing (Beckman Coulter genomics), respectively.

Inserts were digested from PCR®-4Blunt-TOPO with NdeI and BamHI and obtained using gel electrophoresis. The pET15b vector was digested with NdeI and BamHI and inserts were ligated into pET15b and transformed into Rosetta *E. coli.* Colonies with inserts were identified by colony PCR (Fig. 4.8). Sequencing (Beckman Coulter Genomics) was used to confirm that the pET15b vectors with Raf protein expression inserts were 100% correct and in frame with the vector sequence (Fig. 4.9 and 4.10).

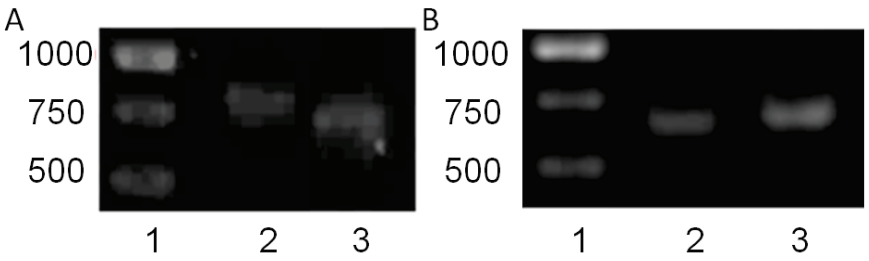

Figure 4.8. Gel electrophoresis confirmation of construction of pET15b vectors containing gene sequences of Raf proteins. (A) Vector inserts obtained by NdeI and BamHI restriction digest of pET15b vectors containing gene sequences of Raf proteins $RafH_{Mtb}$ (lane 2), $RafH_{Msm}$ (lane 3). (B) Vector inserts obtained by NdeI and BamHI restriction digest of pET15b vectors containing gene sequences of Raf proteins $RafS_{Mtb}$ (lane 2), $RafS_{Msm}$ (lane 3). PCR product sizes are $RafH_{Mtb}$ (Rv0079), 822 bp; $RafH_{Msm}$; (MSMEG_3935) 777 bp, $RafS_{Mtb}$ (Rv3241c) 660 bp and $RafS_{Msm;}$ (MSMEG_1878) 693 bp. Bands sizes (bp) are shown from the 1kb ladder (Lanes A1 and B1).

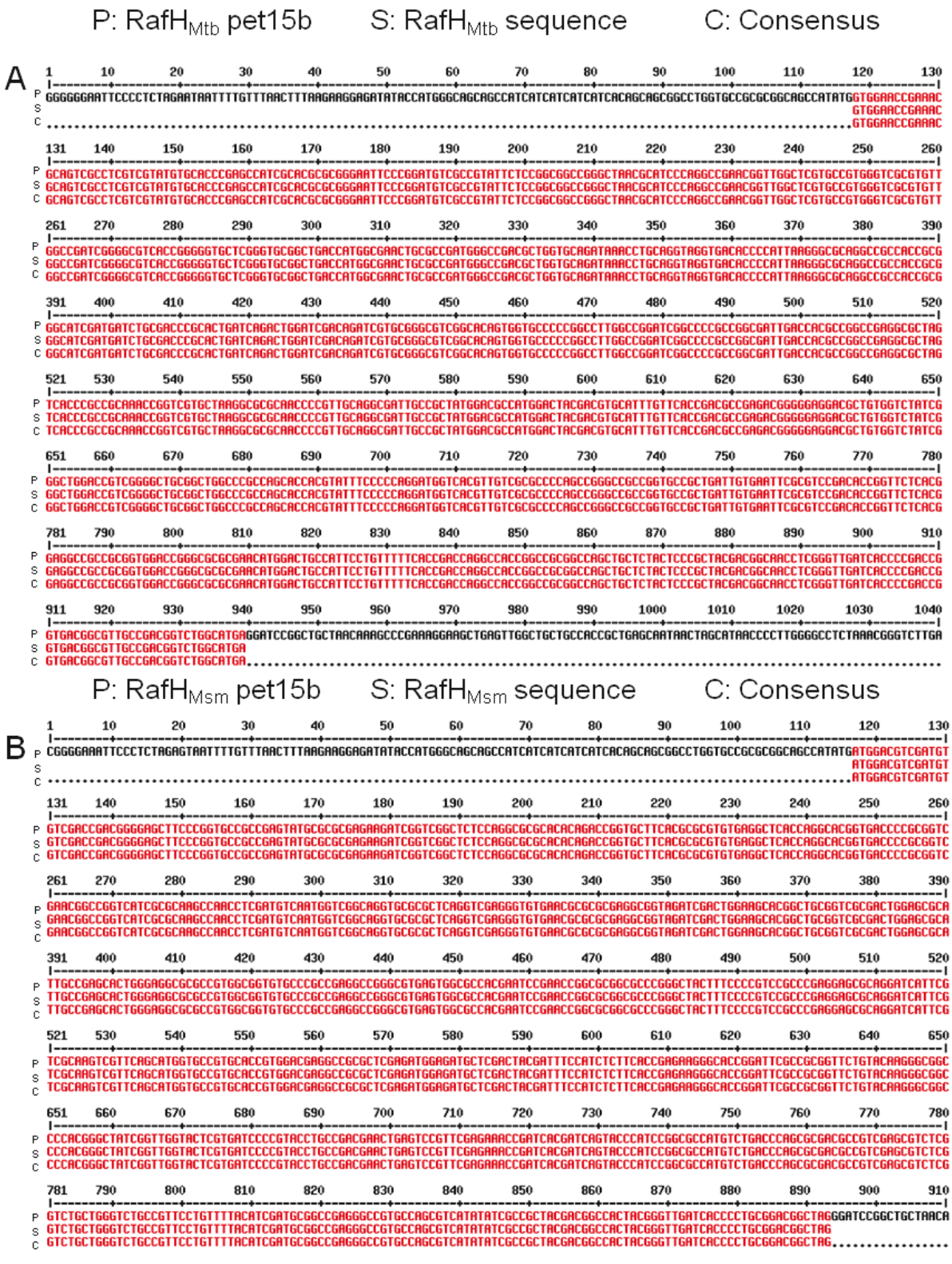

Figure 4.9. Confirmation of correct sequences of (A) RafH$_{Mtb}$ and (B) RafH$_{Msm}$ protein expression inserts of pET15b vectors (Sequencing by Beckman Coulter Genomics). Multiple sequence alignments were carried out with Multalin (Corpet *et al.*, 1988).

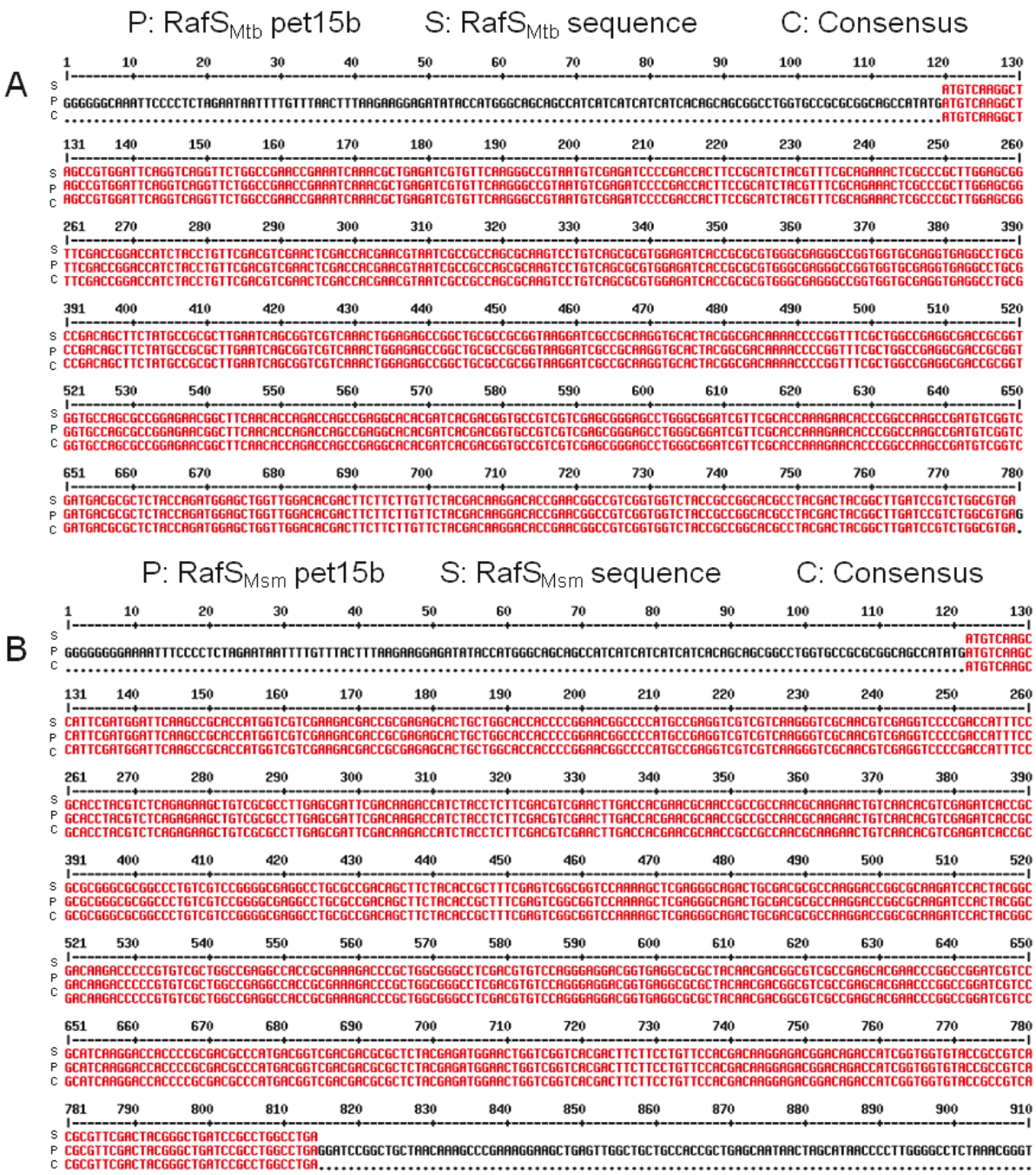

Figure 4.10. Confirmation of correct sequences of (A) RafS$_{Mtb}$ and (B) RafS$_{Msm}$ protein expression inserts of pET15b vectors (Sequencing by Beckman Coulter Genomics). Multiple sequence alignments were carried out with Multalin (Corpet *et al.*, 1988).

4.3.2 RafS and RafH protein expression trials

Expression of Raf protein sequences present on pet15b vectors was induced with IPTG. Recombinant protein induction and SDS-PAGE analysis were carried out as described in Materials and Methods sections 2.5.1, 2.5.2. Soluble Raf proteins were expressed successfully for all strains constructed. Both soluble and insoluble proteins were seen for all strains at 0.1 mM and 1 mM IPTG at 37^{o}C. Raf protein bands were identified by comparing with a control strain carrying the pET15b vector (Fig. 4.11 A). Raf proteins were present in soluble fractions and absent in empty vector control lanes.

The predicted molecular weights of Raf proteins were $RafS_{Msm:}$ 26.4 kDa, $RafS_{Mtb:}$29.47 kDa, $RafH_{Msm}$ 24.53 kDa and $RafH_{Mtb}$: 29.02 kDa. Actual Raf protein gel bands appeared to concur approximately with the predicted sizes (taking into account the additional 1 kDa weight of the His tag), excepting the band for $RafH_{Msm.}$ The protein gel band for $RafH_{Msm}$ was approximately 60 kDa which was twice that as expected (Fig. 4.11 A, B lane 3). It is unclear as to whether the latter finding is an artifact of protein expression or is physiologically relevant. We did not pursue investigating this further due to time limitations. Raf protein predicted physicochemical parameters are listed in Appendix Table 3.

I also attempted Raf protein expression at 18^{o}C overnight to determine whether a lower temperature could enhance the amount of soluble Raf protein expressed by slowing protein folding and thus potentially making the folding more accurate. I was unable to further increase soluble protein expressed using this condition (data not shown). Expression time courses of Raf protein-expressing

strains were carried out as shown in sections 4.3.3 and 4.3.4. In these experiments, relative proportions of soluble to insoluble Raf proteins were compared.

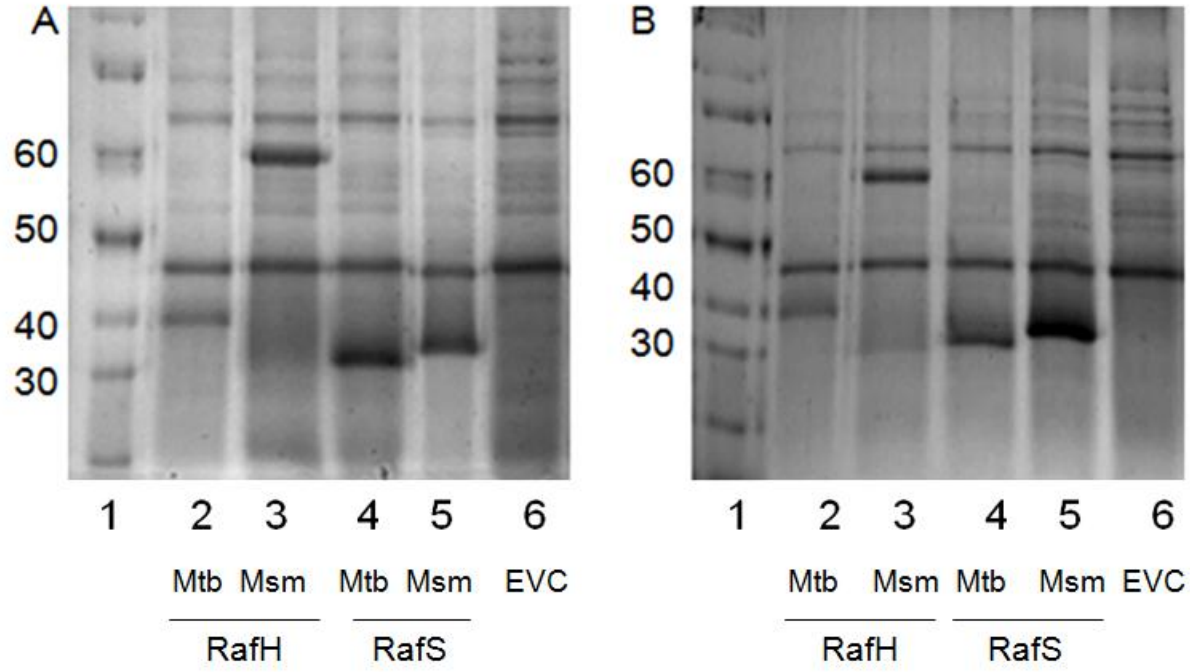

Figure 4.11. SDS-PAGE of soluble protein expression profiles of His-tagged Raf proteins in *E. coli.* His-tagged Raf protein expression was induced with 0.1 mM (A) and 1 mM IPTG (B) for 3 h at 37^{o}C, 220 rpm. Lanes contain soluble protein fractions of strains expressing $RafH_{Mtb}$ (lane 2), $RafH_{Msm}$ (lane 3), $RafS_{Mtb}$ (lane 4), and $RafS_{Msm}$ (lane 5) and empty pET15b vector control (lane 6). Ladder protein weights are indicated in kDa (A and B lane 1). Raf protein migration indicated the following approximate molecular weights; $RafH_{Mtb}$ (40 kDa), $RafH_{Msm}$ (60 kDa), $RafS_{Mtb}$ (32 kDa), and $RafS_{Msm}$ (35 kDa).

4.3.3 $RafS_{Msm}$ purification

I next aimed to determine the optimal time for $RafS_{Msm}$ protein expression. A $RafS_{Msm}$ expression 6 hour (1 mM IPTG) time course assay indicated that the optimal IPTG induction time was 4 - 6 hours (Fig. 4.12). The 4 h time was selected to facilitate carrying out induction and FPLC within 1 working day. The empty vector control indicated that the protein background of the soluble fraction lanes were sufficiently empty in the 30 kDa range where $RafS_{Msm}$ expression was expected (Fig. 4.12).

I employed gradient FPLC to test the elution profile of $RafS_{Msm}$ from 20 mM to 500 mM imidazole. This indicated that the optimal imidazole concentration for removing impurities was 205 mM imidazole (41% buffer B mix). Scaled-up recombinant protein induction (1L cell pellet) and FPLC protein purification were carried out (Materials and Methods sections 2.5.3, 2.5.4). $RafS_{Msm}$ was eluted at 500 mM imidazole i.e. a 24 ml stepwise elution at 100% buffer B (Fig. 4.8 C). The FPLC chromatogram summarizing $RafS_{Msm}$ elution is shown in Fig. 4.13. The SDS-PAGE elution profile of $RafS_{Msm}$ is shown in Fig. 4.14 A. Fractions 3 to 16 were subsequently pooled and concentrated.

Several concentrators showed significant losses when attempting to concentrate $RafS_{Msm}$ (Appendix Table 4). Improved protein concentration was achieved using centrisart concentrators (10 kDa MWCO) (Sartorius) as per the manufacturer's instructions. Centrisart concentrators utilise centrifugation to pull an inner chamber with a polysulfone membrane downwards and buffer to be discarded enters the chamber and can be removed, while the desired protein remains in the tube base. Protein concentrations were determined using a Bradford assay. The final

$RafS_{Msm}$ concentration achieved was 0.6 mg/ml (72% recovery). The aliquots obtained were considered to be of sufficient purity due to the absence of bands in the background of the lanes above and below the $RafS_{Msm}$ bands (Fig. 4.14 B).

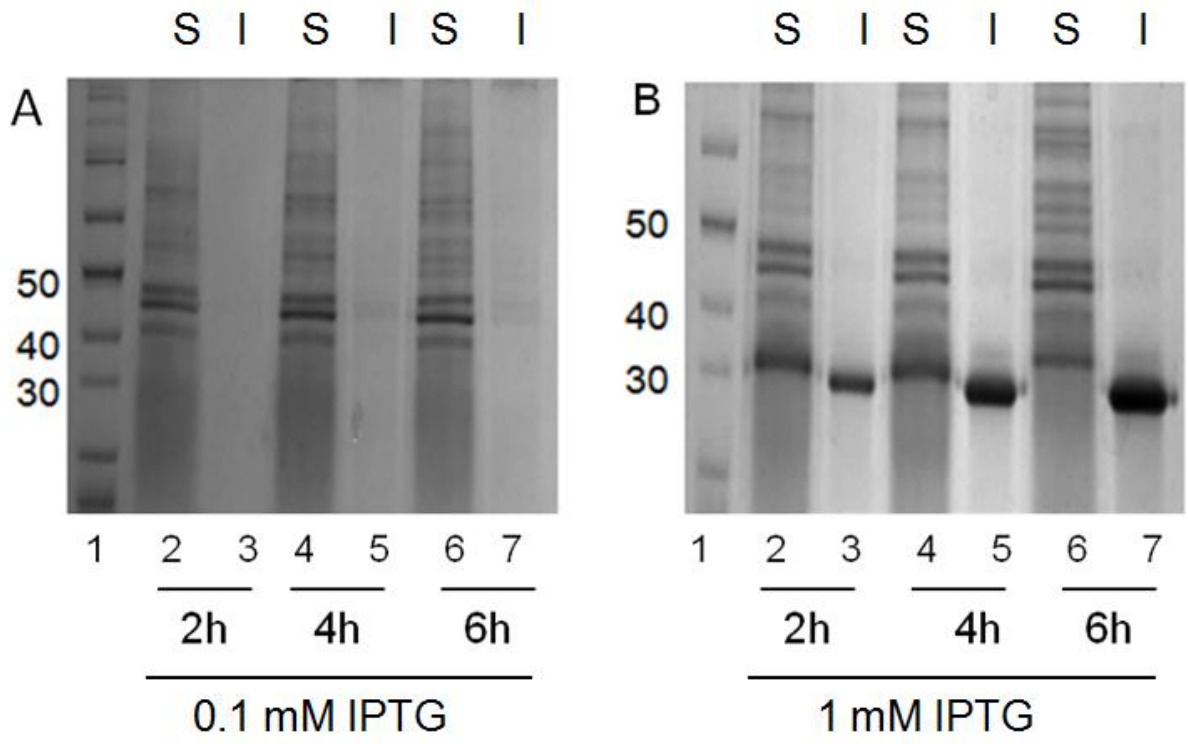

Figure 4.12. $RafS_{Msm}$ protein expression analysis. His-tagged Raf protein expression was induced with 0.1 mM (empty vector control) and 1 mM IPTG ($RafS_{Msm}$) for 6 h at 37^{o}C, 220 rpm. Cells were harvested and lysed and cell extracts were analysed by SDS-PAGE. (A) SDS-PAGE time course assay of protein expression of the pET15b empty vector control at 0.1 mM IPTG. Soluble and insoluble fractions are indicated as “S” and “I” respectively. (B) Time course expression of $RafS_{Msm}$, 1 mM IPTG. Soluble and insoluble fractions are indicated as “S” and “I” respectively. Ladder protein weights are indicated in kDa (A, B Lane 1). $RafS_{Msm}$ protein migration indicated an approximate molecular weight of 28 to 30 kDa.

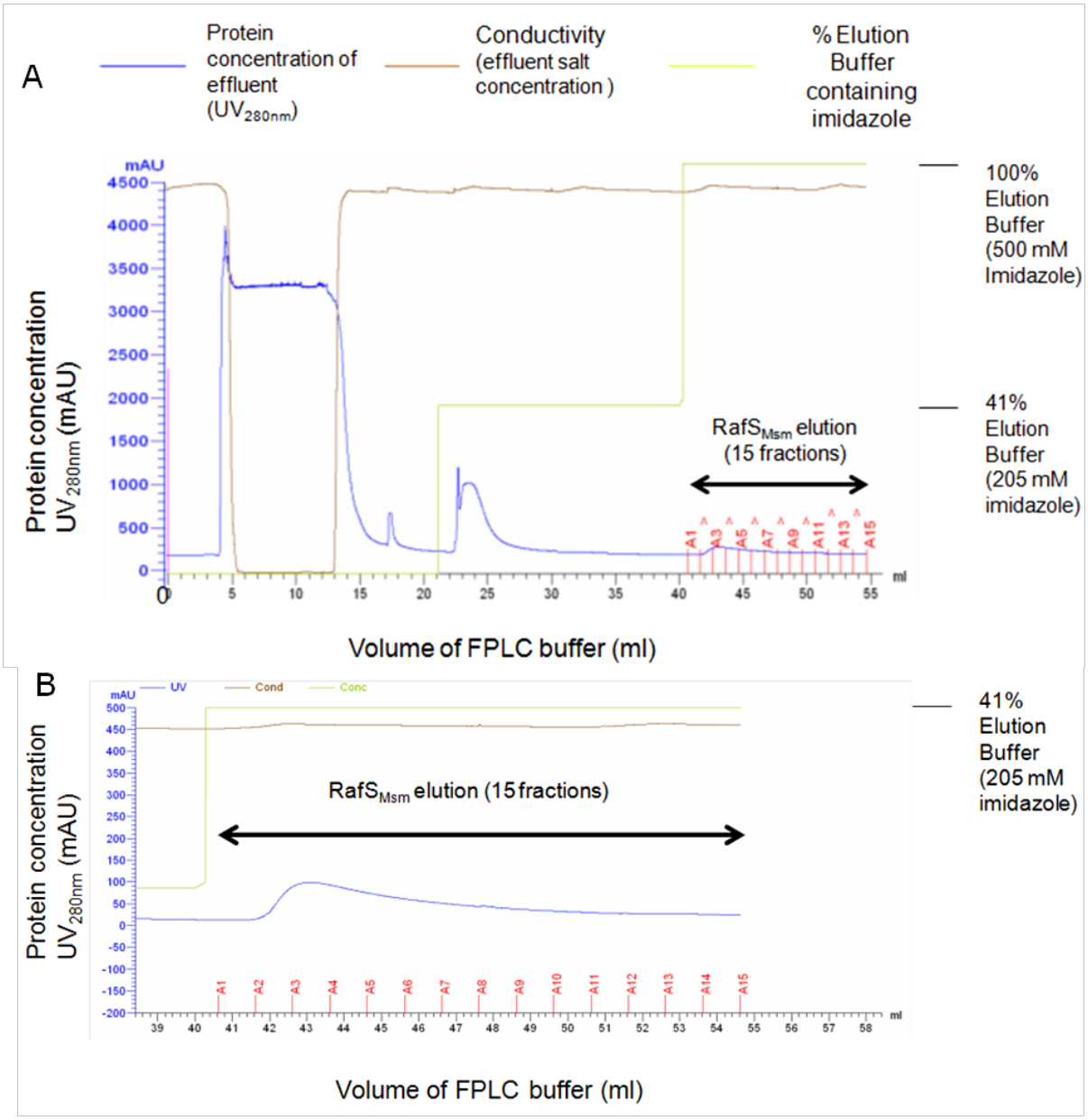

Figure 4.13. FPLC chromatogram indicating purification procedure for $RafS_{Msm}$. His-tagged $RafS_{Msm}$ protein expression was induced with 1 mM IPTG for 4 h at 37°C, 220 rpm. Cells were harvested, lysed and the cell extract was loaded onto a 1 ml His column (GE) using a superloop (GE). Unbound protein was removed with 20 mM and 205 mM imidazole. Subsequently, a 24 ml stepwise elution was carried out at 500 mM imidazole (1 ml fractions were eluted). (A) FPLC chromatogram indicating his column purification procedure for $RafS_{Msm}$ (B) $RafS_{Msm}$ elution profile. Elution of the first 15 fractions is shown. In total, 24 fractions were eluted and are the SDS PAGE elution profile is shown in Fig. 4.14.

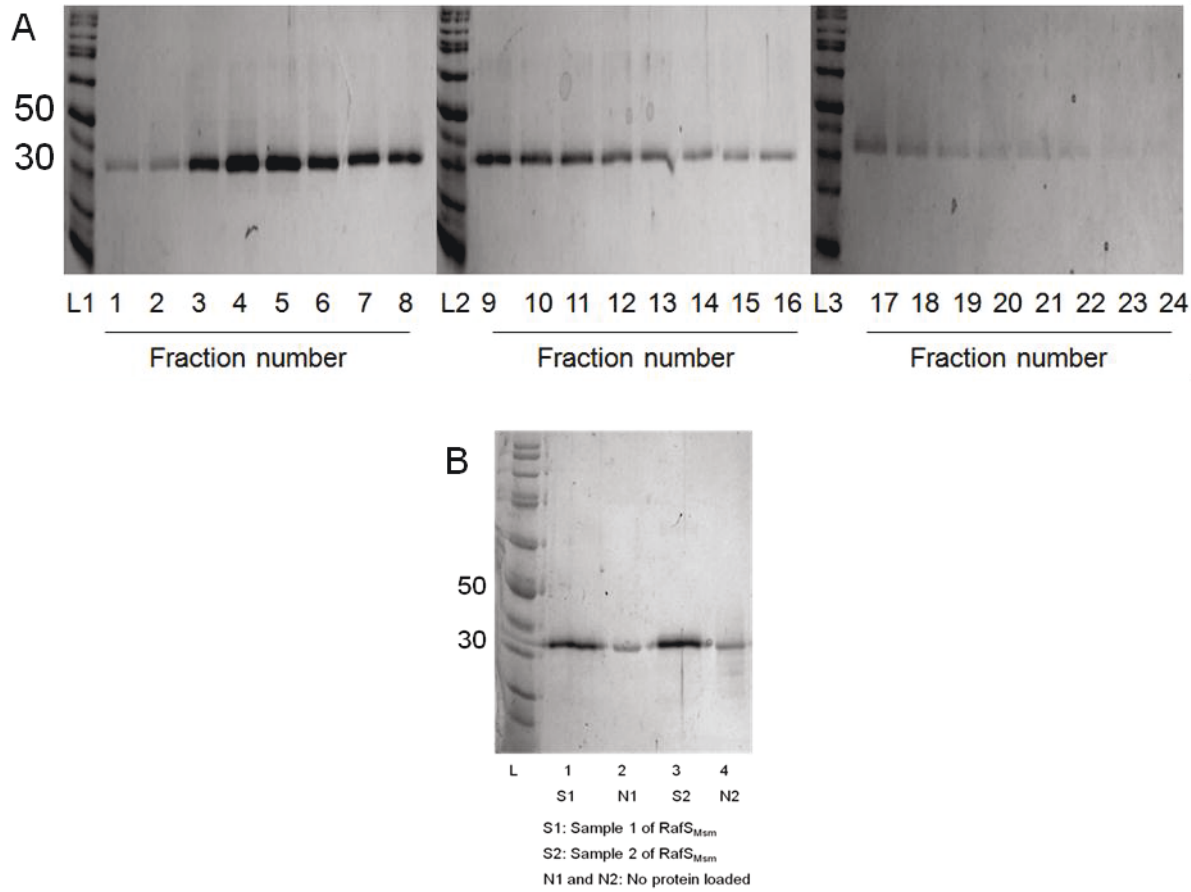

Figure 4.14. $RafS_{Msm}$ FPLC SDS-PAGE elution profile and final product purity analysis. (A) His-tagged $RafS_{Msm}$ protein expression was induced with 1 mM IPTG for 4 h at 37°C, 220 rpm. Cells were harvested, lysed and the cell extract was loaded onto a 1 ml His column (GE) using a superloop (GE). Unbound protein was removed with 20 mM and 205 mM imidazole. Subsequently, a 24 ml stepwise elution was carried out at 500 mM imidazole (1 ml fractions were eluted). A 20 µl sample of each fraction was denatured and loaded to a 12% SDS-PAGE gel. (B) Fractions 3 to 16 were subsequently pooled and concentrated. S1 and S2 indicate concentrated samples of $RafS_{Msm}$. N1 and N2 indicate lanes where no protein was loaded. Ladder protein weights are indicated in kDa (Lanes L1, L2, L3). $RafS_{Msm}$ protein migration indicated an approximate molecular weight of 30 to 35 kDa.

4.3.4 $RafS_{Mtb}$, $RafH_{Msm}$ and $RafH_{Msm}$ expression time courses and purification attempts

I next aimed to determine the optimal induction time for expression of $RafS_{Mtb}$, $RafH_{Msm}$ and $RafH_{Msm.}$ Time course assays indicated an optimal induction time of 4 hours for expression of soluble $RafS_{Mtb}$, $RafH_{Mtb}$ and $RafH_{Msm}$ at 0.1 mM IPTG (Lanes A7, B5 and C5, respectively, Fig. 4.9). For $RafS_{Mtb}$, 4 hours was considered to be the preferred induction time to 6 hours to facilitate protein induction and FPLC purification in 1 working day.

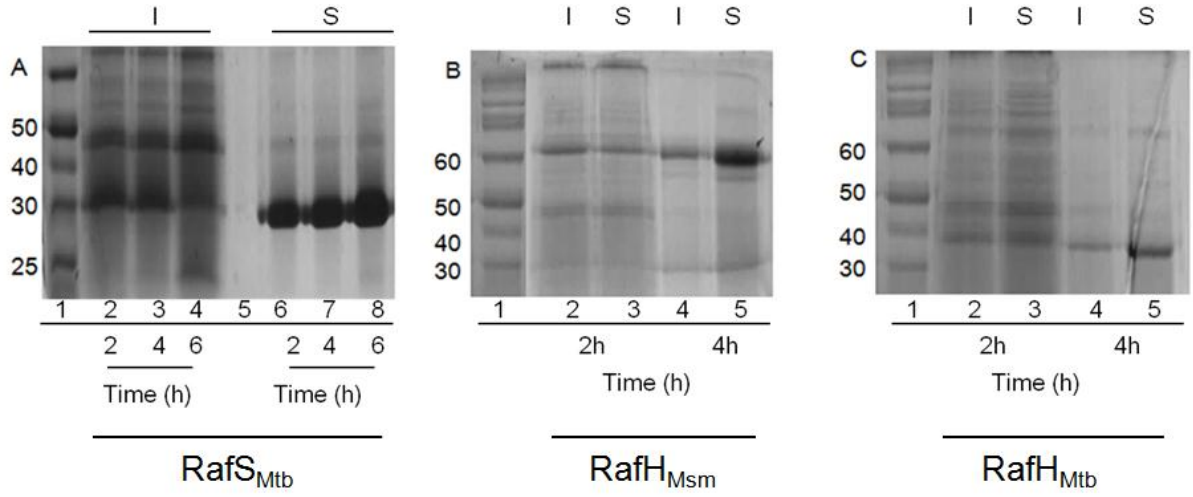

Figure 4.15. SDS-PAGE analysis of time course expression of Raf proteins at 0.1 mM IPTG. His-tagged Raf protein expression was induced with 0.1 mM IPTG for 4 to 6 h at 37°C, 220 rpm. Cells were harvested and lysed and cell extracts were analysed by SDS-PAGE. (A) $RafS_{Mtb}$ 6 hour expression time course. (B) $RafH_{Msm}$ 4 hour expression time course. (C) $RafH_{Mtb}$ 4 hour expression time course. Soluble and insoluble fractions are indicated as “S” and “I” respectively. Protein weights are indicated in kDa for the ladder in lanes A1, B1 and C1. Raf protein migration indicated the following approximate molecular weights; $RafS_{Mtb}$ (28 - 30 kDa), $RafH_{Msm}$ (60 kDa) and $RafH_{Mtb}$ (35 - 38 kDa).

4.3.5 $RafS_{Mtb}$ purification attempts

A considerable amount of soluble $RafS_{Mtb}$ protein was present at 4 hours (Fig 4.16 A) and I attempted to purify soluble $RafS_{Mtb}$ protein from a 1 L culture pellet. I did not obtain $RafS_{Mtb}$ in SDS-PAGE gels via FPLC after several attempts using FPLC buffers as described for $RafS_{Msm}$. Protein appeared not to be eluted since bands corresponding to the size of $RafS_{Mtb}$ were absent from SDS-PAGE elution profiles (data not shown). Due to time limitations, I did not pursue testing other conditions, such as FPLC with buffers adjusted to other pHs, other induction conditions or with a reducing agent additive.

4.3.6 $RafH_{Msm}$ purification attempts

Although $RafH_{Msm}$ is predicted to be 24.53 kDa, a protein gel band (around 60 kDa) (Fig. 4.16) indicates that the soluble version of the protein may form dimers. Whether this is of physiological relevance or is an artifact caused by protein overexpression and aggregation is unknown. The predicted isoelectric point (PI) for $RafH_{Msm}$ was 7.86, suggesting that the protein is likely to be basic and positively charged at pH 7.

Dr. Kathryn Lougheed kindly assisted in this project by attempting to purify $RafH_{Msm}$ by FPLC. She could not purify soluble $RafH_{Msm}$ under the buffer conditions described for $RafS_{Msm}$ with pH adjusted to 8 due to significant aggregation of protein in FPLC fractions (data not shown) (Materials and Methods sections 2.5.3, 2.5.4).

4.3.7 $RafH_{Mtb}$ purification

Dr. Kathryn Lougheed kindly assisted in this project and purified $RafH_{Mtb}$ which was used in translation assays with non-dissociated ribosomes and the polyU mRNA translation assay with dissociated ribosomes (Materials and Methods sections 2.5.3, 2.5.4). $RafH_{Mtb}$ expression was induced in a 2 L culture using 0.1 mM IPTG for 4 h at 37^{o}C. FPLC was carried out with buffers adjusted to pH 8 with stepwise elutions and $RafH_{Mtb}$ was eluted at 200 mM and 300 mM imidazole (data not shown). The predicted isoelectric point (PI) for $RafH_{Mtb}$ was significantly high at 10.21, thus explaining the need for FPLC buffers at pH 8.

Pooled FPLC protein fractions were dialysed using a Slide-a-Lyzer® dialysis cassette 3.5 kDa MWCO (Thermo Scientific) according to the manufacturer's instructions. 1L buffer containing 20 mM Tris, 200 mM NaCl and 10% glycerol, pH 8 was used for dialysis at 10^{o}C overnight. During dialysis, a significant amount of protein aggregated and was spun down so that the supernatant containing soluble protein could be further concentrated. Amicon concentration (Millipore) was carried out as described by the manufacturer. The final concentration of $RafH_{Mtb}$ obtained was 1.5 µg/ml in a 2 ml volume (Fig. 4.18 A).

I subsequently carried out $RafH_{Mtb}$ purification and altered the induction conditions to employ 0.5 mM IPTG for induction of 2 L bacterial culture for 4 h at 37^{o}C, 220 rpm. Given the increased culture volume, I employed two 1 ml His trap columns for FPLC purification. I loaded 24 ml cell lysate to 2 x 1 ml His-trap columns. FPLC buffers (pH8) were modified to include 100 mM sodium phosphate. I carried out stepwise elutions at 300 mM and 500 mM imidazole (60% and 100% buffer B mix, respectively).

Fig. 4.17 indicates the SDS-PAGE analysis of 20 fractions eluted at 500 mM imidazole. Fractions were concentrated with modified TAKM7 buffer (pH 8, 10% glycerol, 2 mM DTT) in Amicon 3 MWCO concentrators (Millipore) (Fig. 4.18 B). $RafH_{Mtb}$ eluted at 300 mM imidazole was of sufficient concentration (1.6 mg/ml, Fig. 4.18 B) and purity and was subsequently utilised in translation assays. Given the ability to concentrate protein with amicon rather than overnight dialysis, I considered the method optimized by myself to be the more convenient of the two methods.

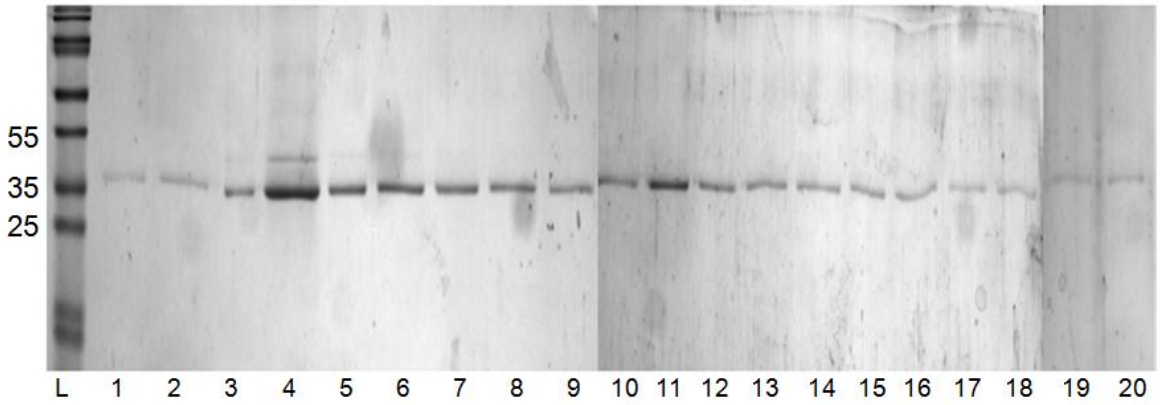

Figure 4.16. SDS-PAGE analysis of $RafH_{Mtb}$ FPLC fractions eluted at 500 mM imidazole. His-tagged $RafH_{Mtb}$ protein expression was induced with 0.5 mM IPTG for 4 h at 37^{o}C, 220 rpm. Cells were harvested, lysed and the cell extract was loaded onto a 1 ml His column (GE) using a superloop (GE). Unbound protein was removed with 20 mM imidazole. Subsequently, a 20 ml stepwise elution was carried out at 500 mM imidazole (1 ml fractions were eluted). A 20 µl sample of each fraction was denatured and loaded to a 12% SDS-PAGE gel. Fraction numbers are indicated. $RafH_{Mtb}$ protein migration indicated an approximate molecular weight of 35 kDa (12% gel). L indicates the Page-Ruler prestained plus protein ladder (Thermosci).

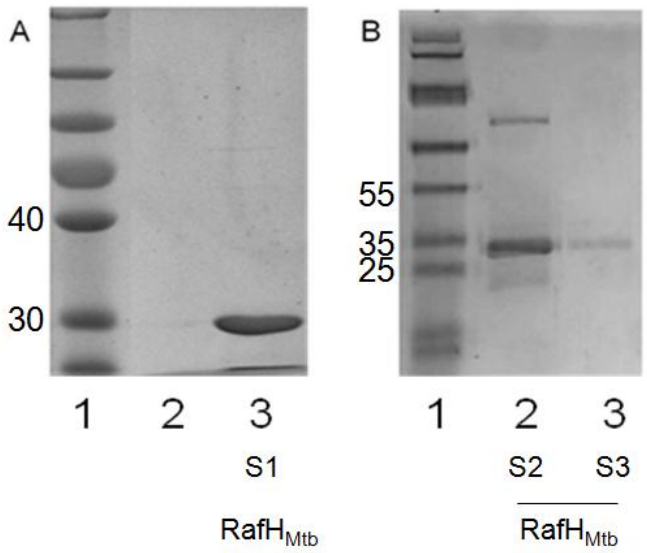

Figure 4.17. SDS-PAGE analysis of purified RafH$_{Mtb.}$ His-tagged RafH$_{Mtb}$ protein expression was induced with 0.1 mM IPTG for 4 h at 37^{o}C, 220 rpm. Cell were harvested lysed and the cell extract was loaded onto a 1 ml His column (GE) using a superloop (GE). FPLC was performed with buffers adjusted to pH8. Unbound protein was removed with 20 mM imidazole. Subsequently, 10 ml stepwise elutions were carried out at (A) 200 mM and 300 mM imidazole (1 ml fractions were eluted) and (B) 300 mM and 500 mM stepwise elutions. Fractions identified as containing pure RafH$_{Mtb}$ were subsequently pooled and concentrated with amicon concentrators and the final sample was analyzed by SDS-PAGE. (A) RafH$_{Mtb}$ purified by Dr. Kathryn Lougheed (8% gel) (lane 3). S1 indicates sample 1. 1 indicates the Page-Ruler prestained plus protein ladder (Thermosci). (B) RafH$_{Mtb}$ protein purified by Nandita Keshavan eluting at 300 mM imidazole (lane 2) and at 500 mM imidazole (lane 3) (12% gel). S2 and S3 indicate samples 2 and 3 respectively. 1 indicates the EZ run protein ladder (FischerSci). Protein weights in kDa are indicated. RafH$_{Mtb}$ protein migration indicated an approximate molecular weight of 30 kDa (8% gel) and 35 kDa (12% gel).

4.3.8 Raf protein expression and purification: summary

Expression conditions that allow soluble Raf protein expression were determined for all N-terminal His-tagged Raf proteins. Raf proteins $RafS_{Msm}$ and $RafH_{Mtb}$ were successfully purified by FPLC (Table 4.1). Raf protein instability indices indicated that $RafS_{Msm}$ is a stable protein with the lowest instability index whereas the other three Raf proteins were classified as unstable. The proteins purified to date were $RafS_{Msm}$ and $RafH_{Mtb}$ for which the instability indices were lowest (Appendix Table 3).

RafH proteins had higher aliphatic indices and a higher proportion of buried residues than RafS proteins (Appendix Table 3). Buried residues are likely to be less accessible to Ni^{2+} ions of the His trap columns and RafH protein binding is likely to be weaker than for RafS proteins. Raf proteins showed a range of isoelectric points (pH at which the protein is of neutral charge). $RafH_{Mtb}$ elution occurred at a lower imidazole concentration than for $RafS_{Msm}$. The larger predicted number of negative than positive residues and negative charge at physiological pH may have contributed $RafS_{Msm}$ affinity to Ni^{2+} upto 500 mM imidazole.

Table 4.1: Summary of outcomes for Raf protein expression and purification

Raf Protein	Soluble protein expression conditions	FPLC Purification outcome
$RafS_{Msm}$	4 h, 1 mM IPTG, 37^{o}C, 1L cell pellet	Purified to 0.6 mg/ml Yield = 3 mg/L culture
$RafH_{Mtb}$	4 h, 0.5 mM IPTG, 37^{o}C, 2L cell pellet	Purified to 1.6 mg/ml Yield = 1.6 mg/L culture
$RafH_{Msm}$	4 h, 0.1 mM IPTG, 37^{o}C, 1L cell pellet	Purification unsuccessful to date
$RafS_{Mtb}$	4 h, 0.1 mM IPTG, 37^{o}C, 1L cell pellet	Purification unsuccessful to date

4.4 Effect of Raf proteins on *in vitro* mycobacterial translation

4.4.1 Effect of Raf proteins on *in vitro* mycobacterial translation: aims

Having purified $RafS_{Msm}$ and $RafH_{Mtb}$ proteins, we next investigated the effect of these proteins on *in vitro* translation by *M. smegmatis* ribosomes. We aimed to investigate translation of 3 types of mRNA with or without a Shine Dalgarno (SD) sequence and translation by 2 types of ribosomes as listed below:

The 3 mRNA translation systems investigated were:

1. *Omega* luciferase mRNA translation (mRNA with SD sequence and translational enhancer sequence from Tobacco Mosaic Virus).
2. *Renilla* luciferase mRNA translation (mRNA with SD sequence).
3. PolyU mRNA translation (mRNA without SD sequence).

The 2 types of *M. smegmatis* ribosomes investigated were:

1. Non-dissociated ribosomes.
2. Dissociated ribosomes (ribosomes are resuspended in low Mg^{2+} buffer, which encourages ribosome dissociation).

The translation systems are further described in section 4.4.2.

4.4.2 *In vitro* mycobacterial translation systems: overview

The *in vitro* translation assays were carried out using $RafS_{Msm}$ and $RafH_{Mtb}$ proteins which were purified by myself ($RafS_{Msm}$ and $RafH_{Mtb}$) and Dr. Kathryn Lougheed ($RafH_{Mtb}$). Dr. Rashid Akbergenov from the laboratory of Prof. Erik C. Böttger, University of Zurich carried out the translation assays and supplied us with raw data and methods. I was involved in the protein purification, experimental design, data plotting and discussion stages.

Translation by non-dissociated and dissociated *M. smegmatis* ribosomes was investigated. Translation assays were attempted by (i) direct incubation of Raf proteins with mRNA and the translation reaction mixture or (ii) pre-incubation of Raf proteins with the translation mixture without mRNA, followed by mRNA addition and incubation. A typical translation reaction mixture consisted of 7.5 pmol *M. smegmatis* ribosomes and 30 µl of a translation mixture containing 0 to 4 µg mRNA, 100 µM amino acid mixture, 40% (vol/vol) of *M. smegmatis* S100 extract, 0.4 µg/µl of total *M. smegmatis* tRNA, 12 µl of commercial S30 Premix without amino acids

We investigated translation of mRNAs which were with and without the SD sequence. The *Omega* and *Renilla* luciferase mRNAs each contained an SD sequence and AUG start codon that is recognized by ribosomes prior to translation. Luciferase originated from *Photinus pyralis* (*Omega* luciferase) or from *Renilla reniformis* (*Renilla* luciferase) and oxidizes luciferin and causes bioluminescence, which was used as an indicator of luciferase mRNA translation. *Omega* luciferase mRNA is a modified firefly luciferase mRNA that contains a translational enhancer

from the Tobacco Mosaic Virus which is present at the 5'UTR of the mRNA and is associated with increased protein synthesis (Zeyenko *et al*., 1994).

PolyU mRNA was also employed, which is a synthetic mRNA, consisting of uracil ribonucleotides only and lacks an SD sequence. Translation of polyU mRNA results in synthesis of a polypeptide made of phenylalanine (Phe) amino acids only. PolyU mRNA translation does not involve initiation and termination, allowing the effect of Raf proteins on translation elongation to be investigated. When luciferase mRNA was employed, bioluminescence (luciferase activity) was measured as an indicator of translation activity. When polyU mRNA was employed, ^{14C}Phe incorporation was measured as an indicator of translation activity (Materials and Methods section 2.5.6).

4.4.3 Effect of Raf proteins on translation by non-dissociated *M. smegmatis* ribosomes

We first investigated whether Raf proteins inhibit translation by non-dissociated *M. smegmatis* ribosomes (see method described in sections 2.5.6 to 2.5.10). $RafS_{Msm}$ and $RafH_{Mtb}$ showed no apparent effect on translation of *Omega* luciferase mRNA by non-dissociated ribosomes (Fig 4.18). Direct incubation of Raf proteins with luciferase mRNA and the translation reaction mixture or pre-incubation of Raf proteins with the translation mixture without mRNA, followed by incubation with mRNA did not show any significant change in translation activity.

Next, we investigated whether Raf proteins inhibit translation by non-dissociated ribosomes when pre-incubated with ribosomes for 1 hour, prior to

incubating with mRNA. Despite the long pre-incubation, Raf proteins did not inhibit translation by non-dissociated ribosomes (Fig. 4.19 A, B). Under these conditions, the effect of incubation of both Raf proteins together with ribosomes did not show any synergistic inhibition of translation by non-dissociated ribosomes. Furthermore, when the antibiotic paromomycine was employed as a positive control, successful inhibition of translation was observed (Appendix Figure 6).

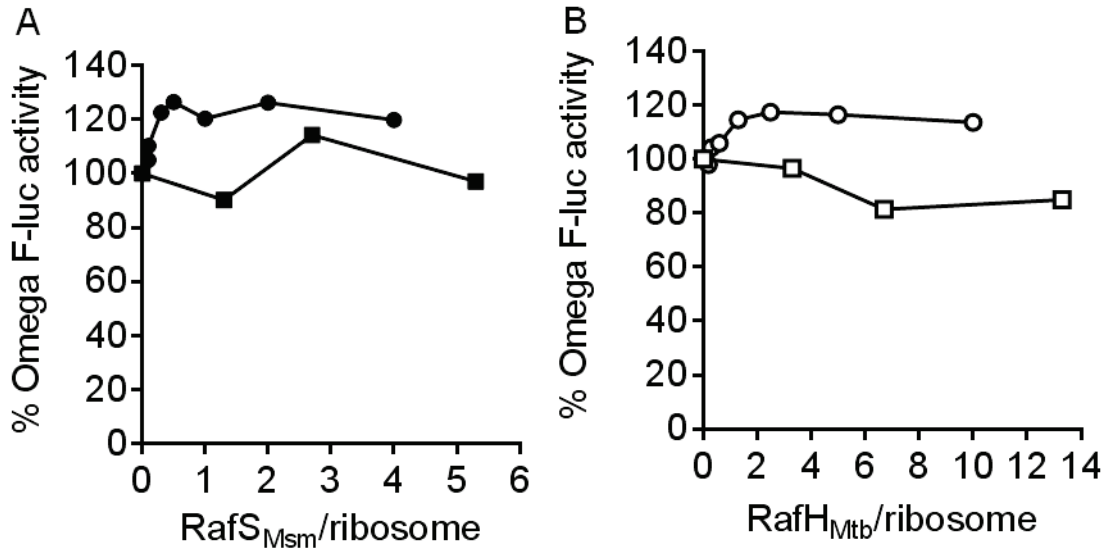

Figure 4.18. RafS$_{Msm}$ and RafH$_{Mtb}$ do not inhibit *in vitro* luciferase mRNA translation by non-dissociated *M. smegmatis* ribosomes. (A, B circles) Translation reaction mixture containing non-dissociated ribosomes was incubated with increasing amounts of Raf proteins (A: RafS$_{Msm}$ and B: RafH$_{Mtb}$) for 35 min at 37^{o}C and *Omega* F-luc activity was measured. (A, B squares) Non-dissociated ribosomes were pre-incubated with increasing amounts of Raf proteins (A: RafS$_{Msm}$ and B: RafH$_{Mtb}$) without mRNA for 10 min at 37^{o}C. The reactions were then incubated for 35 min at 37^{o}C with the remaining components of the translation mixture and *Omega* F-luc activity was measured. F-luc activity indicates firefly luciferase activity.

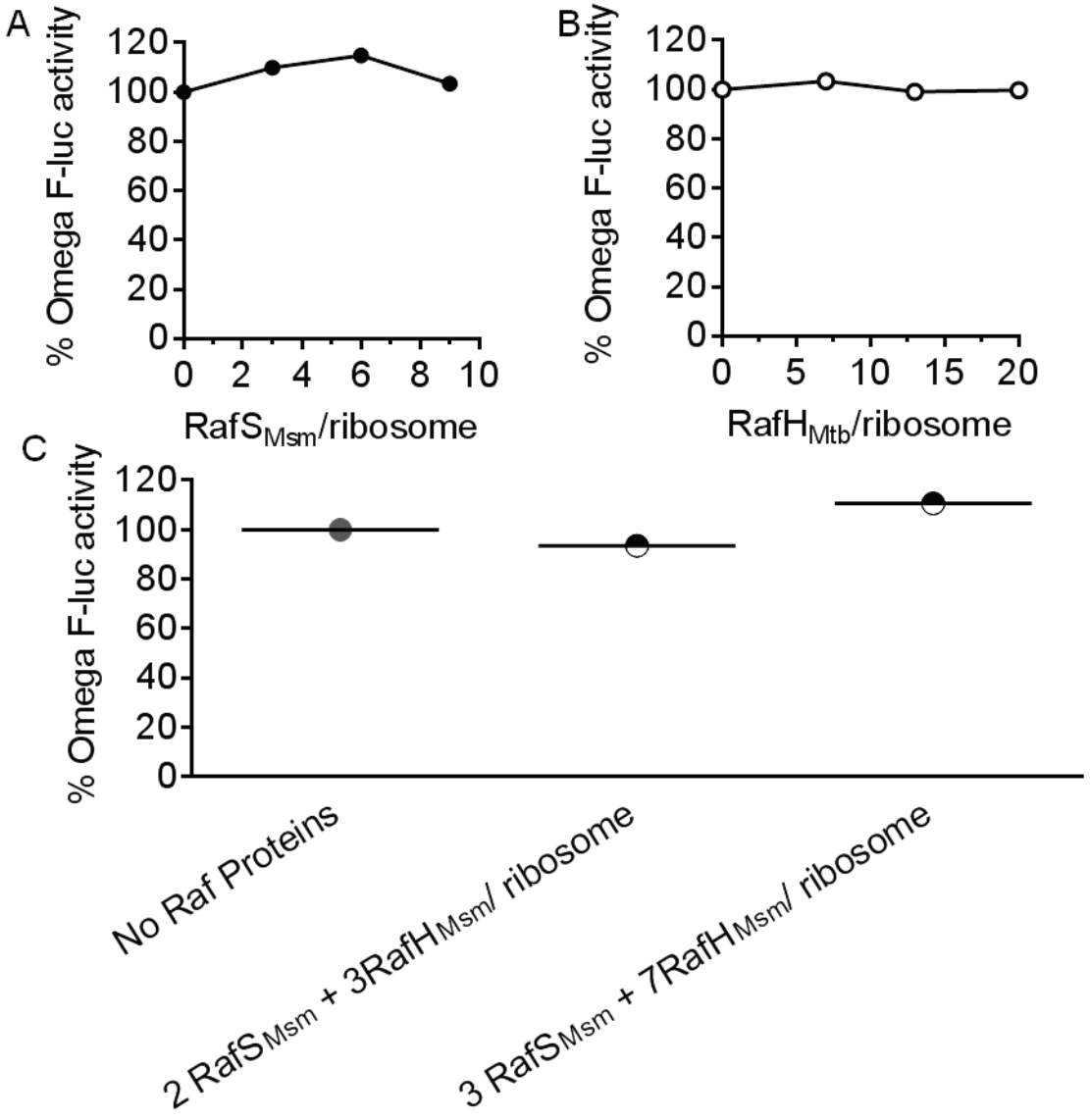

Figure 4.19. RafS$_{Msm}$ and RafH$_{Mtb}$ do not synergistically or individually inhibit *in vitro Omega* luciferase mRNA translation by non-dissociated *M. smegmatis* ribosomes. (A, B) RafS$_{Msm}$ (A) and RafH$_{Mtb}$ (B) do not inhibit *in vitro Omega* luciferase mRNA translation by non-dissociated *M. smegmatis* ribosomes when pre-incubated with ribosomes for 1 hour. (C) RafS$_{Msm}$ and RafH$_{Mtb}$ do not inhibit *in vitro Omega* luciferase mRNA translation by non-dissociated *M. smegmatis* ribosomes when pre-incubated together with ribosomes for 1 hour. (A, B, C) Non-dissociated ribosomes were pre-incubated with increasing amounts of Raf proteins for 60 min at 37^{o}C. The reactions were incubated for 35 min at 37^{o}C with the other components of the reaction mixture and F-luc activity was measured. F-luc activity indicates firefly luciferase activity.

Given that we did not observe any apparent inhibitory activity for the Raf: ribosome ratios investigated thus far, we next investigated the effect of higher amounts of Raf proteins on the translation of *Omega* luciferase mRNA by non-dissociated ribosomes (Materials and Methods section 2.5.6). $RafS_{Msm}$ partially increased *in vitro Omega* luciferase mRNA translation by non-dissociated ribosomes by 42% (13 $RafS_{Msm}$: 1 ribosome) (Fig. 4.20 A) and $RafH_{Mtb}$ partially inhibited *in vitro Omega* luciferase mRNA translation by non-dissociated ribosomes by 30% (Fig. 4.20 B) (34 $RafH_{Mtb}$: 1 ribosome).

Given the partial translation increase that was observed when *Omega* luciferase mRNA and an excess of $RafS_{Msm}$ were employed, we next investigated the effect of Raf proteins on translation of *Renilla* luciferase mRNA, which does not include a translational enhancer, by non-dissociated ribosomes. The data suggested that both Raf proteins inhibited translation of *Renilla* luciferase mRNA, following a temporary increase in translation.

At $RafS_{Msm}$:ribosome 5:1, translation had increased, and by $RafS_{Msm}$:ribosome 8:1, translation had decreased by 75%. At $RafH_{Mtb}$:ribosome 7:1, translation had increased, and by $RafH_{Mtb}$:ribosome 21:1, translation had decreased by 73%. The data suggests that compared to *Omega* luciferase mRNA, *Renilla* luciferase mRNA, which lacks a translational enhancer, is more useful for investigating the effect of Raf proteins on translation by non-dissociated ribosomes due to higher levels of inhibition achieved.

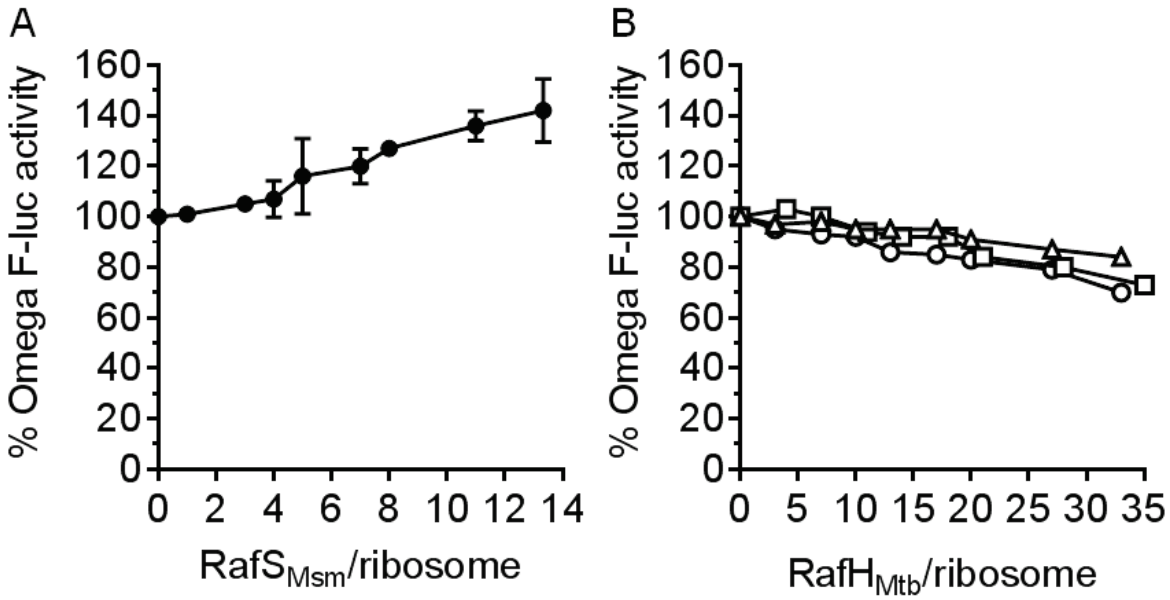

Figure 4.20. Effect of Raf proteins on *in vitro Omega* luciferase mRNA translation by non-dissociated *M. smegmatis* ribosomes. (A) RafS$_{Msm}$ partially increases *in vitro Omega* luciferase mRNA translation by non-dissociated *M. smegmatis* ribosomes. An average of 3 technical replicates is plotted. (B) RafH$_{Mtb}$ partially inhibits *in vitro Omega* luciferase mRNA translation by non-dissociated *M. smegmatis* ribosomes. 3 technical replicates are plotted. (A, B) Non-dissociated ribosomes were pre-incubated with increasing amounts of Raf protein without mRNA for 10 min at 37^{o}C. The reactions were incubated for 35 min at 37^{o}C with the remaining components of the translation mixture, including *Omega* luciferase mRNA. *Omega* firefly luciferase (F-luc) activity was measured.

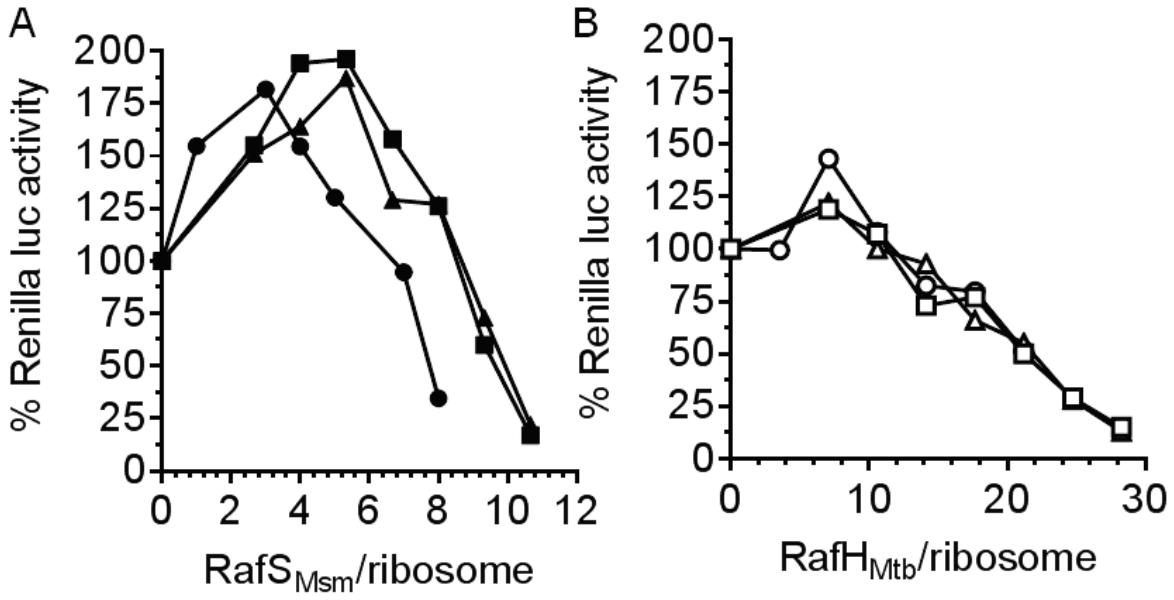

Figure 4.21. RafS$_{Msm}$ and RafH$_{Mtb}$ inhibit *in vitro Renilla* luciferase mRNA translation by non-dissociated *M. smegmatis* ribosomes. Non-dissociated ribosomes were pre-incubated with increasing amounts of RafS$_{Msm}$ without mRNA for 10 min at 37^{o}C. The reactions were incubated for 35 min at 37^{o}C with the remaining components of the translation mixture including *Renilla* luciferase mRNA. *Renilla* firefly luciferase (F-luc) activity was measured. 3 technical replicates per Raf protein are plotted.

Given that the ribosome stabilisation factor PY was shown to inhibit translation of SD-mRNA and also of polyU mRNA, we next investigated the effect of Raf proteins on polyU mRNA translation by non-dissociated ribosomes (see method described in sections 2.5.6 to 2.5.10). PolyU mRNAs are further described in section 4.4.1. RafS$_{Msm}$ and RafH$_{Mtb}$ partially inhibited *in vitro* translation of polyU mRNA by non-dissociated ribosomes by 26% (RafS$_{Msm}$:ribosome 16:1) and 37% (RafH$_{Mtb}$:ribosome 37:1), respectively (Fig. 4.22), indicating that the Raf proteins play a role in partial inhibition of polyU mRNA translation by non-dissociated ribosomes.

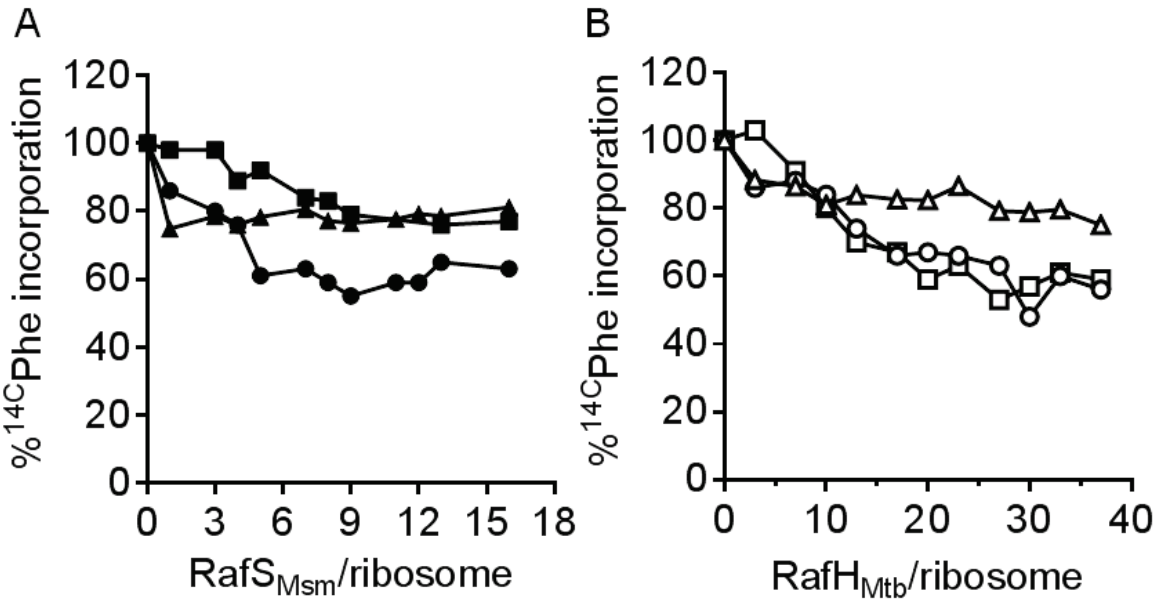

Figure 4.22. Effect of Raf proteins on polyU mRNA translation by non-dissociated ribosomes. (A) $RafS_{Msm}$ partially inhibits *in vitro* luciferase polyU mRNA translation by non-dissociated *M. smegmatis* ribosomes. (B) $RafH_{Mtb}$ partially inhibits *in vitro* luciferase polyU mRNA translation by non-dissociated *M. smegmatis* ribosomes. *M. smegmatis* non-dissociated ribosomes were pre-incubated with increasing amounts of Raf proteins for 15 min (circles) and 30 min (squares, triangles) at 25^{o}C and then the mixture was incubated for 1 hour at 37^{o}C with polyU mRNA and other components of the translation reaction mixture for testing of translational activity. For translation activity detection, RNA was hydrolysed with 5 ml of 5M KOH and protein was precipitated with 5% TCA. The reaction mixture was filtered through a 0.45 mm nitrocellulose membrane and exposed to a phosphoimager screen to obtain the level of ^{14C}Phe incorporation which indicates translational activity.

4.4.4 $RafS_{Msm}$ and $RafH_{Mtb}$ inhibit *in vitro* luciferase mRNA translation by dissociated *M. smegmatis* ribosomes

Given that the *M. smegmatis* Raf proteins were found to bind 30S subunits of stationary phase ribosomes (Trauner, 2010), we next investigated whether Raf proteins may show more potent inhibitory effects on translation when incubated dissociated ribosomes. In order to dissociate ribosomes, non-dissociated ribosomes were resuspended in buffer containing 0.05 mM $MgCl_2$ and 500 mM KCl (see method described in sections 2.5.6 to 2.5.10).

We first investigated the effect of Raf proteins on *Omega* luciferase mRNA translation by dissociated ribosomes (Fig. 4.23). Average translation inhibition percentages were as follows; $RafS_{Msm}$ and $RafH_{Mtb}$ inhibition of *Omega* luciferase mRNA translation were 53% ($RafS_{Msm}$: ribosome 13:1) and 84% ($RafH_{Mtb}$:ribosome 32:1), respectively. Although there was higher variation between replicates in the $RafS_{Msm}$ assay, these assays suggested that $RafS_{Msm}$ inhibited translation of *Omega* luciferase mRNA by dissociated ribosomes.

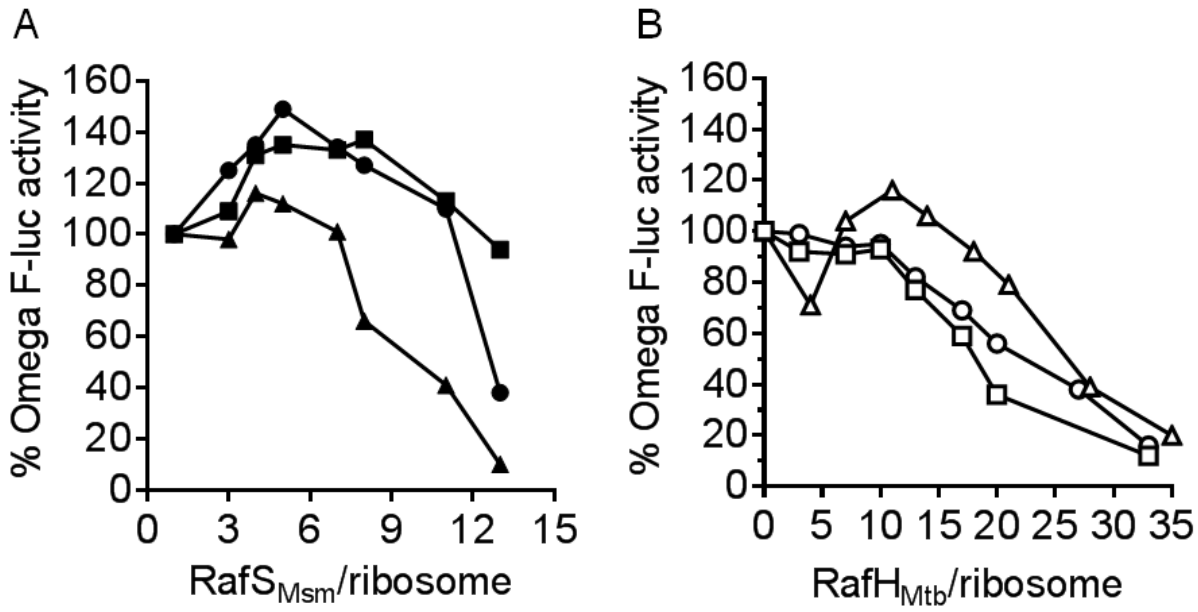

Figure 4.23. RafS$_{Msm}$ and RafH$_{Mtb}$ inhibit *in vitro Omega* luciferase mRNA translation by dissociated ribosomes. (A) RafS$_{Msm}$ inhibits *in vitro Omega* luciferase mRNA translation by dissociated *M. smegmatis* ribosomes. (B) RafH$_{Mtb}$ inhibits *in vitro Omega* luciferase mRNA translation by dissociated *M. smegmatis* ribosomes. In order to dissociate ribosomes, non-dissociated ribosomes were resuspended in a buffer containing 0.05 mM $MgCl_2$ and 500mM KCl. Dissociated ribosomes were pre-incubated with increasing amounts of Raf proteins without mRNA for 10 min at 37^{o}C (circles and squares) or 30 min at 25^{o}C (triangles). Next, the reactions were incubated for 35 min at 37^{o}C with the remaining components of the translation mixture including *Omega* luciferase mRNA. *Omega* firefly luciferase (F-luc) activity was measured.

Given the Raf protein-associated inhibition of translation of *Renilla* luciferase mRNA by non-dissociated ribosomes observed (Fig. 4.24), we next investigated whether Raf proteins affected *Renilla* luciferase mRNA translation by dissociated ribosomes. $RafS_{Msm}$ and $RafH_{Mtb}$ were found to inhibit translation of *Renilla* luciferase mRNA by 93% ($RafS_{Msm}$:ribosome 10:1) and 96% ($RafH_{Mtb}$:ribosome 26:1), respectively. The data indicates that Raf proteins are more potent inhibitors of translation of *Renilla* luciferase mRNA than *Omega* luciferase mRNA.

Given that $RafS_{Msm}$ and $RafH_{Mtb}$ partially inhibited *in vitro* polyU mRNA translation by non-dissociated *M. smegmatis* ribosomes (Fig. 4.25), we also investigated whether $RafS_{Msm}$ and $RafH_{Mtb}$ inhibited polyU mRNA translation by dissociated ribosomes. $RafS_{Msm}$ and $RafH_{Mtb}$ inhibited translation of polyU mRNA translation (Fig. 4.24). Average percentage inhibition of translation for $RafS_{Msm}$ and $RafH_{Mtb}$ were 67% ($RafS_{Msm}$:ribosome 11:1) and 80% ($RafH_{Mtb}$:ribosome 23:1), respectively.

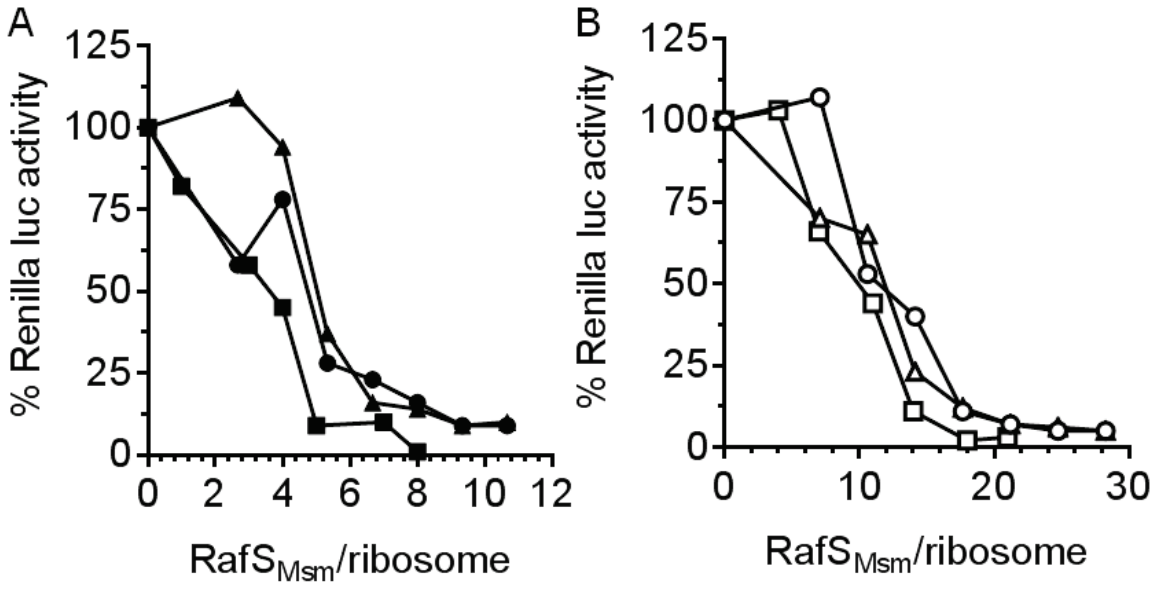

Figure 4.24. RafS$_{Msm}$ and RafH$_{Mtb}$ inhibit *in vitro Renilla* luciferase mRNA translation by dissociated *M. smegmatis* ribosomes. In order to dissociate ribosomes, non-dissociated ribosomes were resuspended in a buffer containing 0.05 mM $MgCl_2$ and 500mM KCl. Dissociated ribosomes were pre-incubated with increasing amounts of RafS$_{Msm}$ without mRNA for 10 min at 37^{o}C. The reactions were incubated for 35 min at 37^{o}C with the remaining components of the translation mixture including *Renilla* luciferase mRNA. *Renilla* firefly luciferase (R-luc) activity was measured.1 replicate per Raf protein is indicated.

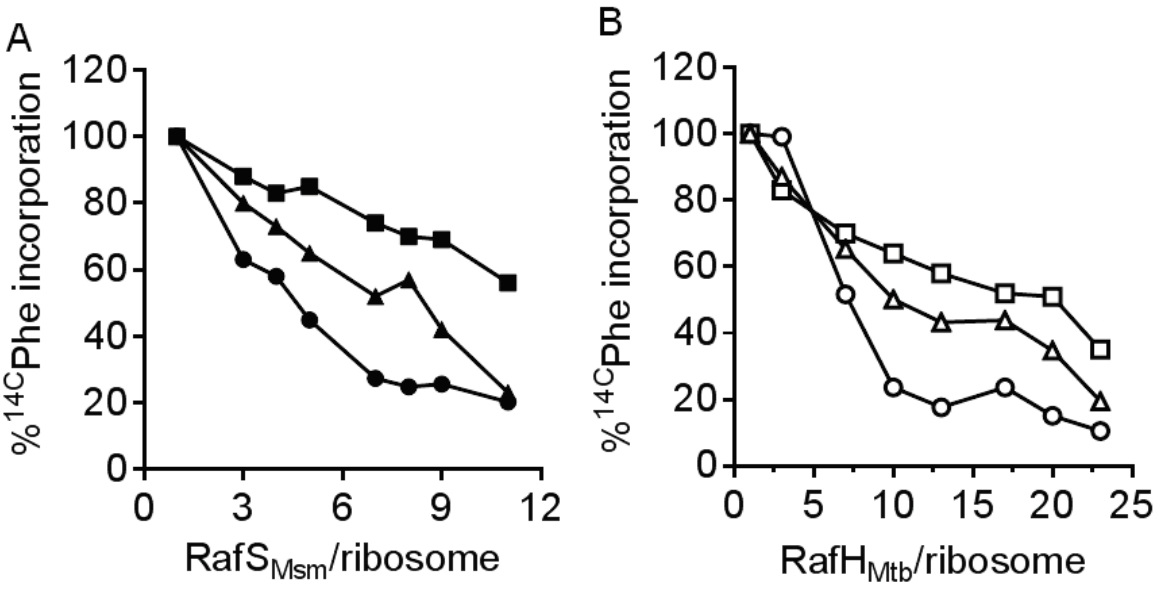

Figure 4.25. $RafS_{Msm}$ and $RafH_{Mtb}$ inhibit *in vitro* polyU mRNA translation by dissociated ribosomes. (A) $RafS_{Msm}$ inhibits *in vitro* polyU mRNA translation by dissociated *M. smegmatis* ribosomes. (B) $RafH_{Mtb}$ inhibits *in vitro* polyU mRNA translation by dissociated *M. smegmatis* ribosomes. In order to dissociate ribosomes, non-dissociated ribosomes were resuspended in a buffer containing 0.05 mM $MgCl_2$ and 500mM KCl. Dissociated ribosomes were pre-incubated with increasing amounts of $RafS_{Msm}$ without mRNA for 15 min at 25°C (circles, squares) or 30°C (triangles). The reactions were incubated for 1 hour at 37°C with the remaining components of the translation mixture including polyU mRNA. For translation activity detection, RNA was hydrolysed with 5 ml of 5M KOH and protein was precipitated with 5% TCA. The reaction mixture was filtered through a 0.45 mm nitrocellulose membrane and exposed to a phosphoimager screen to obtain level of ^{14C}Phe incorporation which indicates translational activity.

4.4.5 Effect of $RafS_{Msm}$ and $RafH_{Mtb}$ on translation by *M. smegmatis* ribosomes: summary.

In summary, $RafS_{Msm}$ and $RafH_{Mtb}$ inhibit *in vitro* translation of dissociated *M. smegmatis* ribosomes. Percentage effects of $RafS_{Msm}$ and $RafH_{Mtb}$ on translation are summarised in Figs. 4.26 and 4.27. The results in this section indicated that $RafS_{Msm}$ and $RafH_{Mtb}$ are inhibitors of translation of *Renilla* luciferase, *Omega* luciferase and polyU mRNA by dissociated ribosomes. Also, $RafS_{Msm}$ and $RafH_{Mtb}$ inhibit translation of *Renilla* luciferase mRNA and polyU mRNA (partial inhibition) by non-dissociated ribosomes. $RafS_{Msm}$ partially stimulated translation of *Omega* luciferase mRNA whereas $RafH_{Mtb}$ partially inhibited translation of *Omega* luciferase mRNA by non-dissociated ribosomes, respectively.

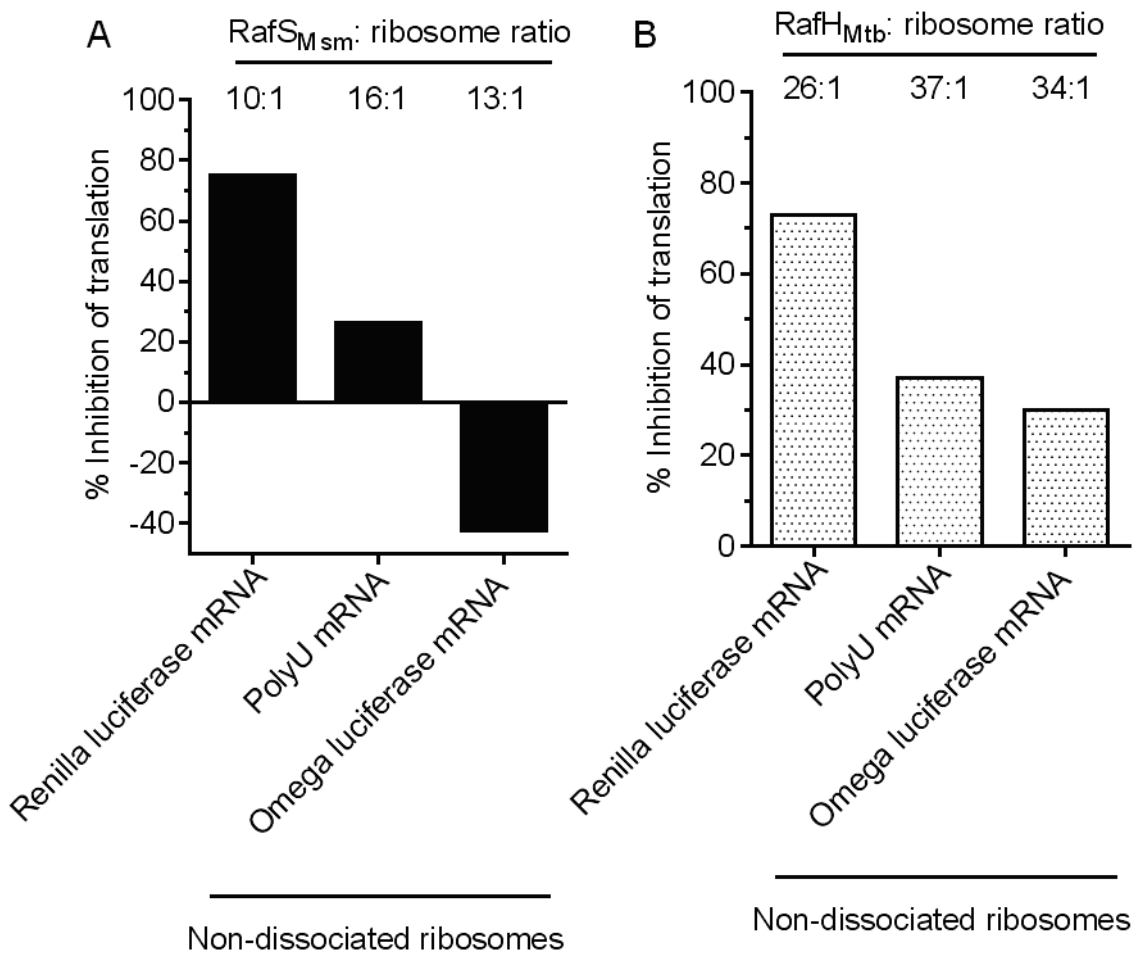

Figure 4.26. Summary of the effects of $RafS_{Msm}$ (A) and $RafH_{Mtb}$ (B) on *in vitro* translation of *Renilla* luciferase, polyU and *Omega* luciferase mRNAs by non-dissociated ribosomes. Percentage inhibition of translation by *M. smegmatis* ribosomes is shown. Number of translation assay replicates = 3 per condition.

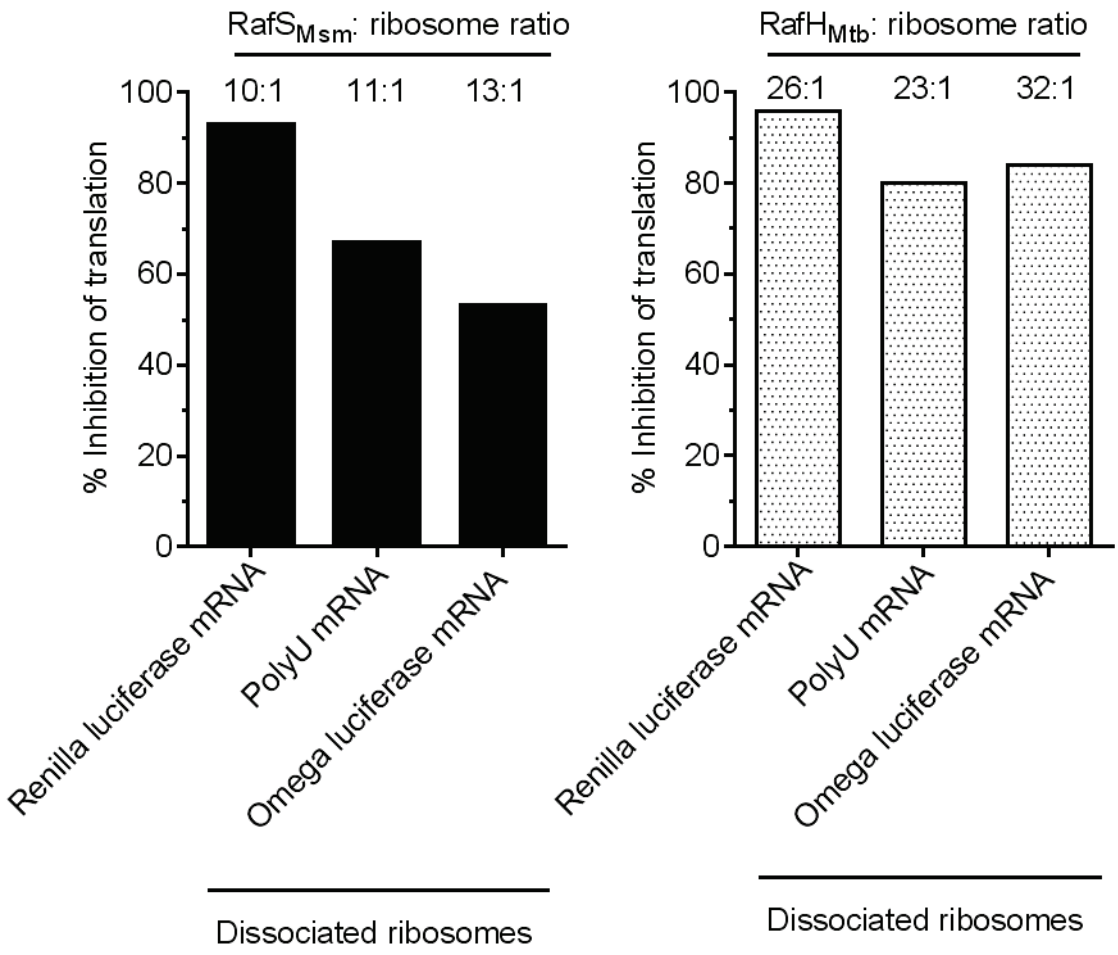

Figure 4.27. Summary of the effects of RafS$_{Msm}$ (A) and RafH$_{Mtb}$ (B) on in vitro translation of *Renilla* luciferase, polyU and *Omega* luciferase mRNAs by dissociated ribosomes. Percentage inhibition of translation by *M. smegmatis* ribosomes is shown. Number of translation assay replicates = 3 per condition.

4.5 Role of $RafS_{Msm}$ in mycobacterial ribosomal subunit association

4.5.1 Role of $RafS_{Msm}$ in mycobacterial ribosomal subunit association: aims

In addition to translation inhibition (section 4.4), ribosomal subunit association is a putative mechanism of ribosome stabilisation. Given the inhibitory effect of Raf proteins on ribosome translation, we next investigated the effect of Raf proteins on ribosomal subunit association.

The aims were:

1. To modify the previous protocol (Trauner *et al.*, 2010) in several ways to incorporate new equipment and improve ease of profiling (Materials and Methods section 2.5.5)
2. To confirm the appropriate magnesium concentration for ribosomal profiling of *M. smegmatis* cell extracts.
3. To investigate the effect of *rafS*$_{Msm}$ deletion on *M. smegmatis* ribosome subunit association in actively growing and early stationary phase cultures by ribosomal profiling.

4.5.2 Optimization of ribosomal profiling: effect of magnesium concentration on *M. smegmatis* normoxic log phase 70S ribosome subunit dissociation

10 mM Mg^{2+} has been employed in ribosomal profiling buffers to provide an environment conducive to ribosomal subunit association, whereas 1 mM Mg^{2+} has been employed to provide an environment conducive to ribosomal subunit dissociation (Trauner *et al.,* 2010). Since log phase cells were less abundant than stationary phase cells, log phase profiling on 1L bacterial culture per replicate was carried out in order to harvest a sufficient amount of cells for ribosomal profiling (Appendix Figure 7).

A typical experiment resulted in 30 to 35 sucrose gradient fractions. The experiments in this section were carried out with cell breakage at room temperature. However, for experiments in section 4.5.3, cell breakage was carried out at 4^{o}C, since this appeared to be beneficial for improving cell disruptor function and ribosomal yield. Further details are given in Materials and Methods section 2.5.5.

Associative and dissociative effects were confirmed by carrying out profiling of ribosomes from wild type and *⊿rafS$_{Msm}$c M. smegmatis* strains (Fig.4.28). Wild type and *⊿rafS$_{Msm}$c* mid log ribosomes were predominantly in the 70S form in 10 mM Mg^{2+} and in the 50S form in 1 mM Mg^{2+} conditions. I next investigated whether 10 mM Mg^{2+} (associative condition) was required in ribosomal profiling gradients. I carried out associative lysis and pelleting (10 mM Mg^{2+}) of mid log ribosomes followed by non-associative gradient centrifugation (1 mM Mg^{2+}) for wild type and *ΔrafS$_{Msm}$c* (Fig. 4.28). In this experiment, the use of lower concentrations of ribosomes may have accounted for the presence of the 30S peak in the ribosomal profile.

Fig. 4.29 indicated lower proportions of 70S ribosomes in wild type and *ΔrafS*$_{Msm}$*c* mutant strains in ribosomal profiles where 1 mM Mg^{2+} was present in sucrose gradients, suggesting that 10 mM Mg^{2+} was required to maintain ribosomal association during sucrose gradient centrifugation. Taken together, the results confirmed that all steps of ribosomal profiling (of *M. smegmatis* cell extracts) should be carried out under associative conditions (with10 mM Mg^{2+}).

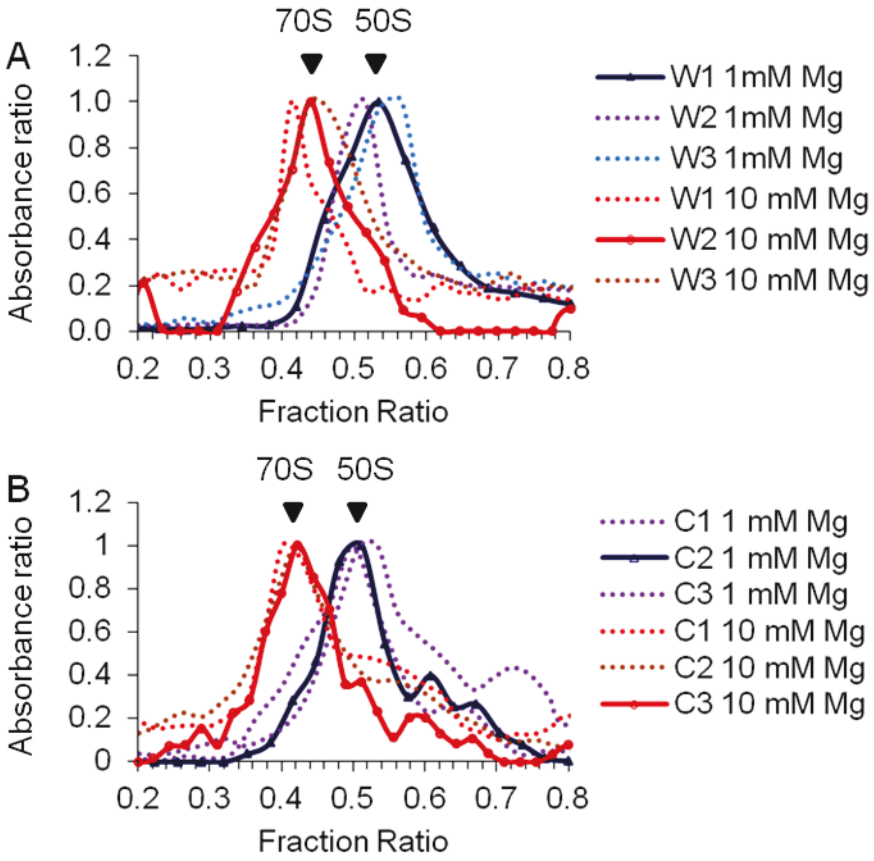

Figure 4.28. *M. smegmatis* wild type (A) and *ΔrafS*$_{Msm}$*c* (B) mid log ribosomes are predominantly associated in 10 mM Mg^{2+} and dissociated in 1 mM Mg^{2+}. (A) and (B) plots were generated by plotting the 6 replicates indicated on the same axes. *M. smegmatis* strains were cultured in LBT media and cells were pelleted and were lysed in associative (10 mM Mg^{2+}) or non-associative (1 mM Mg^{2+}) ribosomal buffer and lysates were clarified by ultracentrifugation. Ribosomes were pelleted by ultracentrifugation on a sucrose cushion. Ribosome sub-species were separated by ultracentrifugation on associative or non-associative sucrose gradients. Absorbance of fractions was measured at 254 nm. Wild type and *ΔrafS*$_{Msm}$*c* independent replicates are indicated (W1 to W3 and C1 to C3 respectively). Representative traces are shown in bold lines. Normalized absorbance and fraction ratios are indicated. Direction of sedimentation is from right to left.

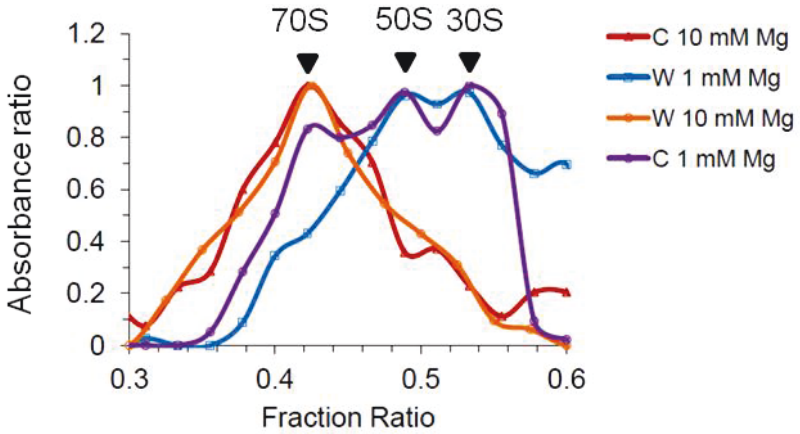

Figure 4.29. 10 mM Mg^{2+} is required during sucrose gradient centrifugation to maintain ribosomal subunit association. The plots were generated by superimposing the 4 replicates indicated. *M. smegmatis* strains were cultured in LBT media and cells were pelleted. Cell pellets were lysed by cell disruption into associative ribosomal buffer (10 mM Mg^{2+}) using a cell disruptor and clarified by ultracentrifugation to remove cellular debris. Ribosomes were pelleted by ultracentrifugation on a sucrose cushion. Wild type and complemented mutant associative ribosome pellets were divided into two halves. One half was centrifuged on a 1 mM sucrose gradient and the other half was centrifuged on a 10 mM sucrose gradient in order to determine the subunit profile. Fractions were collected manually and absorbance of fractions was measured at 254 nm. Results obtained are from a single experiment. Wild type and *ΔrafS*$_{Msm}$*c* independent replicates are indicated (W and C, respectively). Normalized absorbance and fraction ratios are indicated. Direction of sedimentation is from right to left.

4.5.3 Role of $RafS_{Msm}$ in normoxic log phase 70S ribosome subunit association

Having determined the appropriate conditions for ribosomal profiling, we next investigated whether loss of *rafS*$_{Msm}$ affects the ribosomal subunit composition of actively growing *M. smegmatis* cells. Log phase in standard normoxia was defined as an OD_{600nm} of 0.5 to 1 in a 1:2 culture: air ratio based on a growth curve experiment shown in Appendix Figure 5 (Materials and Methods section 2.5.5). A growth curve of strains investigated in these conditions is shown in Appendix Figure 5. Ribosomal profiles of three independently constructed *ΔrafS*$_{Msm}$ *M. smegmatis* mutants were investigated.

In comparison to wild type ribosomal profiles, *ΔrafS*$_{Msm}$ profiles indicated apparently similar proportions of 70S and 50S ribosomal species (Fig. 4.30). Given these results, ribosomal profiling of the *ΔrafS*$_{Msm}$c mutant (complemented mutant constitutively expressing *rafS*$_{Msm}$ via an hsp60 promoter) under these conditions was not pursued further. Thus, it was concluded that there was no ribosomal stability defect for the *ΔrafS*$_{Msm}$ mutant during active growth.

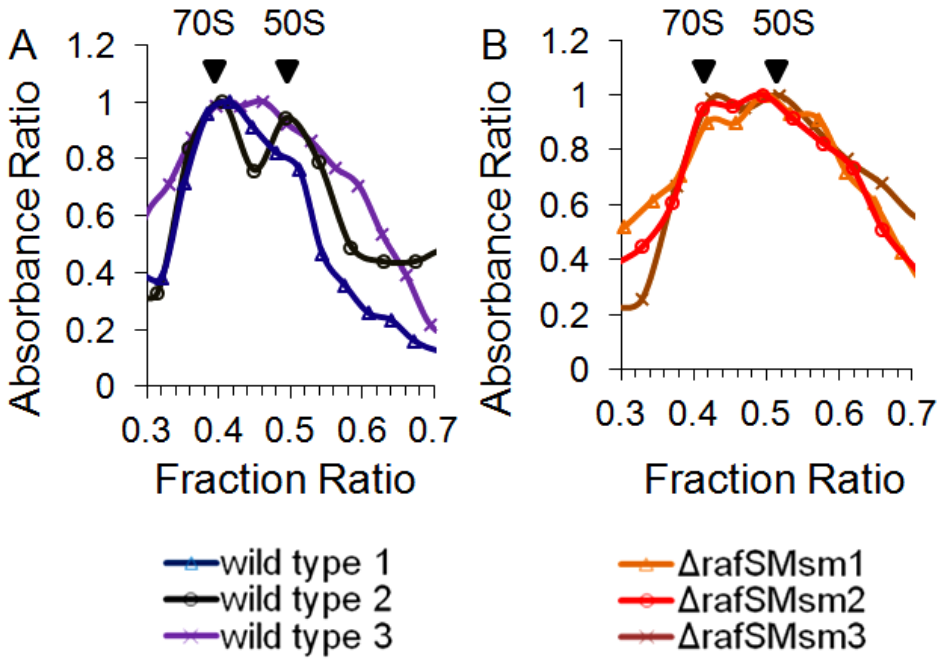

Figure 4.30. $RafS_{Msm}$ is dispensable for ribosome stabilisation in normoxic LBT log phase in associative conditions (10 mM Mg^{2+}). Ribosomal profiling was carried out for independent stationary phase cultures of wild type (A), *Δ$rafS_{Msm}$* (B) *M. smegmatis* strains. Three biological replicates per strain are shown. 70S and 50S ribosomal forms are indicated. *M. smegmatis* strains were cultured in the required media and cells were pelleted. Cell pellets were lysed by cell disruption into associative or non-associative ribosomal buffer using a cell disruptor and clarified by ultracentrifugation to remove cellular debris. Ribosomes were pelleted by ultracentrifugation on a sucrose cushion. Ribosome sub-species were separated by centrifugation on associative or non-associative sucrose gradients. Fractions were collected manually and absorbance of fractions was measured at 254 nm. Direction of sedimentation for is from right to left.

4.5.4 Role of RafS$_{Msm}$ in normoxic stationary phase 70S ribosome subunit association

We next investigated whether RafS$_{Msm}$ plays a role in ribosome stabilisation during stationary phase. It was determined that homogeneous cultures in early stationary phase in LBT in standard normoxia (1:5 culture: air ratio) resulted in reproducible and readable ribosomal profiles (Materials and Methods section 2.5.5). Ribosomal profiles of wild type, *ΔrafS$_{Msm}$* and *ΔrafS$_{Msm}$*c cultures indicated that 70S and 50S ribosomal species were equally predominant or 50S ribosomal subunits were slightly more predominant for all strains (Fig 4.31). Enlarged plots of Fig. 4.31 are shown in Appendix Figures 8, 9 and 10. I concluded that *rafS$_{Msm}$* was dispensable for early normoxic stationary phase ribosome stabilisation in associative conditions.

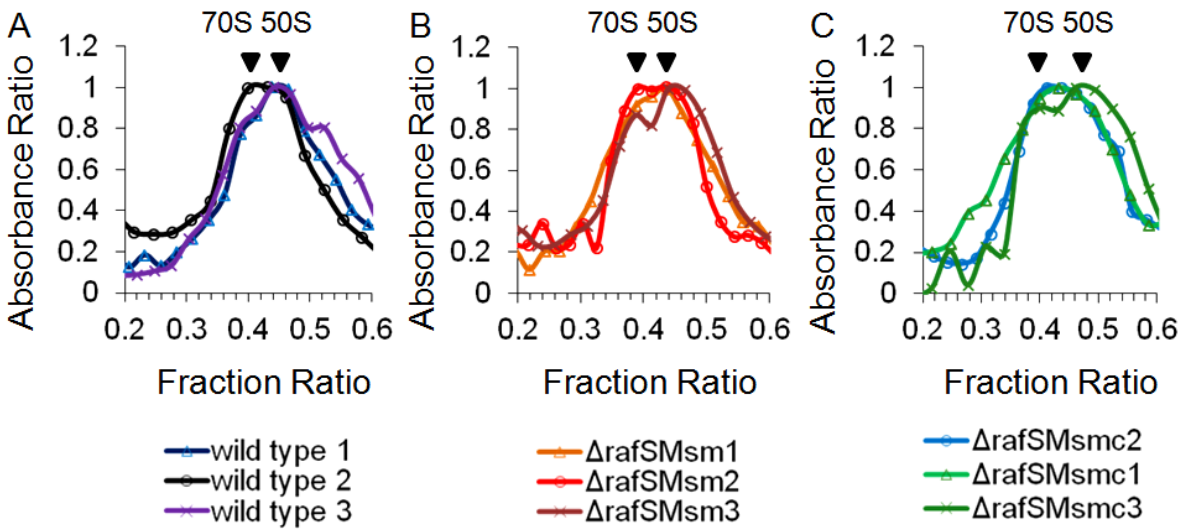

Figure 4.31. $RafS_{Msm}$ is dispensable for ribosome stabilisation in normoxic LBT early stationary phase in associative conditions (10 mM Mg^{2+}). Ribosomal profiling was carried out for independent stationary phase cultures of wild type (A), *Δ$rafS_{Msm}$* (B) and *Δ$rafS_{Msm}$*c *M. smegmatis* strains (C). 3 biological replicates per strain are shown with 3 independent mutant replicates for the *Δ$rafS_{Msm}$* strain. 70S and 50S ribosomal species are indicated with black arrows. Strains were cultured in LBT and cells were pelleted. Cell pellets were lysed by cell disruption into associative ribosomal buffer using a cell disruptor and clarified by ultracentrifugation to remove cellular debris. Ribosomes were pelleted by ultracentrifugation on a sucrose cushion. Ribosome sub-species were separated by centrifugation on associative sucrose gradients. Fractions were collected manually and absorbance of fractions was measured at 254 nm. Direction of sedimentation is from right to left.

4.5.5 Role of $RafS_{Msm}$ in mycobacterial ribosomal subunit association: summary

Taken together, the ribosomal profiling data indicated that $RafS_{Msm}$ is dispensable for ribosome stabilisation in active growth and in early normoxic stationary phase in rich media. In comparing the ribosomal profiles obtained in associative conditions in Fig. 4.28 and Fig. 4.30, it was observed that the 50S ribosomal species were largely absent in Fig. 4.28 and present in Fig 4.30.

This difference was suggested to be due to cell disruption being carried out at $4^{o}C$ in Fig 4.30 and at room temperature in Fig. 4.28. The 30S peak was not always visible in traces and this agreed with what we have seen in previous data from our laboratory (Trauner, 2010). This did not affect the interpretation of results since the 50S peak was taken to be a better indicator of dissociated ribosomes.

In this study, I observed that both 70S and 50S ribosomal species were present in wild type *M. smegmatis* stationary phase cells. However, Andrej Trauner's wild type *M. smegmatis* stationary phase profiling resulted in a single predominant peak which was annotated as 70S ribosomes. Profiling of the *M. bovis* wild type, however, did yield 50S and 70S ribosomal species (Trauner *et al.,* 2010).

The reason for the difference in findings for *M. smegmatis* ribosomes is unclear, although differences in methodology may have contributed to this. Based on these observations, it is suggested that cell disruption at $4^{o}C$ may be important for ribosomal profiling. As shown, deletion of $rafS_{Msm}$ did not affect ribosomal stability in rich normoxic exponential or stationary phase.

4.6 Raf protein biochemical findings: discussion

The most significant finding presented in this chapter is the role of $RafS_{Msm}$ and $RafH_{Mtb}$ in inhibition of *in vitro* translation of *Renilla* luciferase, *Omega* luciferase and polyU mRNAs by *M. smegmatis* dissociated ribosomes, suggesting that these proteins are versatile translation inhibitors, since inhibition occurred despite significant differences in mRNA type. Also, $RafS_{Msm}$ and $RafH_{Mtb}$ both showed significant inhibition of translation of *Renilla*-luc mRNA by *M. smegmatis* non-dissociated ribosomes (see section 4.4.3).

Inhibition of translation was higher when dissociated ribosomes were employed. This finding agrees with what is known about Raf proteins binding to ribosomes. The *M. smegmatis* Raf proteins were found to bind to 30S ribosomal subunits (Trauner *et al*., 2010) and thus Raf protein binding to the ribosome is likely to occur more frequently when ribosomal subunits are dissociated (known to occur in low Mg buffer).

The *Renilla* luciferase translation system is considered to be the closest to physiological of the translation systems investigated here, since it contains a Shine-Dalgarno (SD) sequence and lacks a translational enhancer sequence. Given the data presented indicating Raf-mediated inhibition, it is recommended that *Renilla* luciferase mRNA translation by dissociated and non-dissociated *M. smegmatis* ribosomes be further investigated for $RafS_{Mtb}$ and $RafH_{Msm}$, should they be successfully purified.

However, the increase in translation that preceded inhibition of *Renilla* luciferase mRNA translation by dissociated ribosomes has not been observed

previously in the literature on S30AE ribosome stabilisation factors (Fig 4.23). Whether this biphasic effect is physiologically important is unknown. It may be worthwhile to investigate whether there is a threshold concentration of Raf proteins beyond which they act as inhibitors of translation and below which they do not compete effectively with mRNAs due to being displaced by initiation factors. It remains a possibility that low concentrations of Raf proteins assist in preventing 30S subunit degradation and whether this plays a role in stimulating translation when Raf protein abundance is low.

In comparing the Raf-mediated *Renilla* luciferase mRNA translation inhibition with that of *Omega* luciferase mRNA, the data suggests that the presence of a viral translational enhancer (*Omega* enhancer from tobacco mosaic virus) reduces the translation inhibitory effects of Raf proteins. Nevertheless, the levels of inhibition of translation by dissociated ribosomes were 53% and 84% for $RafS_{Msm}$ and $RafH_{Mtb}$, respectively. It would be interesting to investigate whether Raf proteins are capable of inhibiting translation of viral mRNAs which contain translational enhancers, since such data would suggest that Raf proteins may be capable of anti-viral defense in mycobacteria.

Inhibition of polyU mRNA translation by dissociated ribosomes was significant for both Raf proteins investigated (67% and 80% for $RafS_{Msm}$ and $RafH_{Mtb}$, respectively). This suggests that $RafS_{Msm}$ and $RafH_{Mtb}$ are capable of inhibiting translation of mRNA that lack SD and AUG start sequences. In this assay, inhibition of translation elongation is physiologically relevant since SD sequence recognition by the ribosome does not occur. These findings agreed with that shown for PY (60% to 70% PY: ribosome 1:1) Agafonov also illustrated a role for PY in reducing miscoding

during translation of polyU mRNA, a function which may be worthwhile to investigate with respect to the Raf proteins (Agafonov *et al*., 2004).

Notably, the inhibitory effects of $RafS_{Msm}$ and $RafH_{Mtb}$ on *in vitro* translation have not been demonstrated previously in the existing literature on Raf proteins. In 2012, Kumar *et al.* presented a paper in which $RafH_{Mtb}$ was assigned the name "Dormancy Associated Translation Inhibitor (DATIN)". However, it is unknown as to whether the translation assay presented employ mycobacterial ribosomes and the association of $RafH_{Mtb}$ with mycobacterial dormancy was not experimentally proven. Furthermore, Figure 2 of the paper indicated inhibition of translation by $RafH_{Mtb}$, but ribosome buffer employed was not stated and the extent of inhibition was not quantified (Kumar *et al.,* 2012).

Also, the mycobacterial translation data presented in this work is more reliable than that presented by Kumar *et al*. It is not clear from Kumar's study as to how the ribosomes were prepared and how many replicates of the assay were carried out. Also, they employed an *E. coli* S30 extract. In our study, we have specifically employed *M. smegmatis* ribosomes and indicated the buffer used in all of our translation assays. *M. smegmatis* ribosomes are structurally different to *E. coli* ribosomes and an extra 497 amino acids are present in *M. smegmatis* ribosomes (Shasmal *et al*., 2012).

Furthermore, the S30 extract is from *M. smegmatis* and the Raf: ribosome ratios and percentage inhibition of translation data are indicated in this study, whereas these have not been stated in Kumar *et al*'s work, and cannot be inferred from the amount of Raf protein quoted, since the amount of ribosomes employed was omitted.

Also, the predicted protein structure of $RafH_{Mtb}$ presented in Figure 1 of Kumar's paper (Kumar *et al.,* 2012) is inaccurate and lacks the S30AE domain which has been predicted with high confidence in this work (Figure 4.4). In a further paper, they published a predicted structure of $RafH_{Mtb}$ structure that appeared to be structurally different to the one previously published (Kumar *et al*., 2013). In our predicted structures, one can observe the characteristic βαββββα topology of Raf protein N-terminal domains and its similarity to the S30AE domain of PY and other known S30AE homologues.

Regarding the effect of Raf proteins on ribosome subunit association, it is possible that the presence of $RafH_{Msm}$ compensated for the loss of $RafS_{Msm}$. This can be further investigated by investigating the ribosome subunit composition of a $\Delta rafS_{Msm}$ $\Delta rafH_{Msm}$ strain. We do not rule out the possibility that ribosomal subunit association may be a possible mechanism for Raf protein-mediated inhibition and stabilisation of ribosomes. It is also worthwhile to attempt to purify higher concentrations of Raf proteins and test their effect on association of dissociated ribosomes *in vitro*.

It remains a possibility that the conditions under which Raf proteins are significantly expressed are yet unknown. Thus, it is recommended that further ribosomal profiling assays are carried out in conditions of nutrient starvation, such as carbon starvation and nitrogen starvation. It is also recommended that the *in vitro* effect of Raf proteins on subunit association be characterised.

To inform this investigation, it is suggested that mass spectrometry be used to determine the Raf protein levels under different starvation conditions in order to further investigate the ribosome subunit profile of $\Delta rafS_{Msm}$ conditions under which

Raf proteins are highly expressed. Ribosomal profiling is a key approach which would assist in understanding whether the mechanism of Raf protein-mediated inhibition of translation is related to ribosome subunit association, the physiological stimuli for inhibition of translation, and whether translation inhibition is a key stress tolerance mechanism under a specific physiological condition.

The spinach plastid protein Psrp-1 is a long HPF and S30AE protein and was found to bind at a similar location to that of PY on the 30S subunit. Psrp-1 was associated with an increase in the proportion of *E. coli* 70S ribosomes when incubated *in vitro* with dissociated ribosomes (Sharma *et al.,* 2010). Also, Sharma *et al*. suggested a function for RRF (ribosome recycling factor) and EF-G (elongation factor G) in returning Psrp-1-inactivated ribosomes to the actively translating pool (Sharma *et al.,* 2010). Given that there are effects of Raf proteins on subunit association in vitro, testing the effect of adding factors such as IF3, RRF and EF-G would also help to investigate whether Raf-mediated subunit association can be reversed by adding translation factors.

Ribosome subunit association is not the only mechanism associated with ribosome inactivation. Notably ribosome subunit dissociation can also achieve ribosome inhibition. An example of a factor which achieves this is RsfA or ribosome silencing factor A from *E. coli*. Häuser *et al.* discovered a role for RsfA in independent and competitive growth during the transition from rich to poor media and also in interfering with ribosome subunit association and translation (Häuser *et al.* 2012).

Häuser *et al*. confirmed binding of RsfA to the ribosomal subunit interface and then investigated RsfA binding to previously reported potential interaction partners in

the large ribosome subunit using a yeast two-hybrid assay (Häuser *et al.* 2012). This study highlighted ribosome dissociation as another mechanism of ribosome silencing other than ribosome stabilisation and it also highlighted a role for ribosome silencing in stress tolerance.

Chapter 5: General Discussion

5.1 Scope of the general discussion

The aim of this work was to investigate whether RafS is a ribosome stabilisation factor in mycobacteria and investigate whether it plays a role in stress tolerance. It has been determined that deletion of *rafS*$_{Msm}$ did not have a significant effect on growth and survival in rich media and in carbon–limited media in hypoxic and normoxic conditions. Also, deletion of *rafS*$_{Msm}$ did not affect biofilm and pellicle formation and survival in short term acid stress and heat stress. Deletion of *rafS*$_{Mtb}$ did not affect growth in rich media but was associated with a competitive survival defect in prolonged stationary phase.

Deletion of *rafS*$_{Msm}$ did not affect ribosome subunit association in active growth. However, RafS$_{Msm}$ and RafH$_{Mtb}$ were found to inhibit *in vitro* translation of *Renilla* luciferase mRNA, polyU mRNA and *Omega*-luciferase mRNA when incubated with ribosomes dissociated in a low magnesium buffer. Thus, it has been shown that Raf proteins are ribosome inactivating factors, but it remains to determined as to whether they can act as ribosome stabilisation factors *in vivo* under physiological conditions. The significant findings of this work and recommendations for future study are discussed in the subsequent sections.

5.2 Raf proteins are inhibitors of *in vitro* mycobacterial translation

In this work, ribosome stabilisation is defined as a combination of inhibition of ribosome translation and also ribosome subunit association or ribosome multimer formation. This definition differentiates ribosome stabilisation from ribosome inactivation or ribosome silencing where ribosome subunit association or ribosome multimer formation does not occur. This study has shown that Raf proteins $RafS_{Msm}$ and $RafH_{Mtb}$ satisfy a key requirement that is important for ribosome stabilisation i.e. inhibition of translation.

These findings suggest that it is worthwhile to further investigate the conditions under which $RafS_{Msm}$ and $RafH_{Mtb}$ are expressed and whether they may play a role in conservation of energy and resources. All significant inhibitory effects were observed when Raf proteins were present in a molar excess of ribosomes and it remains to be determined as to whether these ratios are physiologically related and if so, under which conditions.

It is yet unknown as to whether Raf protein-mediated inhibition of translation observed *in vitro* is associated with a change in ribosome subunit composition. In the absence of finding a role for Raf proteins in ribosome subunit association in rich media cultures, it remains to be proven as to whether Raf proteins are ribosome stabilisation factors, although it has been shown in this study that $RafS_{Msm}$ and $RafH_{Mtb}$ are ribosome inactivating factors. Also, it has not yet been demonstrated as to whether RafH is necessary and sufficient for ribosome stabilisation, although RafH is regulated by DosR, which is essential for ribosome stabilisation (Trauner *et al*., 2012).

Raf-mediated translation inhibition shown in this study agrees with what has been shown for *E. coli* PY. PY inhibits both firefly luciferase mRNA translation by approximately 67% (PY: ribosome 1:1) and polyU mRNA translation by approximately 88% (PY: ribosome 4:1) (percentage inhibition estimated based on bar charts of raw numbers) (Agafonov *et al*., 2001). However, Raf-mediated translation inhibition is less similar to *E. coli* HPF-mediated translation inhibition since HPF inhibited polyU mRNA translation significantly (81%, HPF: ribosome 20:1) but only inhibited SD mRNA translation partially (20%, HPF: ribosome 20:1) (Ueta *et al.*, 2008).

The translation assays suggest that Raf proteins are more potent inhibitors of ribosomes dissociated by resuspending in a low magnesium buffer. This finding is consistent with the finding that Raf proteins bind the 30S ribosomal subunit, which has been shown by mass spectrometry (Trauner *et al*., 2010). It would be interesting to further determine whether removing the C-terminal domain affects Raf protein-mediated inhibition of translation, since this would allow investigating whether the N-terminal domain is sufficient for inhibiting translation.

I speculate that there are several possible advantages of ribosome translation inhibition, which include (i) conservation of resources (ii) protection of ribosomes from damage (iii) preservation of ribosomes for restarting growth after prolonged stasis and (iv) translational regulation associated with specific responses, such as persistence-related mechanisms. Further investigations regarding these proposed advantages are discussed in subsequent sections.

5.3 Role of Raf proteins in stress tolerance - $RafS_{Mtb}$ plays a role in maintaining viability in competitive survival in stasis

The correlations between ribosome stabilisation and stress tolerance have been adequately investigated for some ribosome stabilisation factors and have not been proven conclusively for others. For example, deletion of *E. coli* RMF has been associated with decreased survival in acid stress and heat stress (section 1.5.3.2), whereas PY has been associated with cold acclimation but only a partial role has been demonstrated and studies of other stress conditions are lacking (section 1.5.3.5). In this study, a range of physiological stress investigations were conducted to investigate *Δ$rafS_{Msm}$* phenotypes.

As summarised in section 3.8, *$rafS_{Msm}$* was dispensable for growth and survival in several conditions. In this study, the predominant focus of nutrient starvation assays was on carbon limitation. However, it remains to be investigated as to whether RafS plays a role in nitrogen or phosphate starvation, given that $RafS_{Mtb}$ was significantly upregulated after 4 hours and also after 24 hours of stationary phase in general nutrient starvation (section 1.7.2).

A major significant finding of the physiological studies was that $RafS_{Mtb}$ plays a role in maintaining viability during competitive survival in prolonged rich stasis. The stasis competition assay is intended to impose starvation stress on wild type and deletion mutant strains as a direct result of inter-strain competition. Survival of *Δ$rafS_{Mtb}$* was severely compromised at days 164 and 238 (154 – 228 days in normoxic rich stasis) (section 3.7.2). Notably, the phenotype was observed after a long period of time in stasis and it remains to be investigated as to whether more

stringent nutrient starvation would be associated with sooner onset of the *ΔrafS*$_{Mtb}$ survival defect.

These data indicated that, along with maintaining survival of *M. tuberculosis* in prolonged stasis, it is also worth investigating whether *rafS*$_{Mtb}$ plays a role in inter-species competition. The ability to maintain viability under nutrient starvation is a key advantage for survival of *M. tuberculosis* in granulomas. Furthermore, maintaining higher viability would enhance spreading of *M. tuberculosis* to uninfected granulomas (section 1.2.2).

Based on the hypothesis that RafS binds and stabilises 30S subunits and prevents them from being degraded, there is scope for investigation as to whether this process may be a resource conservation mechanism that correlates with the competitive advantage of wild type *M. tuberculosis* in competition with *ΔrafS*$_{Mtb}$. It may also be investigated as to whether RafS$_{Mtb}$ plays a role in preventing other non-mycobacterial species from scavenging 30S subunits which are nutrient-rich and may be released upon cell death during stasis.

It would be necessary to further investigate Raf protein *in vivo* expression levels (in comparison to ribosome levels) in order to investigate these hypotheses and determine whether the Raf: ribosome ratios associated with *in vitro* inhibition of translation are similar. Furthermore, research on this hypothesis would be useful in demonstrating an *in vivo* condition which confers physiological importance to Raf-mediated inhibition of *in vitro* translation.

To our knowledge, the role of an S30AE protein in maintaining viability in competitive stasis has not been shown previously. Furthermore, genes associated with competitive defects in prolonged stasis in mycobacteria are lacking. Hauser *et*

al. demonstrated a competitive defect in log phase growth of the *ΔrsfA* mutant and illustrated that the ribosome silencing factor RsfA plays a role in competitive fitness in 35 generations of active growth (Hauser *et al*., 2012). Taken together with our data, this suggests that investigation of the effect of deletion of Raf proteins on growth and stasis competitive defects in other stress conditions is worthwhile.

Also, it would be interesting to determine whether the loss in viability of the *Δraf*S_{Mtb} mutant is accelerated in independent nutrient-starved stasis. This would assist in understanding whether the competitive defect observed is exclusively a competitive defect or is a result of a survival defect in independent culture. Furthermore, this finding suggests that a competitive assay investigating potential expression regulators of Raf gene expression and survival of Raf gene deletion mutants in macrophage and mouse models is worthwhile. This would assist in understanding whether $RafS_{Mtb}$ can act as a virulence factor that enhances survival in nutrient starvation.

5.4 Recommendations for further work on Raf-mediated inhibition of translation

5.4.1 Structural investigations of Raf proteins

Based on the mechanisms of translation inhibition suggested for *E. coli* RSFs (see section 1.5), it can be investigated as to whether Raf proteins inhibit translation by one or more of the following mechanisms (i) preventing recognition of SD sequences or mRNA by blocking the region of 16S rRNA that contains the anti-SD sequence (ii) binding to the 30S subunit mRNA channel and thus preventing mRNA binding and contact to A and P translation site tRNAs.

Regarding the docking site of Raf proteins on the ribosome, it is recommended that high-resolution crystal structures of Raf proteins in complex with the ribosome are obtained. It is worthy to note that the 70S ribosome-PY structure of Polikanov *et al.* suggested that PY binds to the 30S subunit at its mRNA channel. Furthermore, PY docking to the ribosome is suggested to result in N and C-terminal domains of PY obstructing access of A and P site tRNAs (Polikanov *et al*., 2012). It would be useful to investigate the docking sites of Raf proteins on the ribosome, since this would help to determine whether their mode of inhibition of translation occurs in a similar manner to that of PY.

Ye *et al.* employed NMR spectroscopy to determine the solution structure of PY and determined several conserved residues of basic charge localised to the α helices of the S30AE domain. These helix-localised basic residues were suggested to play a role in binding rRNA, in contrast to the solvent-exposed side of the β

sheets, which consists predominantly of polar and hydrophobic residues (Ye *et al.,* 2002) (Appendix Figure 5).

These findings support the hypothesis that the PY S30AE domain binds the ribosome *in vivo,* since they suggest that there are residues of appropriate charge that can mediate protein-rRNA connections at physiological pH. Similarly, it would be useful to gain similar information for Raf proteins and to investigate ribosome-binding affinities of Raf proteins. Obtaining the structures of RafS proteins in complex with ribosomes would allow determination of which residues of the ribosome are contacted by the RafS proteins.

Ye *et al.* noted a similarity in structure and in amino acid residues (50% conservation of residues) between PY and double-stranded ribosome binding domains of *Drosphila* Staufen and human interferon-induced protein kinase PKR. In addition to the questions raised in this section, this suggests that structural studies of Raf proteins and PY would also contribute to an understanding of the biochemistry of double-stranded ribosome binding domains.

Also, further investigation of the structures of Raf protein C-terminal extensions and orientation of Raf protein linker and C-terminal domains when docking at the ribosome is warranted. Should the C-terminal domain be shown to localise to a binding site on the ribosome that is not involved in translation, it would be interesting to know whether it plays any role in stabilising the conformation of the 30S subunit so as to prevent conformational changes that could induce dimerisation. Alternatively, it may play a role in recognising binding partners or environmental stimuli.

5.4.2 Investigating Raf-mediated inhibition of translation in competition with mRNA and fMet-tRNA and investigating Raf-mediated 30S ribosome subunit protection

As discussed in section 5.2, Raf proteins inhibit *in vitro* translation by *M.F smegmatis* ribosomes. Further evidence is needed to relate *in vitro* Raf-mediated inhibition to *in vivo* mechanisms. For example, it would be worthwhile to investigate whether Raf proteins compete effectively with mRNA and fMet-tRNA for binding to the ribosome. To investigate this, it would be important to attempt translation assays with dissociated ribosomes without pre-incubation of Raf proteins with ribosomes prior to adding the other components of the translation mixture.

Similar questions regarding PY-mediated inhibition of translation are also outstanding. Although it was shown that PY inhibits aminoacyl tRNA binding to the ribosome, this was demonstrated with PY pre-incubation with ribosomes without other components of the translation reaction mixture (Agafonov *et al.,* 2001). If Raf proteins are less effective as translational inhibitors when mRNA and tRNA are abundant, this would lead to the question as to whether their inhibitory effects are therefore less potent during nutrient abundance and more potent during nutrient limitation.

I suggest that direct incubation of proteins with the translation mixture is more close to the physiological conditions of nutrient abundance, whereas pre-incubation of ribosomes and Raf proteins without the other components of the translation mixture is more relevant to conditions of nutrient starvation. These studies would also assist in understanding whether there is a nutrient-dependent mechanism for releasing Raf proteins from ribosomes and restoring ribosomes to active translation.

In addition to these studies, it is worthwhile investigating whether Raf proteins may have a role in protecting 30S subunits from being degraded and if so, whether this plays a role in conservation of cellular resources. Investigating this would involve investigating whether Raf-30S subunit complexes are less prone to degradation by endoribonucleases. Could Raf protein-mediated inhibition of translation be a means of protecting 30S subunits from being degraded post-lysis, so that 30S subunits can be protected as a nutrient source exclusively to mycobacteria?

5.4.3 Investigating Raf-mediated inhibition of response-specific mRNAs

It is still not known as to whether Raf proteins play a role in global shut down of protein synthesis or whether they more specifically inhibit translation of specific transcripts under specific stress conditions. As Di Pietro suggests, it is important not to conclude that ribosome associated inhibitors are causative agents of global translation shut down when ribosome-associated inhibitors' expression or ribosome binding correlates with translation shut down (Di Pietro *et al.,* 2013).

Given the mRNA-dependent inhibition of PY outlined in section 1.5.3.5 (Di Pietro *et al*., 2013), it would be useful to investigate whether Raf proteins may be involved in selectively inhibiting translation i.e. inhibiting translation of mRNA encoding certain types of genes as part of a physiological response. To inform selection of mRNAs for investigating mRNA-dependent translation inhibition, it would be worthwhile to first investigate Raf protein expression levels in different conditions by mass spectrometry. This would assist in determining whether there are specific pathways or stress tolerance conditions under which Raf protein expression is upregulated or downregulated.

For example, to further investigate whether Raf proteins play a role in tolerance of energy-limiting conditions, it would be useful to know whether Raf proteins permit the translation of specific mRNA transcripts that are important for energy-limitation stress tolerance. Given the findings discussed in sections 1.6.4 and 1.7.2, it is worthwhile to investigate Raf-mediated inhibition of translation of a selection of mRNAs that encode proteins that play a role in tolerance of nutrient starvation (RafS) and hypoxia (RafH) in comparison to mRNAs that are not involved in stress tolerance.

5.4.4 Investigating Raf-mediated inhibition of leaderless mRNA translation

Cortes *et al*. determined that there is an extensive leaderless mRNA transcriptome in *M. tuberculosis* which lack a 5' UTR (untranslated region). 5' UTRs contain an SD sequence that is typically recognised by the ribosome during initiation. Given the Raf-mediated inhibition of polyU mRNA observed, it would be interesting to further investigate whether Raf proteins are also capable of inhibiting translation of mycobacterial leaderless mRNA. polyU and leaderless mRNA both lack the Shine Dalgarno sequence that is required for typical mRNA recognition by ribosomes.

Although its role in mycobacterial physiology is not known, genes with active growth functions were notably absent from the *M. tuberculosis* leaderless mRNA transcriptome, suggesting that leaderless mRNA may play a role in stationary phase or persistent mycobacterial physiology (Cortes *et al*., 2013). Although Raf proteins are inhibitors of polyU mRNA translation, it remains a possibility that there are conditions or mRNAs for which translation inhibition is partial or low, since Raf-

protein mediated inhibition of polyU mRNA translation by non-dissociated ribosomes was partial (see section 4.4.2).

The first evidence for the formation of a subpopulation of functionally distinct ribosomes under adverse conditions that are capable of leaderless translation was obtained by Kaberdina *et al.* They demonstrated that treatment of *E. coli* with the antibiotic kasugamycin results in the formation of 61S ribosomes depleted for several essential proteins of the small subunit, including the functionally important proteins S1 and S12 and that these ribosomes were capable of leaderless mRNA translation. The genes that were translated encoded chaperones, stress proteins, ribosomal proteins and ribosome modifying enzymes (Kaberdina *et al.,* 2009).

Kaberdina *et al.* also showed that these respective mRNAs became leaderless in the presence of the antibiotic. The 61S stress ribosomes were found to be protein-depleted ribosomes which allowed translation of selected genes (Kaberdina *et al.,* 2009). It remains to be shown as to whether there are similar ribosome protein depletion mechanisms in mycobacteria and whether these mechanisms occur in response to specific antibiotics or other stresses. Given these findings, it would be worth isolating leaderless mycobacterial mRNAs and investigating whether or not Raf proteins inhibit or permit their translation.

In a more recent study, Vesper *et al.* showed that in *E. coli,* the toxin anti—toxin module *mazEF* (downstream of *rela*) regulates the formation of leaderless mRNA and specialised ribosomes that carry out their translation. MazE acts as an anti-toxin and is bound to toxin MazF after these proteins are synthesised. ClpAP protease degrades MazE and this releases MazF, an endoribonuclease toxin that cleaves single stranded mRNAs at ACA sequences. MazF cleaves closely upstream

of the AUG start codon of specific mRNAs and converts them to leaderless mRNAs. MazF also removes 43 nucleotides from the 3' terminus of 16S rRNA at the decoding centre of 30S ribosomal subunits. The ribosomes then become capable of translation of leaderless mRNA and are known as $70S^{\Delta 43}$ ribosomes (Vesper *et al.,* 2011).

Given that PY binds at this proposed site of the 30S subunit, according to Polikanov *et al.,* it is worthwhile to investigate whether PY-bound ribosomes are protected from modification by MazF or whether MazF is capable of displacing PY in order to mediate leaderless mRNA translation. This leads to the question as to whether a similar system exists in mycobacteria, for which Raf proteins play a role. I suggest that if Raf proteins are displaced by other (hypothetical) mycobacterial proteins involved in leaderless mRNA translation, then it should subsequently be investigated as to whether Raf proteins protect mycobacterial ribosomes from cleavage by non-mycobacterial ribosome-targeting toxins, such as MazF.

5.4.5 Investigating RafS protein cleavage and post-cleavage activity: $RafS_{Mtb}$ and $RafS_{Msm}$ are predicted substrates of Clp protease, a key post-transcriptional regulator in *M. tuberculosis*

Post-transcriptional regulation via Clp protease has been shown to play a role in regulation of *M. tuberculosis* physiology. Inhibition of Clp protease leads to mycobacterial death *in vitro* and in mouse infection models, suggesting that it plays an important role in ensuring cell viability during *in vivo* infection (Raju *et al.,* 2012). In a recent paper, Raju *et al.* showed that several proteins accumulate after Clp protease deletion and that these are putative Clp protease substrates (Raju *et al.,* 2014).

In this study, RafS was highlighted as a putative Clp protease substrate. Deletion of Clp protease resulted in a 2.46 fold increase ($p<0.01$) in both $RafS_{Mtb}$ and $RafS_{Msm}$ accumulation in 48 hours of growth in rich 7H9 media, respectively. RafH was notably absent from this list (Raju *et al.,* 2014). In this work, we have shown for the first time that $RafS_{Msm}$ is an inhibitor of *in vitro* translation. Based on the predicted features of Raf proteins described in section 4.1, it would be interesting to know whether Clp protease degrades Raf proteins or whether Clp-mediated cleavage transforms Raf proteins into structures that are still active but perform a different function. It would be worthwhile to:

1. Investigate whether RafS is cleaved by Clp protease and the effect of this cleavage on protein structure and translation inhibition.
2. Determine whether RafS accumulation is toxic to cells by over-expressing RafS proteins in a strain where the gene encoding Clp protease is deleted.

3. Determine whether Clp protease is capable of cleaving ribosome-bound RafS.
4. Determine whether blocking Clp-dependent degradation of RafS is toxic to mycobacteria.

5.4.6 RafS protein-mediated inhibition of translation as a platform for developing peptide-based anti-mycobacterial therapeutics: is RafS accumulation toxic to mycobacteria?

The primary aim of this work was to characterise the function of RafS in mycobacteria. However, given the potent translation inhibition mediated by Raf proteins, it is apt to ask whether Raf protein accumulation is toxic to mycobacteria. Notably, $RafS_{Mtb}$ was detected in 30-day infected guinea pig lungs but was absent in chronic infection at 90 days (section 1.7.2) (Kruh *et al*., 2010). Furthermore, using microarray analysis, Garton *et al*. found that $rafS_{Mtb}$ was one of 334 genes that were significantly repressed in sputum of infected patients compared to aerobic cultures of *M. tuberculosis* ($p = 5.9 \times 10^{-3}$) (Garton *et al.,* 2008).

Added to the finding that RafS is predicted to be cleaved by Clp protease (see section 5.4.5), these studies indicate that it is worth further investigation as to whether RafS accumulation is toxic to mycobacteria. Also, it is worthwhile to pursue structural characterisation of Raf-mediated inhibition of translation since a more detailed understanding of Raf protein structure and function may be useful for developing small-molecule therapeutic peptides that inhibit ribosome translation.

In order to determine whether this is a viable prospect, it will be important to ensure that Raf proteins are not inhibitors of eukaryotic translation and translation by

ribosomes of species that are important for the natural flora of the lung environment. It will also be important to develop peptides that are not cleaved by mycobacterial Clp protease, since this would allow sustained concentrations of the peptide and to investigate bioavailability and peptide uptake into granulomas.

5.4.7 Recommendations for further investigations of $RafH_{Mtb}$ as a ribosome inactivating stress tolerance factor

In this work, it has been shown for the first time that $RafH_{Mtb}$ inhibits mycobacterial translation. Notably $RafH_{Msm}$ has been shown to contribute to DosR phenotypes, which plays a role in association of 50S and 30S subunits (promoting 70S monomer formation) in hypoxic stasis (Trauner *et al.,* 2012). It remains to be shown as to whether $RafH_{Msm}$ is necessary and sufficient for ribosome subunit association. Provided that $RafH_{Msm}$ can be purified in sufficient amounts, it is recommended that the effect of $RafH_{Msm}$ on ribosome subunit association be investigated *in vitro*.

Based on analyses of gene expression in a fatty acid rich culture stasis model, Rodriguez *et al.* suggested that lipid storage is used by *M. tuberculosis* to ameliorate reductive stress damage and has shown that *devR* (of the DosR 2 component system) and *rafH*$_{Mtb}$ show significantly increased expression in exponential and stationary phase. Analysis of the 500 bp upstream region of the initiation codon of the *rafH*$_{Mtb}$ gene indicated the presence of a lipid signature sequence (Rodriguez *et al.,* 2014).

Rodriguez *et al*. suggested that *M. tuberculosis* requires mechanisms to counteract reductive stress during metabolic changes to adapt to fatty acid metabolism since NADPH is likely to accumulate as a result of these changes (Rodriguez *et al.,* 2014). Given these findings, it would be worthwhile to investigate whether *rafH*$_{Mtb}$ plays a physiological role in protecting ribosomes from reductive stress when *M. tuberculosis* switches to metabolism of fatty acids as the main carbon source.

RafH$_{Mtb}$ was identified to be localised to the cell wall of *M. tuberculosis* by 2D LC-MS (1 of 306 proteins) (Mawuenyega *et al.,* 2005). Furthermore, Commandeur *et al.* found also that RafH$_{Mtb}$ is cell wall-associated and is also a moderate inducer of IFN-γ production in splenocytes of mice infected with *M. tuberculosis* (Commandeur *et al.,* 2013). Since Ortiz *et al*. have also shown that 100S dimers in *E. coli* cluster at the cell wall in nutrient-starved stationary phase, this leads to the question as to whether RafH$_{Mtb}$ plays a role in sequestering 70S ribosomes and/or 30S subunits at the cell wall.

In addition to the recommendations presented thus far, it is worth investigating whether induction of RafH$_{Mtb}$ expression may affect mycobacterial physiology in exponential phase. Pang *et al*. suggests that RafH$_{Mtb}$ expression in exponential phase may be repressed by the *mprAB* two-component system. *M. tuberculosis mprAB* was associated with repressing stress-related genes in exponential phase. Deletion of *mprAB* was associated with significant upregulation of RafH$_{Mtb}$ in exponential phase (4.16 fold) (Pang *et al.,* 2006).

Deletion of *mprAB* was also associated with increased resistance to SDS and enhanced growth in peripheral blood monocytes (Pang *et al.,* 2006). Since it has been shown that $RafH_{Mtb}$ inhibits mycobacterial translation (this work) and is regulated by DosR which promotes 70S monomer formation (Trauner *et al.,* 2012), it would be useful to further investigate whether $RafH_{Mtb}$ expression is repressed by *mprAB* in exponential phase and whether induction of $RafH_{Mtb}$ expression in exponential phase confers stress tolerance benefits, such as those indicated by Pang *et al.*

5.5 Concluding remarks

The data and recommendations for further study presented thus far suggest that RafS and RafH are both inhibitors of mycobacterial ribosome translation and that there are several outstanding research questions which are worth investigation. Further investigation would assist in relating the *in vitro* inhibitory effect of Raf proteins on translation to an *in vivo* mycobacterial role such as stress tolerance or nutrient conservation.

Appendix

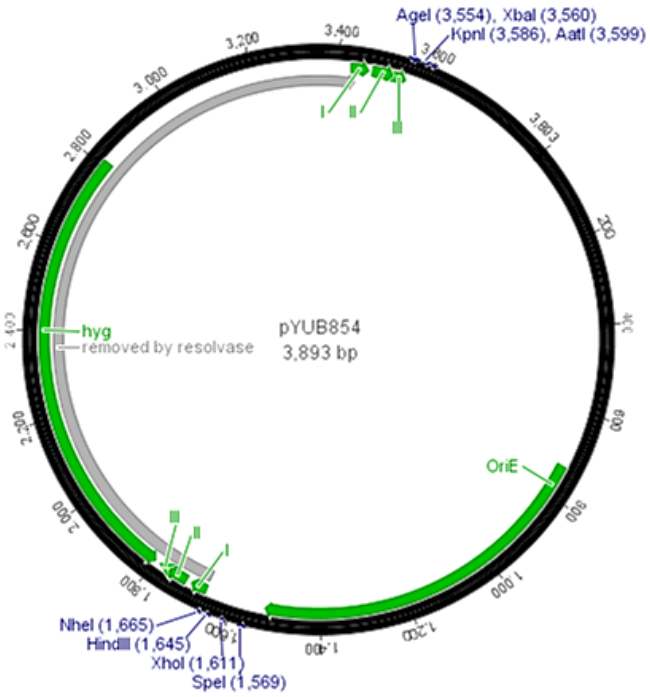

Appendix Figure 2. Map of the plasmid pYUB854 which was employed in mycobacterial recombineering. hyg indicates the hygromycin resistance gene and restriction sites are shown in blue.

Appendix Table 1. Parameters obtained during *M. smegmatis* growth assays

Growth assay (normoxia)	Wild type *M. smegmatis* parameters		
	Mid log active growth optical density range	Duration of one doubling during active growth	Final stationary phase optical density range
LBT	0.5 to 1	3 hours	2.5 to 3
HdB	0.25 to 0.5	4 hours	0.5
Nutrient upshift (HdB to LBT)	0.25 to 0.5	4 hours	0.5
Nutrient downshift (LBT to HdB)	0.2 to 0.4	4 hours	0.4

.

Appendix Table 2. Conditions for investigating *ΔrafS$_{Msm}$1* survival and resuscitation phenotypes. Energy limitation conditions are listed in column 1 in short form. Energy sources or components supplied (+) or lacking (-) are indicated. Complex energy sources refers to Tryptone and Yeast extract.

Energy Limitation Condition (short form)	Normoxia	Complex energy sources	Carbon source (Glycerol)	Tween 80 (dispersal agent, Carbon source)	Nitrogen source
PBS (sealed)	-	-	-	+	-
HdBN (0%G)	+	-	-	-	+
HdBN (0.04%G)	+	-	+	+	+
HdBH (0.04%G)	-	-	+	+	+
LBTH	-	+	-	+	+
LBTN	+	+	-	+	+

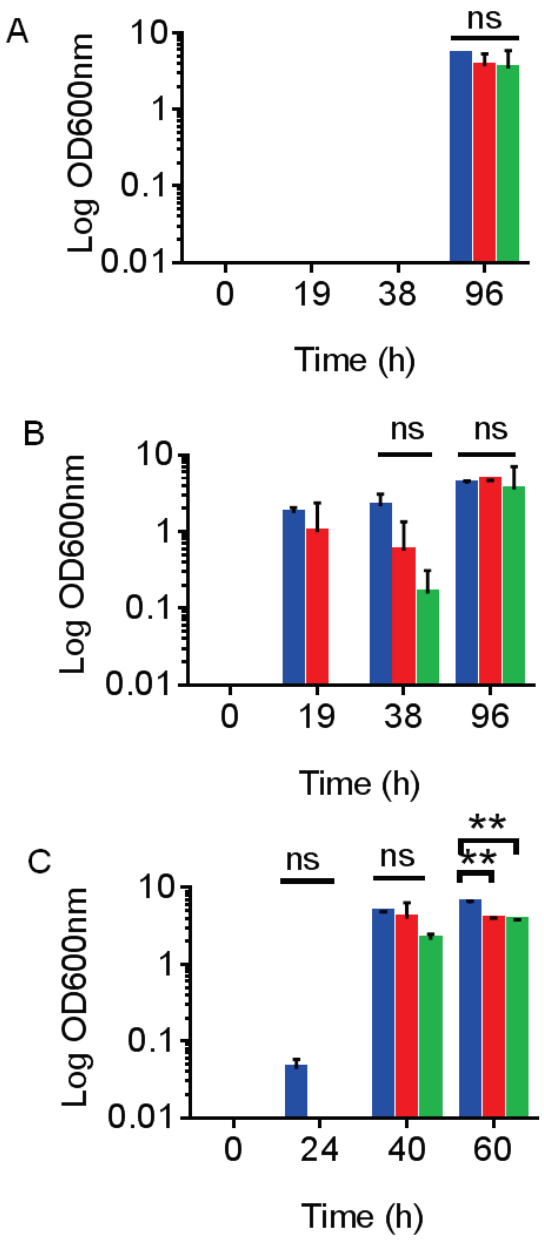

Appendix Figure 2. Role of $RafS_{Msm}$ in resuscitation of aged stasis cultures in rich media. Wild type *M. smegmatis* (blue), *Δ$rafS_{Msm}$1*(red) and *Δ$rafS_{Msm}$c* (green) aged cultures per strain were resuscitated by sub-culturing 1 ml of each culture to fresh LBT medium and monitoring growth in normoxic conditions. (A) Resuscitation of day 64 HdB (0.04% glycerol) normoxic cultures with 2 biological replicates per strain. (B) Resuscitation of day 183 hypoxic LBT stasis cultures with 2 biological replicates per strain. (C) Resuscitation of day 181 hypoxic HdB stasis cultures with 2 biological replicates per strain. Average optical density (600nm) is shown. Error bars indicate standard deviation. Means were compared using a one-way ANOVA with Holm-Šídák multiple comparison test; * : p = 0.001 to 0.01; ns : p > 0.05.

Appendix Table 3: Raf protein predicted physicochemical parameters obtained from ProtParam (Expasy). (A) Raf proteins are listed in order of decreasing stability and other parameters are included. (B) Several parameters affecting thermostability and protein charge are shown. The His tag was not included in these analyses.

(A) Raf protein	Theoretical PI	Expected Charge at pH7.4	Instability index	Classification	Predicted molecular weight (kDa)
$RafS_{Msm}$	6.27	Negative	37.89	stable	26.4
$RafH_{Mtb}$	10.21	Positive	42.05	unstable	29.47
$RafS_{Mtb}$	8.82	Positive	43.33	unstable	24.53
$RafH_{Msm}$	7.86	Positive	48.87	unstable	29.02

(B) Raf protein	Aliphatic index	Grand Average of Hydropathicity	Number of amino acids	Negatively charged residues (Asp + Glu)	Positively charged residues (Arg + Lys)
$RafS_{Msm}$	68.22	-0.790	230	42	38
$RafH_{Mtb}$	86.92	-0.231	273	27	36
$RafS_{Mtb}$	77.43	-0.651	214	34	37
$RafH_{Msm}$	83.22	-0.47	258	38	39

Appendix Table 4. Concentrators that have shown low protein recovery during concentration of $RafS_{Msm}$ at 25 ^{o}C, 5 000 g for 20 min intervals. MWCO indicates Molecular Weight Cut Off.

Concentrator	Details
Amicon Ultra-15 10 kDa MWCO (Millipore)	Cellulose acetate membrane
Vivaspin 10 kDa MWCO and Vivaspin turbo 5 and 10 kDa MWCO concentrators (GE)	Polyethersulfone (PES) membranes

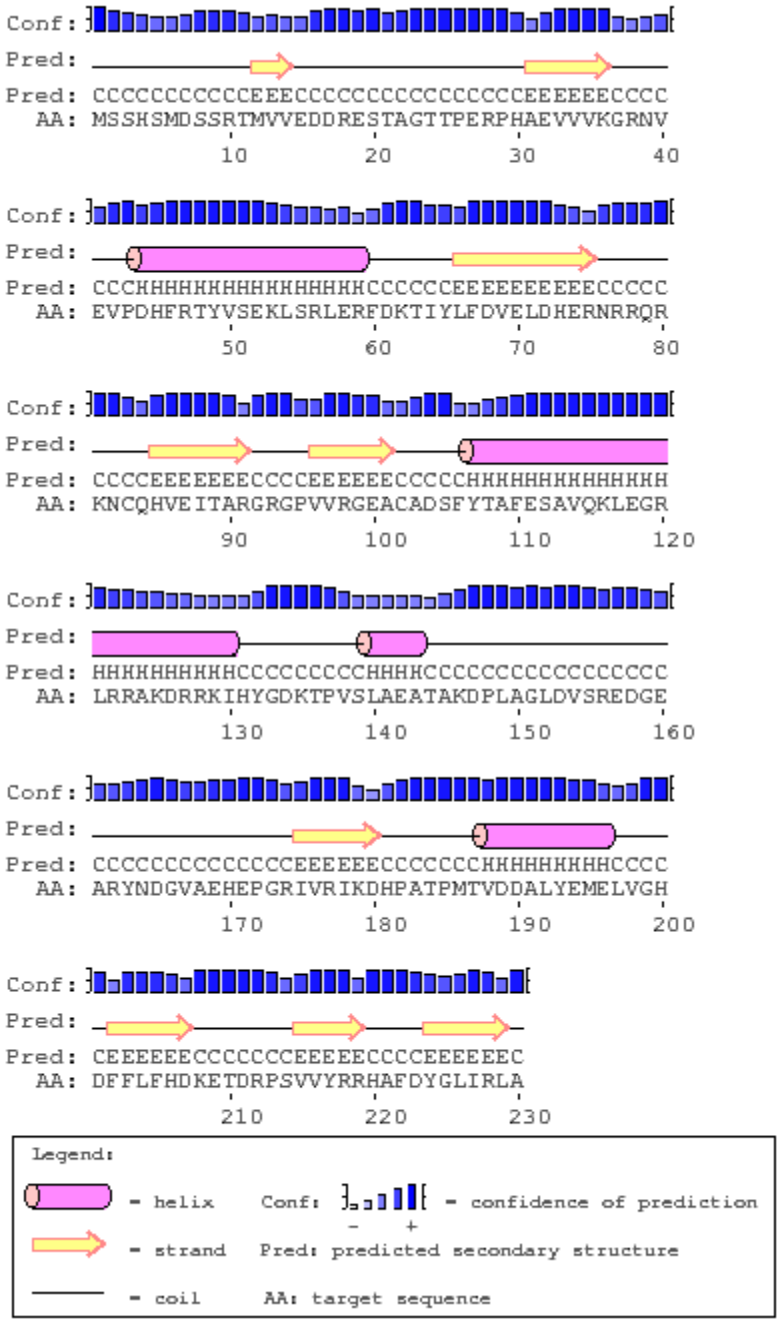

Appendix Figure 3. Secondary structure analysis of $RafS_{Msm.}$ (PSPIRED server, Buchan *et al*, 2013)

Appendix Figure 4. Secondary structure analysis of $RafS_{Mtb}$ (PSPIRED server, Buchan *et al*, 2013).

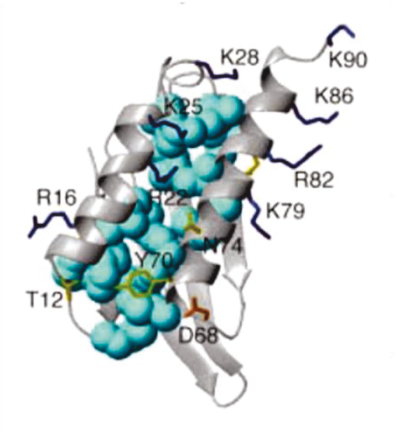

Appendix Figure 5. Several conserved residues of basic charge (blue) are localized to the α helices of the S30AE domain of PY. These helix-localised basic residues were suggested to play a role in binding rRNA. Image adapted from Ye *et al*., 2002.

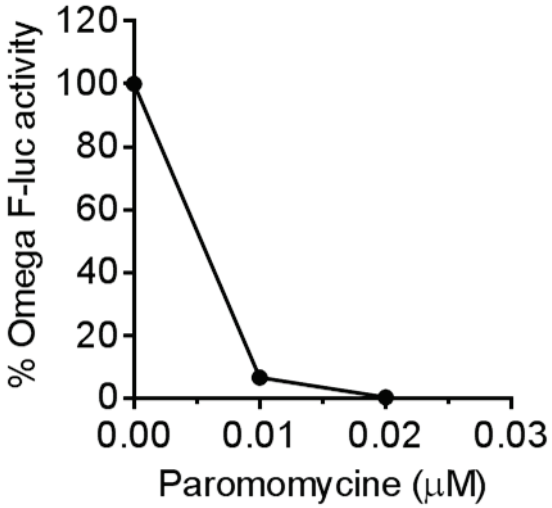

Appendix Figure 6: Paromomycine successfully inhibits translation of *M. smegmatis* non-dissociated ribosomes. Non-dissociated ribosomes were pre-incubated with increasing amounts of paromomycine for 60 min at 37°C. The reactions were incubated for 35 min at 37°C with the other components of the translation reaction mixture and *Omega* F-luc activity was measured.

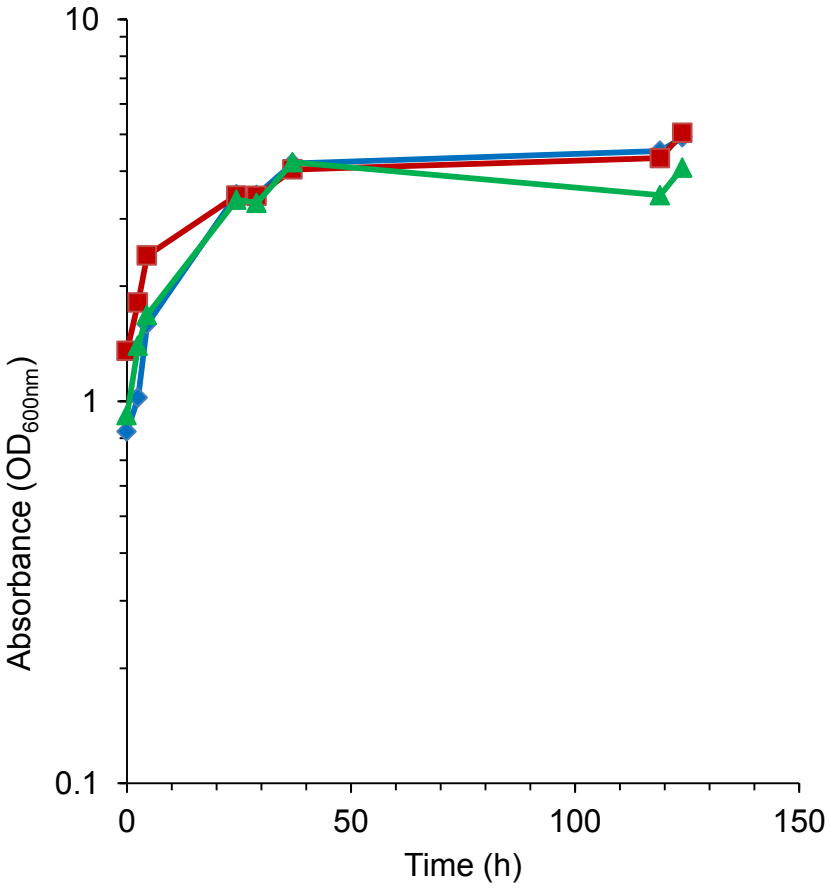

Appendix Figure 7. Growth curves of *M. smegmatis* wild type, Δ*rafS*$_{Msm}$ 1 and Δ*rafS*$_{Msm}$*c* (1 biological replicate each). Strains were cultured in LBT to stationary phase (9 h duration) and subcultured to 1L LBT in 2L flasks (1:2 culture: air ratio).

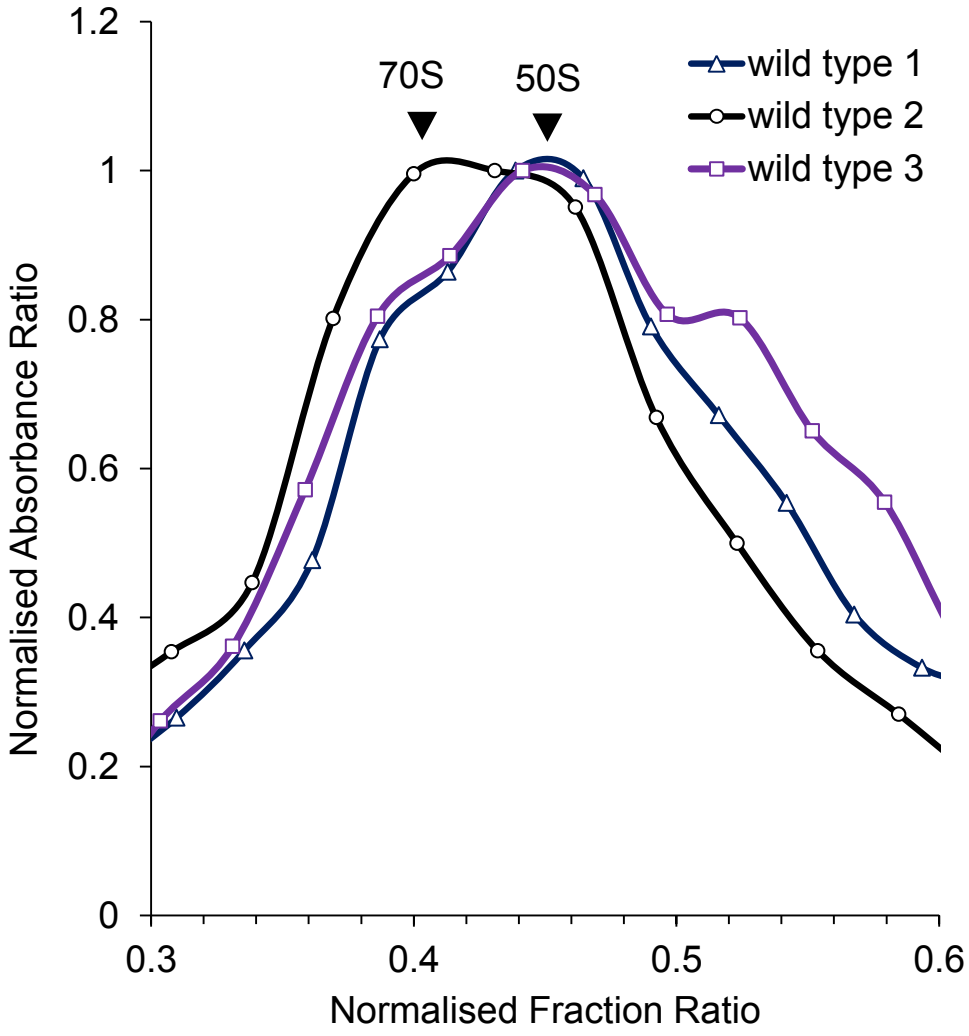

Appendix Figure 8. Enlarged plot shown in Fig. 4.31 A. Ribosomal profiling was carried out for 3 independent stationary phase cultures of wild type *M. smegmatis*. 70S and 50S ribosomal species are indicated with black arrows. Strains were cultured in LBT and cells were pelleted. Cell pellets were lysed by cell disruption into associative ribosomal buffer using a cell disruptor and clarified by ultracentrifugation to remove cellular debris. Ribosomes were pelleted by ultracentrifugation on a sucrose cushion. Ribosome sub-species were separated by centrifugation on associative sucrose gradients. Fractions were collected manually and absorbance of fractions was measured at 254 nm. Direction of sedimentation is from right to left.

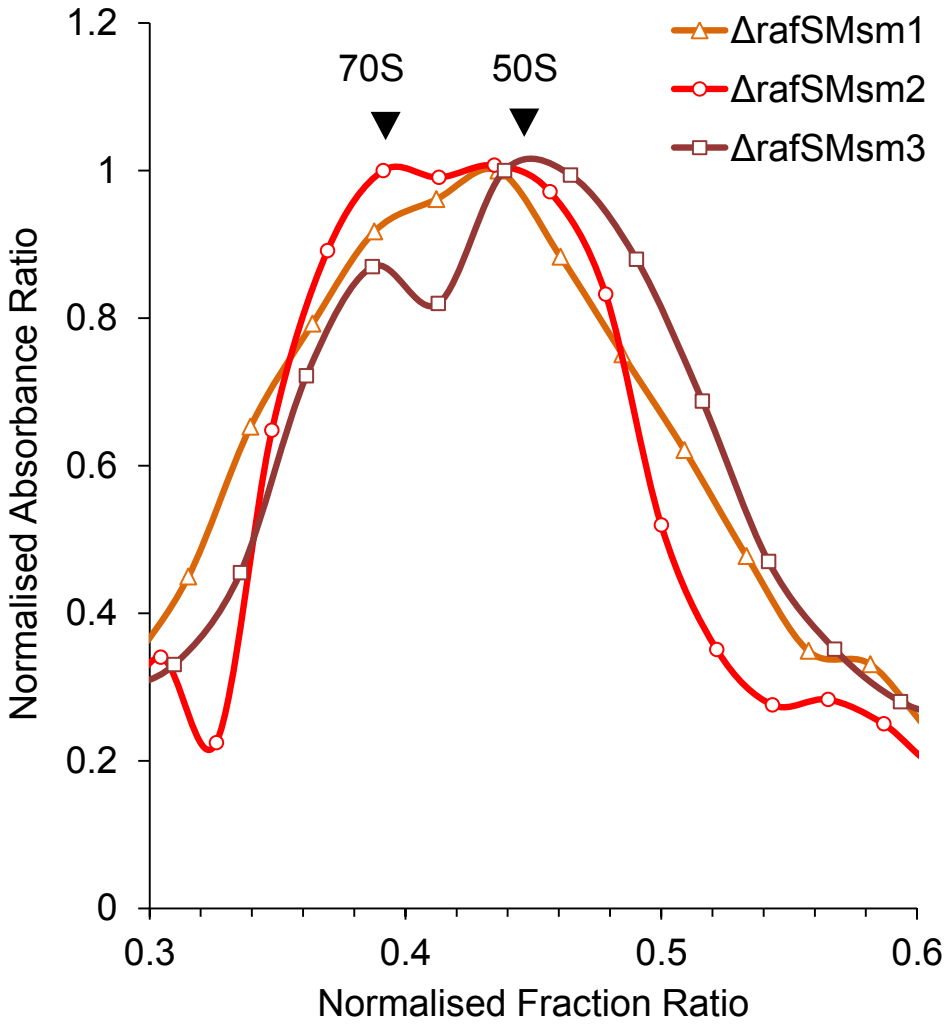

Appendix Figure 9. Enlarged plot shown in Fig. 4.31 B. Ribosomal profiling was carried out for 3 independent stationary phase cultures of *M. smegmatis* 3 independent *ΔrafS*$_{Msm}$ mutants. 70S and 50S ribosomal species are indicated with black arrows. Strains were cultured in LBT and cells were pelleted. Cell pellets were lysed by cell disruption into associative ribosomal buffer using a cell disruptor and clarified by ultracentrifugation to remove cellular debris. Ribosomes were pelleted by ultracentrifugation on a sucrose cushion. Ribosome sub-species were separated by centrifugation on associative sucrose gradients. Fractions were collected manually and absorbance of fractions was measured at 254 nm. Direction of sedimentation is from right to left.

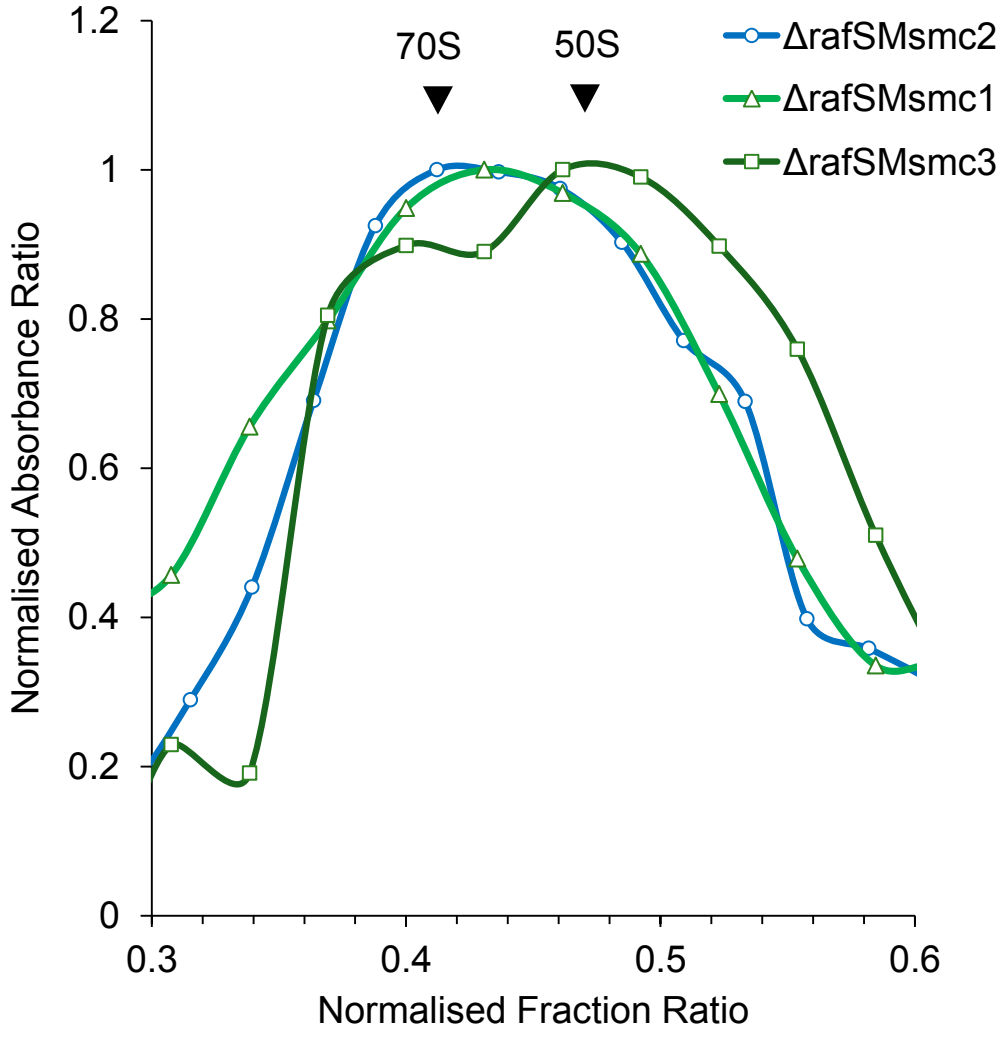

Appendix Figure 10. Enlarged plot shown in Fig. 4.31 C. Ribosomal profiling was carried out for independent stationary phase cultures of *ΔrafS*$_{Msm}$c *M. smegmatis*. 70S and 50S ribosomal species are indicated with black arrows. Strains were cultured in LBT and cells were pelleted. Cell pellets were lysed by cell disruption into associative ribosomal buffer using a cell disruptor and clarified by ultracentrifugation to remove cellular debris. Ribosomes were pelleted by ultracentrifugation on a sucrose cushion. Ribosome sub-species were separated by centrifugation on associative sucrose gradients. Fractions were collected manually and absorbance of fractions was measured at 254 nm. Direction of sedimentation is from right to left.

References

Akbergenov R 2011. Molecular basis for the selectivity of antituberculosis compounds capreomycin and viomycin. *Antimicrob. Agents Chemother*. **55**:4712–7.

Agafonov D.E., Kolb V.A., Nazimov I.V., Spirin A.S. 1999. A protein residing at the subunit interface of the bacterial ribosome. *Proc. Natl. Acad. Sci. U. S. A*. **96**:12345–9.

Agafonov D.E., Kolb V.A., A.S. Spirin. 2001. Ribosome-associated protein that inhibits translation at the aminoacyl-tRNA binding stage. *EMBO Reports* **2**:399-402.

Agafonov D.E., Spirin AS. 2004. The ribosome-associated inhibitor A reduces translation errors. *Biochem. Biophys. Res. Commun*. **320**:354–8.

Anuchin A. M. *et al.* 2009. Dormant forms of *Mycobacterium smegmatis* with distinct morphology. *Microbiology (Reading, England)* **155**:1071-9.

Avarbock A. *et al*. Functional regulation of the opposing (p)ppGpp synthetase/hydrolase activities of Rel_{Mtb} from *Mycobacterium tuberculosis*. *Biochemistry* **44**:9913–23.

Barry C.E. *et al*. 2009. The spectrum of latent tuberculosis: rethinking the biology and intervention strategies. *Nat. Rev. Microbiol*. **7**:845–55.

Beste D.J. *et al.* 2009. The genetic requirements for fast and slow growth in mycobacteria. *PLoS One* **4**:e5349.

Betts J.C., Lukey P.T., Robb L.C., McAdam R. A, Duncan K. 2002. Evaluation of a nutrient starvation model of Mycobacterium tuberculosis persistence by gene and protein expression profiling. *Mol. Microbiol*. **43**:717–31.

Berney M., Cook G.M. 2010. Unique flexibility in energy metabolism allows mycobacteria to combat starvation and hypoxia. *PLoS One* **5**:e8614.

Bibb L.A., Hatfull G.F. 2002. Integration and excision of the Mycobacterium tuberculosis prophage-like element, phiRv1. *Mol. Microbiol*. **45**:1515–26.

Brodersen D.E., Nissen P. 2005. The social life of ribosomal proteins. *FEBS J*. **272:**2098–108.

Bruell C.M. *et al.* 2008. Conservation of bacterial protein synthesis machinery: initiation and elongation in *Mycobacterium smegmatis*. *Biochemistry* **47**:8828–39.

Buchan D.W., Minneci F., Nugent T.C.O., Bryson K., Jones D.T. 2013. Scalable web services for the PSIPRED Protein Analysis Workbench. *Nucleic Acids Res*. **41**:W349–57.

Cecchini G. *et. al.* 2003. Function and structure of complex II of the respiratory chain. *Annu. Rev. Biochem*. **72**:77–109.

Cole C., Barber J.D., Barton G.J. 2008. The Jpred 3 secondary structure prediction server. *Nucleic Acids Res*. **36**:W197–201.

Collins L., Franzblau S.G. 1997. Microplate alamar blue assay versus BACTEC 460 system for high-throughput screening of compounds against *Mycobacterium tuberculosis* and *Mycobacterium avium*. *Antimicrob. Agents Chemother*. **41**:1004–9.

Commandeur S. *et al* 2013. An unbiased genome-wide Mycobacterium tuberculosis gene expression approach to discover antigens targeted by human T cells expressed during pulmonary infection. *J. Immunol*. **190**:1659–71.

Corpet F., Cellulaire L.D.G., Toulouse I., Tolosan C. 1988. Multiple sequence alignment with hierarchical clustering. *Nucleic Acids Res*. **16**:10881–10890.

Cortes T. *et. al*. 2013. Genome-wide mapping of transcriptional start sites defines an extensive leaderless transcriptome in Mycobacterium tuberculosis. *Cell Rep*. **5**:1121–31.

Dahl J.H. *et al*. 2003. The role of Rel_{Mtb}-mediated adaptation to stationary phase in long-term persistence of *Mycobacterium tuberculosis* in mice. *Proc. Natl. Acad. Sci. U. S. A.* **100**:10026–31.

Di Pietro F. *et al.* 2013. Role of the ribosome-associated protein PY in the cold-shock response of *Escherichia coli*. *Microbiologyopen* **2**:293–307

Donoghue H. D. 2009. Human tuberculosis-an ancient disease, as elucidated by ancient microbial biomolecules. *Microbes and infection.* **11**:1156-62.

Dworkin J., Shah I.M. 2010. Exit from dormancy in microbial organisms. *Nat. Rev. Microbiol.* **8**:890–6.

El-Sharoud W.M., Niven G.W. 2007. The influence of ribosome modulation factor on the survival of stationary-phase *Escherichia coli* during acid stress. *Microbiology* **153**:247–53.

Falkinham J.O. 2009. Surrounded by mycobacteria: nontuberculous mycobacteria in the human environment. *J. Appl. Microbiol*. **107**:356–67.

Garton N.J *et. al*. 2008. Cytological and transcript analyses reveal fat and lazy persister-like bacilli in tuberculous sputum. *PLoS Med*. **5**:e75.

Gautam U.S., Chauhan S., Tyagi J.S. 2011. Determinants Outside the DevR C-Terminal Domain Are Essential for Cooperativity and Robust Activation of Dormancy Genes in *Mycobacterium tuberculosis*. *PLoS One.* **6**:1–9.

Gerasimova A., Kazakov A.E., Arkin A.P., Dubchak I., Gelfand M.S. 2011. Comparative genomics of the dormancy regulons in mycobacteria. *J. Bacteriol*. **193**:3446–52.

Ghosh J. *et al*. 2009. Sporulation in mycobacteria. *Proc. Natl. Acad. Sci. U. S. A* **106**:10781-6.

Gilbert W. V. 2011. Functional specialization of ribosomes? *Trends Biochem. Sci*. **36**:127–32.

Goujon M. *et al.* 2010. A new bioinformatics analysis tools framework at EMBL-EBI. *Nucleic Acids Res*. **38:**W695–9.

GraphPad Prism version 6 for Windows, GraphPad Software, La Jolla California USA, www.graphpad.com

Guirado E., Schlesinger L.S. 2013. Modelling the *Mycobacterium tuberculosis* Granuloma - the Critical Battlefield in Host Immunity and Disease. *Front. Immunol*. **4**:98.

Häuser R *et al.* 2012. RsfA (YbeB) proteins are conserved ribosomal silencing factors. *PLoS Genet.* **8**:e1002815.

Henriques A.O., C. P. Moran. 2000. Structure and assembly of the bacterial endospore coat. *Methods (San Diego, Calif.)* **20**:95-110.

Hett E.C., Rubin E.J. 2008. Bacterial growth and cell division: a mycobacterial perspective. *Microbiol. Mol. Biol. Rev.* **72**:126–56.

Honaker R. W., Leistikow R. L., Bartek I. L., Voskuil M. I. 2009. Unique roles of DosT and DosS in DosR regulon induction and *Mycobacterium tuberculosis* dormancy. *Infect. immun.* **77**:3258-63.

Höner zu Bentrup K., Russell D. G.. 2001. Mycobacterial persistence: adaptation to a changing environment. *Trends microbiol*. **9**:597-605.

Hou J.M., *et. al*. 2008. ATPase activity of *Mycobacterium tuberculosis* SecA1 and SecA2 proteins and its importance for SecA2 function in macrophages. *J. Bacteriol*. **190**:4880–7.

Kaberdina A.C., Szaflarski W., Nierhaus K.H., Moll I. 2009. An unexpected type of ribosomes induced by kasugamycin: a look into ancestral times of protein synthesis? *Mol. Cell* **33**:227–36.

Kapopoulou A., Lew J.M., Cole S.T. 2011. The MycoBrowser portal: a comprehensive and manually annotated resource for mycobacterial genomes. *Tuberculosis (Edinb)*. **91**:8–13.

Kelley L.A. and Sternberg M.J.E. 2009. Protein structure prediction on the web: a case study using the Phyre server. *Nature Protocols* **4**, 363 – 371.

Kelkar D.S. *et al.* 2011. Proteogenomic analysis of *Mycobacterium tuberculosis* by high resolution mass spectrometry. *Molecul. Cell Prot*.**10**(12)

Kessel J.C. Van, Hatfull GF. 2007. Recombineering in *Mycobacterium tuberculosis. Nat. Methods* **4**:147–152.

Koul A., Arnoult E., Lounis N., Guillemont J., Andries K. 2011. The challenge of new drug discovery for tuberculosis. *Nature*. **469**:483-490.

Kumar A. *et al*. 2012. *Mycobacterium tuberculosis* DosR Regulon Gene Rv0079 Encodes a Putative, “Dormancy Associated Translation Inhibitor (DATIN)”. *PLoS One* **7**:e38709.

Kumar A., *et al.* 2013. Dormancy Associated Translation Inhibitor (DATIN/Rv0079) of *Mycobacterium tuberculosis* interacts with TLR2 and induces proinflammatory cytokine expression. *Cytokine* **64**:258–64.

Krokowski D. *et al*. 2011. Characterization of hibernating ribosomes in mammalian cells. *Cell Cycle* **10**:2691–2702.

Kruh N. A., Troudt J., Izzo A., Prenni J., Dobos K.M. 2010. Portrait of a Pathogen: The *Mycobacterium tuberculosis* Proteome *In Vivo. PLoS One* **5**:e13938.

Leistikow R. L. *et al*. 2010. The *Mycobacterium tuberculosis* DosR regulon assists in metabolic homeostasis and enables rapid recovery from nonrespiring dormancy. *J. bact*. **192**:1662-70.

Lew J.M., Kapopoulou A., Jones L.M., Cole S.T. 2011. TubercuList--10 years after. *Tuberculosis (Edinb).* **91**:1–7.

Liljas, A. Structural Aspects of Protein Synthesis. (World Scientific Publishing Co, London, U.K. 2004).

Loebel R. O., Shorr E., Richardson H. B. (1933a). The influence of adverse conditions upon the respiratory metabolism and growth of human tubercle bacilli. *J Bact.* **26**, 167–200.

Lougheed K.E. *et al.* 2011. Effective inhibitors of the essential kinase PknB and their potential as anti-mycobacterial agents. *Tuberculosis (Edinb*) 1-10

Magnusson L.U., Farewell A., Nyström T. 2005. ppGpp: a global regulator in *Escherichia coli*. *Trends Microbiol*. **13**:236–42.

Maki Y., Yoshida H., Wada A. 2000. Two proteins, YfiA and YhbH, associated with resting ribosomes in stationary phase *Escherichia coli*. *Genes Cells* **5**:965–74.

Mawuenyega K.G. *et al.* 2005. *Mycobacterium tuberculosis* functional network analysis by global subcellular protein profiling. *Mol. Biol. Cell* **16**:396–404.

Miotto P. *et al.* 2012. Genome-wide discovery of small RNAs in *Mycobacterium tuberculosis. PLoS One* **7**:e51950.

Niven G.W. 2004. Ribosome modulation factor protects *Escherichia coli* during heat stress, but this may not be dependent on ribosome dimerisation. *Arch. Microbiol*. **182**:60–6.

Notredame C., Higgins D.G., Heringa J. 2000. T-Coffee: A novel method for fast and accurate multiple sequence alignment. *J. Mol. Biol*. **302**:205–17.

Ortiz J.O. *et al.* 2010. Structure of hibernating ribosomes studied by cryoelectron tomography in vitro and in situ. *J. Cell Biol*. **190**:613–21.

Pang X. *et al.* 2007. Evidence for complex interactions of stress-associated regulons in an *mprAB* deletion mutant of *Mycobacterium tuberculosis*. *Microbiology* **153**:1229–42.

Piir K., Paier A., Liiv A., Tenson T., Maiväli U. 2011. Ribosome degradation in growing bacteria. *EMBO Rep.* **12:**458–62.

Polikanov Y.S., Blaha G.M., Steitz T. A. 2012. How Hibernation Factors RMF, HPF, and YfiA Turn Off Protein Synthesis. *Science*. **336**:915–918.

Pozos T.C., Ramakrishnan L., Ramakrishan L. 2004. New models for the study of Mycobacterium-host interactions. *Curr. Opin. Immunol*. **16**:499–505.

Primm T.P. *et al*. 2000. The stringent response of *Mycobacterium tuberculosis* is required for long-term survival. *J. Bacteriol*. **182**:4889–98.

Puri P *et. al.* 2014. Lactococcus lactis YfiA is necessary and sufficient for ribosome dimerization. *Mol. Microbiol*. **91**:394–407.

Raju R.M. *et al.* 2012. *Mycobacterium tuberculosis* ClpP1 and ClpP2 function together in protein degradation and are required for viability *in vitro* and during infection. *PLoS Pathog*. **8**:e1002511.

Raju R.M. *et al.* 2014. Post-translational regulation via Clp protease is critical for survival of *Mycobacterium tuberculosis*. *PLoS Pathog*. **10**:e1003994.

Rengarajan J., Bloom B. R., Rubin E. J.. 2005. Genome-wide requirements for *Mycobacterium tuberculosis* adaptation and survival in macrophages. *Proc. Natl. Acad. Sci. U. S. A* **102:**8327-32.

Rodríguez J.G. *et al.* 2014. Global adaptation to a lipid environment triggers the dormancy-related phenotype of *Mycobacterium tuberculosis*. *MBio* **5**:e01125–14.

Russell D. G. 2007. Who puts the tubercle in tuberculosis? *Nat. Rev. Microbiol*. **5**:39-47.

Rustad T. R., Sherrid A. M, Minch K. J., Sherman D. R.. 2009. Hypoxia: a window into *Mycobacterium tuberculosis* latency. *Cell. Microbiol*. **11**:1151-9.

Servin J. A, Herbold C. W., Skophammer R. G., Lake J. A. 2008. Evidence excluding the root of the tree of life from the actinobacteria. *Mol. Biol. Evol.* **25**:1-4.

Shajani Z., Sykes M.T., Williamson J.R. 2011. Assembly of bacterial ribosomes. *Annu. Rev. Biochem*. **80**:501–26.

Sharma M.R. *et al*. 2010. PSRP1 is not a ribosomal protein, but a ribosome-binding factor that is recycled by the ribosome-recycling factor (RRF) and elongation factor G (EF-G). *J. Biol. Chem*. **285**:4006–14.

Shasmal M., Sengupta J. 2012. Structural Diversity in Bacterial Ribosomes: Mycobacterial 70S Ribosome Structure Reveals Novel Features. *PLoS One* **7**:e31742.

Shiloh M., P. Di Giuseppe C. 2010. To catch a killer. What can mycobacterial models teach us about *Mycobacterium tuberculosis* pathogenesis? *Curr Opin Microbiol.* **13**:86-92.

Shleeva M.O. 2011. Dormant ovoid cells of *Mycobacterium tuberculosis* are formed in response to gradual external acidification. *Tuberculosis* (Edinb). **91**:146–54.

Simonetti A. *et. al*. 2009. A structural view of translation initiation in bacteria. Cell. Mol. Life Sci. 66:423–36.

Singh B., Ghosh J., Islam N. M., Dasgupta S., Kirsebom L. A. 2010. Growth, cell division and sporulation in mycobacteria. *Antonie van Leeuwenhoek* **98**:165-77.

Singh S., Saraav I., Sharma S. 2014. Immunogenic potential of latency associated antigens against *Mycobacterium tuberculosis*. *Vaccine* **32**:712–6.

Smeulders M.J., Keer J., Speight R.A., Williams HD. 1999. Adaptation of *Mycobacterium smegmatis* to Stationary Phase Adaptation of *Mycobacterium smegmatis* to Stationary Phase. *J. Bacteriol*. **181:**270.

Starosta A.L., Lassak J., Jung K., Wilson D.N. 2014. The bacterial translation stress response. *FEMS Microbiol. Rev*. E publication ahead of print.

Stephen F.A. *et al.* "Gapped BLAST and PSI-BLAST: a new generation of protein database search programs". *Nucleic Acids Res*. **25**:3389-3402.

Tan X., Varughese M., Widger W. 1994. A Light-repressed Transcript Found in Synechococcus PCC 7002 Is Similar to a Chloroplast-specific small subunit ribosomal protein and to a transcription modulator protein associated with Sigma 54. *J Biol. Chem* **269**:20905–20912.

Traag B. *et al*. 2010. Do mycobacteria produce endospores? *Proc. Natl. Acad. Sci. U. S. A* **107**:878-81.

Trauner A. 2010. On the stability of mycobacterial ribosomes during stasis. Imperial College Thesis. Imperial College London.

Trauner A., Lougheed K.E., Bennett M.H., Hingley-Wilson S.M., Williams H.D.. 2012. The dormancy regulator DosR controls ribosome stability in hypoxic mycobacteria. *J. Biol. Chem*. **287**:24053–63.

Ueta M. *et al*. 2008. Role of HPF (hibernation promoting factor) in translational activity in *Escherichia coli*. *J. Biochem*. **143**:425–33.

Ueta M., Wada C., Wada A.. 2010. Formation of 100S ribosomes in *Staphylococcus aureus* by the hibernation promoting factor homolog SaHPF. *Genes Cells* **15**:43–58.

Ueta M. *et al*. 2013. Conservation of two distinct types of 100S ribosome in bacteria. Genes Cells 1–21.

van de Kassteele J *et al.* 2012. New statistical technique for analyzing MIC-based susceptibility data. *Antimicrob. Agents Chemother***. 56**:1557–63.

van Kessel J.C., Marinelli L.J., Hatfull G.F. 2008. Recombineering mycobacteria and their phages. *Nat. Rev. Microbiol*. **6**:851–7.

Ventura M., C. *et al.* 2007. Genomics of Actinobacteria: tracing the evolutionary history of an ancient phylum. *Microbiol Mol Biol Rev*.**71**:495-548.

Vesper O., *et*. *al*. 2011. Selective Translation of Leaderless mRNAs by Specialized Ribosomes Generated by MazF in *Escherichia coli. Cell* **147**:147–157.

Vila-Sanjurjo A., Schuwirth B., Hau C., Cate J.. 2004. Structural basis for the control of translation initiation during stress. *Nat. Struct. & Mol. Biol.* **11**:1054-1059.

Wada A., Igarashi K., Yoshimura S., Aimoto A.I. S. 1995. Ribosome modulation factor: stationary growth phase-specific inhibitor of ribosome functions from Escherichia coli. *Biochem. Biophys. Res. Commun*. **214**:410–417.

Wada A. 1998. Growth phase coupled modulation of *Escherichia coli* ribosomes. *Genes Cells* **3**:203–8.

Wayne L.G. 1996. An *in vitro* model for sequential study of shiftdown of *Mycobacterium tuberculosis* through two stages of nonreplicating persistence. *Infect. Immun.* **64**(6):2062.

WHO Report 2013. Global Tuberculosis Control. *World Health Organization*. 2013. Retrieved 21 July 2014.

Wilson D. N., K. H. Nierhaus. 2004. The how and Y of cold shock. *Nat. Struct. & Mol. Biol* **11**:1026-8.

Ye K., Serganov A., Hu W., Garber M., Patel D.J. 2002. Ribosome-associated factor Y adopts a fold resembling a double-stranded RNA binding domain scaffold. *Eur. J. Biochem*. **269**:5182–5191.

Yoshida H., Ueta M., Maki Y., Sakai A., Wada A. 2009. Activities of *Escherichia coli* ribosomes in IF3 and RMF change to prepare 100S ribosome formation on entering the stationary growth phase. *Genes cells* **14**:271-80.

Zeyenko V. V., Ryabova L. A., Gallie D.R., Spirin A. S. 1994. Enhancing effect of the 3'-untranslated region of tobacco mosaic virus RNA on protein synthesis in vitro. *FEBS Lett*. **354**:271–3.

Zhukov I., P. Bayer, Schölermann B., Ejchart A.. 2007. 15N magnetic relaxation study of backbone dynamics of the ribosome-associated cold shock response protein Yfia of *Escherichia coli*. *Acta biochim Pol.* **54**:769-75.